The Institute of Paper Chemistry

Appleton, Wisconsin

Doctor's Dissertation

An Examination of
Longleaf Pine Cell-Wall Morphology
by Electron Microscopy of Single Fibers

Charles E. Dunning

June, 1968

AN EXAMINATION OF LONGLEAF PINE CELL-WALL MORPHOLOGY BY ELECTRON MICROSCOPY OF SINGLE FIBERS

A thesis submitted by

Charles E. Dunning

B.S. 1963, North Carolina State College
M.S. 1965, Lawrence University

in partial fulfillment of the requirements
of The Institute of Paper Chemistry
for the degree of Doctor of Philosophy
from Lawrence University,
Appleton, Wisconsin

June, 1968

TABLE OF CONTENTS

SUMMARY

In order to investigate the cell-wall structure of wood-pulp fibers directly, methods were developed for the microdissection of single fibers. The cylindrical freeze-dried fibers (ca. 40 μm. x 5 mm.) were slit open lengthwise and then spread out flat. Subsequently, either the exterior surface or the lumen surface was scraped to expose the lamellar deposition of microfibrils. Shadow-cast replicas of the exposed surfaces were prepared according to specially adapted techniques and then examined in a transmission electron microscope. The fibers studied were latewood tracheids of longleaf pine (Pinus palustris Mill.) which had been delignified in acidified sodium chlorite solution and then extracted with various concentrations of potassium hydroxide (KOH).

Using the developed methods, a generalized model of the cell wall was derived. Inside of the primary wall, the outer layer of the secondary wall (S1) was found to consist of at least five lamellae: one lamella with its fibrils lying nearly perpendicular to the fiber axis, one lamella resembling a left-hand (S) helix pitched about 65° from the axis, and one lamella resembling a right-hand (Z) helix about 60° from the axis. Below the last-mentioned lamella, several other lamellae perform a gradual transition to the microfibril angle of the S2 layer (central layer of the secondary wall). The S2 layer was found to be made up of fibrils deposited in a Z helix with an angle to the axis of approximately 15°. The S3 layer (inner layer of the secondary wall) was found to include at least twelve lamellae. These lamellae demonstrate a gradual stepwise transition of fibril orientation. If one visualizes a line segment which assumes the fibril direction of any given lamella in the S3, this line of orientation rotates in a clockwise motion (as seen from a point in the S2) in stepping from one lamella to the next--moving from the S2 to the lumen. Starting at the orientation of the S2, this rotation progresses more than 270°, ending with an S helix about 60° from the fiber axis. Then, a reversal in direction of rotation takes place

with a few lamellae making a small counterclockwise rotation to the lumen-surface fibril orientation, which is nearly perpendicular to the fiber axis.

As for the effects of the alkaline extractions, both the exterior and the lumen surfaces of the nonextracted fibers were found to be plastered over with a mudlike material. This material (probably pectin or other carbohydrates, together with some "soluble lignin") was largely removed by extraction with 0.1N KOH. The extractions with 9% KOH and with 9% KOH plus borate left some of the surface lamellae in a loosened condition. In fact, some of the loosened lamellae had been completely removed, allowing the underlying fibrils to loosen. Possibly, the loosened lamellae had been bonded to the cell wall by a hemicellulose that was removed by the extraction.

In addition to the studies of single fibers, some of the delignified chips were cleaved apart into radial shives, and the shive surfaces were replicated. The gaps between the adjacent fibers were found to be bridged over by nearly intact fibrillar membranes (presumably parent-cell walls). Practically all of the gaps were bridged over--some of them by multiple membrane thicknesses. Further study of the radial shives also permitted direct comparison of torus-type versus primary-wall-type pit membranes in ray crossings. As a result of this comparison, the author concludes that the torus structure is not a drying artifact as some workers had suggested, but that it is most probably a real structure produced during cell growth, a conclusion which reinforces the older concepts of pit structure.

INTRODUCTION

Starting with the assumption that the single fiber* is the fundamental construction unit of paper, several theories have recently been developed in an effort to relate the mechanical properties of paper to the properties of the fiber. Furthermore, other workers have proceeded with efforts to determine and interrelate the mechanical properties and structural parameters of single fibers. However, the explaining and interrelating of these properties inevitably require a knowledge of the fiber structure. At the same time, research concerning the isolation of the fibers from wood and the subsequent modification of the fiber characteristics also involves fundamentals of fiber structure--as well as wood structure. Therefore, the broad objective of this thesis research was to enlarge current knowledge of wood and fiber structure. Thus, with the objective of the program in mind, a brief historical review of the current knowledge in this field will be presented. Then, a more detailed discussion of the objectives and approach of this research will be given in THE APPROACH OF THE THESIS.

HISTORICAL REVIEW

CELL-WALL STRUCTURE

According to a recent textbook of wood anatomy (1), the concept of multilayered cell-wall structure of woody cells proposed by Kerr and Bailey (2, 3) has become classical. The basic concept, illustrated in Fig. 1, is that the cell wall is composed of a primary wall plus a secondary wall, the latter of which is generally divided into three separate layers. (The citing of a three-layered structure emerges from microscopical observations with polarized light and crossed nicols. Under such conditions, cross sections of the tubular cell wall appear as two, thin, bright,

*In the context of the present work, the term "fiber" refers to elongated wood cells in general, and to softwood longitudinal tracheids in particular.

concentric rings separated by a wider, darker, central band.) As noted by Bailey and cited by Roelofsen (4, p. 209) later, Dippel had already (1878) observed the triple layering of normal secondary walls. However, his terminology was somewhat variable and confused. Therefore, Kerr and Bailey's main contribution lay in their application of uniform terminology based on ontogenetic principles. Thus, they define the primary wall as the cambial wall, or the "original wall of the cell which is formed in the meristematic region and is carried over in more or less modified form into the fully differentiated tissues..." This wall alone is capable of expanding in length and diameter during growth. The secondary wall refers to the "strongly anisotropic layers of secondary thickening which are formed after a cell has attained its final size and shape." At this point, a further definition by Wardrop (5) might be helpful. He defines the primary wall as "the structure formed at cell division in the cambium and which encloses or enclosed the protoplast during the phase of surface growth of the cell during differentiation." Likewise, he defines the secondary wall as "the structure which is formed after the surface growth has ceased."

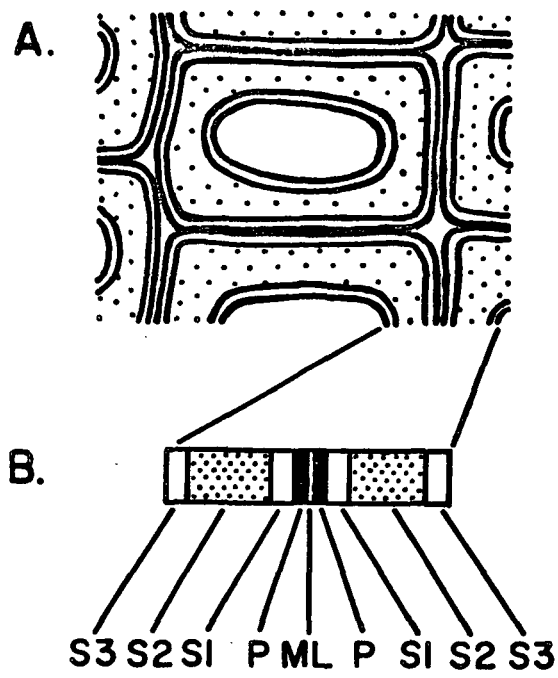

Figure 1. The Classical Schematic Diagram of Cell Wall Structure by Kerr and Bailey (2)

In general, the terminology of Kerr and Bailey has been accepted. The four layers have come to be designated as follows: P--primary wall; S1--outer layer of the secondary wall (layer adjacent to P); S2--central layer of the secondary wall; and S3--inner layer of the secondary wall (layer adjacent to the cell lumen). However, some workers (6-10) still adhere to a form of the terminology in existence before Kerr and Bailey's work. They use the terms primary wall, transition lamella (S1), secondary wall (S2), and tertiary wall (S3). The main point of contention is the S3 or tertiary lamella, which these workers maintain should be divorced from the secondary wall in terminology because of its behavioral differences. (The tertiary wall is claimed to be different in texture, reaction to chemicals, and resistance to enzymatic decomposition. It is also claimed to be mechanically separable from the cell wall.)

Bailey (11) has met the disagreement by saying that though the "tertiary wall" of a particular type of cell from a particular plant may behave in a given way, another cell may not even have a "tertiary wall" or, if it does have, the layer may behave differently. Therefore, he contends that use of the more generalized "secondary wall," be it three-layered or not, would be more acceptable. Furthermore, Wardrop, et al. (5, 12-18), who have been quite active in cell-wall research, have continued to use, and have defended from time to time, the terminology of Kerr and Bailey on the basis of its physiological foundation. A possible resolution of the disagreement is the terminology of Frey-Wyssling (19), who suggests that in addition to the three-layered secondary wall, the cell may have a "tertiary lamella" on its lumen surface. Apparently, Wardrop and Harada (17) agree to the possible presence of a "tertiary lamella" consisting of the "denatured remains of the cytoplasm," but insist that as such it "should receive no special designation in the terminology of wall structure."

As the electron microscope became available and cellulose fibers were examined, the cell wall was found to be made up of fine "subfibrils" or "filaments" (20-22).

Although a good beginning, these first micrographs of bare, untreated strands were low in contrast and detail. Therefore, Frey-Wyssling, et al. (23) used metal shadowing to make replicas of fiber surfaces. Their detailed micrographs showed the primary wall to be made up of randomly interwoven microfibrils and the secondary wall to be made up of uniformly arranged microfibrils. Other workers have subsequently generalized that the S1 layer is made up of spirally oriented microfibrils with an angle of about 60° to the fiber axis; that the S2 microfibrils lie at an angle of about 15°; and that the S3 microfibrils, similarly to those of the S1, lie in a transverse orientation of 60 to 90°. [Most of the recent papers already mentioned (6-10, 12-18) were based on electron microscopy and bear out these generalizations.]

More detailed study of the S1 has shown this layer to be made up of not just one, but several, crossed sublayers (24-29). Each sublayer is thought to be made up of microfibrils deposited in a spiral with about a 60° angle to the fiber axis. However, the successive sublayers are believed to have alternating right- and left-hand spirals. (Figures 2, 3, and 4 show three recent schematic models of the cell wall, and each bears out this detail of the S1.)

The S2, also, is believed by many workers to be lamellated. Bailey (32) observed concentric light and dark rings in cross sections of delignified and swollen tracheids and interpreted these rings as lamellae. Wardrop and Dadswell (13) and Harada (33) have interpreted some of their electron micrographs of ultra-thin cross sections of untreated wood as showing concentric lamellation of the S2. Jayme and Fengel (34) and Stone and Scallan (35) have solvent exchanged delignified pulps from water to methacrylate and then polymerized the methacrylate for sectioning. After sectioning, the methacrylate was dissolved away, leaving fiber cross sections with nearly concentric lamellae. However, Stone and Scallan admitted that the appearance was an artifact in part, since sections cut from fibers embedded in Epon 812 had a different appearance, and since Borysko (36) had found methacrylate

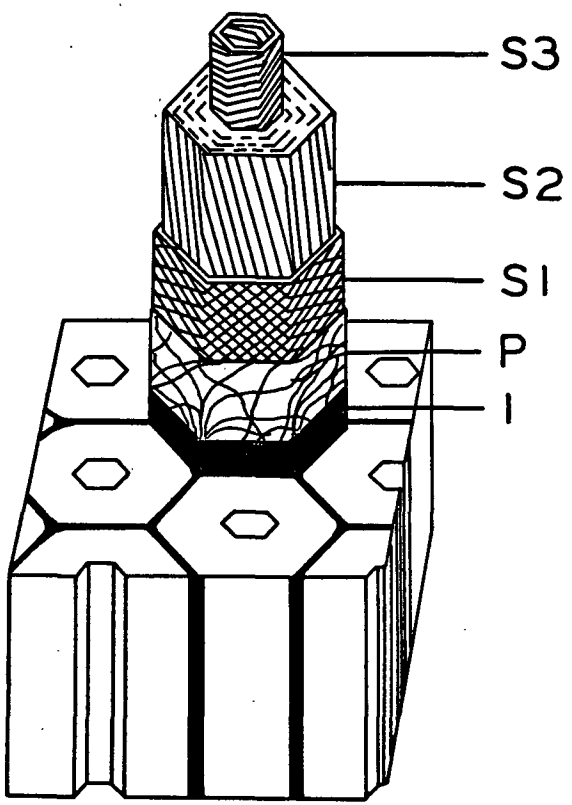

Figure 2. Cell-Wall Model by Wardrop and Dadswell (30)

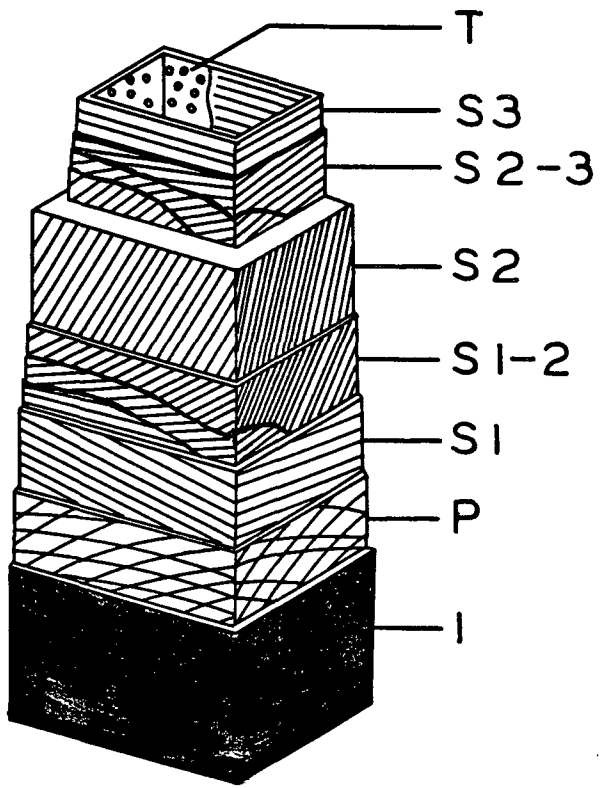

Figure 3. Cell-Wall Model by Harada, et al. (31)

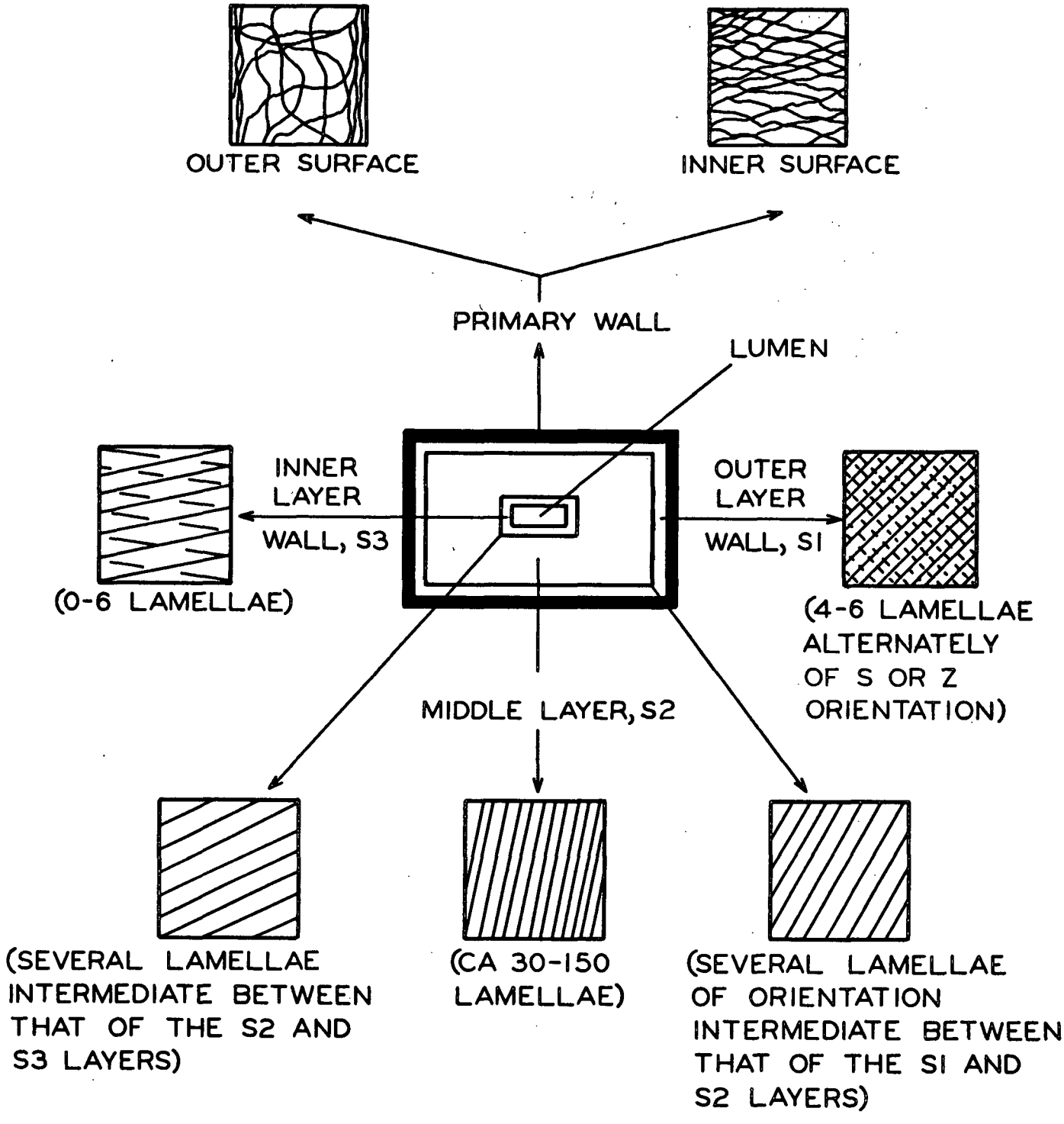

Figure 4. The Cell-Wall Organization of a Typical Fiber or Tracheid According to Wardrop (16)

to deform embedded materials during polymerization. Thus, this evidence obtained by methacrylate embedding is questionable.

On the other hand, Wardrop and Harada (17) have presented some evidence that the secondary wall is deposited layer by layer, and thus would be considered lamellated. Furthermore, they estimated the number of lamellae or sublayers in each of the basic cell-wall layers by measuring the cross-section thicknesses of the layers and then dividing the measured thicknesses by an assumed lamella thickness of 300 A. These estimated numbers of lamellae are indicated in Fig. 4. However, the conclusion of this discussion should still indicate that the matter of lamellation is still not decided conclusively--especially in the case of the S2.

As to the angle of orientation of the S2 microfibrils, uniform angles of 5 to 30 degrees have been indicated, depending on species, springwood, or summerwood, etc. As to the direction of spiraling, Wardrop indicated a left-hand spiral in the S2 (13, 30). However, Meier (8) found the same species examined by Wardrop (Pinus radiata) to have right-hand spiraling in its S2. Wardrop has subsequently indicated right-hand spiraling in his later model (Fig. 4).

The S3 is generally thought to consist of fibrils lying in a "flat helix" with an angle of about 60 to 90 degrees to the cell axis (1). However, the actual structure of this layer is still very much in question. For example, some workers believe the S3 to consist of one layer (sublayer) of microfibrils [Fig. 2, Fig. 3, Liese (9)]. On the other hand, Wardrop and Harada (17) have suggested that the S3 is made up of from zero to six lamellae with alternating orientation similar to that of the S1. (Their number estimate is based on the previously mentioned assumption of lamellae 300 A. thick.)

Thus, one can assemble evidence to indicate that the three basic secondary layers are themselves lamellated. However, the secondary wall may be even more

complex. Harada (37) records Kobayashi and Utsumi (38) as having suggested that "all the layers of the secondary wall are of a minute obliquely crossed structure" (apparently meaning that lamellae of intermediate orientation may lie between the S1 and S2 and between the S2 and S3). Harada, et al. (31) examined surface replicas of longitudinal sections of Picea jezoensis and Pinus densiflora cut with a microtome. They found that:

> The layers S1, S2, and S3 are each composed of several lamellae, and the angles and directions of the microfibrillar orientation in these lamellae are almost the same. Between the S1 and the S2, however, or between the S2 and S3, there can be seen some lamellae where the angle of microfibrils changes gradually...until the direction of their orientation becomes quite reversed.... Though it is possible to regard such a gradual change of the angle of the microfibrillar orientation as attributable to a very few lamellae, at any rate in this case it can be seen that the microfibrils change the direction of their orientation in a form like a spread fan, between the S2 and S3.... (37).

Practically all of Harada's (31) micrographs of intermediate layers were made from Picea jezoensis; only one micrograph showed a transition in Pinus densiflora, and that picture indicated just one "veering layer" between the S1 and S2. Even for Picea jezoensis, the number of transition layers shown between the S2 and S3 varied from none to four.

Wardrop (14) indicates that he and Harada, working together, later concluded "that the number of lamellae of intermediate orientation must be few." In still another paper, Wardrop and Harada (17) reported that they did not observe intermediate lamellae in differentiating tracheids and fibers of Pinus radiata and Eucalyptus elaeophora. However, they did find intermediate lamellae in mature fibers of these woods. On the other hand, some instances of sharp transition (without intermediate lamellae) between the S1 and S2 were found even in mature wood, suggesting that the organization of the cell wall is somewhat variable. In accord with these uncertain results, Wardrop's recent model (Fig. 4) indicates

"several" transition lamellae between the S1 and S2 and between the S2 and S3. Likewise, Necesany (39) reports from his work that "the transition between the individual parts of the cell wall can be but not always continuous." Thus, in agreement with Harada (37), the conclusion of this discussion is that the matter of layer transition must be further examined. In particular, extension to other species, together with more thorough verification of the continuity of transition, would improve the base of evidence for a suitable model of the cell wall. Also, Berlyn's (40) suggestion that the continuity of transition attests "to the essential unity of the entire secondary wall" could possibly be strengthened in the light of better evidence for that continuity.

THE WARTY LAYER

One structure of the fiber which should be mentioned is the "warty layer" on the lumen surfaces of some species. According to Wardrop (14), the structure was first observed by Kobayashi and Utsumi (1951) and Liese (1951). Liese and Hartmann-Fahnenbrock (41) first applied the term "warzenahnlich" (wartlike), because the material had the appearance of small granular or hemispherical bodies. [The diameters range from less than 0.01 μm. to more than 1.0 μm. with an average of 0.1 to 0.2 μm. (10).] Liese (42, 43) has subsequently examined over 80 species of Pinus, as well as species of several other genera, in order to determine the absence or presence of warts in these species. Also, Wardrop, Liese, and Davies (44) have made an extensive study of the chemical reactivity of the warty layer and found the material quite resistant toward most solutions, including concentrated acids and bases. However, the layer could be dissolved by treatment with chromic acid (50%, cold), boiling NaOH followed by chlorine water, or hydrogen peroxide followed by acetic acid. (Table I summarizes their findings.)

TABLE I

THE SOLUBILITY REACTIONS OF THE WART STRUCTURE OF *Actinostrobus pyramidalis*, WARDROP, ET AL. (44)

Treatment	Condition of the Wart Structure
Boiling water, 4 hr.	Unchanged
Sulfuric acid, 72%, 2 hr.	Unchanged
Sulfuric acid, 98%, 2 hr.	Unchanged
Alcohol (boiling 4 hr.) followed by ether (boiling 4 hr.)	Unchanged
Urea, 5M, 4-hr. boiling	Unchanged
Sodium hydroxide, 17.5%, 4-hr. boiling	Unchanged
Hydrogen peroxide, 100 vol., 0.5 hr., 98°C.	Unchanged
Sodium hydroxide, 0.25M, 4-hr. boiling	Unchanged
Pyridine, boiling 2 hr.	Unchanged
Butanol and hydrochloric acid, 2-hr. boiling	Unchanged
Sodium hypochlorite, cold, 8 hr.	Unchanged
Chromic acid, 50%, cold	Slowly dissolved after 24 hr.
Sodium hydroxide, 5-min. boiling followed by chlorine water, 6 g./l., cold	Dissolved rapidly
Hydrogen peroxide, 100 vol., + glacial acetic acid, 1:1, boiling	Dissolved after 4 hr.

The exact origin of this "warty layer" or "tertiary lamella" is still unknown. Liese (43) believes the layer to consist of dead protoplasmic material dried onto the lumen surface. By contrast, Wardrop and Davies (45) obtained evidence that wart-like protrusions are formed as a part of the last-deposited secondary-wall layer (S3). Wardrop (5) therefore concluded that the warty layer was made up of these protrusions plus cytoplasmic remnants dried onto the surface.

CELL-WALL PITS

Another structure of the cell wall is its pitting. A recent discussion of pits by Liese (46) indicates the large amount of study that has been done on this feature. [Panshin, et al. (1) also summarized present concepts of pit structure.] Basically, a pit is a hole through the cell wall, allowing communication with the lumen. The cells are arranged in wood so that opposite pits in adjacent cells usually lie in line with a "pit membrane" separating them. Two such facing pits constitute a "pit pair." Pits located in longitudinal or ray tracheids in softwoods have a dome or border arching over the pit membrane. Two such "bordered" pits together constitute a "bordered pit pair." As illustrated in Fig. 5, the membrane separating the opposite bordered pits in most softwoods is thought to have a thickened center. This thickened disk has come to be called the torus. The torus is believed to be suspended in place by spokes of microfibrils running radially to the surrounding wall. The perforated ring made up by these radial strands is termed the margo.

On the other hand, the pits in the thinner-walled parenchyma cells do not have the overarching border and are termed simple pits. Furthermore, the once-accepted concept was that the simple pit was an open cavity, as in Fig. 6a (48). However, Harada (49) has shown that, at least for sugi (Cryptomeria japonica D. Don) and hinoki (Chamaecyparis obtusa S. et Z.), the inner wall of the ray cell is continuous over the "pit," as in Fig. 6b. Thus, in partial agreement with the previous concept, he pictures the membrane to be continuous, lacking the torus construction of Fig. 5. Incidentally, this pairing of a simple pit with a bordered pit is termed a "half-bordered pit pair."

In the study of pit structure, too, Bailey (3) was largely responsible for present concepts, though the work of Sachs (1879) and Russow (1883) preceded his early work (1913). Although his concepts were based on the results of light

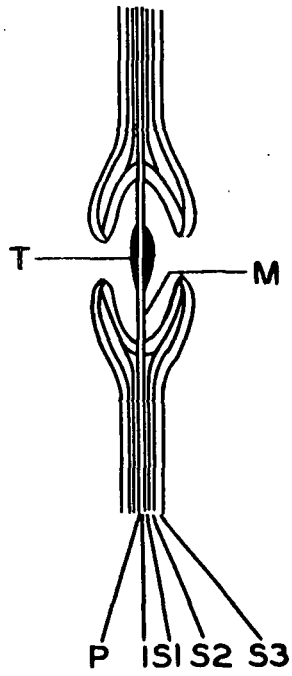

Figure 5. A Diagrammatic Representation of a Tangential Section Through a Bordered-Pit Pair

T = torus; M = Margo [Wardrop (30)]

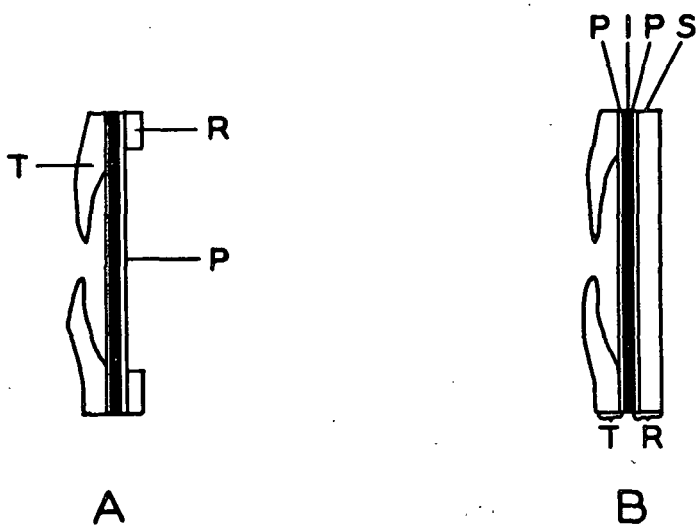

Figure 6. (A) The Older Concept of a Half-Bordered Pit Pair, Showing the Absence of Parenchyma-Cell Secondary Wall over the Pit Membrane (T = Tracheid, R = Ray-Parenchyma Cell, P = Pit Membrane). (B) The Newer Concept of Secondary Wall Continuing over the Pit Opening [Harada (49)]

microscopy and particle-filtration experiments, those concepts have generally agreed with the results of electron microscopy. Harada (31, 49) and Coté (50-52), among others, have supported Bailey's picture of bordered pits, as well as the concept of continuous-membrane structure in half-bordered pit pairs.

However, other workers have questioned some of the details of pit structure on the basis of electron microscopy. A repetitive question has been the matter of whether the membrane actually has microscopic pores, or whether the primary walls are continuous through the margo, thus meaning that the pores are only submicroscopic in size. Frey-Wyssling and Bosshard (53) questioned Liese's early electron micrographs showing microscopic pores between the radial strands and then presented micrographs showing what they called an ultrafilter woven among these radial microfibrils. However, Liese, et al. (6, 41, 54) were able to pass 200 nm. particles through the membranes, indicating that the pores of the membranes would have to be at least 200 nm. in diameter. According to Jayme and Fengel (55), Frey-Wyssling and Bosshard then modified their position by saying that the primary wall remains intact up to the sixth year, but that then the radial bundles unite into radial strands in a form of differentiation. On the other hand, Frey-Wyssling (19) in his book still upheld the submicroscopic porosity of bordered-pit membranes.

Jayme and Hunger (56) also observed pit membranes with the continuous, randomly woven textile of the primary wall. In order to explain the apparent disagreement with the concept of torus-type membranes, Jayme, et al. (55, 57, 58) hypothesized that all softwood membranes were of the primary-wall type, but that the torus-type membranes were artifacts resulting from the drying process. They explained the development of the torus construction as resulting from the aspiration (displacement of the membrane to a position blocking one of the pit apertures) of the pit. According to their explanation, the stress established in the radial fibrils in the membrane caused those fibrils to stretch and align themselves into radial bundles

(Fig. 7). The loose (nonstretched) fibrils were thought to migrate inward to the membrane center and thus form the torus. The aspiration itself was thought to be caused during drying by surface-tension effects of retreating water-air interfaces. Therefore, Jayme, et al. developed a method of replication intended to maintain the water-swollen condition of the pulp. Their approach was to prevent the rapid evaporation of water during the high-vacuum shadowing of the specimen by impregnating the specimen with a sorbitol solution. As to the success of the method, both torus-type and primary-wall-type membranes were still found, though the workers concluded that the sorbitol-treated wood had fewer of the torus-type membranes. They thus concluded that the primary-type membranes belonged to non-aspirated pits and torus-type membranes belonged to aspirated pits.

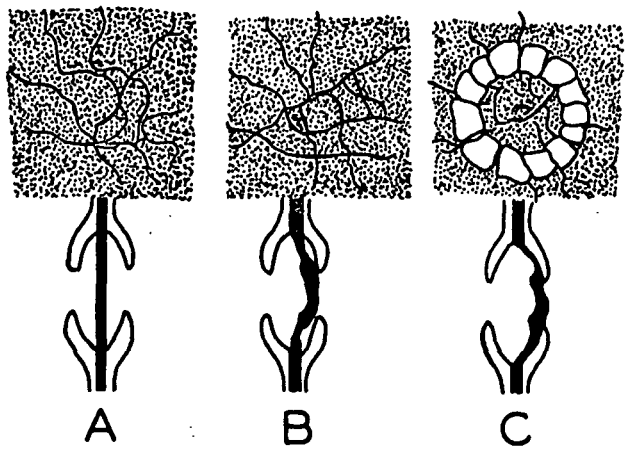

Figure 7. The Mechanism of Torus Formation Hypothesized by Jayme, et al. (58). (A) The Original Primary-Wall-like Membrane, (B) Aspiration of the Membrane, Causing Tension in the Radially Oriented Fibrils, (C) Aggregation of the Radial Fibrils and Migration of the Loose Fibrils Toward the Center

The same method of sorbitol treatment has since been tried by Jutte and Spit (59), but without success. They were not able to offer any conclusive evidence as to whether the torus is formed by aspiration. However, several workers (46, 54, 60, 61) have definitely objected to the hypothesis of Jayme, et al. that the torus

is a drying-process artifact. Their objections include several comments: (1) Tori can be found in nonaspirated membranes of green wood; (2) Some coniferous woods generally do not have tori, even in the aspirated condition; and, (3) Several workers (3, 6, 41, 51, 54) have been able to pass microscopic (0.05-0.2 μm.) particles through green wood. Tsoumis (60) therefore suggests that the observations of Jayme, et al. could be explained by assuming that the continuous primary-wall-type membranes are located in half-bordered pit pairs and that the torus membranes belong to true bordered-pit pairs.

Later, Thomas and Nicholas (62) applied a different approach in examining the question of drying artifacts and used solvent-exchange drying. Their idea was that by reducing the surface tension of the final liquid evaporated from wood sections, the tendency toward aspiration of pits by the retreating capillary interface could be reduced. Their micrographs indicate that, as expected, nonaspirated pits with torus-type membranes can be prepared. However, they are not sure that their micrographs represent the "green" state of the membranes, since even pentane (which they used) has some surface tension.

Finally, Fengel (63) (one of Jayme's colleagues in the artifact hypothesis) has studied the question by examining ultrathin sections of differentiating pit membranes. He concluded that the initial membrane is different from the surrounding primary wall in that its margo fibrils do have a preferred radial orientation. However, he still expressed the importance of pit aspiration in achieving the final membrane appearance. His concept was that the newly differentiated pit is in a labile condition which is set in final form by aspiration. In conclusion, the debate is still not definitely settled. Thus, further evidence as to the development and final form of the pit membranes would be most beneficial in this presently active discussion.

CHEMICAL CONSTITUENTS OF THE CELL WALL

The chemical constituents of wood-cell walls are divided into three main groups: cellulose, hemicellulose, and lignin, plus a fourth group of miscellaneous materials such as pectinaceous substances, inorganic salts, etc. In keeping with the general interest in delignified materials to be pursued later in this thesis, lignin will not be discussed. However, the other materials should be considered briefly. Cellulose is considered to be the essential strength factor of the cell and at least in large part makes up the microfibrils already mentioned. Basically, of course, cellulose is made up of β-1,4 linked polymer chains of anhydroglucose units. However, the manner of organization of the glucose polymers into "crystalline" regions and ultimately into microfibrils is unfortunately not known. [For example, books by Ott, et al. (64) and Hearle and Peters (65) and a paper by Manley (66) review some of the currently held theories of cellulose structure.]

The hemicelluloses are "those polysaccharides occurring in the cell wall that dissolve either in cold or in hot alkali but are insoluble or only slightly soluble in cold and hot water" (4). The major hemicelluloses in softwoods are o-acetyl-galactoglucomannan and arabino-(4-O-methylglucurono)xylan (67). Because of obvious difficulties, no direct method has been found for determining the location of the hemicelluloses within the cell wall. Probably the most reliable indirect method to date is that of Meier (68), who isolated cells of different states of maturity from an active zone of differentiation and then chromatographically analyzed the carbohydrate fraction of those cells. Working with Pinus sylvestris, he found higher galactan and arabanan contents in the middle lamella and primary wall, high glucuronoarabinoxylan content in the S1 and S3, and high glucomannan content in the S2.

Finally, the pectic substances are basically galacturonic-acid polymers and are found mostly in the middle lamella and primary wall (68A). Depending on the

source of these materials and the methods used in isolating them, they are found to have varying methyl-ester contents. Also, the free-acid groups are thought to be bound to varying degrees as calcium salts.

THE APPROACH OF THE THESIS

The objective of the thesis was to examine more thoroughly the microfibrillar structure of the cell wall. The microfibrillar structure was assumed as the dimensional scale of emphasis (rather than the molecular scale, for example), since Jentzen (69), Spiegelberg (70), and Hill (71), as well as others, had emphasized the importance of the fibrillar structure in analyzing the physical properties of single fibers. In the judgment of the author, this approach is well justified. The reasoning is that the factors of fibril orientation and behavior could completely overshadow the factors of molecular and crystal structure within the fibrils in the analysis of the fiber mechanical properties.

Once the microfibrillar structure (submicroscopic) was established as the dimensional realm of investigation, the logical choice of method was electron microscopy, since this instrument is readily capable of resolving the desired detail. However, as was implied in the HISTORICAL REVIEW, existing methods of specimen preparation were somewhat questionable. Therefore, a significant amount of time was spent in developing modified replication procedures. Furthermore, methods of dissecting single pulp fibers were also developed.

As to the choice of pulp for examination, wood holocellulose was chosen because of its minimal degradation and high yield. As a bonus, information obtained from such a pulp was expected to be translatable into knowledge of the untreated wood cell. Such knowledge is, of course, quite valuable in pulping research. Also, in addition to studying some of the pulp in the untreated form, the author examined other samples of the pulp which had been subjected to progressive stages of alkaline

extraction. The objective of this phase of the program was to obtain some indication of the location and influence of the hemicelluloses in the fiber wall, as well as the reaction of the fiber wall to chemical treatment. Thus, the approach of the program was such as to fulfill the general objective, which was to gain understanding of the overall fiber structure and its behavior during treatment.

EXPERIMENTAL MATERIALS AND METHODS

SOURCE OF THE FIBERS TO BE STUDIED

The fibers used in this study were obtained from Spiegelberg following his thesis research (70). The availability of his holocellulose pulp samples was quite fortunate, because the relating of the physical properties he observed to the fiber structure observed in this study became possible. Also, Hill (71) has used some of the same fibers, and Jentzen (69) had used very similar ones.

Briefly, the pulp was prepared from the summerwood of the 27th and 28th growth rings of a 49-year-old longleaf pine (Pinus palustris). The chips to be defibered were extracted with chloroform-ethanol and then treated for three weeks in a sodium chlorite solution initially buffered to pH 6.8. The final holocellulose had a Klason-lignin content of 0.45%, and the yield was 72.1%.

In order to obtain nonextracted fibers, some of the delignified chips were tumbled with water and rubber balls in plastic bottles. Other chips were subjected to the following procedure:

"(1) 0.1N KOH for two hours at room temperature,

(2) 2% KOH for one hour at room temperature, and 9% KOH for one-half hour at 45°C. ± 2°C. (twice),

(3) 9% KOH-3% H_3BO_3 for one-half hour at 45°C. ± 2°C. (twice)" (70).

After each extraction the pulp was thoroughly washed and a sample was removed from the batch, labeled, and stored. (The samples have been stored in a 0.05% solution of phenyl mercuric acetate at 40°F. since preparation.) The sugar analysis of those pulp samples is given in Table II.

TABLE II

SUGAR ANALYSIS OF HOLOCELLULOSE PULP CORRECTED FOR YIELD [SPIEGELBERG (70)][a]

Sample	Yield, %[b]	Glucan, %	Xylan, %	Mannan, %	Araban, %	Galactan, %
Unextracted holocellulose	72.1	55.5	6.68	15.6	1.29	1.82
Holocellulose extract with 0.1N KOH	62.1	56.0	5.52	15.2	0.86	1.13
Holocellulose extract with 0.1N KOH + 2% + 9% KOH	54.2	53.0	1.35	11.9	--	0.86
Holocellulose extract with 0.1N KOH + 2% + 9% + 9% KOH - 3% H_3BO_3	50.1	51.1	1.28	7.76	--	0.78

a All percentages referred to unextracted holocellulose as 72.1%.

b Based on extractive- and moisture-free wood.

PREPARATION OF FIBERS FOR REPLICATION

Although the electron microscope is capable of extremely fine resolution and good focal depth, it does have limitations. One of these is that the microscope column, including the specimen chamber, must operate under a high vacuum and, hence, the specimen must be dry. However, the more important limitation is that the penetration depth of the electron beam in organic materials is extremely small. For example, in the present work even single thicknesses of the cell wall were far too thick to allow transmission of the beam. Partial thicknesses of the wall were also tried, but only the very thinnest fragments (fractional thicknesses of the S3) were thin enough to permit sufficient transmission for imaging. Because of this limitation, metal replicas (copies of the fiber surfaces) were prepared for

observation. The developed replication procedures will be described in a later section. The purpose of the present section will be to discuss the procedures used in preparing the fibers and exposing the surfaces to be replicated.

FIBER DRYING

Several attempts had been made in the past to replicate the surfaces of materials as they appear in the water-swollen condition. Fischbein (72) pressed wet specimens into heat-softened polyethylene and polystyrene films. After the film had been allowed to cool and harden, the specimen was stripped away, and the plastic film was coated with a metal film. The metal film (replica) was separated from the plastic film and placed on a supporting screen for viewing in the microscope. Another method of wet preparation is that of Jayme and Fengel (55). With the idea that artifacts were caused by drying, they impregnated wet pulp specimens with a sorbitol solution in order to retard drying during the high-vacuum shadowing operation. However, both the method of Fischbein and that of Jayme and Fengel involve questions of interface effects. For example, would free standing surface fibrils (if such should be present) force themselves through the water-polymer interface of the first method, or through the sorbitol solution-air interface in the second method? In any case, neither worker presents micrographs indicating the presence of such fibrillated fibrils, standing above the surface.

Therefore, in an effort to avoid the effects of interfacial surface tension, the technique of freeze drying (freezing followed by sublimation) was applied in the present work. In fact, this technique had already been used to dry wet-web samples for study in the scanning electron microscope (73). However, an uncertainty in the use of freeze drying for replica specimens was whether the surface fibrillation would survive the subsequent replication process, even if it did survive the freeze drying. The initial results indicated a surprisingly good retention of the

loose, fibrillar texture, and, therefore, the technique was adopted for general use in this work.

In the adopted method of freeze drying, the first step was to pour a very dilute suspension of the fibers into a disposable aluminum weighing dish. Then, the bottom of the dish was touched to the surface of a dry ice-acetone bath until freezing was complete. The dish of ice was placed in the vacuum chamber of an N.R.C. Type 3505-2 Dehydration Unit and held under vacuum until the ice had sublimed. The dry fibers were then transferred to glass weighing bottles for storage. Because of possible interest, Appendix I is a discussion of an attempt to use liquid nitrogen freezing and of the chip defibering that resulted. Also, Appendix II discusses the possibility of using solvent-exchange drying.

DISSECTION OF FIBER SPECIMENS

Quite obviously, if the lumen surfaces of fibers were to be examined, some method of cutting open the fibers to expose those surfaces had to be developed. Furthermore, if the lumen could be exposed by slitting out one side of the cylindrical fiber and spreading out the fiber wall as a wide, flat sheet of fiber wall, one would have a much wider width of fiber-wall surface to replicate. Also, in the case of the exterior fiber surface, one might be able to compare the radial faces of the fiber with the tangential faces. Therefore, with these considerations in mind, such a method for spreading out the walls of single fibers was developed. Furthermore, since the electron-microscopy techniques of surface replication permit examination of surfaces only, the internal wall structure still could not be studied immediately. Hence, a method of scraping and peeling away surface wall layers to expose inner surfaces was devised. Finally, because of the essential role of the slitting and peeling operations in the present work, and because the success of

these techniques gave a new perspective of possible hand manipulations of single pulp fibers, these techniques will be discussed in detail.

The Slitting Technique

The basic slitting technique consisted of inserting the point of a fine knife into the lumen of the fiber and then pushing the knife along the fiber. The rounded knife point followed the lumen and the sharp upper edge of the knife slit open the upper side of the fiber wall as in Fig. 8. Because of the microscopic size of the pulp fiber (20 to 40 μm. in diameter, 3 to 6 mm. in length), several problems were encountered. The crucial matter was the development of a suitable knife. Techniques of preparing such knives were developed and are discussed in Appendix III. Secondly, the movement of the knife was extremely tedious and had to be done mechanically. This problem was solved by using a Bausch and Lomb Micro Manipulator similar to the one used by A. J. Bailey (74). The dissection was carried out under a Bausch and Lomb Stereozoom (0.7 to 3.0-power) microscope fitted with 10-power oculars and a 2-power objective lens (total magnification 14X to 60X). (This microscope was found quite suitable and nontiring to the eyes--even for extended periods of close work.) The microscope was mounted to a machining stage by a combination of Bausch and Lomb and homemade adaptors. The movable machining stage allowed two-directional movement over the working area. A light source made for use with lamp-and-scale galvanometers was mounted with the microscope and moved with the field of view.

The freeze-dried fiber to be cut open was laid on a rubber disk placed on the working stage. (Attempts to use wet fibers are discussed in Appendix IV.) A steel needle bent into the shape of a hairpin was used to hold the fiber in place. The blunt end of the needle was held in a hole bored into the edge of the working stage. The sharpened needle point lay over the fiber end, and the spring action of the needle pressed the fiber to the rubber surface. The fiber lay in a right-to-left

direction with its right end clamped in place. The slitting knife was mounted in the right manipulator with its point toward the left.

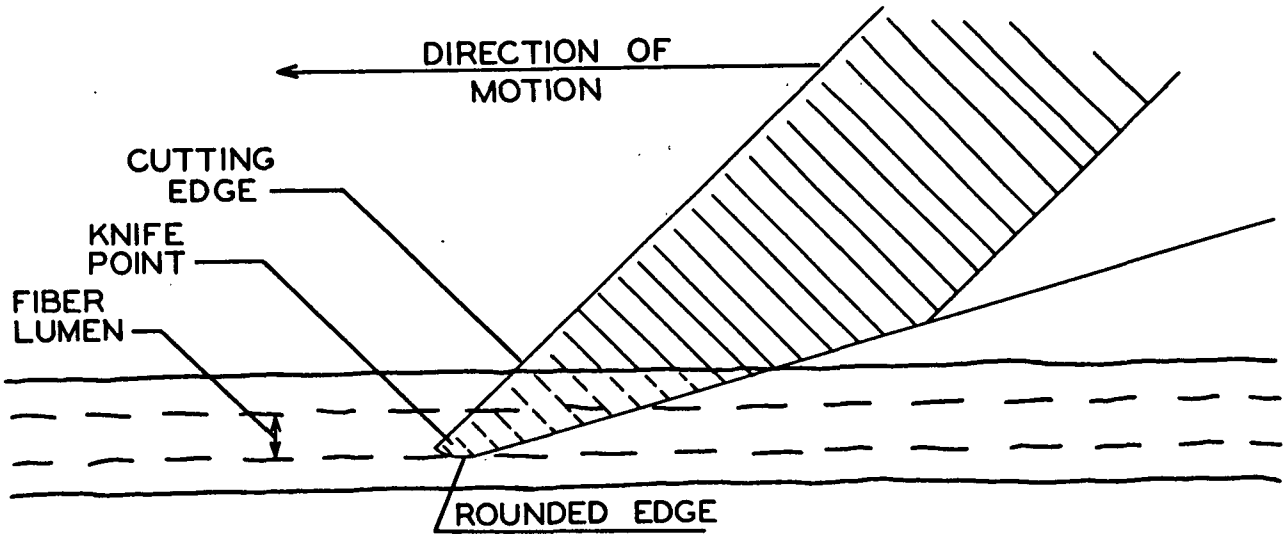

Figure 8. A Schematic Drawing of the Basic Slitting Technique

The point of a hand-held needle was laid across the fiber, near the clamping needle, and pressed down to make a dent or indentation in the fiber surface. The knife point was maneuvered into position over the dent and then gently lowered and pushed forward slightly until the point had gained entrance to the fiber lumen (Fig. 9). At the same time, care had to be exercised to see that the point did not pass right on through the underside fiber wall as the fiber was pressed to the rubber surface. Once, however, the leading point of the knife had gained entrance to the lumen, the knife and fiber were lifted slightly above the rubber surface to reduce the danger of forcing the knife through the lower fiber wall. Then the knife was pushed slowly along the fiber. The point of the knife followed the lumen while the trailing, sharp upper edge did the slitting. (The microscopic point of the knife was intentionally rounded at the bottom so that it would "ride" more easily along the lumen surface without pushing through the lower wall.)

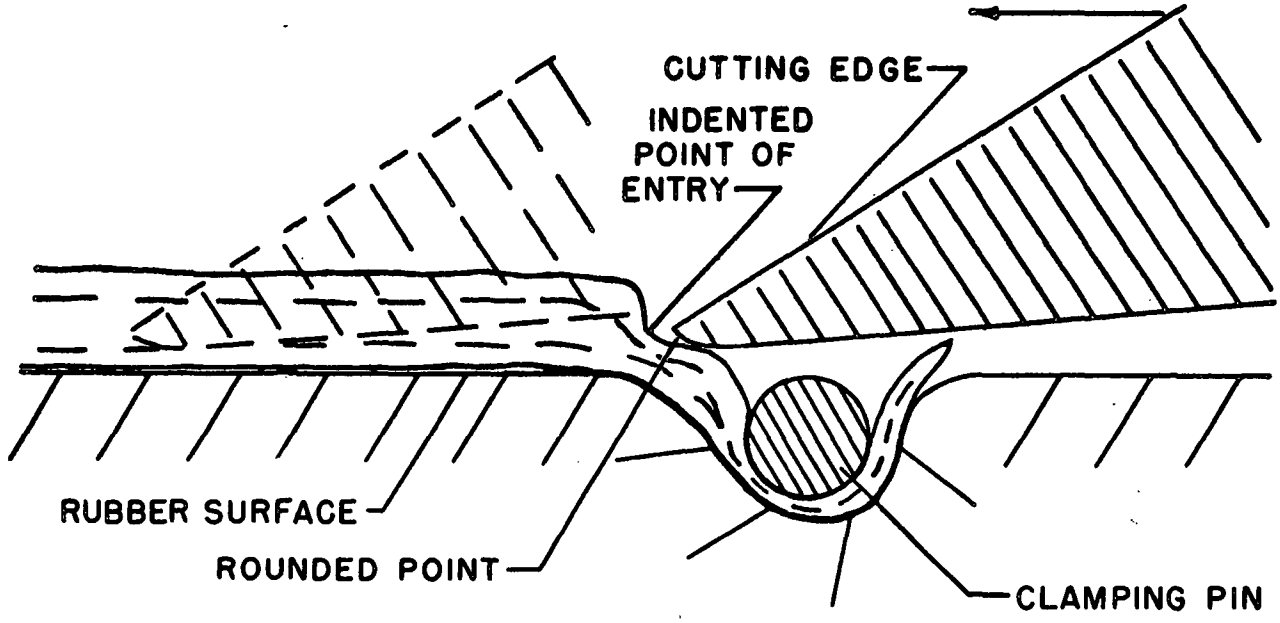

Figure 9. The Method of Entering the Knife Point into the Cell Lumen

Once the fiber had been slit open, it still did not open up of its own accord but, on the contrary, it had to be forced open. This operation was a manual one, performed with two dissecting needles, one of which had been sharpened to a slender tip small enough to enter the lumen, yet rounded at the very end. The needle with the rounded point was placed nearly parallel to the fiber, pushed into the lumen, and moved away from the clamping needle. The other needle, lying across the fiber and pressing down on it, followed the first needle and forced the standing edges of the fiber wall to lie down (Fig. 10). Thus, the fiber was opened up and flattened out as a fiber wall sheet (FWS). However, one precaution had to be taken. Once the FWS was released from the clamped position, discernment between the outside and lumen side of the flat sheet became very difficult. Therefore, a customary diagonal cutoff prior to release became as meaningful as the skewed corner of IBM cards (Fig. 11). If no treatment of the surfaces was to be done, the FWS's thus prepared were ready for application of the metal replica film, which will be discussed separately.

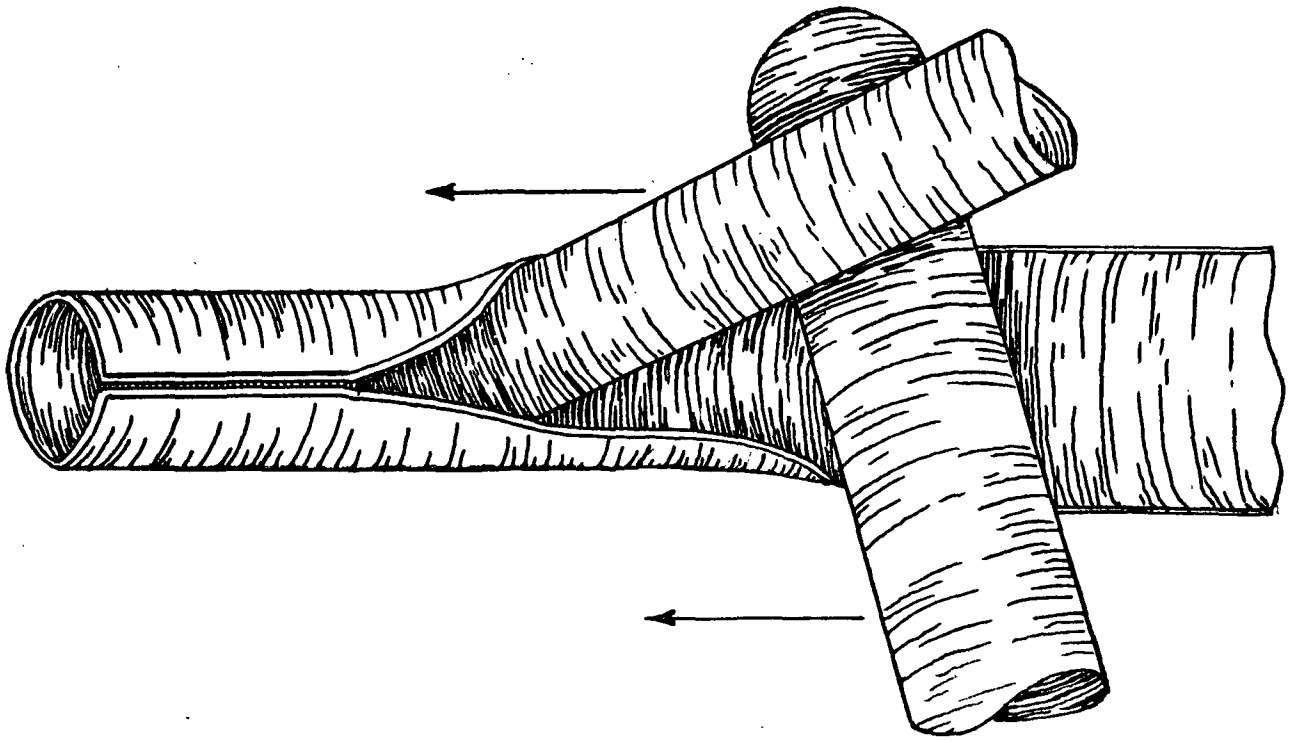

Figure 10. The Technique of Using Slightly Rounded Dissecting Needles to Spread Out Slit Fibers

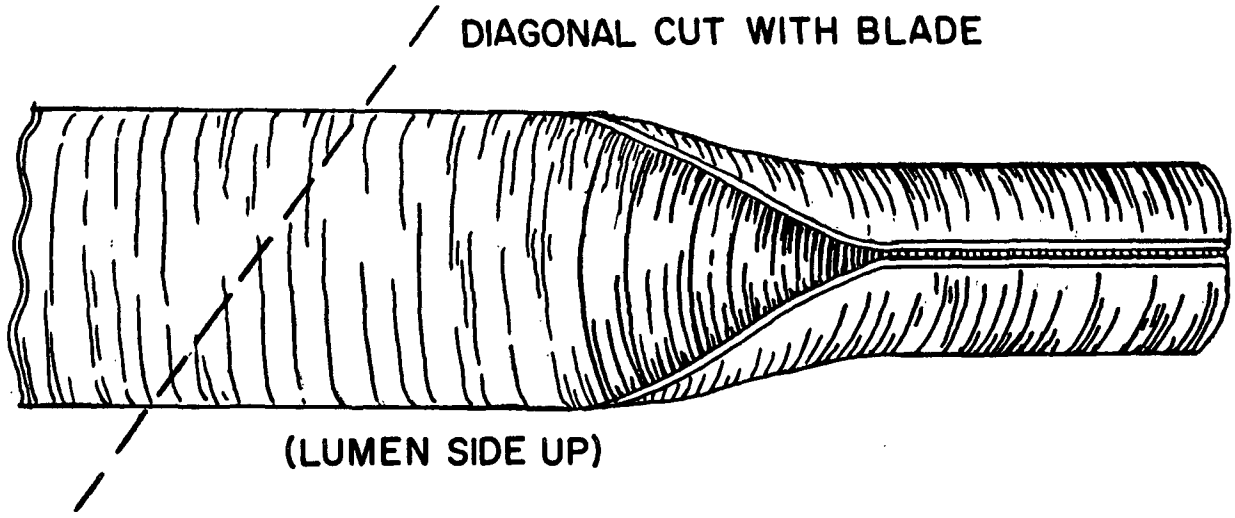

Figure 11. The Diagonal Cut-Off Used to "Label" the Exterior Versus Lumen Surfaces of the Fiber Segments

Peeling Away of Surface Layers

In order to expose internal layers of the FWS for replication, the surface layers had to be removed. The removal of these layers was started by scraping the surface with a small knife made from a dissecting needle. By repeated scraping of a given area, a small tab of layer material could be loosened. Then, a pair of stainless steel tweezers, which had been precision reground with an "Arkansas" stone and with pink rouge, was used to grasp the raised tab and peel back the surface layer. As will be understood upon examination of the micrographs, the peeling back of the "layer" was not a separation between morphological layers, but rather it was a random tearing apart of several lamellae. Because of this random tearing, the operation was quite beneficial, as it permitted study of the multiple layering within the S1 and S3.

PREPARATION OF SURFACE REPLICAS

The techniques of replication and microscopy of wood and paper have been well developed and extensively practiced (75). However, the application of these techniques to portions of single fibers required considerable modification. For this reason, the techniques developed for single fibers will be explained in some detail. The replicas were of two types: "shadow-transfer" replicas [so-called by Côté, et al. (75)] and "negative" replicas.

SHADOW-TRANSFER REPLICAS

The shadow-transfer replicas (STR) were considered the more reliable and, therefore, were generally used. Basically, the method consisted of metal shadowing the surface of the specimen directly, and then separating the metal replica from the specimen for examination in the microscope. The fact that the metal shadowing was applied to the surface of the specimen directly--and not to some intermediate impression of the specimen surface--was reason to assume that replicas produced by

this method would be less likely to include artifacts. Incidentally, these STR were also more easily interpreted than the other replica forms tried.

Figure 12 is a schematic outline of the STR process. The FWS was mounted for shadowing by being pressed into the surface of rubber cement, which had been spread on the surface of a microscope slide and allowed to dry. Then, the metal replica film was applied to the FWS under high vacuum by evaporating metal atoms from a palladium wire wound around an electrically heated tungsten filament. The palladium source, placed at an angle of 30° with the plane of the specimen surface, cast "shadows" behind the features of the specimen surface. Then, a film reinforcing was applied over the metal film by evaporating carbon atoms from pointed, touching carbon electrodes through which a heating current was passed. After the application of the carbon and metal films, tweezers were used to pull the FWS from the surface of the rubber cement.

In order to separate the fragile replica film from the specimen, the replica side of the specimen was first pressed into melted polystyrene (PS). This embedding was done by a technique adapted from Hunger (76, 57) and designed by him to eliminate the problem of air-bubble formation in the PS. The FWS was placed, replica side up, on a tab of 0.05 μm-pore-size Metricel (Polypore) filter (Gelman Instrument Co.) and covered with a 1/4-in. PS disk. (The PS disk edges had been dipped lightly into rubber cement in order to insure its staying in position on the filter.) The filter tab was then placed on a slip of scratch paper which was subsequently laid on a sintered-glass disk in a brass holder (Fig. 12B). (The paper prevented melted PS from plugging the sintered glass.) A gum-rubber membrane sealed the assembly to allow application of a vacuum and simultaneously submerging in a glycerine bath at 190°C. The vacuum assembly was held in the glycerine for 2.5 minutes, during which time the PS melted and conformed to the replica surface. The assembly was then cooled for 30 seconds in a water bath to

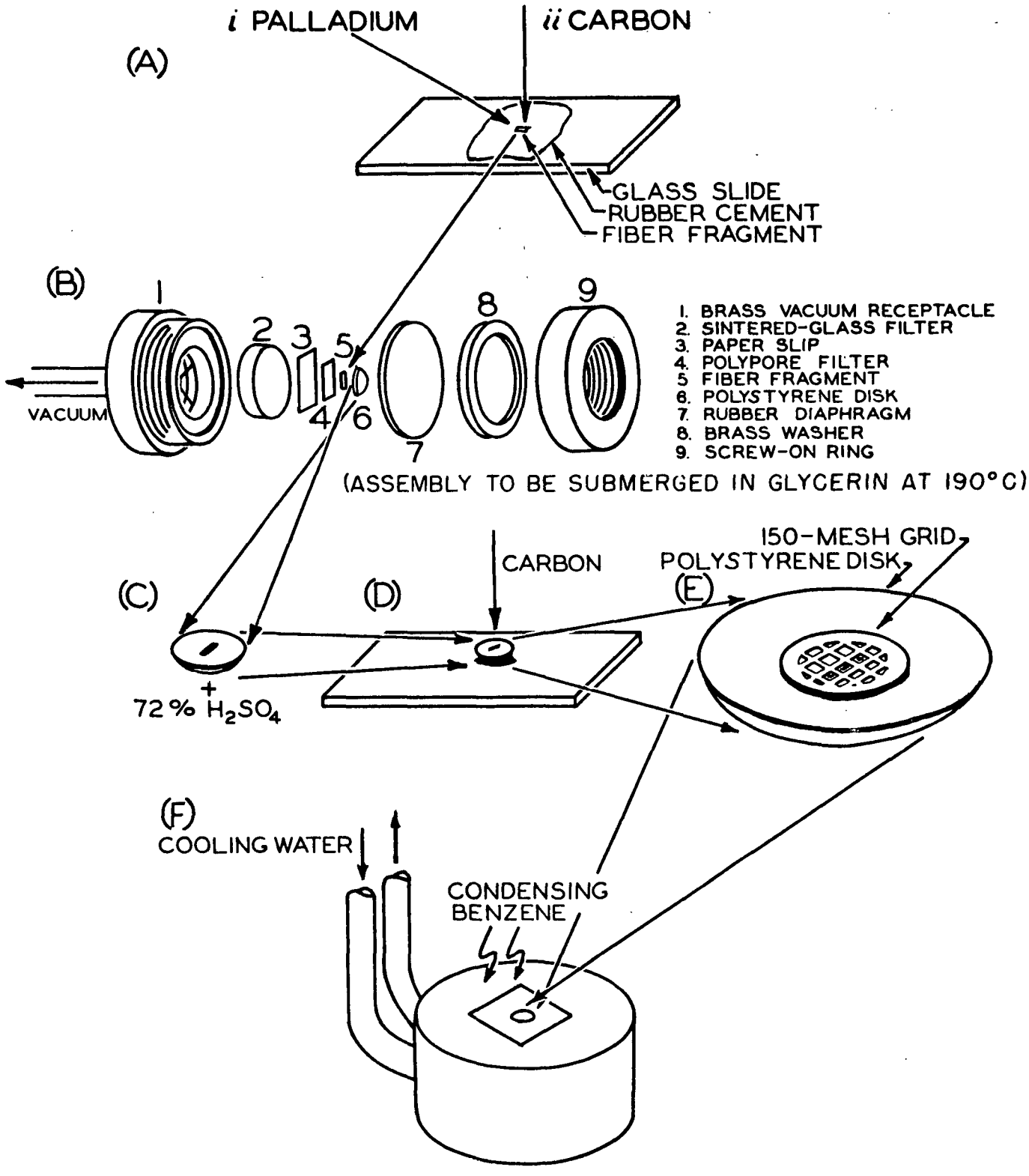

Figure 12. Schematic Outline of the Replication Procedure. (A) Shadowing with Palladium and Coating with Carbon; (B) Vacuum Embedding of the Replica in Polystyrene; (C) Removal of the Cell Wall from the Replica; (D) Application of Second Carbon Coating; (E) Placement of Supporting Grid over Replica; (F) Washing Away the Polystyrene to Deposit the Replica Film on the Grid

harden the PS. The PS disk was removed from the vacuum apparatus and washed in glacial acetic acid and then water to allow softening and removal of the filter material from the surface of the disk. Then the disk was washed in 72% sulfuric acid for one hour to remove the cell wall material. Thus, the replica film alone was left embedded in the PS.

Since the replica film was no wider than the original FWS and was normally cracked and fractured when the FWS was pulled away from the rubber cement, its pieces were certain to fall through the holes of even the finest mesh screen upon release from the PS. Therefore, the PS disk and embedded replica were coated with a second carbon film. This carbon film reinforced the replica fractures and afforded areas broad enough to be supported on the fine-mesh screens (grids) normally used to support replicas and thin sections in the microscope.

The final step of the procedure was to wash away the PS, allowing the replica and supporting film to drape over a supporting grid. The apparatus used for this operation was a water-cooled metal box similar to one used by Hunger (76, 77). The replica to be washed was covered with a 150-mesh grid which had been tipped with rubber cement to keep it in place on the PS disk. (The manipulation of placing the grid over the fiber replica was done under the stereo microscope in order to insure that as little as possible of the fiber replica was covered by the bars of the grid.) Also, a line was scored around the grid so that the desired area of the carbon film would be deposited on the grid without having the mass of the film adhering to the grid upon washing. Then, the PS disk was placed on a slip of Whatman No. 1 filter paper, which was subsequently laid on the surface of the cooling box (Fig. 12f). The box was lowered into the vapor space of a beaker of boiling benzene. Benzene vapor condensed on the cool surface of the box and washed away the PS. Thus, the STR was left to drape over the grid. Finally, tweezers were used to lift the grid from the wet paper surface, and upon being

exposed to the air, the remaining benzene on the grid evaporated. The supported, dry replica was then ready for study in the microscope.

NEGATIVE REPLICAS

In a few special cases, negative replicas were used to supplement the information gained from the STR. The surface to be replicated was pressed into melted PS without prior shadowing. Depending on the effect desired, the specimen was then removed from the PS surface either with 72% sulfuric acid or by being mechanically stripped away. The PS impression thus prepared was shadowed with palladium and coated with carbon. The PS was then washed from the replica film in the same way as for the STR's.

Because the metal shadowing was not applied to the fiber surface directly but to an intermediate impression, the negative replicas were thought to be more apt to form artifacts. Also, the micrographs of these replicas were more difficult to interpret, since the surface shadowed had a topography negative to that of the original surface. However, the negative replicas were quite beneficial in special applications, one of which was the analysis of the PS behavior during the preparation of STR's.

PREPARATION OF ULTRATHIN SECTIONS

As a means of supplementing some of the observations made from surface replicas, a few holocellulose slivers were embedded and sectioned. The slivers (0.5 x 0.5 mm.) were first stained one to three hours with 2% osmium tetroxide. Then they were dehydrated by exchange into ethyl alcohol. The specimens were exchanged into propylene oxide and then into D. E. R. 332-732 (a diepoxide resin manufactured by Polysciences, Inc., and prepared according to Formula "B" of the manufacturer's data sheet number 113). After curing, the embedded specimens were sectioned to thicknesses of about

1/20 μm. in a Porter-Blum microtome with either glass or diamond knives. Finally, the sections were caught on collodion-covered grids and stained with 1.2% potassium permanganate to further enhance the contrast.

ELECTRON MICROSCOPY

The replicas and thin sections were examined and photographed in an RCA EMU-3F electron microscope equipped with high-voltage fine focusing. The images were recorded on Kodak projector slide plates (medium, 3-1/4 in. x 4 in.) and developed with VDH film developer manufactured by Brandywine Photo Chemical. To facilitate the recording of stereo views without having to change specimen holders, the stereo specimen holder supplied with the microscope was generally used for all of the pictures. The stereo views were usually taken on 35-mm. Adox KB 14 film and mounted in Realist stereo masks (21-20, distant) for observation in Realist stereo viewers.

EXPERIMENTAL RESULTS AND DISCUSSION

INTERCELLULAR STRUCTURE AND ADHESION IN THE HOLOCELLULOSE CHIPS

Somewhat incidental to the main objective of examining the structure of individual fibers, some effort was given to study of the intercellular structure and adhesion in the delignified chips. This interest grew out of an observation of the definite cohesiveness or "strength" of the delignified chips and, also, the way in which the nonextracted fibers appeared to have been damaged during separation from the chips.

As a first step in this examination, some of the holocellulose chips were pulled apart manually and studied with the dissecting microscope. In agreement with previous observations (78), the chips easily delaminated along their radial planes, resulting in sheets or shives of fibers with the tangential faces of the fibers bonded together. However, these tangential faces were considerably more difficult to pull apart. In other words, the fibers appeared to be held together much more tightly along their tangential faces than along their radial faces. Several experiments were subsequently carried out in an effort to examine more thoroughly the nature of this interfiber adhesion.

THE SURFACES OF THE RADIAL SHIVES

In order to get a better view of the shive surfaces, replicas of the radial surfaces were prepared and studied. Figure 13 is a micrograph of one such replica. The picture shows parts of three longitudinal tracheids. The immediate question about the micrograph is the location of the gaps between the adjacent fibers. Careful study of the picture shows that the gaps are not directly visible but are actually covered over by smooth coverings or bridges. (The irregular vertical

Figure 13. A Surface View of a Radial Shive Showing Parts of Three Different Tracheids

FA: fiber axis
G: covered gaps between the tracheids
W: surface wrinkles in the radial face of the central tracheid

Plate Number[a]: 3696 AF

Magnification[b]: 6600X (The scale marking is ten microns, or micrometers--μm.)

Specimen Preparation[c]: Shive manually separated from delignified chip while still wet, air dried, STR[d].

---

a
The IPC file number for the electron micrograph.

b
The magnification of the actual print shown (adjusted for reduction or enlargement by the printer).

c
The notes on specimen preparation are included only because of possible incidental interest on the part of the reader. Any information deemed essential for the point being derived will also be placed in the figure caption.

d
STR (Shadow Transfer Replica) explained in the discussion of methods used.

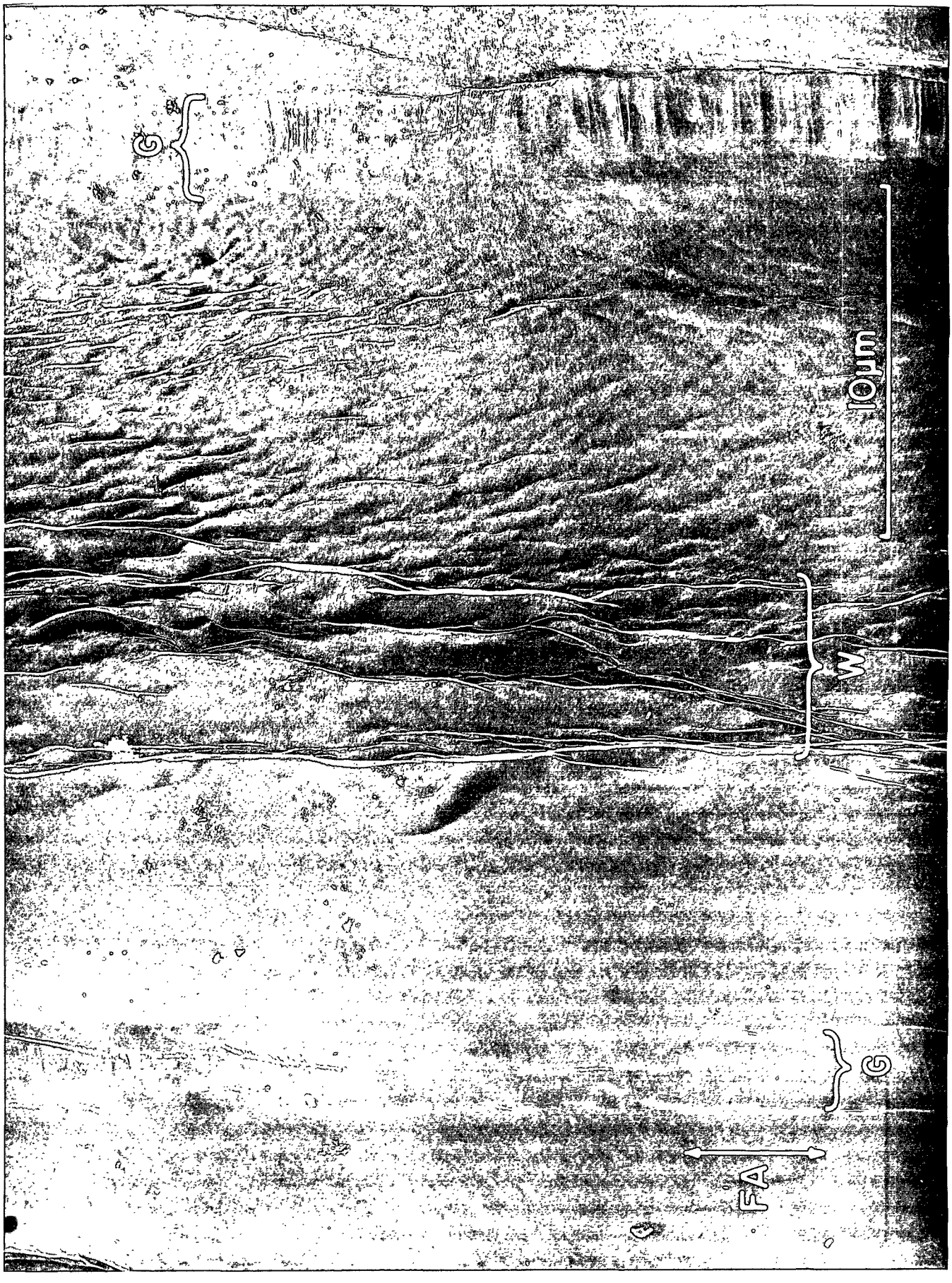
10μm
W
G
FA

lines which may be mistaken for a gap are wrinkles or folds in the radial fiber face.) Figure 14 is a higher magnification of a similar gap covering. Close examination of this picture indicates the gap covering to contain microfibrils. These microfibrils appear to continue into the coverings over the tracheids themselves. Furthermore, no discontinuity can be found in the covering layer over the fiber faces. In other words, the picture suggests the presence of a microfibrillar lamella or membrane, deposited on the surfaces of the adjacent fibers and bridging the gap between them. Incidentally, Thompson, Heller, and Smith (79) had already observed single microfibrils bridging across pairs of pulp fibers which had never been completely separated. Possibly, those single fibrils could have been remnants of membranes such as those observed in this case.

In the particular case of Fig. 14, the microfibrils in the membrane appear somewhat randomly oriented. However, wide variations in membrane appearance have been found. Figure 15 pictures an interfiber gap over which the microfibrils appear to be aligned in a nearly parallel fashion. These microfibrils could have been either deposited directly in this nearly parallel manner, or else they were deposited as a randomly oriented sheet which was then stretched in the transverse direction (the more likely case). Even more drastically stretched microfibrils (if stretching should be the case) are shown in Fig. 16. These fibrils appear to be consolidated in raised bands or belts across the gap. Furthermore, even though the bridging membrane appears to have split transversely and divided into these several contracting bands, the true gap between the fibers is still not definitely visible. [A fine, white (electron-scattering) vertical line can be seen, but this line is most probably a slight wrinkle in the replica.] In any case, a smooth continuity over the gap can be seen between the two uppermost bands, as if still another bridging membrane lies underneath the raised bands.

Still another variation in the gap covering can be seen in Fig. 17 which shows a nearly level, nonstretched bridge. This gap is also different in that the microfibrils appear to be plastered over and are only slightly visible.

In addition to variations in the appearance of the membrane, the different locations of the membrane within the wood structure should also be mentioned. The micrographs presented thus far have shown the membrane to be present over the tracheid faces and above or below ray-cell crossings. Figure 18 shows the edge of one such ray crossing. The ray cells have been removed, leaving the pits in the tracheids exposed. As in this representative picture the intertracheid gaps were definitely bridged over in the ray-crossing areas. In fact, even additional bridging layers may have been present in these areas. The horizontal curled films separating horizontal rows of pits were common and could have been the edges of added layers produced by the ray cells themselves. The lower portion of Fig. 18 shows the area of the radial face below the ray crossing and reinforces the idea that the bridging membranes are not limited to ray-crossing areas. The raised but torn membrane in the center of the picture may be similar to the raised bridges of Fig. 16, or may also accompany the ray crossing.

Bridging membranes were also found associated with the ray cells themselves. In a few cases the cleaved faces of the shives retained the ray cells in undisturbed form. Thus, Fig. 19 shows two ray tracheids along the edge of a ray crossing. Of significance in the present discussion is the observation that both the gap between the two ray cells and the gap between the upper ray tracheid and the longitudinal tracheids appear to be bridged over by a deposited membrane. This observation was the usual case for the ray cells.

One final area of the radial shive face is the area of overlapping tips of longitudinal tracheids. Figure 20 is possibly a micrograph of such a tip. The

Figure 14. A Surface View of a Radial Shive Showing a Fibrillar Membrane Bridging Across the Gap Between Two Adjacent Cells. [By Careful Observation, One Can Trace Single Fibrils (Arrows) Which Are Continuous from the Tracheid Faces and into the Covering Membrane]

G: the gap between the fibers
FA: fiber axis. (This abbreviation will be used throughout the thesis, and the explanation will not be repeated except in cases for which some note is added.)

Plate Number: 3695 AF

Magnification: 17,600X

Specimen Preparation: Same specimen as in Fig. 13.

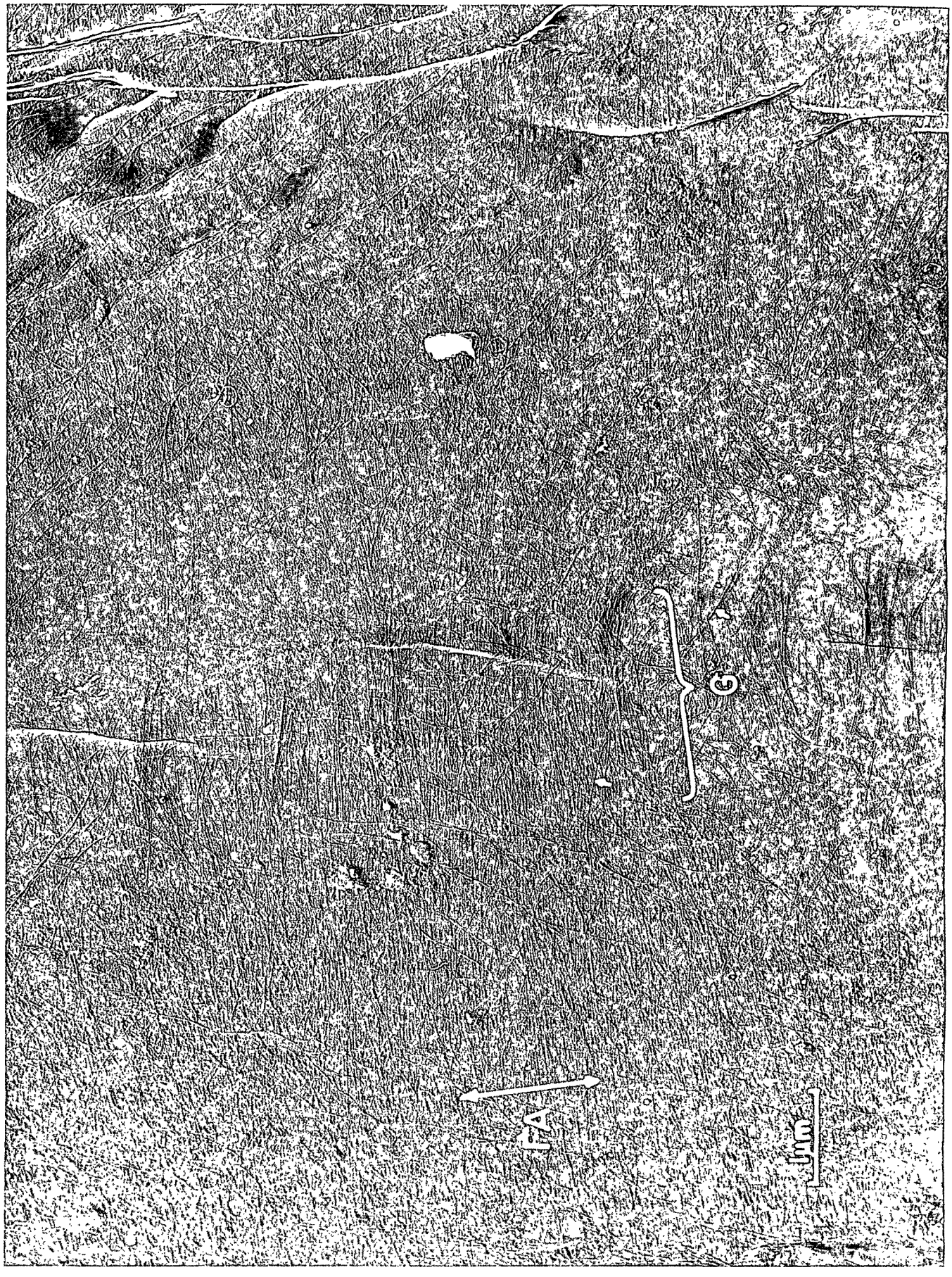
1mm
A
G

Figure 15. A Surface View of a Radial Shive, Showing Well-Aligned Fibrils Lying Across The Gap Between Two Adjacent Fibers

G: the gap between the fibers

Plate Number: 3703 AF

Magnification: 17,600X

Specimen Preparation: Shive manually separated from delignified chip while still wet, air dried, STR.

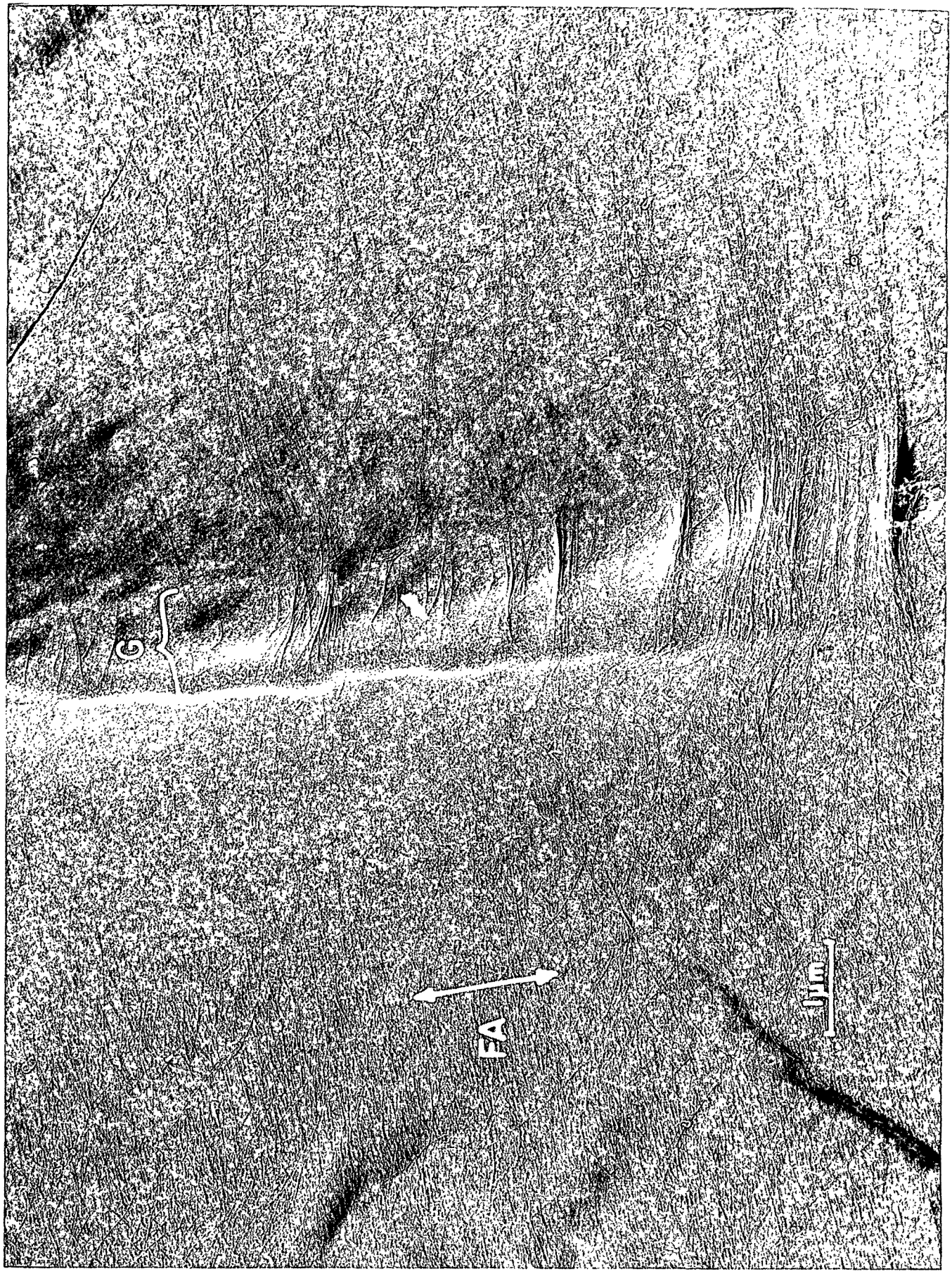
FA
1 µm

Figure 16. A Surface View of a Radial Shive, Showing Raised Bands of Well-Aligned Fibrils Lying Across the Gap Between Two Adjacent Tracheids

B: raised bands of fibrils across the intertracheid gap
CM: a continuous membrane underlying the bands
W: a wrinkle in the replica
RF: a displaced replica fragment

Plate Number: 3458 AF

Magnification: 12,700X

Specimen Preparation: Shive manually separated from delignified chip while still wet, freeze dried (FD), STR

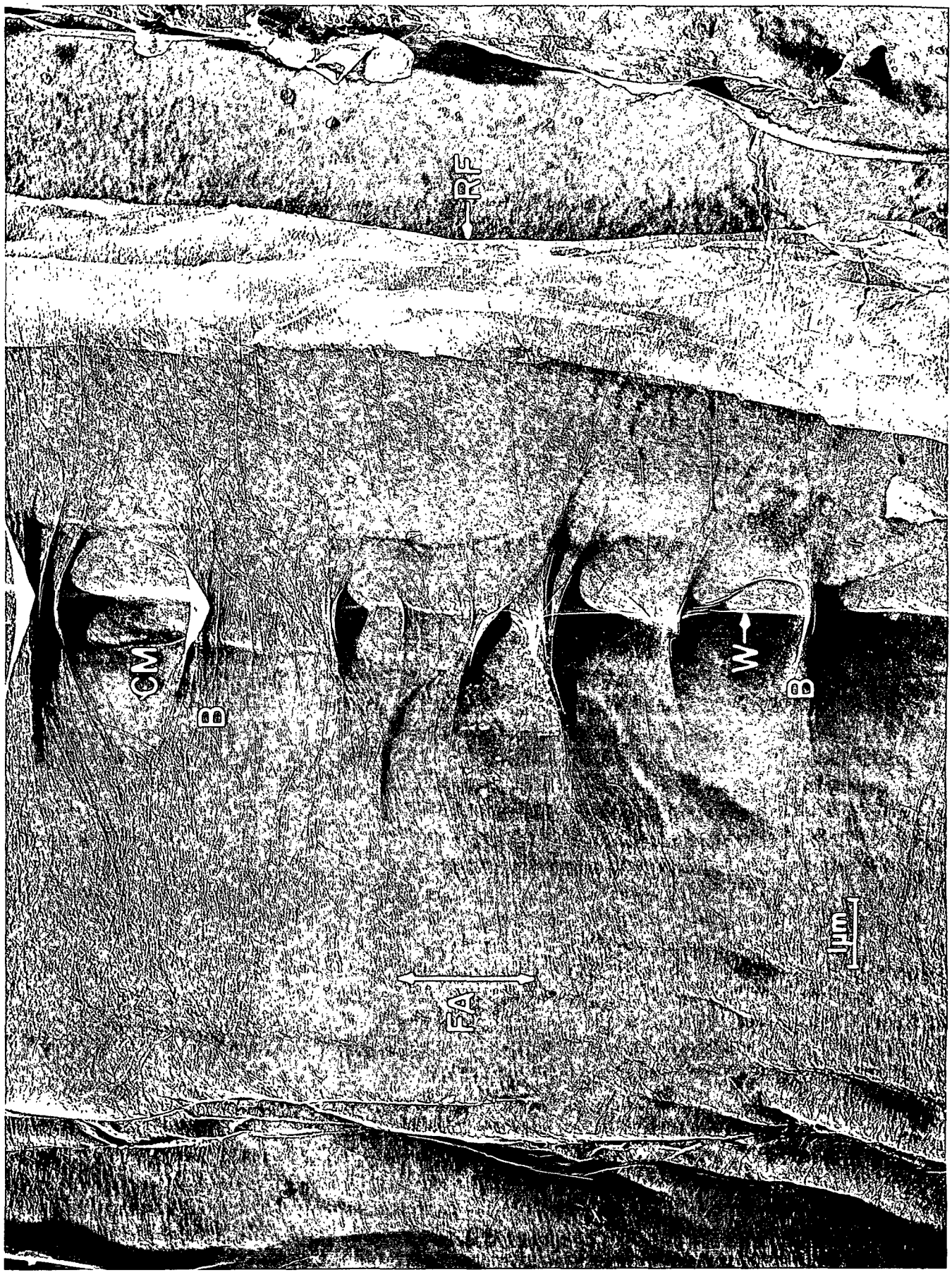
CM
BB
FAPE
FAPE
W
BB
1μm

Figure 17. A Bridged Gap Between Two Adjacent Tracheids. The Gap Covering Appears to be Nearly Level and Quite Smoothly Plastered Over

G: the intertracheid gap

Plate Number: 3461 AF

Magnification: 12,700X

Specimen Preparation: Same specimen as in Fig. 16

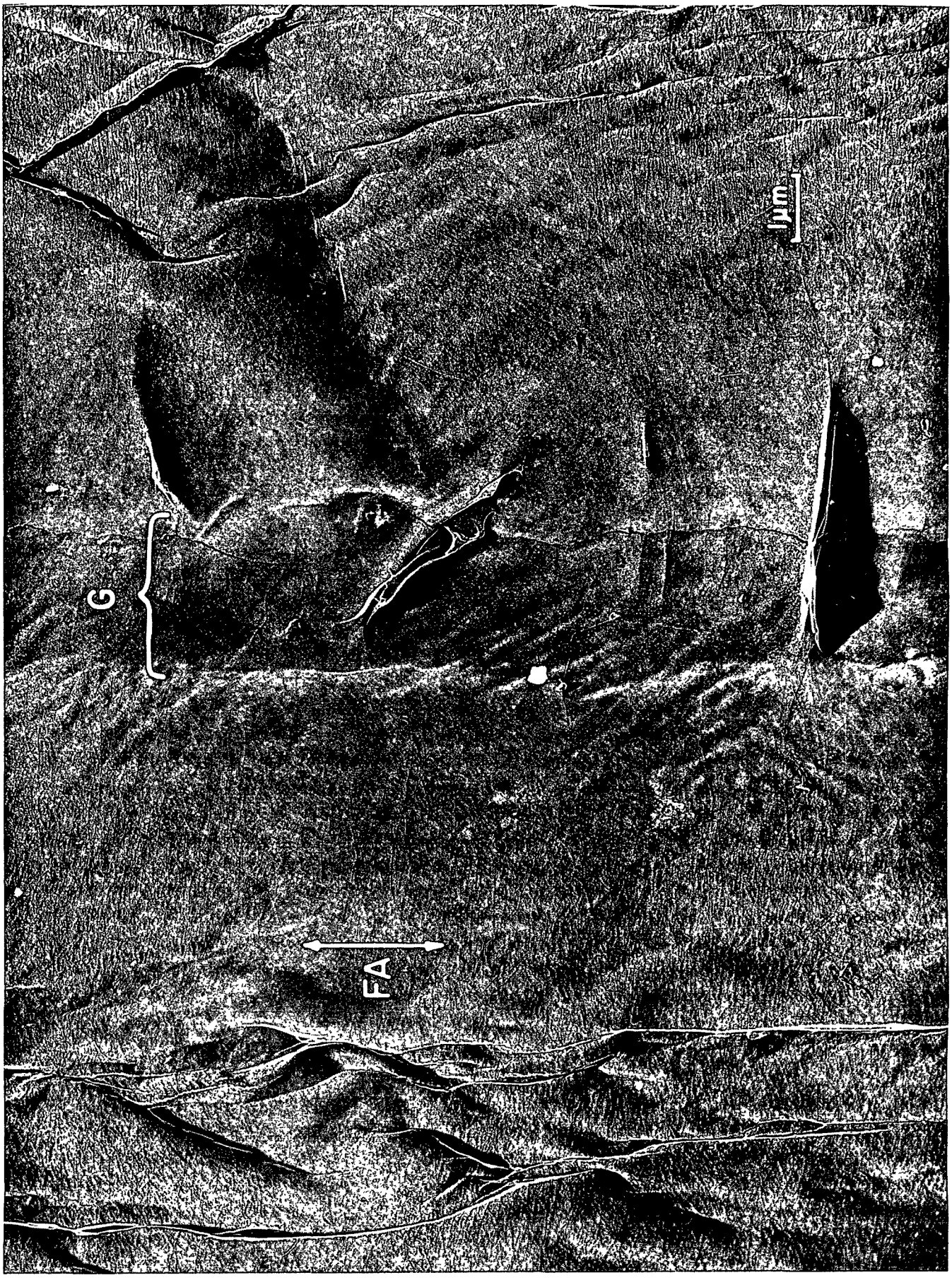
FA
G
1m

Figure 18. A Surface View of a Radial Shive, Showing an Intertracheid Gap Passing Through the Edge of a Ray Crossing

CL: unknown curled layers lying in the ray crossing
M: a raised, torn, intertracheid membrane lying outside the ray crossing
P: pits in the tracheid walls

Plate Numbers: 3435-3437 AF

Magnification: 3100X

Specimen Preparation: Delignified chip freeze dried, shive manually separated from the dry chip, STR


P
P
CL
P
P
P
CL
FA
P
M
10μm

Figure 19. Two Ray Cells Retained in Place on the Face of a Radial Shive

B: the border between the upper ray cell and the vertical, longitudinal tracheids. (This junction was apparently bridged over by a membrane)
GR: the gap between the two ray cells (also bridged over)
P: pits in the ray cell
FA: fiber axis (of the longitudinal tracheids)

Plate Number: 4678 AF

Magnification: 6200X

Specimen Preparation: Same specimen as in Fig. 13


10µm
FA
B
GL
GL
GL
GL
GL
GR

Figure 20. A Surface View of a Radial Shive, Including a Possible Fiber Tip

T-T-T: suspected blunt tip of an overlapping tracheid
G: gap between the two underlying tracheids

Plate Number: 3455 AF

Magnification: 8200X

Specimen Preparation: Same specimen as in Fig. 16

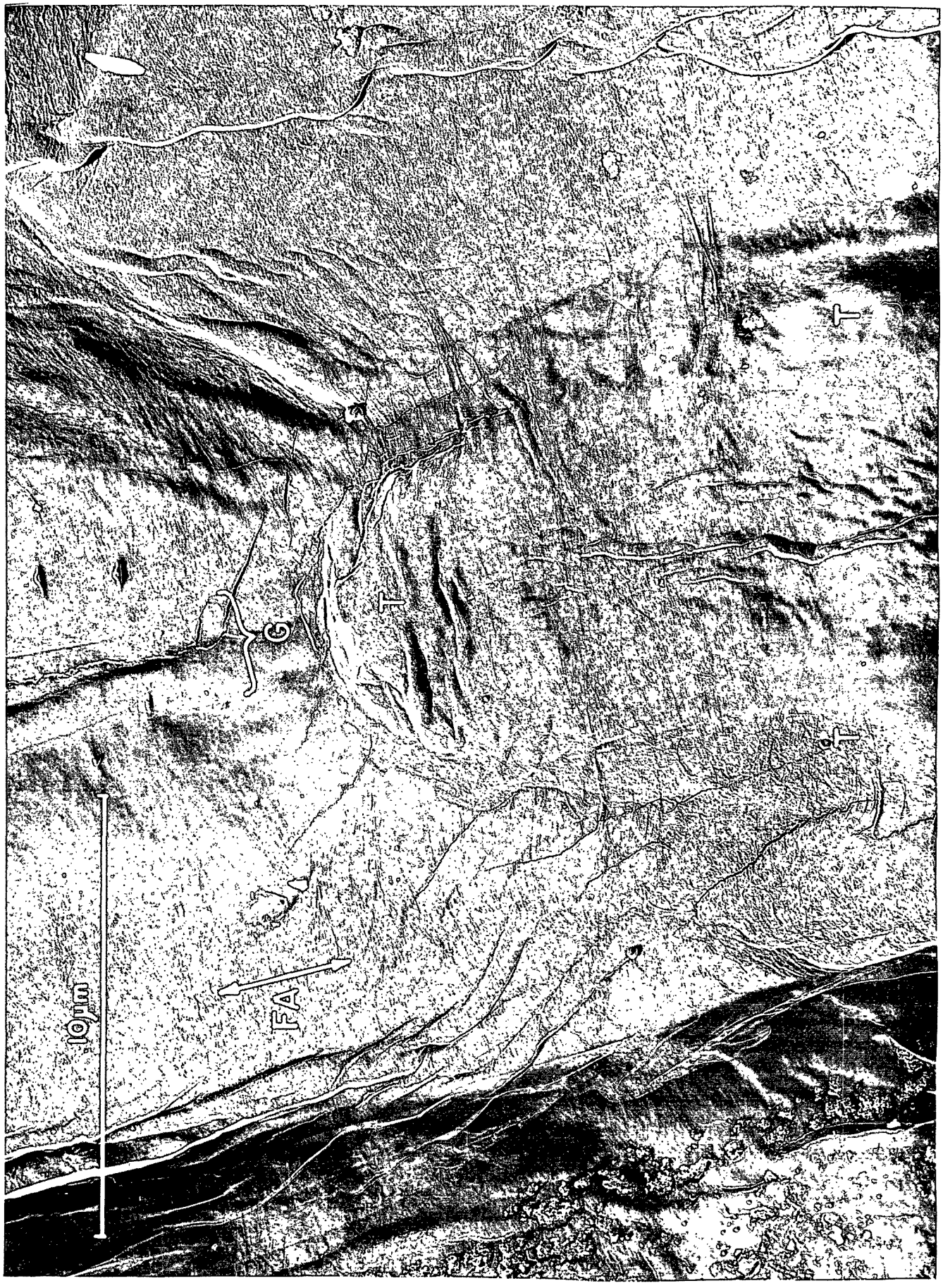
10m
FA
T
T
T

depression which outlines the suspected blunt cell tip is also covered over by membranelike material. However, this matter of coverings over the tracheid tips remains somewhat in question, since the suspected tip in this picture was not verified as such. Also, even if the cited example was in fact a tracheid tip, one would not be safe in claiming a general case on the basis of one example.

The discussion thus far has emphasized the variations in the membrane. The more general appearance of the membrane is shown in Fig. 21. Two parallel grooves appear to run along the corners of the adjacent tracheids. In fact, stereo views of this area (Fig. 22A) verify this picture of parallel "Vee" grooves with an arched surface between them.

CROSS SECTIONS OF HOLOCELLULOSE CHIPS

In order to examine further intercellular connections in the holocellulose chips, several chips were embedded and sectioned for the electron microscope. Figures 23 through 26 are representative micrographs of the sections. Figure 23 includes a cross-sectioned, exposed radial face and shows that the gap coverings are indeed membranelike in nature. Furthermore, the stereo image of parallel "Vee" grooves with an arched membrane between is also verified. Finally, one of the arches appears to have a double thickness of membrane material, in agreement with the speculation of possible double membranes in Fig. 16 and 18.

Figure 24 gives a better overall view of a delignified but not defibered chip. (The parallel slits should be ignored as they are scratches from the diamond knife.) By careful examination, one can find the bridging membranes of one radial row of fibers lying quite close to the cell walls of the adjacent row. Also, the picture points up the significance of a seemingly minor feature of the cell-wall drawing by Kerr and Bailey (2, 3) (Fig. 1, this thesis). The adjacent tangential faces appear quite tightly bonded together, just as they have shown.

A closeup of a ray-crossing zone is shown in Fig. 25. Some separation of the ray cell and longitudinal cell has taken place without destruction of the bridging membrane, indicating again that the two can well be independent. Finally, Fig. 26 gives a closeup of a thicker bridging membrane.

THE ORIGIN OF THE BRIDGING MEMBRANE

Generally, one assumes that the microfibrils of the wood-cell walls were generated in some manner by the living cells. Then, with regard to the bridging membrane, what cell could have deposited the layer common to at least two tangentially adjacent cells? The logical explanation is that the membrane could have been formed by the parent cell of the two adjacent cells. This explanation is quite plausible when one remembers that the two adjacent daughter cells could have been formed side by side in the mother cell, being bound together by the primary wall of the mother cell. Thus, the bridging membrane is probably the cast-off cell wall of the parent cell.

In fact, careful examination of the literature reveals that several workers (1, 80, 81) have actually observed intercellular membranes in light-microscope cross sections and have in general referred to the membranes as parent cell walls. However, the interesting observation is that none of these workers has included an intercellular membrane in his model of wood and cell-wall structure. Possibly, the membrane is not included in the models because of the accepted view that the parent-cell wall is drastically ruptured upon the enlargement of the daughter cells (1, 82-84) (Fig. 27). The idea of a ruptured membrane apparently grew out of the failure to observe the membrane at every intercellular gap. However, considering the probable fragility of the membrane in the alkaline extraction used to prepare the specimens, the evidence for profuse rupturing of the membrane is not conclusive.

Figure 21. A Surface View of a Radial Shive Showing an Example of the Gap-Covering Appearance More Generally Observed

G: the covered gap

Plate Numbers: 3503-3505 AF

Magnification: 6200X

Specimen Preparation: Shive manually separated from delignified chip while still wet, FD, STR

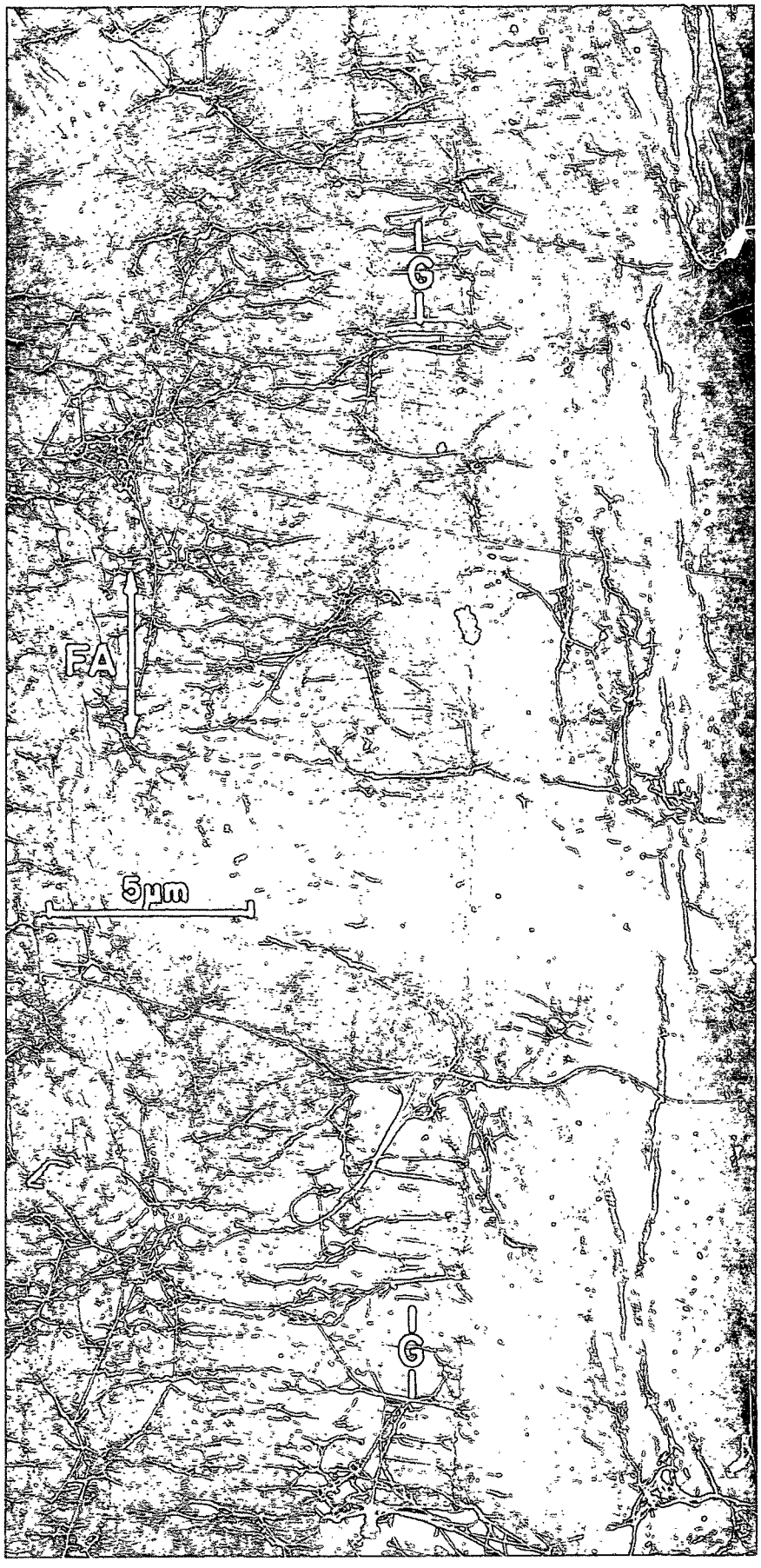
G
FA
5μm
G

Figure 22A. A Typical View of a Bridging Membrane

Plate Number: 5132 AF

Magnification: 3200X

Specimen: Same as in Fig. 21

Figure 22B. One Bridging Membrane Suspended Above a Lower One

Plate Number: 5133 AF

Magnification: 2400X

Specimen: Radial shive extracted ten seconds with 0.1N KOH at 28°C., washed, FD, STR

Figure 22C. A Bridging Membrane Which Has Survived an Overnight Extraction with 0.1N KOH

Plate Number: 5134 AF

Magnification: 3200X

Specimen: Same as in Fig. 34

Note: Some suggested methods of viewing the stereo pictures are given in Appendix V.

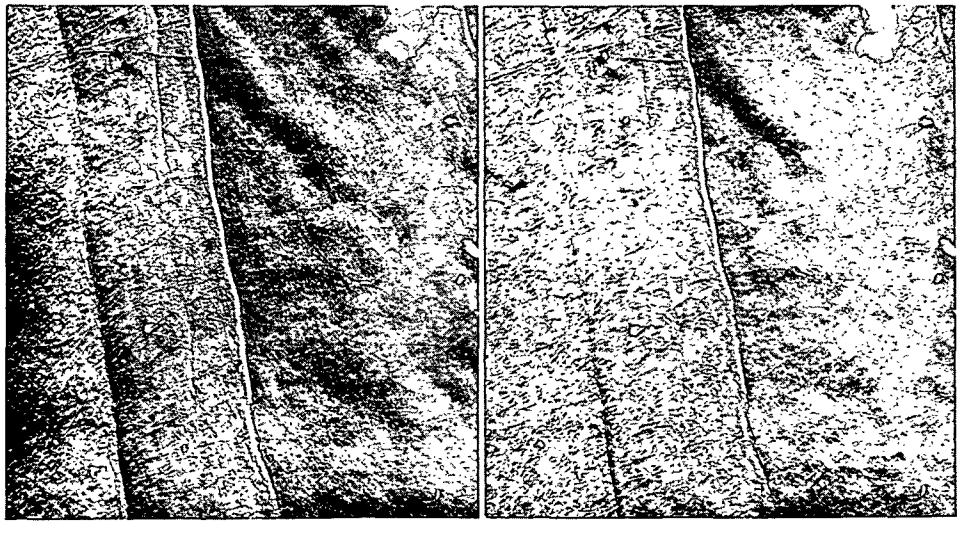

Figure 23. An Ultrathin Cross Section of a Shive

RD: radial direction
RF: the exposed radial face of the shive
M: membrane gap coverings (with double thickness pointed out by small arrows)
V: "Vee" grooves
RC: ray cell
LC: lumen cavity

Plate Number: 4466 AF

Magnification: 3900X

Specimen Preparation: Shive stained one hour with osmium tetroxide, embedded*, sectioned, stained one hour with potassium permanganate

*The details of the embedding and sectioning are discussed in the section concerned with materials and methods.


10μm
V
M
V
RD
S1
S2
S3
LC
RF
V
M
V

Figure 24. An Ultrathin Cross Section of a Delignified Wood Chip

RD: radial direction
BM: bridging membranes across the intertracheid gaps
RF: radial faces (loosely bonded)
TF: tangential faces (tightly bonded)
SC: scratches in the section caused by the diamond knife
LC: lumen cavities

Plate Number: 4462 F

Magnification: 3900X

Specimen Preparation: Stained one hour with osmium tetroxide, embedded, sectioned


RD
S1
S2
S3
LC
SC
SC
-TF-
BM
BM
LC
10 cm

Figure 25. An Ultrathin Cross Section of a Delignified Wood Chip Showing a Ray-Crossing Zone

RD: radial direction
RC: ray cell
LT: longitudinal tracheid
S: separation of the ray cell (RC) from the longitudinal tracheid (LT)
BM: the bridging membrane uncovered by the separation

Plate Number: 4474 F

Magnification: 7500X

Specimen Preparation: Stained one hour with osmium tetroxide, embedded, sectioned, stained one hour with potassium permanganate


LT
RD
PC
BM
S
S1
S2
LT
LT
PC
10 μm

Figure 26. An Ultrathin Cross Section of a Radial Shive, Showing Especially a Thicker Bridging Membrane

BM: bridging membrane across the intertracheid gap
RF: radial face
LC: lumen cavity

Plate Number: 4481 F

Magnification: 9800X

Specimen Preparation: Stained three hours with osmium tetroxide, embedded, sectioned, stained one hour with potassium permanganate


5µm
RF
BM
S1
S2
S3
LC

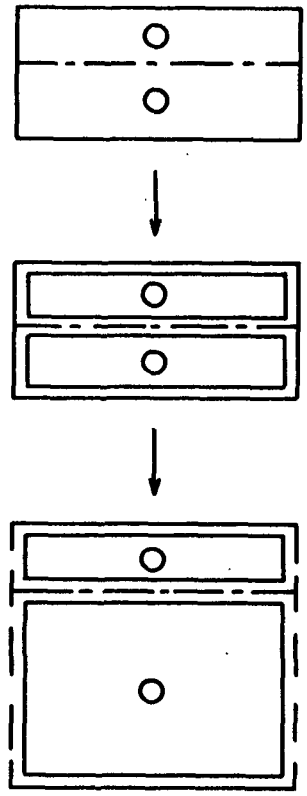

Figure 27. The Assumed Rupturing of the Parent-Cell Wall upon Enlargement of the Daughter Cells [Wardrop (82)]

More recently, Jayme and Fengel (34, 85) have made ultrathin cross sections of delignified sprucewood for the electron microscope and have observed inter-tracheid fibrils and lamellae. Also, Fengel (86) sectioned beechwood in a direction perpendicular to the axes of ray cells and observed parent-cell-wall lamellae between ray-parenchyma cells. These electron micrographs of cross sections did show the intercellular layering but still did not give any indication of the frequency of membrane rupture. In fact, no micrographs showing the membrane in surface view have been found in the literature.

One excellent picture showing the intercellular membrane to be parent-cell-wall material is a micrograph prepared by Kerr and Bailey (2) and reproduced in Fig. 28. This picture was made from a cross section of a cambial zone in the resting winter condition and shows the cells to be grouped within intact parent-cell walls. The grouping exists because the xylem daughter cells produced by division of the "cambial

Figure 28. A Cross Section of Dormant Immature Cells, Showing Intact Parent-Cell Walls Enclosing Groups of Cells. From Textbook of Wood Technology, Vol. I, 2d ed., by Panshin, H. J., de Zeeuw, Carl, and Brown, H. P. Copyright 1964 by McGraw-Hill, Inc. Used by Permission of McGraw-Hill Book Company

initial" subdivided and then resubdivided. Thus, two cells are paired together in one surrounding membrane, and then two pairs of cells are bound together as a group of four cells. The manner of cell division and subdivision which could have resulted in this grouping is summarized in Fig. 29.

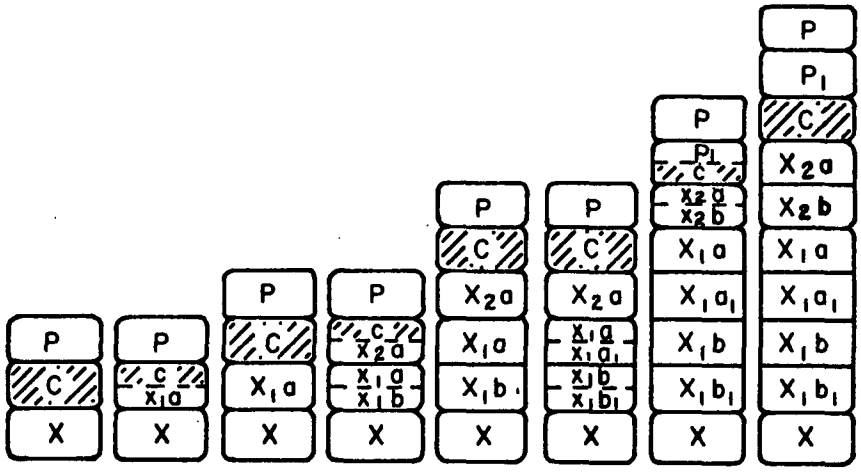

Figure 29. A Schematic Drawing of the Cell Subdivision Which Results in the Grouping of Cells as Seen in Fig. 28 (c: cambial initial; P: phloem; X: xylem). From Textbook of Wood Technology, Vol. I, 2d ed., by Panshin, H. J., de Zeeuw, Carl, and Brown, H. P. Copyright 1964 by McGraw-Hill, Inc. Used by Permission of McGraw-Hill Book Company

Figure 28 also shows some fragments of wall material which appear to be separate from, and would have preceded, even the group parent cell. However, the existence of such a fragment is quite possible in view of the fact that even the group parent cell was at some previous time produced by division of another cell and, therefore, would have been completely surrounded by another membrane. Furthermore, extension of this reasoning indicates that the many ancestral cell walls could not possibly have stretched enough to contain all of their descendent cells and, for this reason, certainly would have broken into fragments. One would, then, expect to find these fragments "floating" in the intercellular region.

QUESTIONS OF MEMBRANE STRUCTURE AND CHEMICAL CONSTITUENCY

The Continuity of the Bridging Membrane

After studying the cell grouping in Fig. 28 one wonders whether all of the spaces between fibers could be bridged over or whether, for example, only three out of four would be bridged. In an effort to answer this question, several replicas of radial shives were specially prepared and studied. Since the bars of the 150-mesh grids normally used obscured about one interfiber gap out of four, special grids with elongated windows (Ti grids) were used to mount the several replicas. The longer windows permitted examination of many more adjacent interfiber areas. Figure 30 is a representative micrograph from one of these grids and shows eleven adjacent gaps. Of these eleven gaps, several are without question bridged over by a continuous membrane. The continuity over the remaining gaps, though, may be questionable because of cracks and wrinkles in the replica film itself. In the case of these gaps with uncertainty of membrane continuity examination of the same gap but in different windows of the grid revealed that continuous bridges could in fact be found across each of the gaps. Figures 31-33 present representative micrographs from this examination and demonstrate the conclusion that the eleven consecutive gaps are all bridged over (though not necessarily by the same membrane).

One can see from these pictures that experimental problems such as cracking and wrinkling of the replica film seriously limit extended surveys such as this one. Otherwise, one would most likely be able to find many more than eleven consecutive gaps bridged over.

Finally, Fig. 33D is included, not only to demonstrate the continuity of a membrane over gap number two, but also to demonstrate the presence of double membranes--a high one over a low one. This possibility had already been supported by Fig. 16, 18, and 23. Still another example of a high bridge over a low one is shown as a stereo view in Fig. 22B. Furthermore, Fig. 29 indicates that multiple bridging membranes are to be expected.

Behavior of the Bridging Membrane in Caustic Extraction

People have generally observed that holocellulose chips are more easily defibered during extraction with dilute alkali [as did Spiegelberg (70)] than by mechanical action alone. The cohesiveness of the chips has generally been explained as resulting from the bonding together of the fibers by pectin materials (2, 87). On the other hand, other workers (78, 88, 89) have been able to extract delignified wood cross sections with pectin and hemicellulose solvents without maceration. (They considered the sections to be macerated when the segments of the different cells in the cross sections had completely separated from one another.) In fact, Wardrop (78) floated delignified sections on solutions of pepsin, dilute hydrochloric acid, ammonium oxalate, monoethanolamine, hot 2.5% sodium hydroxide, cold 17.5% sodium hydroxide, and a 10% mixture of chromic and nitric acid--all without maceration of the sections. He concluded that the bond must be as resistant as Cross and Bevan cellulose and that some form of mechanical linkage was more reasonable than some resistant intercellular material. Furthermore, Wardrop and Dadswell (82) later suggested that the fragments of the parent-cell wall may have been responsible for the cohesion of the delignified wood sections that they studied.

Figure 30. A Surface View of a Radial Shive Showing Eleven Consecutive Intertracheid Gaps (Denoted by Pairs of Numbers)

Plate Numbers: 3964-3969 AF

Magnification: 1500X

Specimen Preparation: A delignified chip was freeze dried, during which the chip of its own accord delaminated into radial shives. An STR of one of these shive faces was prepared

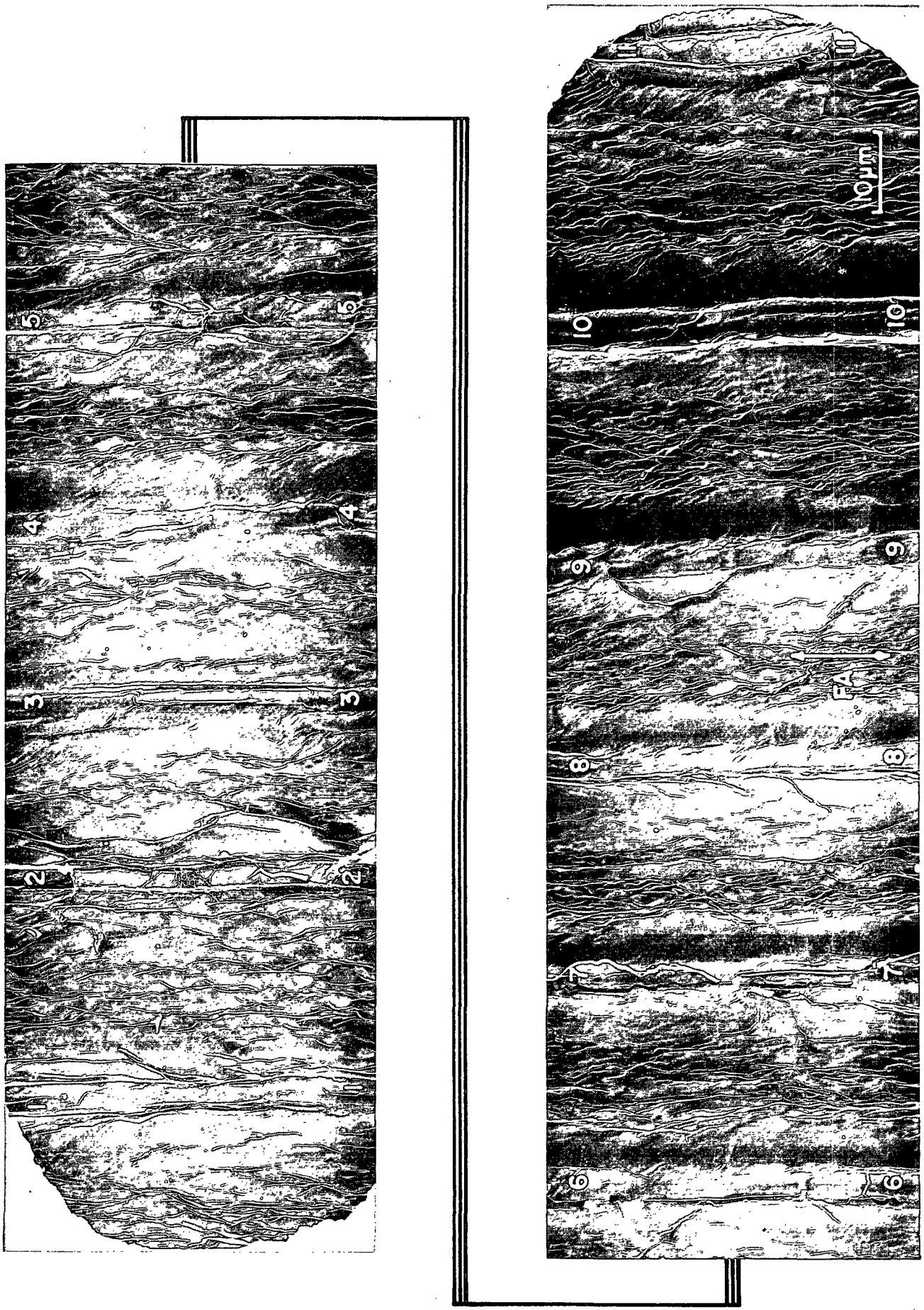
10 µm
1
2
3
4
5
6
7
8
9
10

Figure 31A. Gap Number One

17 Grid frames below the frame in Figure 30

Plate Number: 3970 AF

Magnification: 10,000X

Figure 31B. Gap Number Two

9 Frames below the frame in Figure 30

Plate Number: 3974 AF

Magnification: 6300X

Figure 31C. Gap Number Three

A higher magnification from Figure 30

Plate Number: 3979 AF

Magnification: 6300X

Figure 31D. Gap Number Four

A higher magnification from Figure 30

Plate Number: 3977 AF

Magnification: 6300X

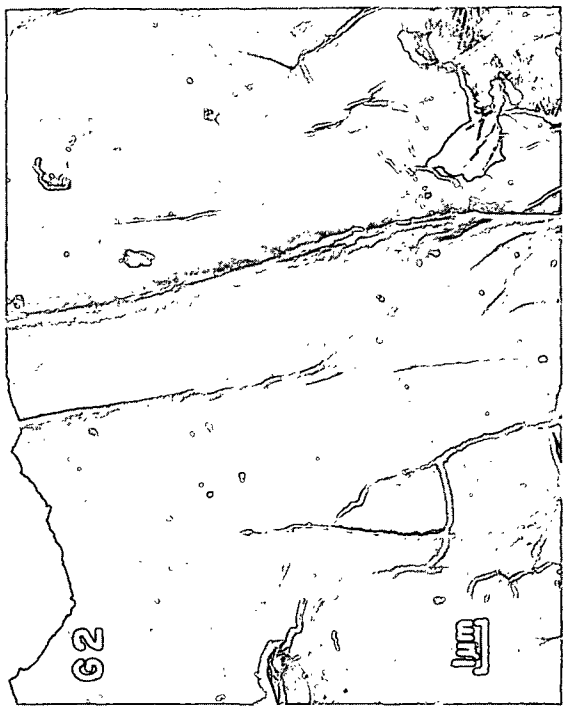
62
1cm

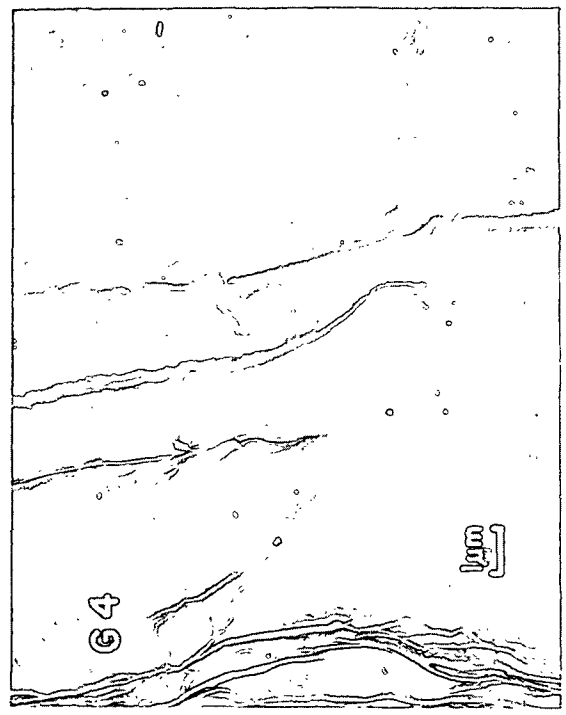
64
1cm

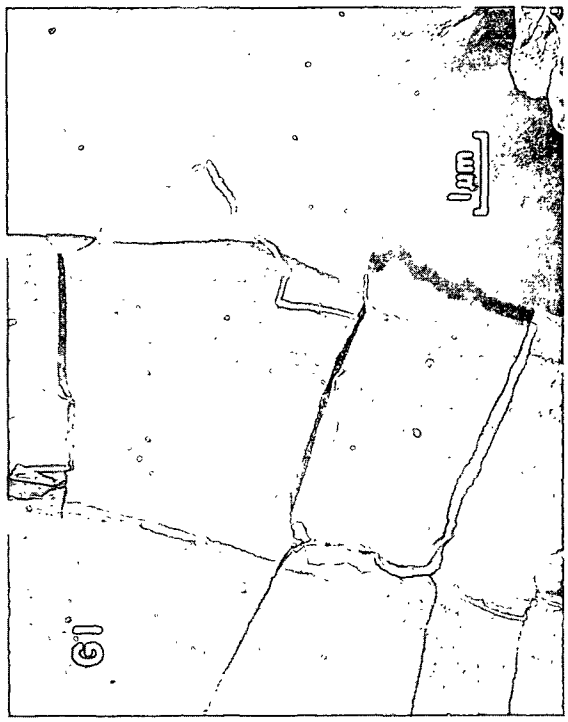
61
1cm

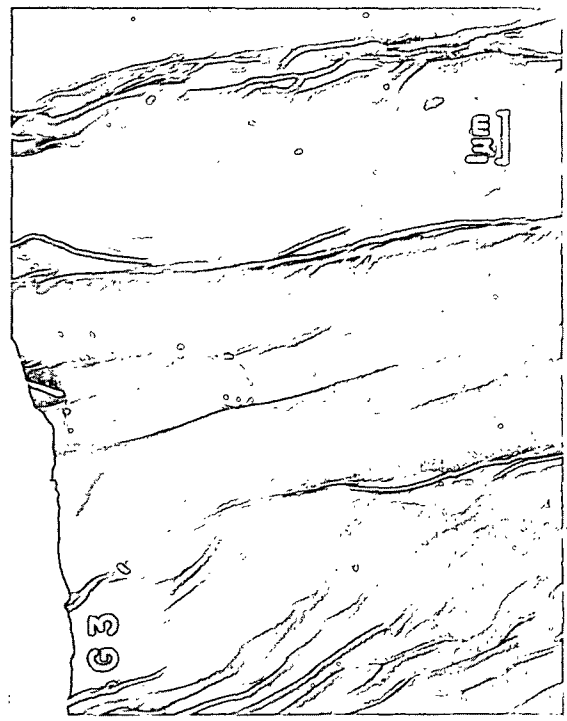
63
1cm

Figure 32A. Gap Number Five

A higher magnification from Fig. 30

Plate Number: 3981 AF

Magnification: 6300X

Figure 32B. Gap Number Six

A higher magnification from Fig. 30

Plate Number: 3983 AF

Magnification: 4600X

Figure 32C. Gap Number Seven

A higher magnification from Fig. 30

Plate Number: 3984 AF

Magnification: 8600X

Figure 32D. Gap Number Eight

Four grid frames below the frame in Fig. 30

Plate Number: 3986 AF

Magnification: 4600X

Figure 33A. Gap Number Nine

A higher magnification from Fig. 30

Plate Number: 3987 AF

Magnification: 4600X

Figure 33B. Gap Number Ten

A higher magnification from Fig. 30

Plate Number: 3988 AF

Magnification: 6300X

Figure 33C. Gap Number Eleven

Six grid frames below frame in Fig. 30

Plate Number: 3989 AF

Magnification: 6300X

Figure 33D. Gap Number Two

Six grid frames below frame in Fig. 30

Plate Number: 4680 AF

Magnification: 1600X

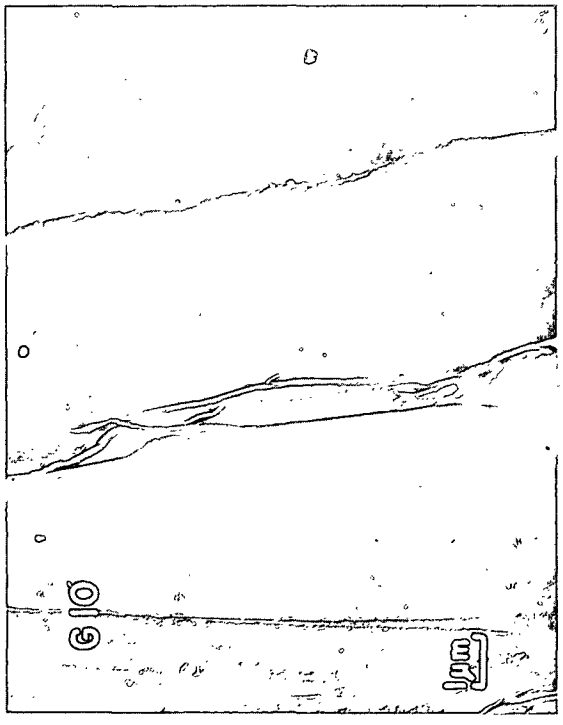
E3
610

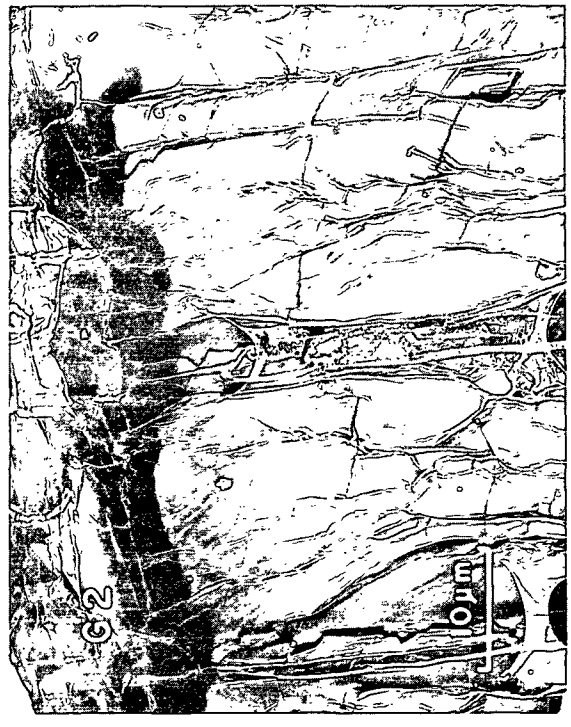
E3
620

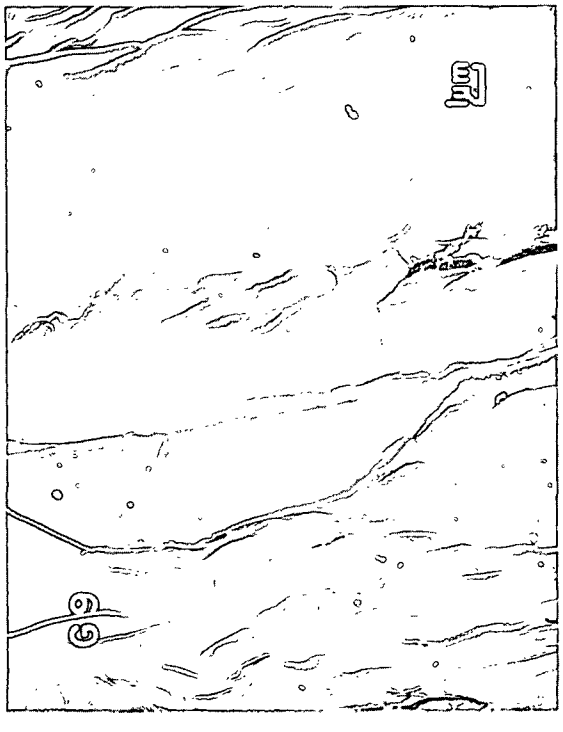
E3
630

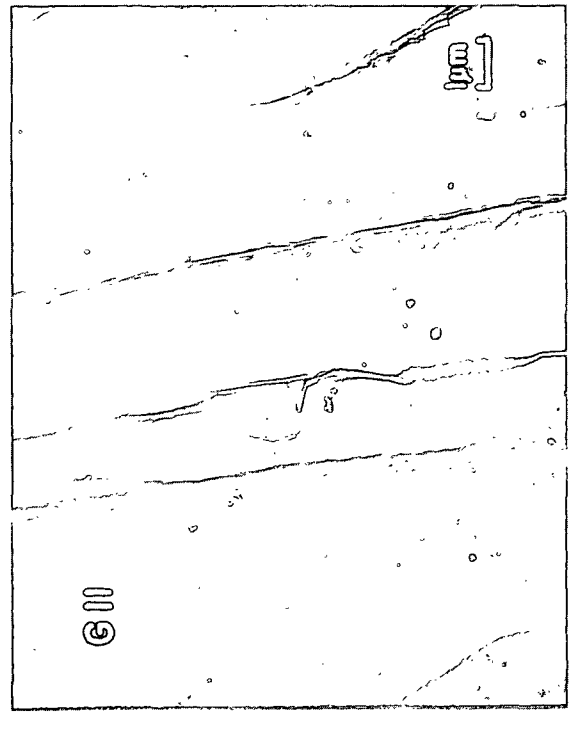
E3
640

In order to observe the effect of mild caustic on the holocellulose chips of the present work, some radial shives were separated and placed under the stereo microscope. A drop of 0.1N potassium hydroxide placed on the surfaces of the shives caused the fibers to loosen quite readily. In fact, only with extreme caution could the shives even be moved without coming apart. (Apparently, Wardrop's method of floating the sections on solutions must have been very gentle indeed!)

Certainly, one wonders what was happening to the bridging membranes to allow the chips to defiber so readily. One possible explanation was that the membrane was being dissolved. Roelofsen and Kreger (90) had obtained evidence that pectin can be present as fibrils [though their conclusion has been questioned (12)]. Could the membrane, then, be made up of alkali-soluble pectin? To test this possibility, some of the shives were extracted very carefully with 0.1N potassium hydroxide (KOH) and then washed with water before drying for replica preparation. Figures 34 and 22C show one such shive extracted overnight with alkali and then washed with water and air dried. As can be seen, the bridging microfibrils are clearly present, even on the extracted shive. Furthermore, they can be seen much more clearly with the previous plastering materials having been removed from the surface. In conclusion, the defibering of the holocellulose chips in alkali must be explained by some means other than a dissolving of the intercellular membrane.

THE SURFACES OF MANUALLY SEPARATED FIBERS

Some of the holocellulose chips were manually defibered under water in an effort to see whether nonextracted fibers could be separated without damage to their surface layers. The chips were first peeled into radial shives of fibers (joined on their tangential faces). Several micrographs of such exposed radial faces have already been presented in this section of the thesis. In general, the surfaces exposed appeared to be quite smooth and showed little sign of layer damage

during separation. The evidence is that the delaminations took place along the planes between adjacent intercellular membranes.

Once the radial sheets of fibers had been separated, the fibers in the sheets were forced apart, still under water. This separation along the tangential faces was more difficult and resulted in some disruption of the surface layers. Figure 35 shows the tangential face of one such fiber with torn, loose, layer material on its surface. Close examination of this loose material indicates that it is most probably a portion of primary wall pulled from the adjacent fiber. The disruption of this primary layer apparently took place upon separation of the adjacent tangential faces, and suggests that the adhesion between the primary layers of the two tangentially adjacent cells may have been equal to, or even greater than, the adhesion between the primary and S1 layers of the fiber pulled away.

Another type of layer damage observed on the fibers separated wet is shown in Fig. 36. This micrograph shows both a radial face (to the left) and a tangential face (to the right) with the included "corner" of the cell between. (A more complete discussion of the cell "corner" is given on page 119.). As was frequently observed, a loose, torn layer can be seen along the corner of the cell. The torn edges on some of the cells, in fact, were large enough to be seen in the light microscope used for dissection. However, though they were sometimes large and easy to find, the exact source of these exposed layers still hasn't been determined. One would judge that the layers are torn fragments of the intercellular membrane. On the other hand, the layers could be disrupted layer material from the tangential faces. Thus, the exact explanation remains uncertain.

Finally, some of the delignified chips were freeze dried and then pulled apart. In this case, even some areas of the adjacent radial faces were tightly bonded together and were damaged by the separation. Figure 37, showing the radial face

Figure 34. A View of a Bridging Membrane Which Has Been Extracted Overnight with 0.1N KOH but Has Remained Intact

G: the covered gap

Plate Number: 3780 AF

Magnification: 17,600X

Specimen Preparation: Delignified shive extracted overnight with 0.1N KOH at room temperature, washed with water, air dried, STR


EA
G
G
1μm

Figure 35. A Tangential Face of a Fiber Separated from its Adjacent Fiber While Still Under Water

L: loose layer material, possibly retained from the adjacent fiber

P: exposed primary layer of the fiber being studied

FA: fiber axis (The nominal direction of the fiber axis in most of the micrographs is either perpendicular to the caption lines--as in this micrograph--or parallel to them. However, because of the difficulty of specimen preparation and because of the image rotation in the microscope, the actual direction may be somewhat different from vertical or horizontal. Therefore, the indicated direction might be slightly adjusted in accord with any indicators in the given pictures. In this picture, the line has been drawn parallel to the surface wrinkles, as suggested by Fig. 13)

Plate Number: 3523 AF

Magnification: 17,600X

Specimen Preparation: Delignified fiber manually separated from shive under water. FD, slit open, STR of exterior surface of fiber (not lumen surface)


L
L
L
P
EA

Figure 36. The Exterior Surface of a Fiber Manually Separated from a Delignified Chip While Still Under Water

RF: one of the radial faces

TF: one of the tangential faces

C: the fiber "corner"* between the two faces

TL: an unexplained torn layer associated with the corner

Plate Number: 3509 AF

Magnification: 11,800X

Specimen Preparation: Delignified fiber manually separated from shive under water, FD, slit open, STR

*The "corners" are the thickened-wall areas originating at the corners of fibers with rectangular cross sections. This feature is discussed in more detail on page 119

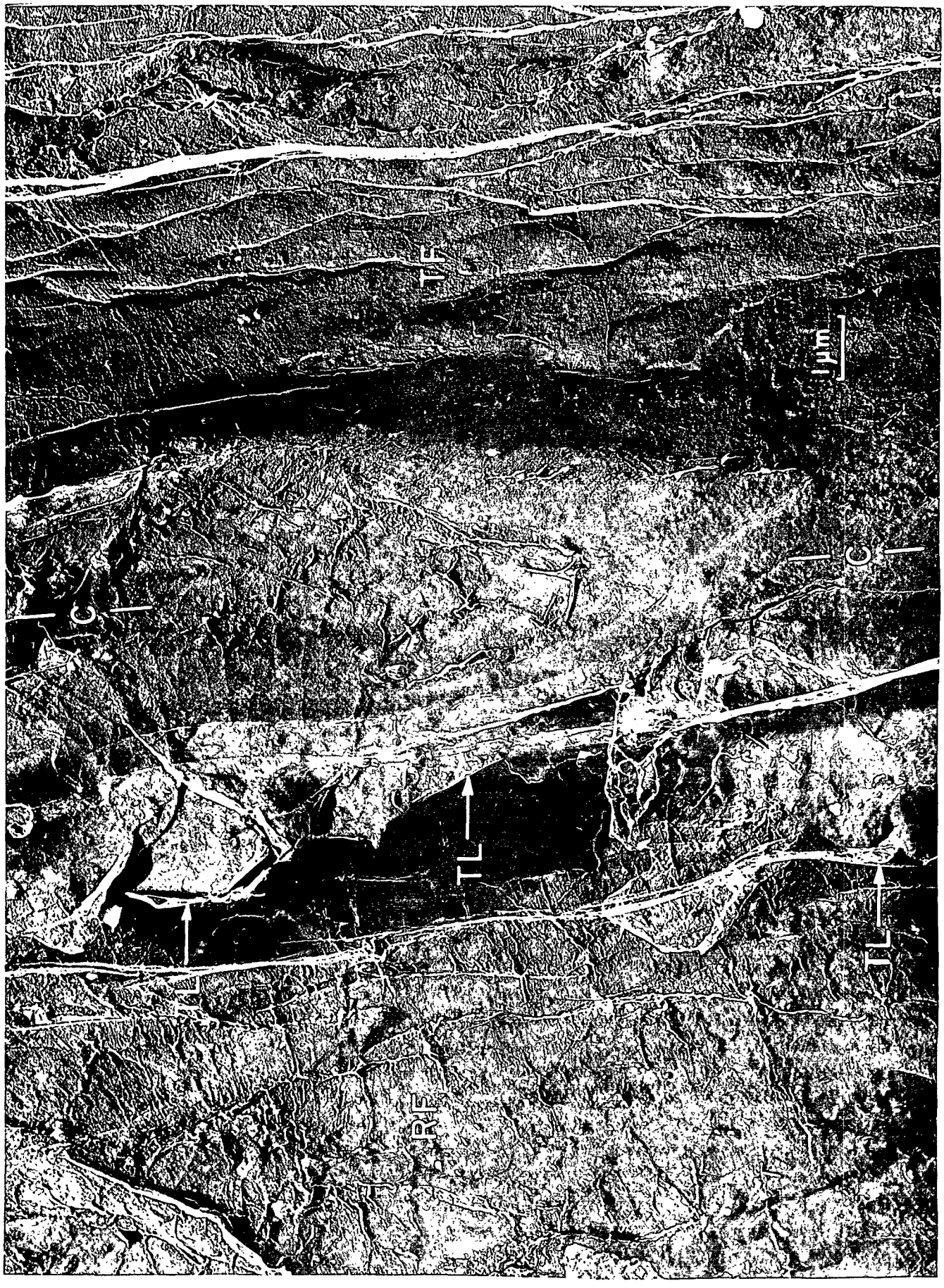
PE
1 µm
G
G
TJ
TJ
PE

Figure 37. The Face of a Radial Shive Pulled from a Freeze-Dried Chip, Showing Some of the Layer Damage that Took Place upon Separation of the Adjacent Faces

S1-R: S1 fibrils retained from adjacent fiber

P: primary layer, probably of the fiber being studied

S1-E: S1 fibrils of the present fiber exposed by removal of primary layer

FA: fiber axis (the axis direction was drawn parallel to the two grooves, which were probably associated with an intertracheid gap)

Plate Number: 3497 AF

Magnification: 11,800X

Specimen Preparation: Delignified chip FD, internal radial-shive surface exposed by pulling the chip apart, STR


SI-R
SI-R
SI-R
SI-R
FA
1m

of such a shive pulled from a freeze-dried chip, illustrates this kind of damage. In some areas of this surface, both the intercellular layers and the primary layers appear to have been torn away, exposing the S1 layer. At the same time, other parts of the area seem to have retained parts of the adjacent fibers which had been pulled away.

With regard to the tangential faces of those fibers pulled apart after freeze drying, these surfaces indicated even more damage than the tangential faces pulled apart wet, just as one would expect. Figure 38 pictures the tangential face of one such fiber which has retained much of the layering of the adjacent fiber. The regular alignment of the retained material suggests that it may even be part of the S1 (outer layer of the secondary wall) of the adjacent fiber.

In conclusion, the adjacent tangential faces appear to be well bonded in either the wet or dry condition. The radial faces, though, are easily separable while wet, but appear to become somewhat bonded during drying. This conclusion is not surprising in light of the closely associated tangential faces and separated radial faces seen in Fig. 24.

DISCUSSION OF THE CONCLUSIONS

The important general result of the experimentation just discussed was the observation of the intercellular membranes in surface view. Others had already observed the membranes in cross-section view, primarily by light microscopy, and had concluded that they were parent-cell walls. However, the surface views from the present work permitted more detailed examination of the membrane structure and resulted in tentative adjustment of previous concepts. For example, the micrographs of the surface replicas indicate that the parent-cell wall is not as profusely ruptured as had been suggested, but is actually quite continuous along a given interfiber gap. Furthermore, as many as eleven consecutive gaps have been

found bridged over, strongly suggesting that the bridged gap is the general case for latewood. This designation of latewood cells must be borne in mind as one makes extensions of these conclusions to earlywood, because the earlywood cells grow much more in diameter than the latewood cells and would be more likely to rupture or, at least, drastically stretch the parent-cell wall.

On the question of stretching versus rupturing of the parent-cell wall during expansion of the daughter cells, the micrographs of raised, segmented bridges over lower, continuous bridges suggested that a stretching of the membrane is quite possible. The microfibrils of the raised bridges appeared to have been drawn out to lie nearly parallel to one another. Furthermore, those bridges appeared to have been reduced in width, as if by Poisson contraction during stretching. Incidentally, the apparent greater stretching of the upper membrane relative to the lower one is quite plausible, because the upper membrane would have preceded the lower membrane in time and would have been subjected to more extension by the added generation of daughter cells. In contrast to the plausible evidence for a stretching of the intercellular membrane, little evidence for the alternative rupturing of a rigid membrane has been found. No definite vertical breaks in the membrane have been observed, though such breaks could have been obscured by the wrinkles in the radial faces and by the plasterlike material over the surface. Thus, no definite conclusions can be drawn from this work regarding the relative importance of membrane stretching versus rupturing. However, a simple stretching of the membrane would appear to the author to be the more plausible explanation.

One factor which should be reflected in the manner of membrane stretching or rupturing is the degree of bonding between the parent-cell walls and the developing cell walls just before secondary thickening. If, for example, the membrane were not bonded to the cells but were free to slide over them, one would expect a uniform tension along the entire membrane and a subsequent uniform elongation along its

Figure 38. A Tangential Face of a Fiber Manually Separated from a Delignified, Freeze-Dried Chip

S1-R: fibrils retained from the adjacent fiber which has been pulled away

P: the exposed primary wall of the present fiber

Plate Number: 3425 AF

Magnification: 11,800X

Specimen Preparation: Delignified chip FD, fiber pulled from chip, slit open, external-surface STR

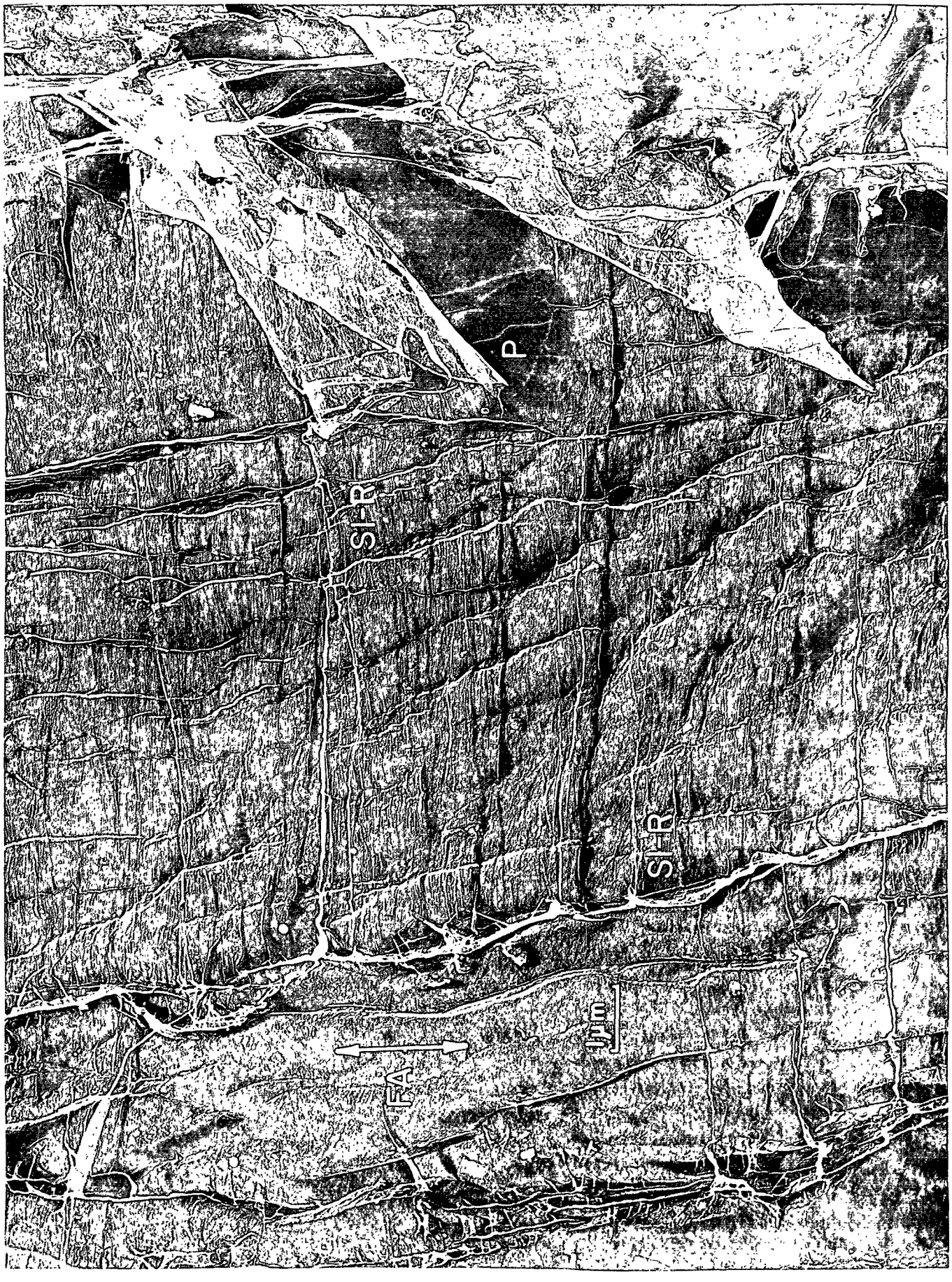
P
Sl-Pa
Sl-Pa
FA

length (assuming a uniform thickness of the membrane). On the other hand, if the membrane were tightly bonded to the cell faces, its elongation would be dependent on the expansion of the cell faces. In other words, the extension of the membrane-cell wall combination would be similar to the extension of a laminated sheet. At the same time, the extension of the bridges between cells would depend on whether the configurations and separations of the cell corners were altered during the diameter enlargement of the cells. For instance, if the membrane were tightly bonded to the cell corners and the corners did not move apart, the unsupported segment of the membrane would not have to stretch. In this case, little breaking of the membrane at the gaps would be expected. Obviously, the true extent of bonding between the bridging membrane and the cell wall cannot be conclusively stated on the basis of the work to date. However, a combination of the two extremes of bonding and nonbonding is at least suggested by some of the micrographs. For instance, the raised, stretched fragments may not have been tightly bonded to the next layer in the wet condition. The lower, continuous membrane bridges, though, appear to have been uniformly bonded in place and not extensively stretched.

Nor is the easier defibering of the delignified chips in caustic solution fully understood. If the bridging membranes are merely flat sheets or fragments of sheets draped over the fibers and bonded to them by pectic materials, dissolution of the pectin should release the membranes and allow the fibers to separate. On the other hand, if the membranes are, in fact, continuous around groups of fibers, the caustic might first loosen the membrane from the fiber faces and then lubricate the fibrils, allowing them to slide apart. Needless to say, more work is needed to fully explain the manner of defibering in the membrane-bound mass.

Another unknown about the intercellular membranes is their relative effect on the strength of wet holocellulose chips. One is prone to speculate that the membranes "bind" the fibers together into radial shives. The fibers would thus

be relatively easier to separate along radial faces than along tangential faces, as is observed. However, the binding strength of the membrane is probably not the full explanation. For instance, the observation of tightly bonded tangential faces and loosely connected radial faces in ultrathin sections has already been mentioned (Fig. 24). Since the observed feature of the chips is the relative strength in the two directions, possibly the membrane is influenced not by its added mechanical strength in the radial direction, but by its limitation of chemical bonding in the tangential direction. In other words, could the presence of the membrane between radially adjacent cells reduce the effectiveness of pectinaceous bonding between those cells? Of course, another possibility is that the bond between the tangential faces, believed to have been established during the formation of the cell plate (61), is of a chemical nature inherently different from the bond between the radial faces. If this is the case, even the presence of membranes in the radial intercellular space may be of little significance. Thus, the relative importance of mechanical and chemical bonding in holocellulose chips is still uncertain.

Finally, the observation of the intercellular membrane suggests some interesting questions in connection with pulping and papermaking. First, with regard to pulping, does the presence of isolating membranes in the radial direction contribute to an anisotropy of chemical bonding in the radial versus tangential directions in wood? Secondly, assuming the intercellular membrane to be largely cellulosic in composition, to what extent would a loss of the membranes by colloidal dispersion account for the decreasing yield of cellulose as the reaction time of chemical pulping increases? With regard to the quality of the pulp, how much would the colloidally dispersed membranes add to the specific surface area of the pulp if they should be retained? Also, could these membrane fines become "temporary" specific surface area by being dispersed and then redeposited? Finally, to what extent would this membrane material be significant as bonding fines in the final sheet?

THE CELL-WALL ORGANIZATION

INTRODUCTION

The central goal of the thesis research was to examine the organization of the tracheid cell wall. The first specific objective was to study the microfibril orientation, especially in the S1 and S3 layers. The efforts to study this structure were quite successful and resulted in substantiated concepts of wall structure. The second objective was to gain some understanding of the distribution of hemicelluloses through the cell wall. Though the attempt to meet this second objective in a direct manner was unsuccessful, an indirect approach of examining fibers extracted with alkali solutions was quite fruitful. Thus, the results of the alkali extraction will also be discussed, not only because of the implications involving the hemicelluloses, but also because of the observed effects of the alkali on the wall structure. As to the order of discussion, the outer layers of the cell wall will be considered first--both their microfibrillar structure and their reaction to alkali extraction. Then, the lumen-surface layers will be considered in a similar manner. Finally, some discussion of the S2 layer, lying between those two regions, will be given.

THE PRIMARY-S1 STRUCTURE

The Microfibril Orientation

As was explained earlier, the organization of the microfibrils in the cell wall was studied by examining surface replicas of fiber-wall sheets (FWS) which had been randomly scraped to expose the different layers. Figure 39 is a representative micrograph showing the external surface of one fiber prepared in this manner. The area with randomly oriented fibrils is tentatively designated as the outer surface of the primary layer, in accord with the characteristic picture of that layer obtained by others (5, 15, 16, 37). Close observation indicates that large areas of this

randomly oriented primary layer have been torn away, revealing other layers of fibrils with orientations nearly transverse to the fiber axis. These "transverse" fibrils could be ascribed to the S1 layer or even to the primary layer, since some workers (5) have concluded that the inner surface of the primary layer has transversely oriented fibrils. Actually, an exact labeling of these layers in this case cannot be applied, because the definition of the primary layer is not one of layer appearance but of ontogenetic derivation. Furthermore, even the ontogenetic definition is not fully satisfactory, because the process of growth during the early stages of cell development is still not completely understood (4, 61). Because of this uncertainty of definition, the randomly oriented layer will be arbitrarily designated as the primary layer and the transverse layer as the outer layer of the S1, simply in agreement with the practice of earlier workers.

More of the S1 structure can be seen in Fig. 40-42. These micrographs show that the transverse "layer" is actually not very thick--certainly not as thick as the S1 "layer" is generally considered to be. (The transverse layers observed are estimated to be only a few fibrils thick--or about 1000 A. By comparison, the micrographs of the cross sections, Fig. 23-26, generally indicate an S1-layer thickness of about 10,000 A.) In any case, a sharpening of the terminology is seen to be necessary for the purposes of the present discussion. Therefore, the much thinner aggregate of only a few fibrils thickness will be referred to as a lamella. On the other hand, the thicker S1, S2, and S3 structures will be referred to as layers, in agreement with present custom. Thus, a given layer may be found to be made up of several lamellae.

Another common feature of Fig. 40-42 is that below the transversely oriented lamellae, other lamellae with lines of orientation rotated about 25° clockwise from the transverse can be seen. Furthermore, the lamellae below these inclined lamellae are also inclined--but at about 30° counterclockwise from the transverse.

Figure 39. The Exterior Surface of a Fiber Which Has Been Scraped to Expose the Internal Fibrillar Structure

P: primary layer

TE: torn edge of the primary layer

S1: the outer layer of the secondary wall

SC: scraped surfaces

FA: fiber axis (drawn parallel to the wrinkles)

Plate Number: 4307 AF

Magnification: 11,800X

Specimen Preparation: 9% KOH[a], FD[b], FWS[c], exterior surface scraped, STR[d]

---

a
The designation 9% KOH will be used to refer to the delignified fibers extracted with 9% KOH by Spiegelberg (70) and used as a starting material in the present work. Likewise, NONEXTR will refer to his nonextracted fibers; 0.1N KOH will refer to the fibers that he extracted with 0.1N KOH; and KOH-BOA will refer to fibers that he extracted with a solution of 9% KOH plus 3% boric acid.

b
FD indicates that the fiber was freeze dried.

c
FWS indicates that the fiber was slit open along one side and then spread out flat as a fiber wall sheet.

d
STR indicates that a shadow-transfer replica of the surface was prepared.


SS
SP
FE
FE
SI
FA
1mm

Figure 40. A View of an External Fiber Surface Showing the Surface Lamellae Torn Back to Expose the Structure

LL: the loose layer torn back

P: the primary layer

TE: torn edge of the primary layer

TL: the transverse lamella

SI - B: the lamella with its angle of orientation rotated clockwise from the transverse direction

SI - C: the lamella with its angle of orientation rotated counterclockwise from the transverse direction

FA: fiber axis (drawn parallel to the wrinkles)

Plate Number: 4528 AF

Magnification: 19,000X

Specimen Preparation: 0.1N KOH, FD, FWS, surface scraped, SFE: KOH-BOA*, FD, STR

*The designation SFE refers to the single-fiber extraction procedure discussed in Appendix VI. KOH-BOA, again, indicates that the single fiber was extracted with 9% KOH plus 3% borate (Fig. 145, Sequence B).


1 µm
FA
SfB
SfG
HE
HF
P

Figure 41. Exposed Lamellar Structure of an S1 Layer

P: primary layer

TL: transverse lamella

S1 - B: lamella with line of orientation inclined clockwise from the horizontal

S1 - C: lamella inclined counterclockwise from horizontal

SC: a scraped surface

FA: fiber axis (drawn parallel to the cut edge of the cell wall)

Plate Number: 4324 AF

Magnification: 8800X

Specimen Preparation: KOH-BOA, FD, FWS, external surface scraped, STR


FA
SI-B
SI-C
TL
P
SS
5mm

Figure 42. Exposed Lamellar Structure of an S1 Layer

P: primary layer

TL: transverse lamella

S1 - B: lamella inclined clockwise from the horizontal

S1 - C: lamella inclined counterclockwise from the horizontal

FA: fiber axis (parallel to the fiber "corner" on which the arrow is drawn)

Plate Number: 4506 AF

Magnification: 14,000X

Specimen Preparation: 0.1N KOH, FD, FWS, exterior surface scraped, SFE:KOH-BOA (Fig. 145, Sequence B), FD, STR

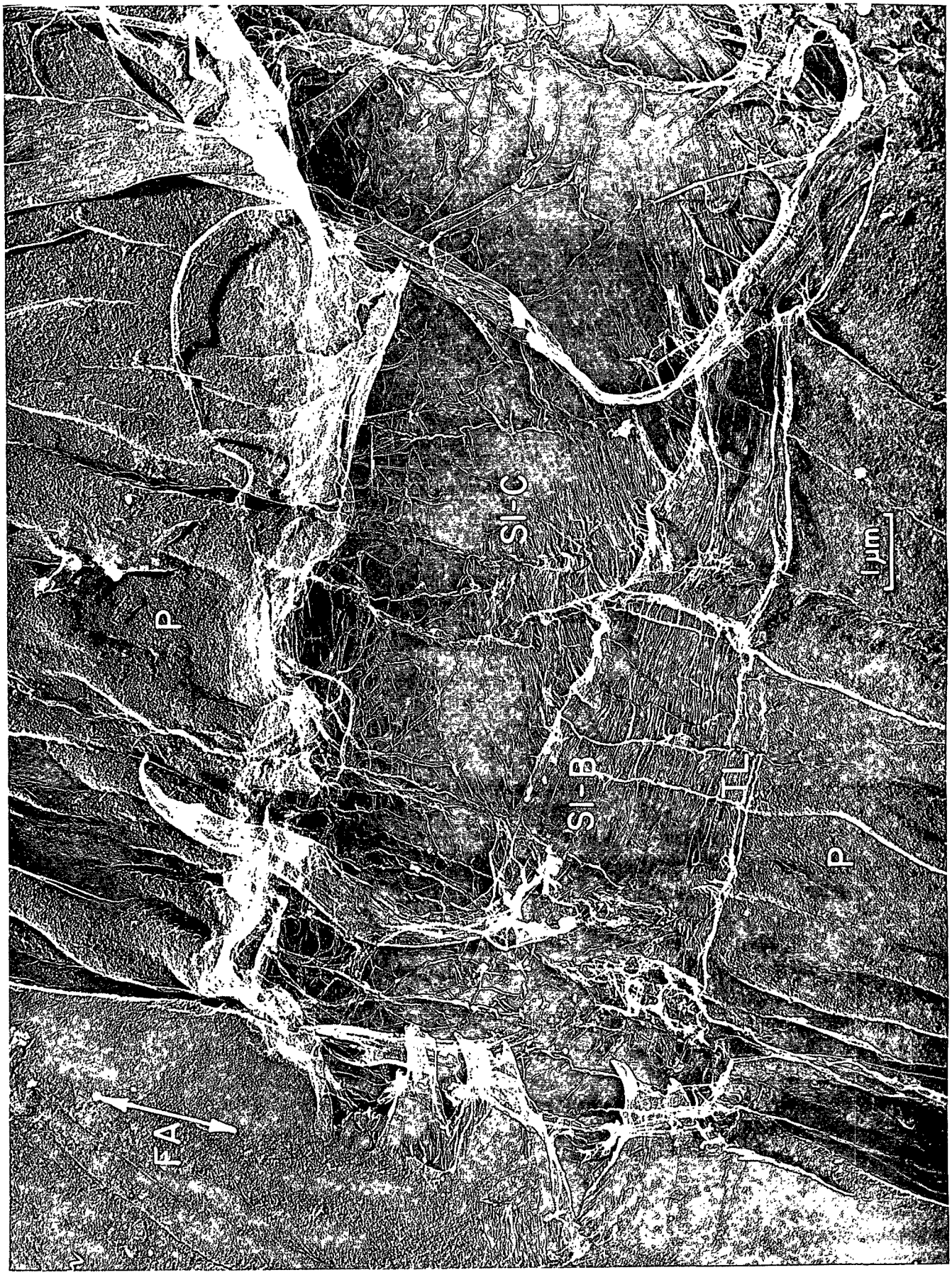
FA
P
SI-C
SI-B
P
1μm

Figure 43. A View of the Gradual Transition from the S1 to the S2

P*: primary layer

S1*: outer layer of secondary wall

SF: a "spread-fan" structure in the S1

S2*: central layer of the secondary wall

FA: fiber axis (nominally vertical--or perpendicular to the lines of the caption)**

Plate Number: 4525 AF

Magnification: 14,000X

Specimen Preparation: 0.1N KOH, FD, FWS, exterior surface scraped, SFE:KOH-BOA (Fig. 145, Sequence B), FD, STR

*These designations of the cell-wall layers will be used throughout this section and will not be redefined with each usage.

**Since most of the fiber axes are nominally vertical and are marked as such, the identification of the abbreviation will not be repeated unless some note is to be added.


FA
1cm
S2
S1
S3
PL

Figure 44. A View of the Gradual Transition from the S1 to the S2

SF: a "spread-fan" structure in the S1

Plate Number: 4298 AF

Magnification: 12,000X

Specimen Preparation: 0.1N KOH, FD, FWS, exterior surface scraped, SFE:10% KOH saturated with barium hydroxide (Fig. 140, Sequence A), FD, STR


S4
S3
S2
S1
S5
S6
S7
S8
S9
S10
S11
S12
S13
S14
S15
S16
S17
S18
S19
S20
S21
S22
S23
S24
S25
S26
S27
S28
S29
S30
S31
S32
S33
S34
S35
S36
S37
S38
S39
S40
S41
S42
S43
S44
S45
S46
S47
S48
S49
S50
S51
S52
S53
S54
S55
S56
S57
S58
S59
S60
S61
S62
S63
S64
S65
S66
S67
S68
S69
S70
S71
S72
S73
S74
S75
S76
S77
S78
S79
S80
S81
S82
S83
S84
S85
S86
S87
S88
S89
S90
S91
S92
S93
S94
S95
S96
S97
S98
S99
S100
S101
S102
S103
S104
S105
S106
S107
S108
S109
S110
S111
S112
S113
S114
S115
S116
S117
S118
S119
S120
S121
S122
S123
S124
S125
S126
S127
S128
S129
S130
S131
S132
S133
S134
S135
S136
S137
S138
S139
S140
S141
S142
S143
S144
S145
S146
S147
S148
S149
S150
S151
S152
S153
S154
S155
S156
S157
S158
S159
S160
S161
S162
S163
S164
S165
S166
S167
S168
S169
S170
S171
S172
S173
S174
S175
S176
S177
S178
S179
S180
S181
S182
S183
S184
S185
S186
S187
S188
S189
S190
S191
S192
S193
S194
S195
S196
S197
S198
S199
S200
S201
S202
S203
S204
S205
S206
S207
S208
S209
S210
S211
S212
S213
S214
S215
S216
S217
S218
S219
S220
S221
S222
S223
S224
S225
S226
S227
S228
S229
S230
S231
S232
S233
S234
S235
S236
S237
S238
S239
S240
S241
S242
S243
S244
S245
S246
S247
S248
S249
S250
S251
S252
S253
S254
S255
S256
S257
S258
S259
S260
S261
S262
S263
S264
S265
S266
S267
S268
S269
S270
S271
S272
S273
S274
S275
S276
S277
S278
S279
S280
S281
S282
S283
S284
S285
S286
S287
S288
S289
S290
S291
S292
S293
S294
S295
S296
S297
S298
S299
S300
S301
S302
S303
S304
S305
S306
S307
S308
S309
S310
S311
S312
S313
S314
S315
S316
S317
S318
S319
S320
S321
S322
S323
S324
S325
S326
S327
S328
S329
S330
S331
S332
S333
S334
S335
S336
S337
S338
S339
S340
S341
S342
S343
S344
S345
S346
S347
S348
S349
S350
S351
S352
S353
S354
S355
S356
S357
S358
S359
S360
S361
S362
S363
S364
S365
S366
S367
S368
S369
S370
S371
S372
S373
S374
S375
S376
S377
S378
S379
S380
S381
S382
S383
S384
S385
S386
S387
S388
S389
S390
S391
S392
S393
S394
S395
S396
S397
S398
S399
S400
S401
S402
S403
S404
S405
S406
S407
S408
S409
S410
S411
S412
S413
S414
S415
S416
S417
S418
S419
S420
S421
S422
S423
S424
S425
S426
S427
S428
S429
S430
S431
S432
S433
S434
S435
S436
S437
S438
S439
S440
S441
S442
S443
S444
S445
S446
S447
S448
S449
S450
S451
S452
S453
S454
S455
S456
S457
S458
S459
S460
S461
S462
S463
S464
S465
S466
S467
S468
S469
S470
S471
S472
S473
S474
S475
S476
S477
S478
S479
S480
S481
S482
S483
S484
S485
S486
S487
S488
S489
S490
S491
S492
S493
S494
S495
S496
S497
S498
S499
S500
S501
S502
S503
S504
S505
S506
S507
S508
S509
S510
S511
S512
S513
S514
S515
S516
S517
S518
S519
S520
S521
S522
S523
S524
S525
S526
S527
S528
S529
S530
S531
S532
S533
S534
S535
S536
S537
S538
S539
S540
S541
S542
S543
S544
S545
S546
S547
S548
S549
S550
S551
S552
S553
S554
S555
S556
S557
S558
S559
S560
S561
S562
S563
S564
S565
S566
S567
S568
S569
S570
S571
S572
S573
S574
S575
S576
S577
S578
S579
S580
S581
S582
S583
S584
S585
S586
S587
S588
S589
S590
S591
S592
S593
S594
S595
S596
S597
S598
S599
S600
S601
S602
S603
S604
S605
S606
S607
S608
S609
S610
S611
S612
S613
S614
S615
S616
S617
S618
S619
S620
S621
S622
S623
S624
S625
S626
S627
S628
S629
S630
S631
S632
S633
S634
S635
S636
S637
S638
S639
S640
S641
S642
S643
S644
S645
S646
S647
S648
S649
S650
S651
S652
S653
S654
S655
S656
S657
S658
S659
S660
S661
S662
S663
S664
S665
S666
S667
S668
S669
S670
S671
S672
S673
S674
S675
S676
S677
S678
S679
S680
S681
S682
S683
S684
S685
S686
S687
S688
S689
S690
S691
S692
S693
S694
S695
S696
S697
S698
S699
S700
S701
S702
S703
S704
S705
S706
S707
S708
S709
S710
S711
S712
S713
S714
S715
S716
S717
S718
S719
S720
S721
S722
S723
S724
S725
S726
S727
S728
S729
S730
S731
S732
S733
S734
S735
S736
S737
S738
S739
S740
S741
S742
S743
S744
S745
S746
S747
S748
S749
S750
S751
S752
S753
S754
S755
S756
S757
S758
S759
S760
S761
S762
S763
S764
S765
S766
S767
S768
S769
S770
S771
S772
S773
S774
S775
S776
S777
S778
S779
S780
S781
S782
S783
S784
S785
S786
S787
S788
S789
S790
S791
S792
S793
S794
S795
S796
S797
S798
S799
S800
S801
S802
S803
S804
S805
S806
S807
S808
S809
S810
S811
S812
S813
S814
S815
S816
S817
S818
S819
S820
S821
S822
S823
S824
S825
S826
S827
S828
S829
S830
S831
S832
S833
S834
S835
S836
S837
S838
S839
S840
S841
S842
S843
S844
S845
S846
S847
S848
S849
S850
S851
S852
S853
S854
S855
S856
S857
S858
S859
S860
S861
S862
S863
S864
S865
S866
S867
S868
S869
S870
S871
S872
S873
S874
S875
S876
S877
S878
S879
S880
S881
S882
S883
S884
S885
S886
S887
S888
S889
S890
S891
S892
S893
S894
S895
S896
S897
S898
S899
S900
S901
S902
S903
S904
S905
S906
S907
S908
S909
S910
S911
S912
S913
S914
S915
S916
S917
S918
S919
S920
S921
S922
S923
S924
S925
S926
S927
S928
S929
S930
S931
S932
S933
S934
S935
S936
S937
S938
S939
S940
S941
S942
S943
S944
S945
S946
S947
S948
S949
S950
S951
S952
S953
S954
S955
S956
S957
S958
S959
S960
S961
S962
S963
S964
S965
S966
S967
S968
S969
S970
S971
S972
S973
S974
S975
S976
S977
S978
S979
S980
S981
S982
S983
S984
S985
S986
S987
S988
S989
S990
S991
S992
S993
S994
S995
S996
S997
S998
S999
S1000

Thus, these adjacent lamellae are crisscrossed, as had already been found in S1 layers by other workers (24-29).

Below the crossed lamellae, a gradual transition to the S2 layer takes place, as in Fig. 43 and 44. A first glance at these micrographs suggests some form of fan structure--as if the fibrils of a given lamella might converge on a given point (Fig. 45). However, another explanation is that the fan vanes are made up of the exposed edges of several overlapping lamellae--each with an orientation slightly different from the one above it (Fig. 46). This second interpretation has already been suggested by Harada, et al. (31, 37, 91) and, in the opinion of the author, is the better explanation. One reason for preferring this interpretation is that this type of fan formation has been seen many times in the exposed layer structure prepared in this work. However, it seems unlikely that chance areas of misalignment in single lamellae would be exposed so frequently. Also, frequent occurrence of convergent fan structures within single lamellae would violate the generally observed simplicity of the lamellae. Furthermore, close scrutiny of Fig. 43 and 44 reveals the presence of overlapping lamellae, in agreement with the interpretation of a stepwise transition.

Thus, this discussion so far has consisted of detailed explorations of small transition steps within the S1. None of the micrographs has shown the complete transition from primary to S2 layer. Three example micrographs which meet this need for an overall view are given in Fig. 47-49. Comparison of these pictures, together with those micrographs already discussed, allows one to synthesize a general model of the S1 lamellar structure. A representative model would appear to include at least three features: (1) an outer lamella of transversely oriented fibrils, (2) two underlying lamellae of crisscrossed orientation, and (3) several intermediate lamellae making a gradual stepwise transition to the orientation of the S2 layer.

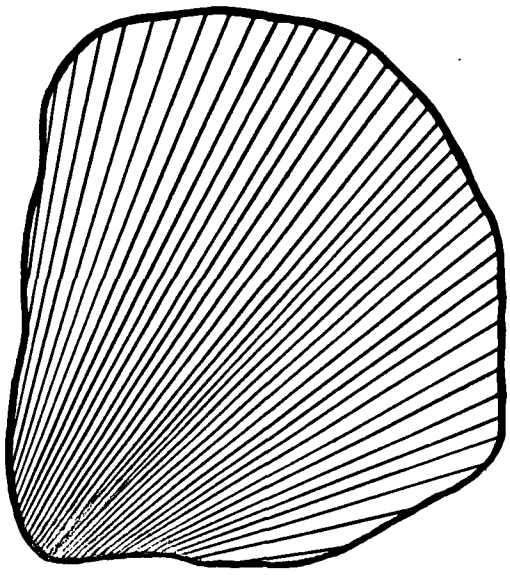

Figure 45. One Possible Interpretation of the Spread-Fan Appearance: Fibrils of a Single Lamella Having a Converging Pattern

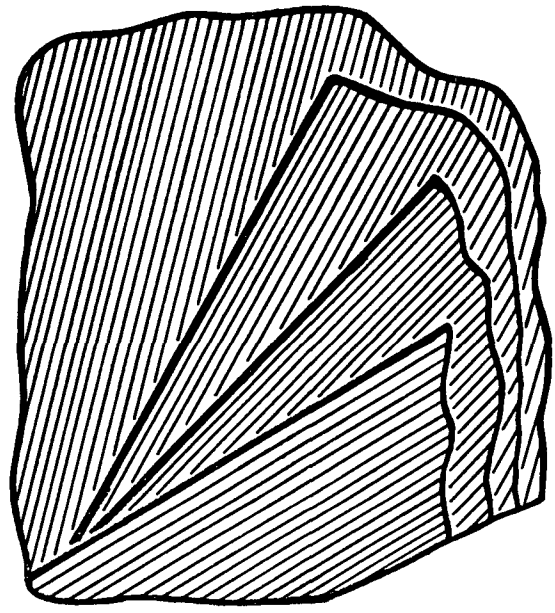

Figure 46. The More Probable Interpretation of the Spread Fan: Overlapping Lamellae of Slightly Different Orientations

The Effect of Alkali Extraction on the P and S1 Layers

Quite fortunately, the actual fiber samples prepared by Spiegelberg (70) were available for further examination. The fibers to be examined were selected at random from the freeze-dried aliquot samples and then were slit open into FWS. The FWS were each cut in half; one half was mounted for replication of the exterior surface, and the other half was mounted for replication of the lumen surface. (The lumen surfaces will be discussed in a later section.)

Because of the fiber-to-fiber variation within the different samples, at least 12 fibers from each sample were replicated and studied. Even then, no effort was made to develop statistical charts of variation within the different samples. Instead, the spectrum of variation in surface characteristics within a given sample, together with the general or "average" condition, was cited. This system was sufficient to

Figure 47. An Overall View of the Complete Primary-S2 Transition

1: transverse lamella

2: lamella inclined clockwise from horizontal

3: lamella inclined counterclockwise from horizontal

4: intermediate or "transition" lamellae making a gradual transition to the S2 orientation (this transition may be considered a continuation of 3)

C: probable "corner" of the fiber

FA: fiber axis (parallel to the corner)

SC: scratches in the surface left by the scraping blade

Plate Number: 4183 AF

Magnification: 8800X

Specimen Preparation: 9% KOH, FD, FWS, exterior surface scraped, STR


C
FA
C
C
S2
S1
C
P
1
2
3
4
5
6
5 mm

Figure 48. An Overall View of the Complete Primary-S2 Transition

1: transverse lamella (nearly hidden under the primary layer)

2: lamella inclined clockwise from horizontal

3: lamella inclined counterclockwise from horizontal

4: intermediate or "transition" lamellae making a gradual transition to the S2 orientation

Plate Number: 4312 AF

Magnification: 12,600X

Specimen Preparation: 9% KOH, FD, FWS, exterior surface scraped, SFE:10% KOH saturated with barium hydroxide (Fig. 140, Sequence A), FD, STR


FA
S2
4
3
2
P
1μm

Figure 49. An Overall View of the Complete Primary-S2 Transition

1: transverse lamella

2: lamella inclined clockwise from horizontal

3: lamella inclined counterclockwise from horizontal

4: intermediate or "transition" lamella making a gradual transition to the S2 orientation

FA: fiber axis (drawn perpendicular to the transverse lamella)

Plate Number: 4538 AF

Magnification: 13,000X

Specimen Preparation: KOH-BOA, FD, FWS, exterior surface scraped, SFE:KOH-BOA, FD, STR


S2
4
P
2
4
P
2
4
2
P
1mm

expose the trends of surface treatment resulting from the progressive stages of alkali extraction. Incidentally, one could conceivably obtain statistical information by some system of photographic recording of large surface areas. Alternatively, one might obtain such information by marking a grid on the fluorescent screen of the microscope and counting squares as the specimen is viewed. However, the expense and tedious labor of either system would have to be justified against the anticipated gains.

The Nonextracted Fibers

Figures 50-52 are three example micrographs of unextracted fiber surfaces. As exemplified by these micrographs, those surfaces were generally plastered over with structureless, mudlike materials, leaving the fibrils covered and not visible. (In some areas, though, segments of fibrils could be seen protruding through the smooth material.)

Another feature occasionally observed on the nonextracted fibers was the evidence of layer or membrane damage. By chance, such evidence is visible in each of Fig. 50-52. Figure 50 shows loose sheets of disrupted layer material standing on a fiber surface, but the source of the layers is not obvious. If these loose flags had been torn out of the primary layer of this fiber, one would expect to see tear lines and areas of exposed S1 layering from which the flags had been torn. In fact, a torn edge is visible but the surface exposed does not have the characteristic appearance of the S1 layer. Another explanation then is that the loose layer material resulted from damage to the intercellular membrane. However, this explanation has not been verified either.

In a similar manner, Fig. 51 (stereo: Fig. 53A) shows a partial layer of fibrillar material adhering to the surface of another fiber. In this picture, the torn edge of the adhering layer crosses the raised "corner" of the fiber, meaning

that the unknown layer is lying across two adjacent faces of the fiber. [The presence of raised ribs or "corners" along the length of dried fibers was first observed by Jayme and Hunger (92, 93) and was explained as resulting from the thickened corners of the originally rectangular fiber. A stereo view of another raised corner is given in Fig. 53B.) The fact that the torn layer lies across the two faces of the fiber is an indication that the layer was a part of an intercellular membrane rather than a part of a primary layer surrounding one fiber. The reasoning in this interpretation is that the two fiber faces in question could not have simultaneously touched the primary layer of another fiber, meaning that a firm bonding together of the surfaces during growth would not have occurred. On the other hand, an intercellular membrane (parent-cell wall) could touch three faces of a given tracheid during growth. Quite plausibly, then, such a membrane could have touched and bonded to the two fiber faces in question during the growth of the cell--thus being in a position to be partially retained by the cell faces during defibering of the chip.

On the other hand, definite damage to a fiber surface is shown in Fig. 52. Two tear lines across the picture enclose an area of nearly parallel fibrils, almost certainly an exposed area of the S1 layer. Again, this layer damage probably resulted from the separation of two firmly bonded adjacent fibers.

Even more significant than the surface damage to the fibers shown thus far, some of the nonextracted fibers had been damaged to an extent visible with the light microscope. Some of the freeze-dried fibers appeared to be ballooned in a manner resembling fibers swollen in caustic. However, closer examination showed that the fibers had actually frayed much like a cane stalk that is repeatedly bent back and forth but still does not break. In fact, a few half-fiber ends which looked as if they had actually broken in just such a manner were found in the sample.

Figure 50. The Exterior Surface of a Nonextracted Fiber. The Surface is Generally Plastered Over with Mudlike Material and also Includes some Loose Sheets of Layer Material

LS: loose sheets of layer material

TE: torn edge in the surface layer

ES: unidentified exposed surface surrounded by the torn edge (a patch of the surface layer is thought to have been torn away)

FA: fiber axis (drawn parallel to the wrinkles)

Plate Number: 3150 AF

Magnification: 12,600X

Specimen Preparation: NONEXTR, FD, FWS, STR


LS
LS
LS
LS
LS
1m

Figure 51. The Exterior Surface of a Nonextracted Fiber

C: a "corner" of the fiber

PL: a partial layer of fibrillar material lying across the corner

P?: a possible primary layer of the present fiber

Plate Number: 3138 AF

Magnification: 12,600X

Specimen Preparation: NONEXTR, FD, FWS, STR


1μm

Figure 52. The Exterior Surface of a Nonextracted Fiber

P?: probable primary layer on the surface of the fiber

TE: torn edge of the primary layer

S1?: probable S1 layer exposed by the tearing away of the surface layer

F: exposed fibrils not covered by the mudlike material

Plate Number: 3143 AF

Magnification: 16,100X

Specimen Preparation: NONEXTR, FD, FWS, STR


1μm
FF
TF
P?
P?
TF
SI?
FF

Figure 53A. A Torn Layer Edge Lying Across a Corner and Two Faces of a Fiber

Plate Number: 5135 AF

Magnification: 4700X

Specimen: Same as in Fig. 51.

Figure 53B. A More Apparent Fiber Corner

Plate Number: 5136 AF

Magnification: 3300X

Specimen: Same as in Fig. 67

Figure 53C. Surface Crevices Lying Perpendicular to the Fiber Axis

Plate Number: 5137 AF

Magnification: 4700X

Specimen: Same as in Fig. 58

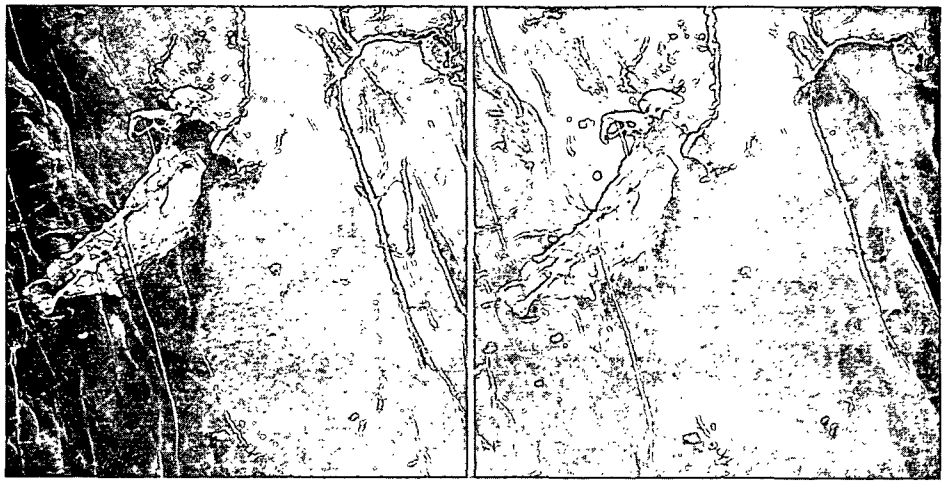

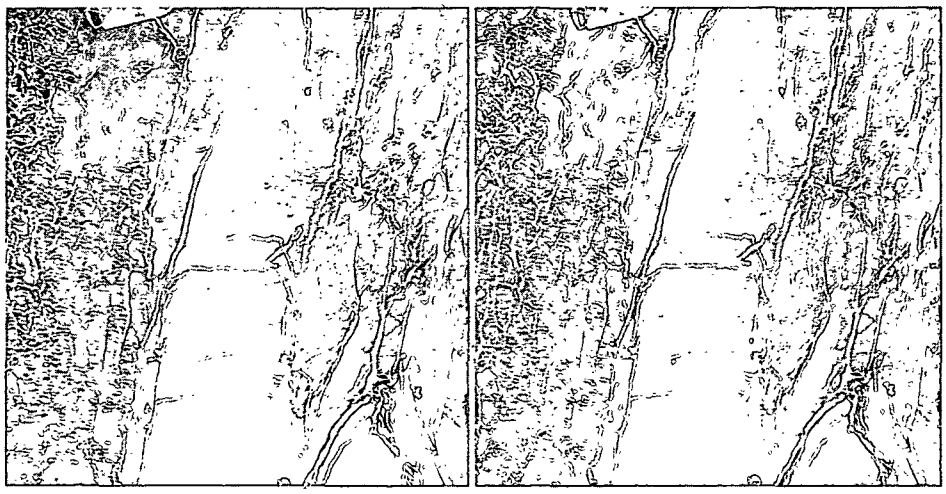

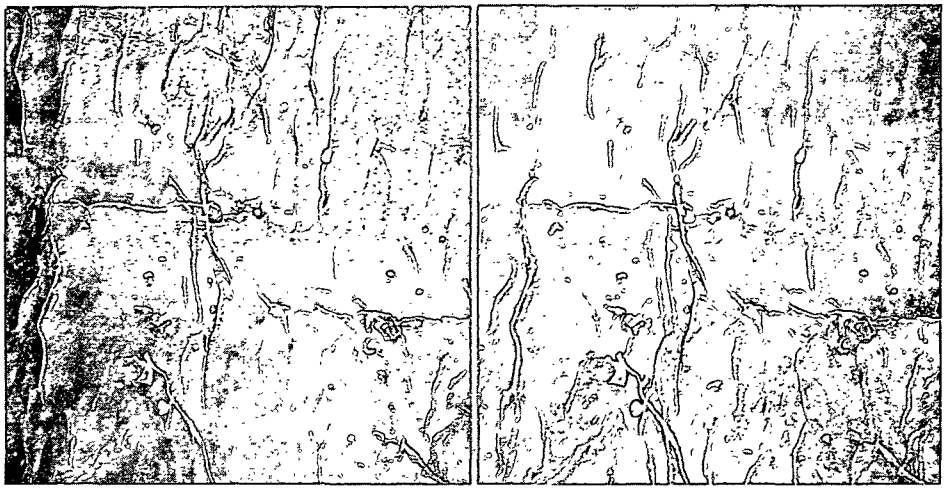

In order to determine approximately what percentage of the fibers had been damaged, a "floc" of the freeze-dried fibers was drawn from the sample bottle. Then, each fiber was examined and counted. A total of 103 fibers were counted. Seventy-two of the fibers appeared undamaged. Of the remaining 31 fibers, nineteen were either drastically frayed or broken. Twelve of the fibers appeared only slightly damaged. These slightly damaged fibers generally had a small amount of localized peeling of their outer layers. If these fibers were manually caused to buckle by pushing the two ends together, a sharp bend usually occurred at the previously observed area, indicating a weak "joint" in the fibers. (Examples of these broken and damaged fibers are shown in Fig. 54 and 55, respectively.) Thus, one should be aware that even the mild mechanical action of tumbling in water with rubber balls can cause severe fiber damage.

After the damaged fibers were observed, the results of Spiegelberg (70) were studied in an effort to determine whether the fiber damage was reflected in his measurements. However, no definite effect could be detected. According to breaking stresses, the nonextracted fibers were somewhat stronger than the 0.1N KOH-extracted fibers when dried under no load, but the strengths of the two samples were nearly the same for fibers dried under load. Also, his standard-deviation figures do not indicate a significantly wider variation in the nonextracted-fiber breaking-stress measurements, though one would expect a wider variation because of "weak-link" considerations.

The Fibers Extracted with 0.1N Potassium Hydroxide

The general appearance of the fiber surfaces extracted with 0.1N potassium hydroxide (KOH) is illustrated in Fig. 56-59. Two differences between these surfaces and those of the nonextracted fibers are apparent. First, most of the plastering material has been removed by the extraction, leaving the randomly oriented fibrils of the surface quite visible. Secondly, the primary layers are

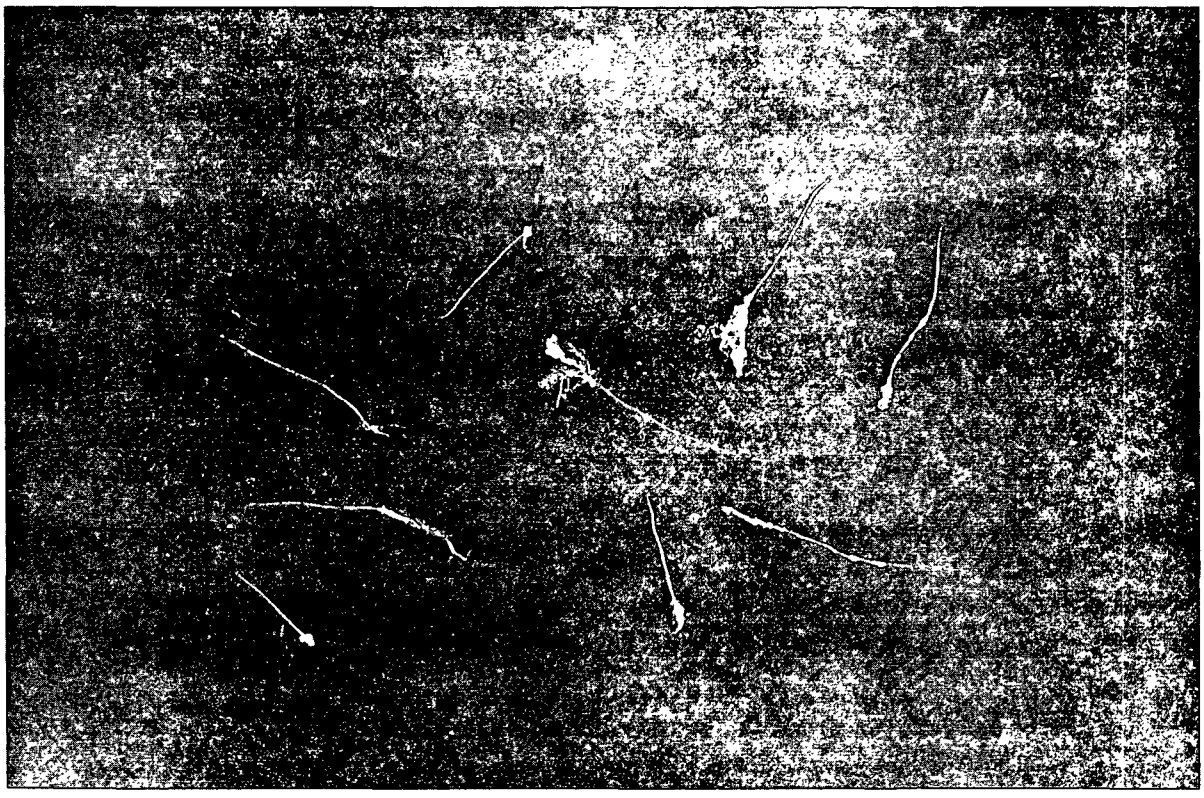

Figure 54. Broken Fiber Ends from a Sample of Nonextracted, Freeze-Dried Fibers. Negative No. 67M630 A, Magnification 8.7X

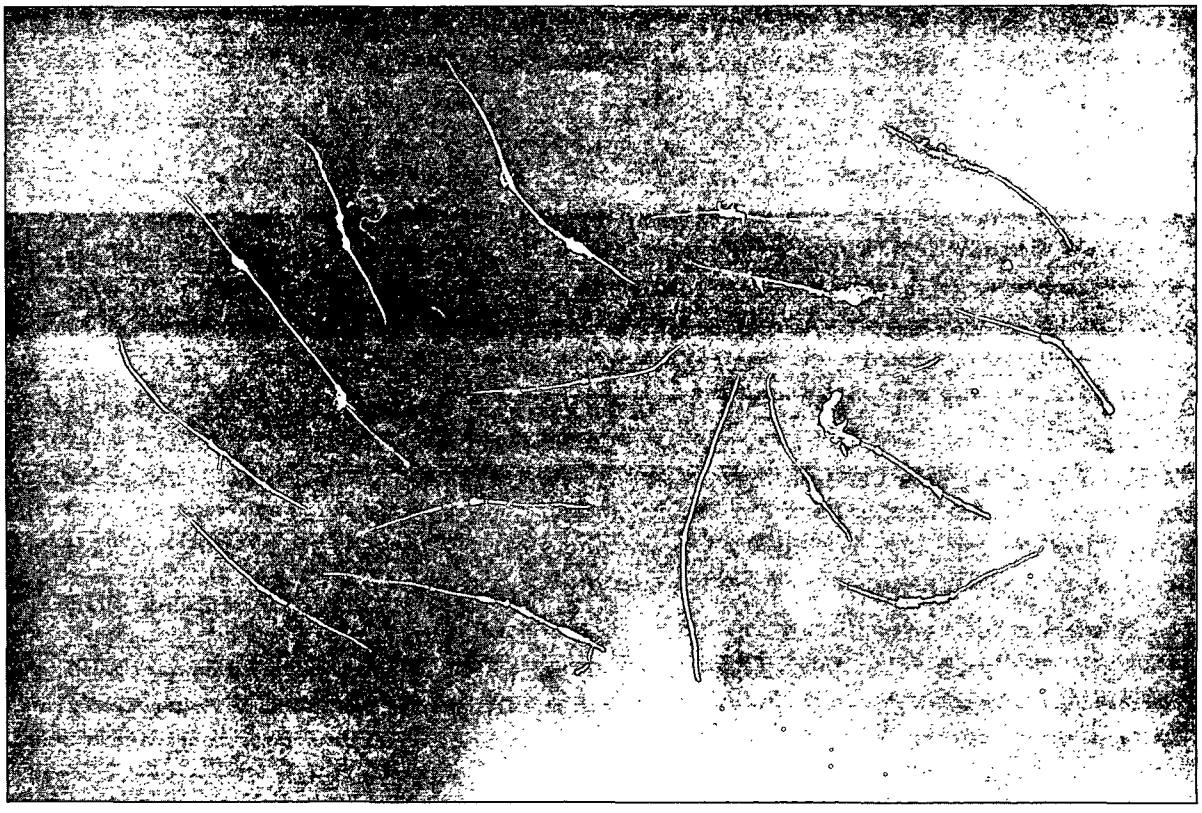

Figure 55. Badly Damaged Fibers Which Are Frayed but not Broken. Negative No. 67M630 B, Magnification 8.7X

Figure 56. The Exterior Surface of a Fiber Extracted with 0.1N KOH. The Mudlike Plastering Material Has Been Generally Removed, Exposing the Fibrillar Structure

TE: a torn edge in the primary layer

F: a flag of the surface layer, torn away along the torn edge and then folded back, exposing the S1

FA: fiber axis (approximately aligned with the suspected corner at the right)

Plate Number: 3192 AF

Magnification: 17,300X

Specimen Preparation: 0.1N KOH, FD, FWS, STR


SI
P
FA
1 µm

Figure 57. The Exterior Surface of a Fiber Extracted with 0.1N KOH, Including an Overlapping, Randomly Oriented Lamella

P: possibly, the primary layer of the fiber

OL: an overlapping, randomly oriented lamella

FS: a long fibrillar strand attached to the overlapping lamella

M: a trace of mudlike material remaining on the surface

Plate Number: 3264 AF

Magnification: 16,100X

Specimen Preparation: 0.1N KOH, FD, FWS, STR


NW
NW
SE
Pg
Tm
Tm
Tm

Figure 58. The Exterior Surface of a Fiber Extracted with 0.1N KOH

CR: crevices across the fiber surface

W: wrinkles in the surface

FA: fiber axis (drawn parallel to the wrinkles)

Plate Number: 3190 AF

Magnification: 11,700X

Specimen Preparation: Same specimen as in Fig. 56


CR
W
W
CR
W
CR
A
B
1 mm

Figure 59. The Exterior Surface of a Fiber Extracted with 0.1N KOH

FS: fibrillar strands standing above the surface

SH: the shadows of the strands

C: a corner of the fiber

W: wrinkles in the surface

Plate Number: 2433 AF

Magnification: 9600X

Specimen Preparation: 0.1N KOH, FD, FWS, STR

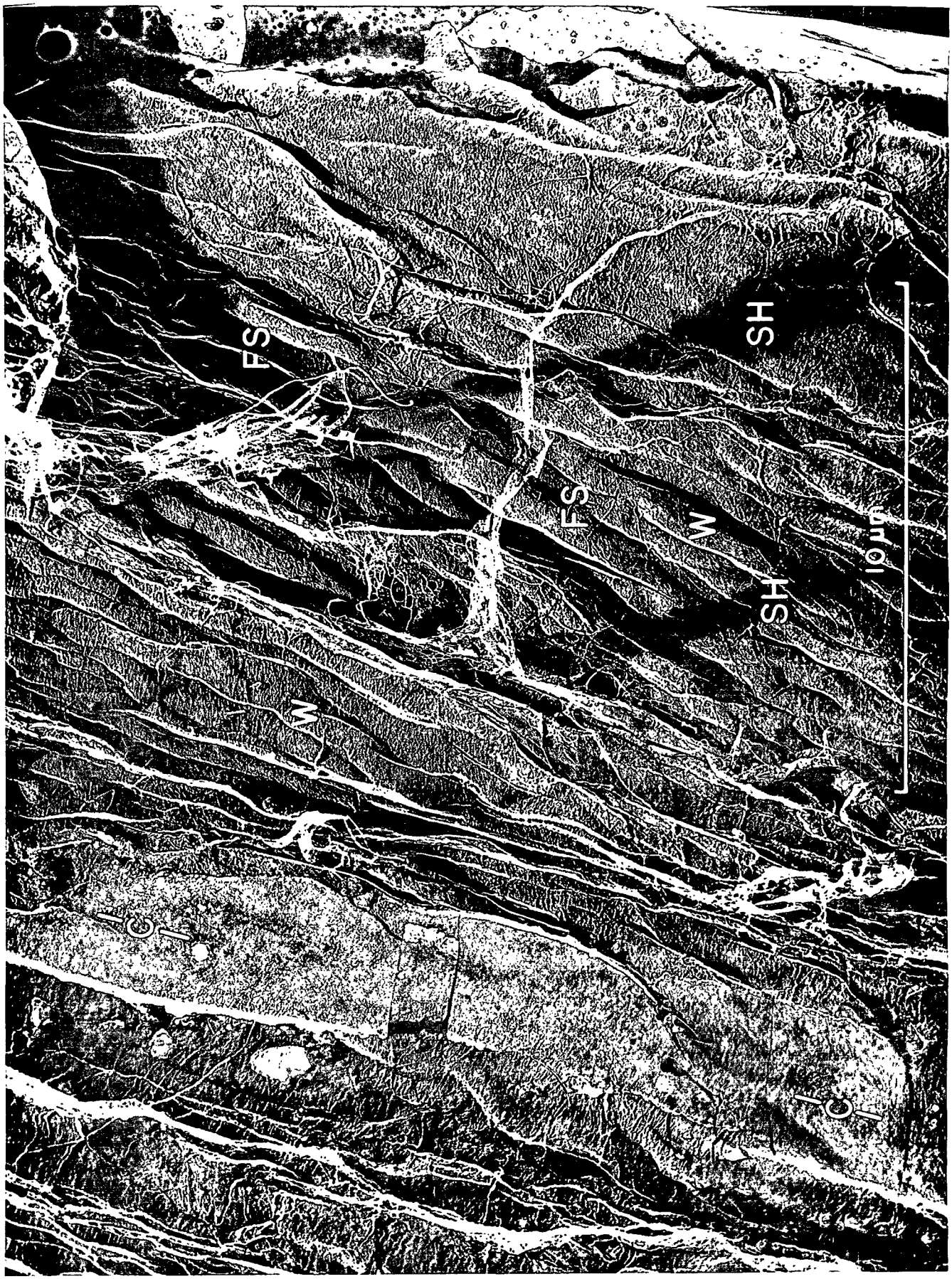
FS
SH
LFS
W
SH
W
W
1 cm

generally intact and cover the entire exterior surfaces. With regard to this second difference, the relative extent of primary-layer damage in the two samples is actually somewhat uncertain. More damaged layer fragments were visible on the nonextracted surfaces. However, many of these fragments were probably portions of intercellular membrane, meaning that the actual amount of damage to the primary layers of the non-extracted fibers is unknown. Nevertheless, the fiber damage observed with the light microscope is sufficient evidence that the nonextracted fibers were definitely damaged by the mechanical separation.

Figures 56-59 not only illustrate the general appearance of the mildly extracted fibers; they also display some other features that were occasionally observed. One such feature was the presence of small holes torn in the primary layer. Figure 56 shows one such hole which exposes a portion of the S1. Though holes like this one were observed on a few of the fibers, no conclusion has been reached as to their origin. The layer material torn back was usually present beside the hole, as if it had been simply torn mechanically. However, the most severe mechanical action involved in the preparation was a tumbling of the fibers over one another as the extracting solution was stirred by bubbling nitrogen.

Figure 57 shows another feature of common occurrence. Examination of this micrograph reveals the presence of one randomly oriented lamella overlapping another. The primary layer is generally assumed to be one continuous lamella over the entire cell. Thus, the observation of this overlapping structure was quite unexpected. A possible explanation is that the upper, overlapping sheet may have been a fragment of an intercellular membrane.

Figure 58 shows some crevices lying across a fiber. [At first, the crevices look like ridges, but careful study of the shadows and of the stereo view (Fig. 53C) should correct the idea.] These crevices have the appearance of a mechanical

dislocation in the wall structure. The fibers extracted with 0.1N KOH were generally straight, but occasionally they were bent with sharp joints similar to the way that a drinking straw bends. (Figure 155, Appendix VII is an overall view of some of these fibers.) Quite probably, these crevicelike features were compression failures at such a bend.

This micrograph also clearly illustrates another phenomenon which was commonly observed and should be mentioned--the presence of longitudinal "wrinkles" along the fiber faces. These "wrinkles" or "folds" have been observed by others (4, 16, 92-94) and usually lie nearly parallel to the fibrillar angle of the S2. The generally accepted explanation of these features is that they are wrinkles in the S1 and primary layers. These wrinkles are thought to be caused by the compressive stress exerted on these P and S1 layers when the S2 layer contracts in perimeter during drying. Incidentally, the question was raised at the beginning of this work as to whether the wrinkles could have been caused by compressive stresses in the outer cell layers when the slit fibers were spread out into FWS. However, Fig. 13 showed wrinkles on the radial face of a nonslit fiber still included in a shive. Thus, this explanation is not sufficient.

One surface feature which could be seen even in the light microscope was the presence of long, loose strands on the fiber surfaces. Examples of these strands are shown in Fig. 59. The longer one is at least 11 μm. long, but according to the shadows, the other one could have been even longer before it was apparently broken off. Waving strands like these were seen in all three of the extracted samples, but their source has not been definitely explained. The most reasonable explanation is that they might be drawn fragments of intercellular membrane material, although in some cases they could also be fragments of primary layer.

Finally, two other micrographs of one fiber are given to show that larger areas of primary-layer damage could be found in the mildly extracted sample, though such

Figure 60. The Exterior Surface of a Fiber Extracted with 0.1N KOH, Showing an Unusual Loosened Surface Layer.

LP: a loosened layer (probably the primary layer) suspended above the fiber surface

M: mudlike material retained on the surface

W: wrinkles in the surface

FA: fiber axis (drawn parallel to the wrinkles)

Plate Number: 3208 AF

Magnification: 16,100X

Specimen Preparation: 0.1N KOH, FD, FWS, STR

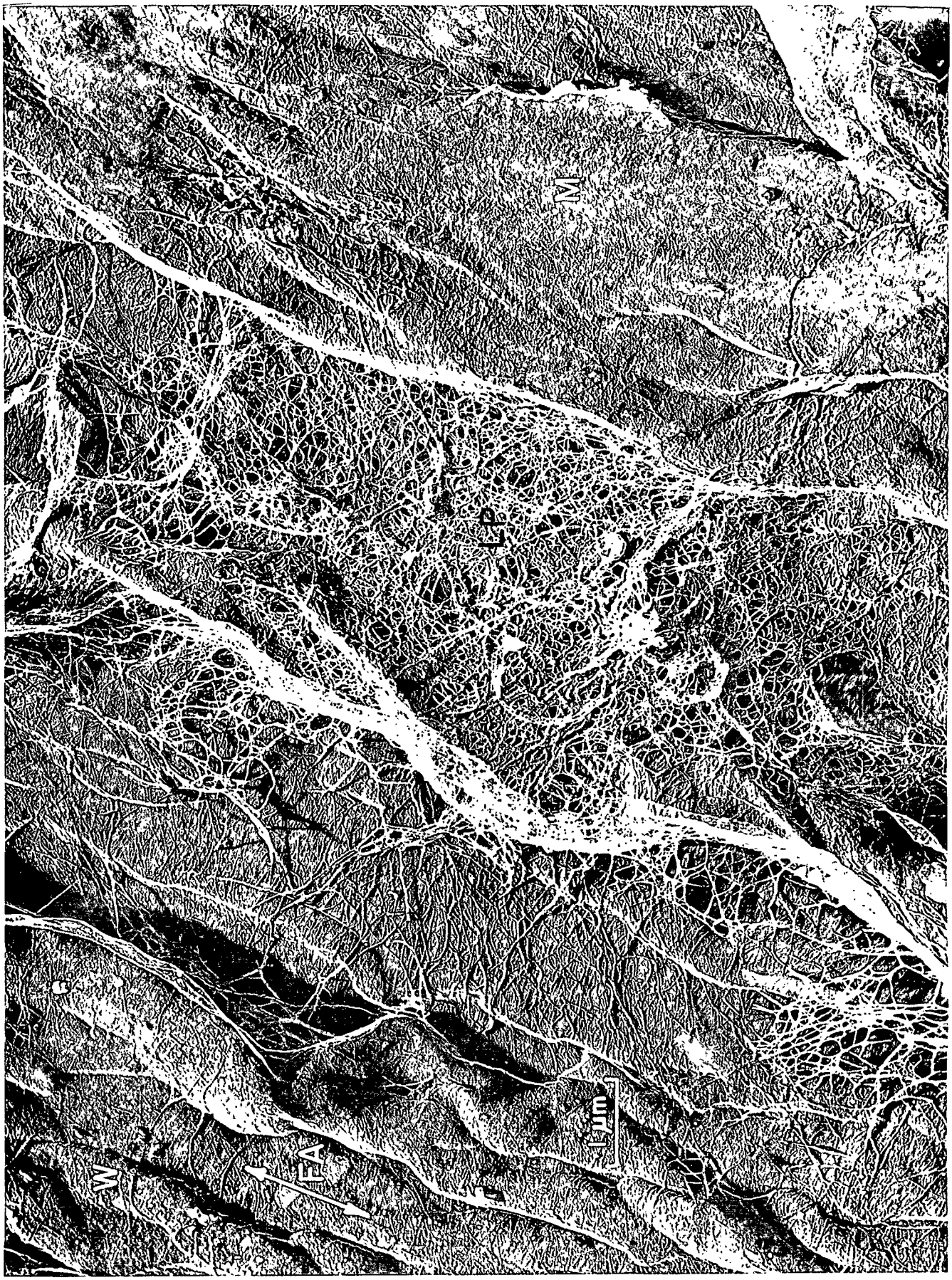
M
M
1 km
E
W

areas were quite rare. Figure 60 shows one surface over which the primary layer had been loosened. Presumably, the primary layer in such a condition would be quite vulnerable to damage. Possibly, a similar loose condition preceded the removal of the layer shown in Fig. 61 (stereo, Fig. 62A). In any case, this second micrograph shows an area of the fiber where much of the primary layer has been removed, and even some of the S1 layering has been loosened. Again, one should remember that these pictures show the extreme case of layer damage observed for this sample and that this extent of damage was quite rare. In fact, the general case was that the primary layers were quite intact.

The Fiber Surfaces Extracted with 9% Potassium Hydroxide

The fiber surfaces extracted with 9% KOH were definitely different from those extracted with 0.1N KOH only. Even more of the plasterlike material had been removed from the fibrillar structure, as seen in Fig. 63. Also, the extent of layer damage was noticeably more severe when the sample as a whole was considered, though the particular fiber in Fig. 63, as well as others like it, had retained its primary layer generally intact.

Actually, Fig. 63 introduces a trend which was observed for many of the fibers extracted with 9% KOH--a preferential loosening and removal of the primary layer from the tangential faces. Close examination of this micrograph indicates that the randomly oriented layer over the tangential face (to the left of the "corner") is loosening, but that the layer over the radial face (to the right) is still tightly bonded to the cell wall. Even more definite loosening of the primary layer can be seen in Fig. 64. As was frequently observed, whole sheets of loose layer material with only a few bonding contacts remaining can be seen draped over the cell surface. Furthermore, many areas were seen in which the primary layer was actually tearing away in sheet form, as in Fig. 65. Also, once the randomly oriented primary layer had been removed, the S1 fibrils began to loosen and disassociate, as seen in Fig. 66.

An overall view of one fiber surface, including one tangential and two radial faces separated by two fiber corners, is given in Fig. 67. Quite obvious in this picture is the removal of the primary layer from the tangential face, though the primary layer over the radial faces is generally intact. Actually, closer study of the picture reveals that fragments of the primary layer are still present on the tangential face and that some loosening of the layer over the radial faces is taking place. Incidentally, the denoting of radial and tangential faces of this fiber, as well as those fibers already discussed, was done on the basis of the location of the pits. The tangential walls of the hard pines generally do not have pitting (1); so the pitted faces of the fibers were designated as radial faces.

Two other micrographs have been included in this discussion of the 9% KOH-extracted fibers, because they indicate the presence of more than one primarylike layer on some of the fiber surfaces. Figure 68 shows a hole torn in one such layer, revealing another similar layer. Another area with a thin, lacy layer overlying a primary layer is pictured in Fig. 62B. Again, the most likely explanation of these double layers is that fragments of the intercellular membranes have survived the alkali extraction and are held in place on the surface of the primary layer.

The Fibers Extracted with 9% KOH plus 3% Borate

The visible differences between the sample extracted with 9% KOH and the sample extracted with 9% KOH plus 3% borate were differences of degree of surface degradation rather than categorical differences of layer attack. Figure 69 shows one fiber surface subjected to this latter stage of extraction. In this unusual picture, the four faces of the fiber are seen side by side, together with three of the cell corners. In this area, the primary layer has been removed from the tangential faces and part of one radial face.

Figure 61. The Exterior Surface of a Fiber Extracted with 0.1N KOH, Showing an Unusual Removal of the Primary Layer and a Loosening of the S1 Fibrils

S1: uncovered S1 layer

LS1: loosened S1 fibrils

P: a portion of the primary layer retained in place

FA: fiber axis (drawn parallel to the wrinkles)

Plate Number: 3209 AF

Magnification: 12,600X

Specimen Preparation: Same specimen as in Fig. 60


1μm
FA
D
ISI
SI

Figure 62A. A Fiber Surface from Which the Primary Layer Has Been Removed, Permitting the S1 Fibrils to Loosen

Plate Number: 5138 AF

Magnification: 3300X

Specimen: Same as in Fig. 61

Figure 62B. A Thin, Lacy Layer Overlying a Primary Layer

Plate Number: 5139 AF

Magnification: 6500X

Specimen: 9% KOH, FD, FWS, STR

Figure 62C. Extensive Fibrillation of a Fiber Surface Extracted with 9% KOH Plus 3% Borate

Plate Number: 5140 AF

Magnification: 2500X

Specimen: Same as in Fig. 70

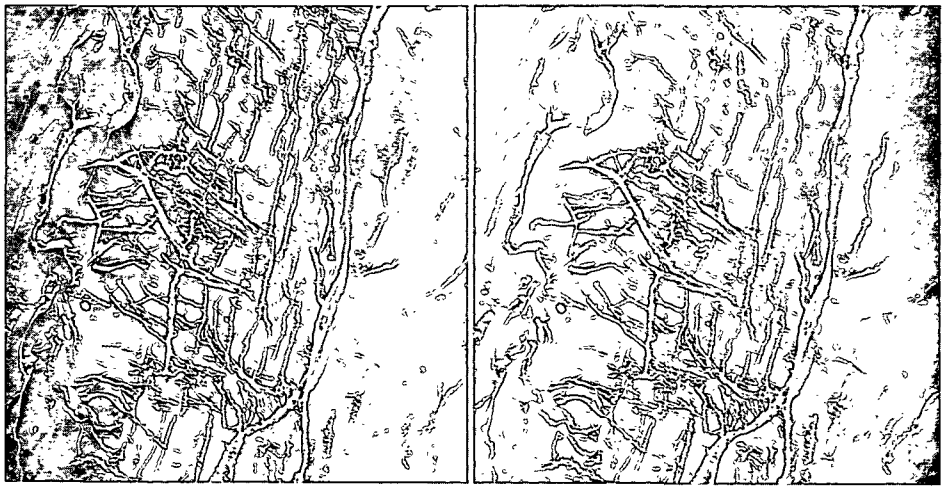

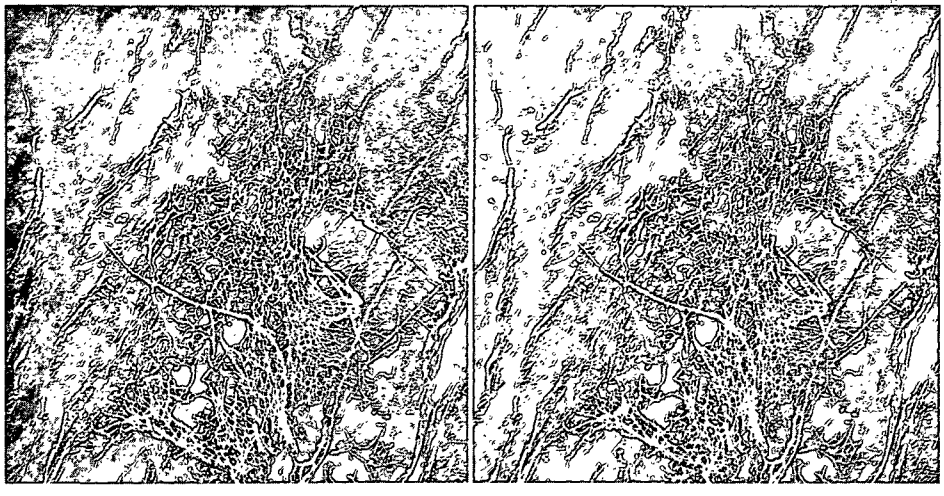

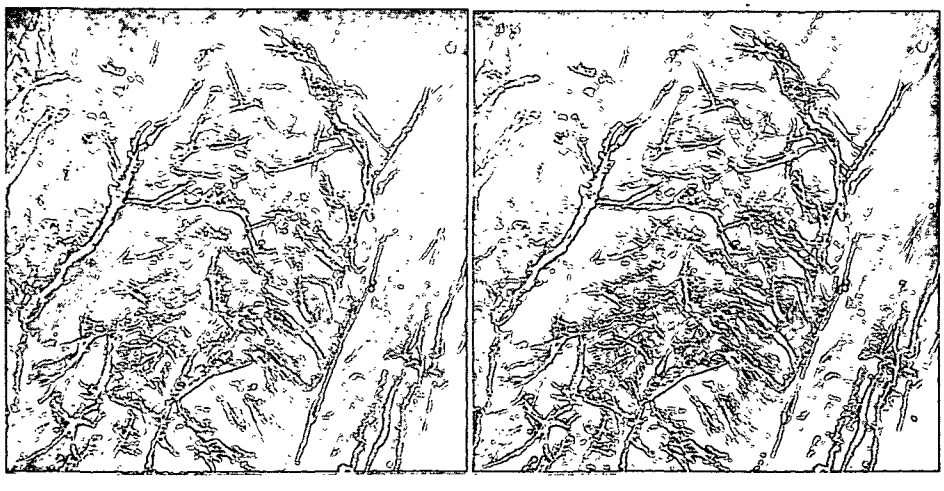

Figure 63. The Exterior Surface of a Fiber Extracted with 9% KOH

C: a corner of the fiber

TF: a tangential face of the fiber

RF: a radial face

LP: loosening primary layer

Plate Numbers: 3000, 3001 AF

Magnification: 8500X

Specimen Preparation: 9% KOH, FD, FWS, STR


10μm
RF
LP
LP
LP

Figure 64. The Exterior Surface of a Fiber Extracted with 9% KOH, Showing a Loosening of the Surface Layer.

LS: loosening of the surface (primary) layer

C: a corner of the fiber (the fiber-axis direction would be parallel to the corner if it were to be shown)

WR: a wrinkle in the replica

Plate Number: 2946 AF

Magnification: 14,300X

Specimen Preparation: 9% KOH, FD, FWS, STR


WR
LS
LS
LS
S
S

Figure 65. The Exterior Surface of a Fiber Extracted with 9% KOH

TE: a torn edge in the primary layer

LP: a loosened area of the primary layer torn away in sheet form

S1: the S1 layer exposed by the removal of the primary layer

FA: fiber axis (drawn parallel to the wrinkles)

Plate Number: 2940 AF

Magnification: 14,300X

Specimen Preparation: 9% KOH, FD, FWS, STR

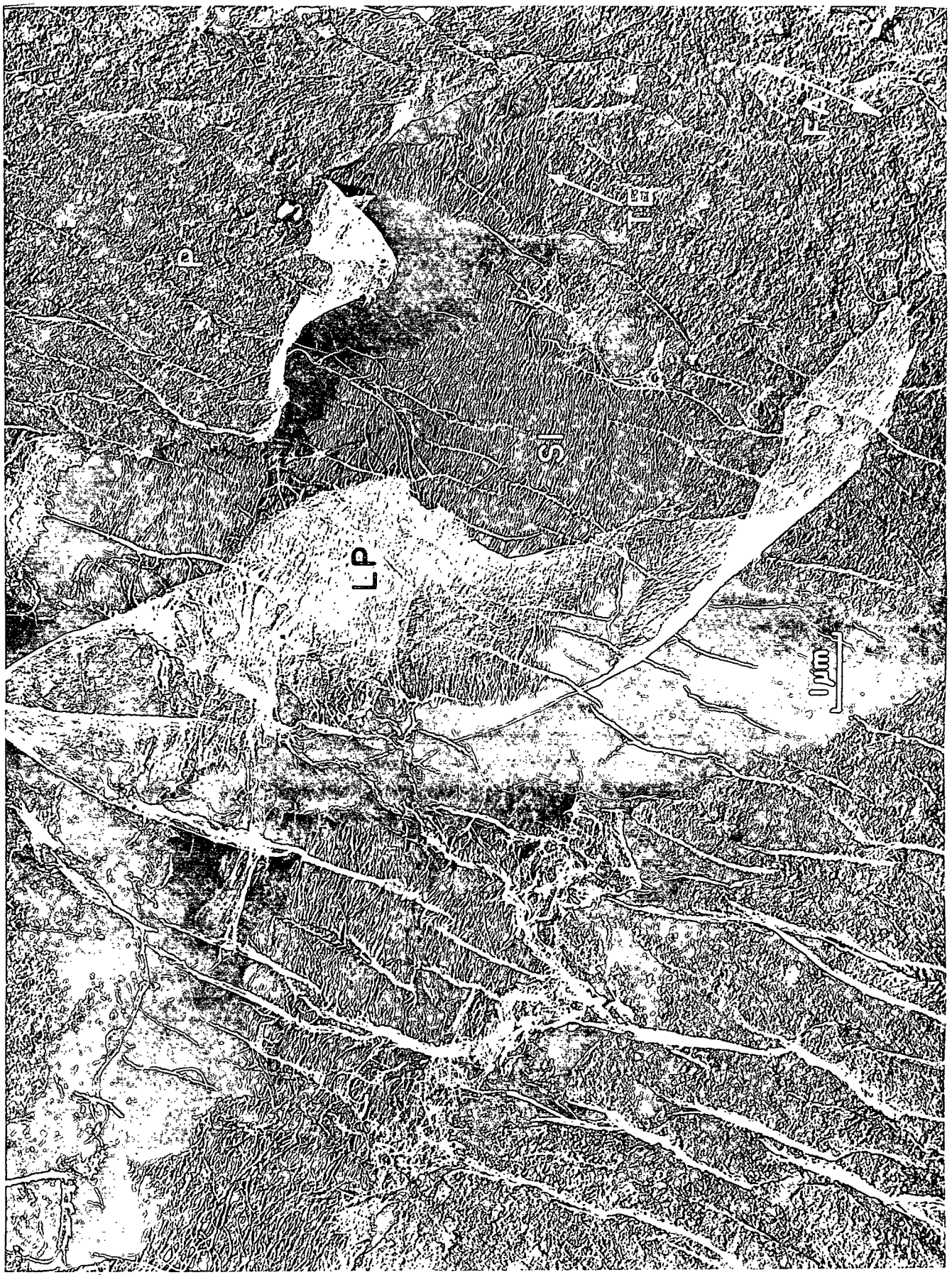
e
LP
SP
1 mm

Figure 66. The Exterior Surface of a Fiber Extracted with 9% KOH, Showing an Exposure of the S1 and a Loosening of the S1 Fibrils

P: possible fragment of the primary layer retained on the surface

TE: torn edge in the primary layer

S1: exposed S1 surface

LS1: loosening S1 fibrils

Plate Number: 2920 AF

Magnification: 20,900X

Specimen Preparation: 9% KOH, FD, FWS, STR

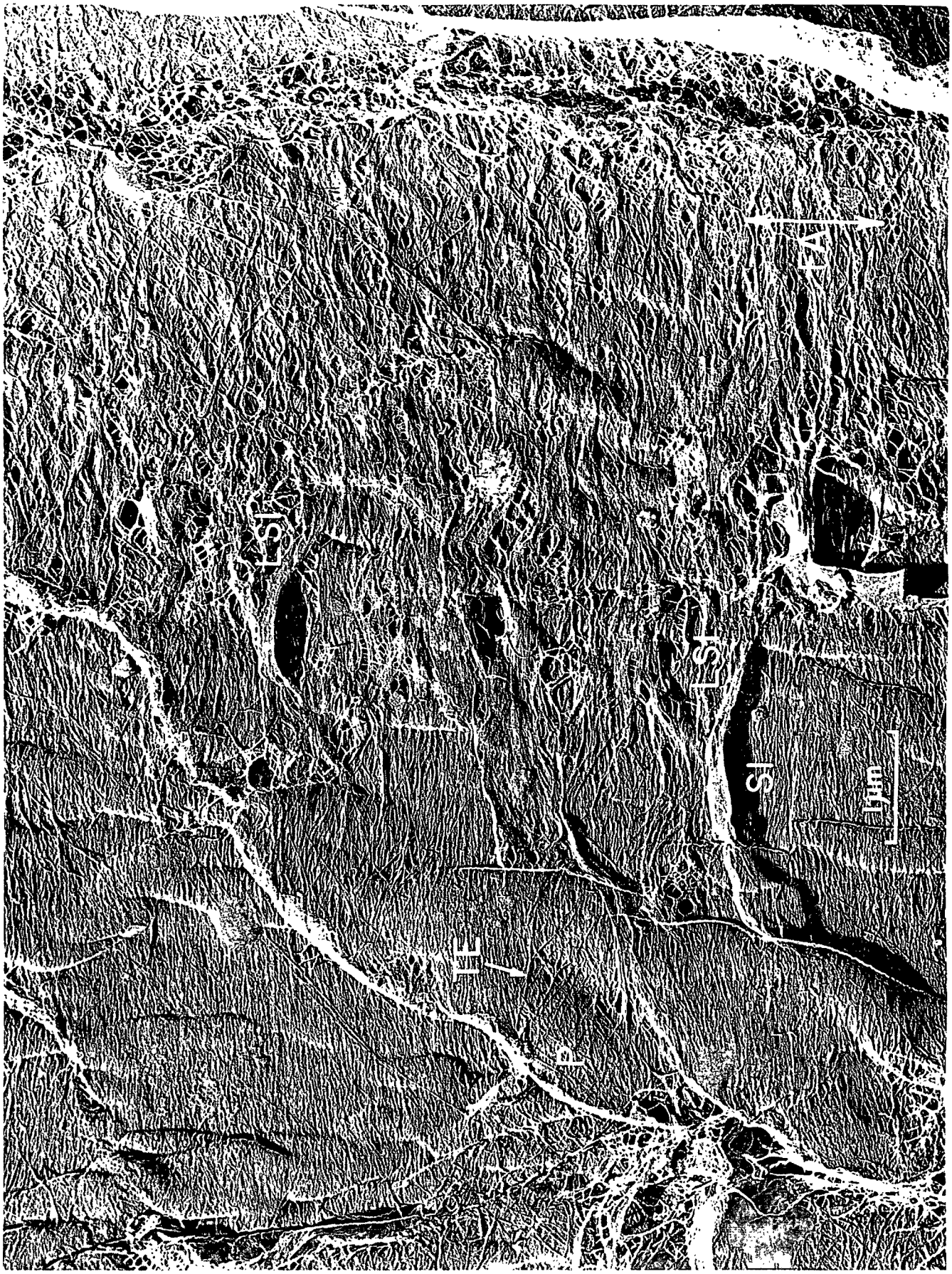
A
SF
SF
SL
1 µm
E
B

Figure 67. The Exterior Surface of a Fiber Extracted with 9% KOH. The Primary Layer Has Been Largely Removed from the Tangential Face, but is Generally Intact over the Radial Faces

C: corner of the fiber

P: cell pits

RF: radial faces (denoted by pits)

TF: tangential face

S1: exposed S1 layer

FP: fragment of the P layer retained on the tangential face

LP: loose primary layer on the radial face

Plate Number: 2975-2980 AF

Magnification: 3700X

Specimen Preparation: 9% KOH, FD, FWS, STR


RF
ICI
TF
RF
SI
LP
FP
P
SI
FP
P
P
10 µm
P
P
ICI
ICI

Figure 68. The Exterior Surface of a Fiber Extracted with 9% KOH, Including a Hole Torn in the Surface Layer and Revealing the Underlying Layer

RO: randomly oriented surface layer

TE: torn edge in the surface layer

LL: loose layer of the surface material torn back

E: the exposed, underlying, randomly oriented layer

I: a possible intermediate layer between the surface and underlying layers

M: mudlike material retained on the surface

Plate Number: 2904 AF

Magnification: 31,100X

Specimen Preparation: 9% KOH, FD, FWS, STR


EA
RC
TE
M
E
LL
RO
1 μm

Figure 69. The Exterior Surface of a Fiber Extracted with KOH Plus Borate. Most of the Primary Layer Has Been Removed--Even from One of the Radial Faces

C: the fiber corners (the fourth corner is indicated as "C?", since one cannot be sure that the wrinkle shown actually is the corner)

M: mudlike material on the corners

P: cell pits

RF: radial faces (one radial face includes two pits)

TF: tangential faces

S1: exposed S1

RP: a remnant of the primary layer

Plate Number: 2959, 2960 AF

Magnification: 4200X

Specimen Preparation: KOH-BOA, FD, FWS, STR


TF
SI
10 μm
M
RF
RP
TF
P

One other aspect of Fig. 69 should also be mentioned--the observation that, even after extensive extraction, the corners still appear plastered over. Certainly, the alkali solutions used should have removed any exposed hemicelluloses. Possibly, this mudlike material is residual lignin, though the Klason-lignin content of the chips was only 0.45%. This explanation is at least compatible with the views of other workers (47, 95, 96), who indicate that the cell corners contain the highest concentration of the cell-wall lignin, and that, even after pulping, the corners retain part of this lignin.

Figures 70 and 62C illustrate the extensive surface fibrillation which could be found in this sample of fibers extracted with KOH plus borate. In these micrographs, one sees an area which has its primary layer removed and its outer S1 fibrils definitely loosened, all without any mechanical "beating." Incidentally, these micrographs are also quite informative in demonstrating the capability of the freeze-drying and replication processes to retain and reproduce this form of fibrillation.

Actually, no "general" condition for all of the fibers in this sample can be cited. Of twelve fibers examined, three had retained their primary layers nearly intact. Five had their primary layers nearly completely removed--even from their radial faces. The other four fibers were intermediate in amount of primary-layer damage and had varying amounts of this layer removed. Thus, the conclusion is that these fibers are not different from those extracted with 9% KOH only, except as a matter of degree of damage. These fibers did appear to have more of their primary-layer material removed and, subsequently, a greater loosening of their S1 fibrils.

THE S3 "LAYER"

The Microfibril Orientation

As was indicated in the Historical Review, the structure of the S3 "layer" has remained in question (in contrast to the S1, which has been studied somewhat more thoroughly). Furthermore, as will become apparent in this discussion, the S3 layer is also more complex, at least in the longleaf pine tracheids studied in this work. For these reasons, the structure of this layer will be discussed in more detail than was the S1.

The Lamellae Near the Lumen Surface

This discussion will begin with the orientation of the microfibrils on the lumen surface, and then proceed to the lamellae uncovered when the surface lamella is torn away. Figure 71 illustrates this kind of tearing and uncovering. The fibrils at the top of the figure constitute the lumen-surface lamella, and lie in a characteristic orientation nearly perpendicular to the fiber axis. However, much of this layer has been torn away leaving a fractured or torn lamella edge. Below this lamella edge, other torn edges can be seen, meaning that several lamellae lie beneath the lumen-surface lamella. More specifically, two barely visible and one abruptly visible tear lines with angles only slightly different from the first one can be seen in this picture. Thus, the fibrillar orientations of the four lamellae nearest the lumen differ from one another only slightly, but they differ in a continuous, stepwise, counterclockwise rotation (counting from the lumen surface toward the S2).

Below the last-mentioned definite tear line in Fig. 71, other lamellae can be seen. However, these lamellae are noticeably different from the first ones in their appearance. For one thing, some of these inner lamellae are made up of only a few, separated fibrils. One can, in fact, look between two adjacent fibrils of one

Figure 70. The Exterior Surface of a Fiber Extracted with KOH Plus Borate, Showing an Example of Extreme Surface Fibrillation

FA: fiber axis (drawn parallel to the suspected fiber corner)

Plate Number: 2954 AF

Magnification: 14,300X

Specimen Preparation: KOH-BOA, FD, FWS, STR

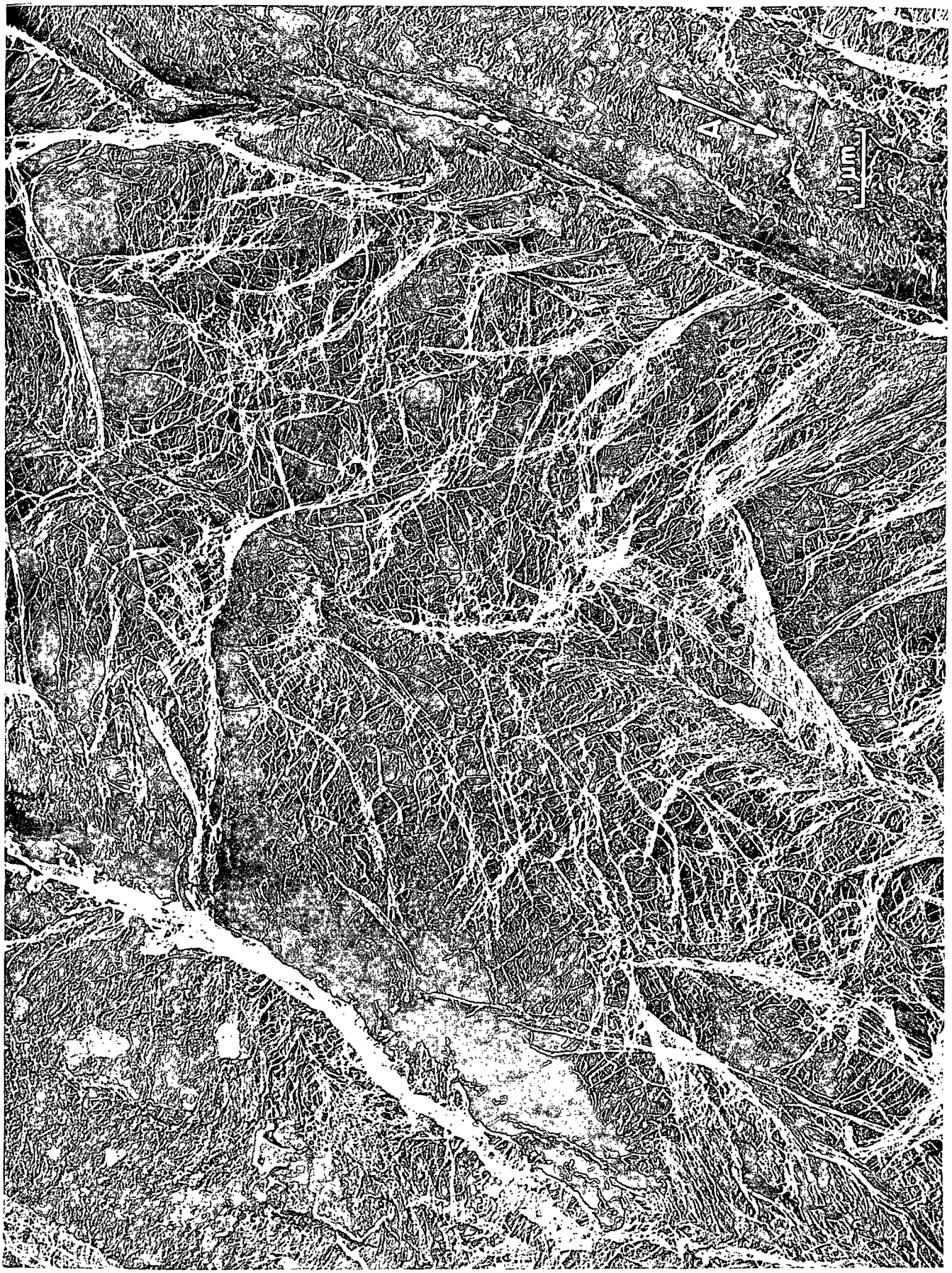
A
1mm

Figure 71. A Fiber Lumen Surface from Which Some of the Lamellae Have Been Peeled Back to Expose the S3 Structure

(The lamella orientations have been numbered in order, counting from the lumen surface toward the S2 layer. Lamellae 1-4 demonstrate a counterclockwise rotation of orientation, and 5-10 demonstrate a clockwise rotation. The abrupt tear line and the reversal in rotation occur between 4 and 5. The dotted line enclosures designate the locations of slits in the lamellae.)

LS(1): the lumen-surface lamella (No. 1 in the transition)

LS: a slit through which an underlying lamella is visible

W: waves in the surface giving possible indication of the orientation of an underlying lamella

FA: fiber axis (nominally vertical)*

Plate Numbers: 4388-4390 AF

Magnification: 5800X

Specimen Preparation: KOH-BOA, FD, FWS, lumen surface scraped and peeled, STR

*In practically all of the lumen-surface micrographs to be shown, no definite indicators of the fiber-axis direction could be found. Therefore, the arrows were drawn in a vertical direction in accord with the nominal direction of placement of the specimen in the microscope.


LS(II)
2
3
4
5
6
6
5
6
6
6
8
10
TE
6
8
9
W
10
SLI
9
8
FA

lamella (i.e., through a slit in the lamella) and see the orientation of the underlying fibrils. Incidentally, this means of comparing the orientation angles of two successive lamellae is considered more reliable than comparing the angles at a tear line, since one cannot otherwise be sure that only one lamella was torn at a given tear line.

These inner lamellae (beneath the sharp tear line and starting with number five) are also different in that their lines of orientation reverse their direction of incremental rotation, stepping down in a clockwise rotation, rather than a counterclockwise rotation like that of the first layers. In the case of these particular lamellae, the incremental rotations are not visible from definite lamella edges, but rather are seen at the slits in the thin lamellae as one looks through one lamella to the next. Furthermore, a definite counting of the number of lamellae is somewhat difficult, because no definite lamella edges are discernible. In other words, the peeling back of the surface lamellae did not leave sharply defined torn edges. Instead, the layer of material removed from this surface appears to have tapered in thickness, with a resultant erratic gradient through each remaining lamella.

In any case, the number of lamellae has been estimated by counting the number of noticeably different angles of orientation in scanning from the top to the bottom of the picture. In this manner, about five of the thinner lamellae, or a total of nine lamellae counting the four above the abrupt tear line, can be seen in Fig. 71. However, the significant factor is not the exact number of lamellae, but the way in which the lamellae exhibit a stepwise rotation in angle. In fact, the five thinner lamellae alone demonstrate a rotation of 180° (from horizontal to horizontal), or an average of about 45° per increment. Furthermore, this picture still does not show all of the S3 lamellae, since the S2 layer is not visible.

To return to the question of the abrupt transition at the tear line between the four upper lamellae and the five underlying lamellae, Fig. 72 and 73 show the same transition but at other parts of the same fiber. Both of these pictures show smoother gradients and indicate the presence of another, longitudinally oriented lamella. The orientation of this lamella is such that it is considered by the author to be just one further step in the counterclockwise rotation of the four surface lamellae already mentioned. Thus, the presence of this longitudinally oriented lamella does not destroy the basic pattern already mentioned. In both Fig. 72 and 73, the beginning of the clockwise rotation in fibrillar angle can still be seen as other lamellae underlie the longitudinal lamella and have fibrils at an angle clockwise from those of this lamella.

After examining the conflict between Fig. 71 and Fig. 72 and 73, one raises the question of whether the lamellar structure is uniform throughout the fiber. However, this apparent conflict does not constitute conclusive evidence of nonuniformity. The longitudinal lamella could have been originally present in the area shown by Fig. 71, but then it could have been torn away in such a manner as to not be visible. This possibility is demonstrated quite well by Fig. 74. Examination of the diagonal tear line in this micrograph indicates that at least one lamella (Area I), and possibly a second lamella, is torn at the upper segment of that line. However, a third lamella (Area II) definitely overlaps the lower left corner of the first-mentioned lamella (as shown by the overlapping torn edge of this lamella TE_{II}). The significant observation is that both lamellae were torn simultaneously along the lower segment of the tear line. This demonstration that several lamellae can be torn simultaneously along a single, common tear line is definite support for the suggestion that a longitudinally oriented lamella could have been torn away in Fig. 71. Thus, the possibility of consistent lamellar structure throughout a fiber is not necessarily violated by the disagreement between Fig. 71 and Fig. 72 and 73.

Figure 72. Another View of the Same Fiber as in Fig. 71, Showing a Vertically Oriented Lamella that Was not Visible in that Earlier Micrograph

LS: the lumen surface

TE: a torn edge of the surface lamella

LL: a loose layer rolled back to expose lamella edges making a gradual rotation in angle (as shown by the short lines indicating orientation angles)

UL: the upright or longitudinally oriented lamella

Plate Number: 4398 AF

Magnification: 17,400X

Specimen Preparation: Same specimen as in Fig. 71.

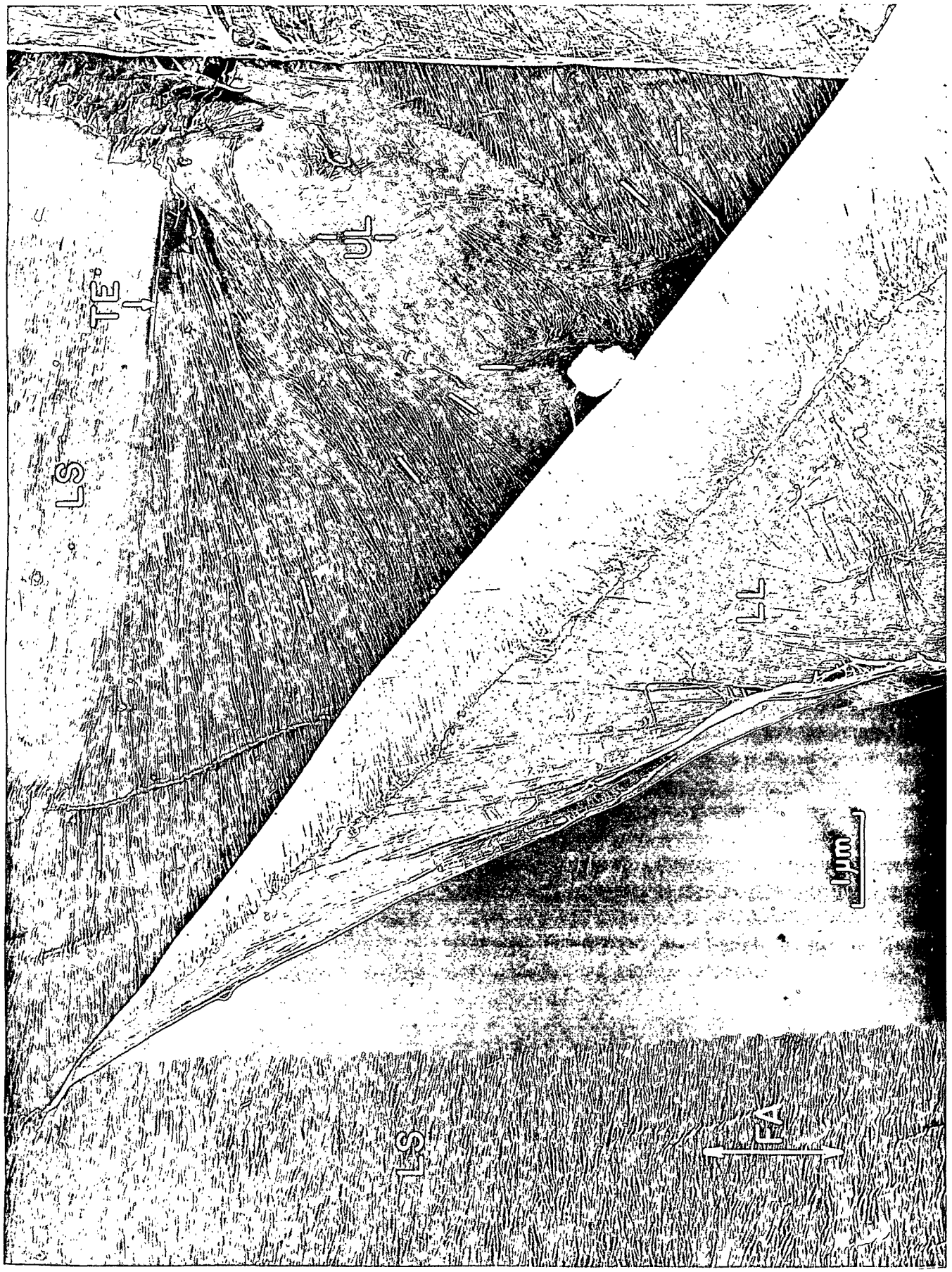
LS
LS
LL
LL
LL
1μm
N
W

Figure 73. Another View of the Same Fiber as in Fig. 71, Showing a Vertically Oriented Lamella that Was not Visible in that Earlier Micrograph

LS: the lumen surface

TE: a torn edge of the surface lamella

UL: the upright or longitudinally oriented lamella

FR: a displaced fragment of a replica

SC: a scratch in the lumen surface, probably caused by the back of the slitting knife

Plate Number: 4397 AF

Magnification: 17,400X

Specimen Preparation: Same specimen as in Fig. 71.


FA1
FA2
FA3
FA4
FA5
FA6
FA7
FA8
FA9
FA10
FA11
FA12
FA13
FA14
FA15
FA16
FA17
FA18
FA19
FA20
FA21
FA22
FA23
FA24
FA25
FA26
FA27
FA28
FA29
FA30
FA31
FA32
FA33
FA34
FA35
FA36
FA37
FA38
FA39
FA40
FA41

Figure 74. An Internal Surface of an S3 Layer. This Micrograph Demonstrates One of the Problems Involved in Interpreting the Micrographs--the Problem of Deciding how many Lamellae Are Torn at a Given Tear Line

DTL: a diagonal tear line

I: Area I, including one and probably two lamellae (1 & 2)

TE_I: the torn edge of the lamellae in Area I

TE_{II}: the torn edge of an overlapping lamella (3)

II: Area II, the overlapping lamella

$TE_{I \& II}$: torn edge of all three lamellae

SL: slit in 3, through which 2 is visible

W: waves in I generated by underlying fibrils

O & OO: two underlying lamellae, which make a total of five lamellae visible in this area (the five lamellae do fit into the trend of clockwise rotation observed earlier, though they are numbered in reverse fashion in this micrograph)

Plate Number: 4383 AF

Magnification: 11,700X

Specimen Preparation: Same specimen as in Fig. 71.

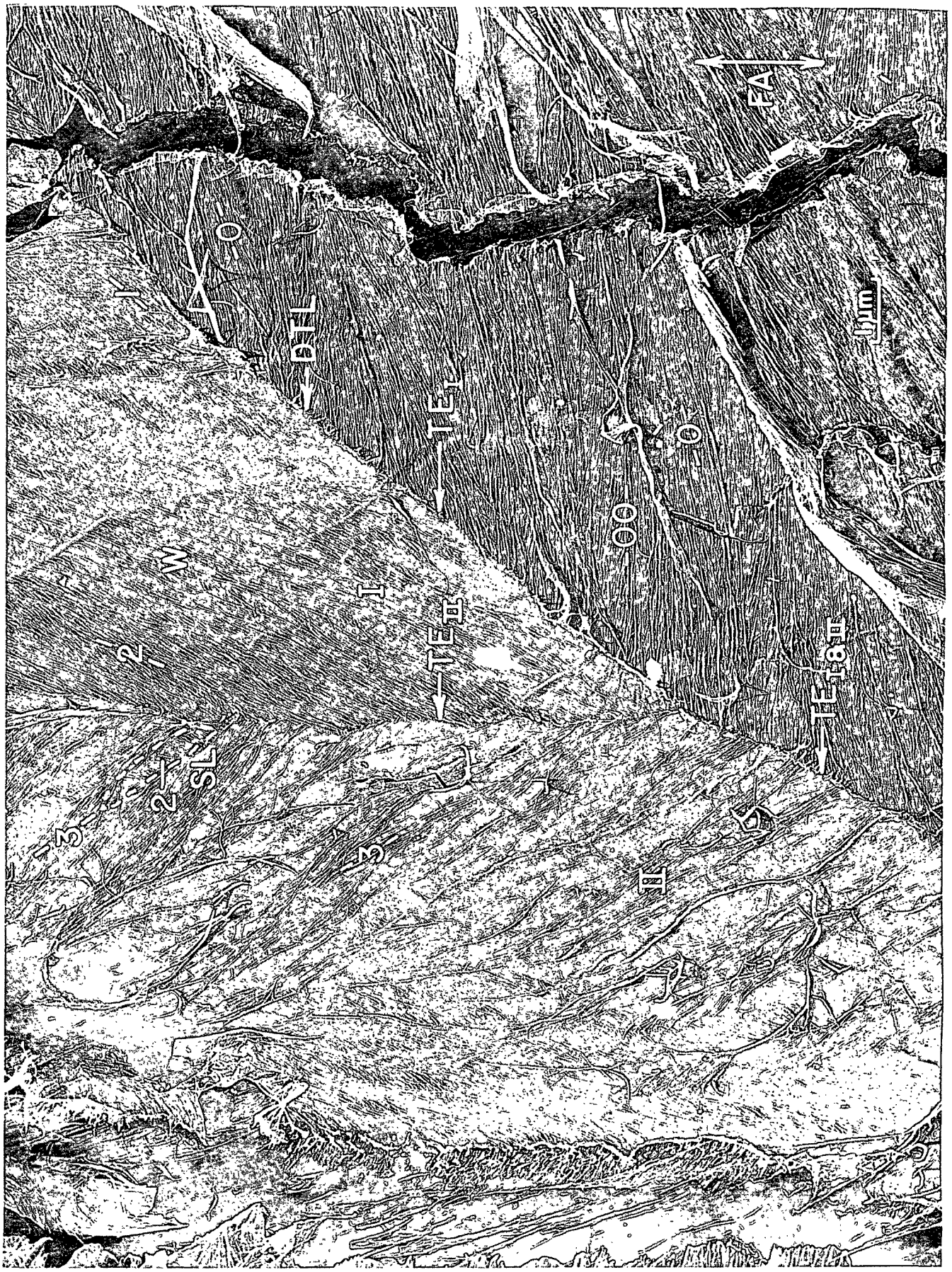
PA1
WM
TE1
TE2
TE3
TE4
TE5
TE6
TE7
TE8
TE9
TE10
TE11
TE12
TE13
TE14
TE15
TE16
TE17
TE18
TE19
TE20
TE21
TE22
TE23
TE24
TE25
TE26
TE27
TE28
TE29
TE30
TE31
TE32
TE33
TE34
TE35
TE36
TE37
TE38
TE39
TE40
TE41
TE42
TE43
TE44
TE45
TE46
TE47
TE48
TE49
TE50
TE51
TE52
TE53
TE54
TE55
TE56
TE57
TE58
TE59
TE60
TE61
TE62
TE63
TE64
TE65
TE66
TE67
TE68
TE69
TE70
TE71
TE72
TE73
TE74
TE75
TE76
TE77
TE78
TE79
TE80
TE81
TE82
TE83
TE84
TE85
TE86
TE87
TE88
TE89
TE90
TE91
TE92
TE93
TE94
TE95
TE96
TE97
TE98
TE99
TE100

However, a definite conclusion about this question of intrafiber variation must await further study.

In addition to discussing intrafiber variation, one also has to examine the matter of whether all of the tracheids from a given tree would be alike in their microfibrillar structure. Actually, Liese (10) has obtained evidence which indicates that they are not alike. In fact, he found large differences in the angle of lumen-surface fibrils, even for adjacent fibers of sectioned wood surfaces. Furthermore, one can determine from the micrographs of the present work that the internal lamellae, also, exhibit fiber-to-fiber variations, both in their angles of orientation and in their interlamella interval angles. Thus, the author agrees with the conclusion of Liese that the fibers do not follow an exact pattern of lamellar structure.

However, a certain degree of generalization about the progression of angles does appear realistic. For instance, Fig. 75 shows the progression of lamella transition in another fiber. This picture shows again the counterclockwise rotation, reversal, and clockwise rotation in lamella orientations already observed in Fig. 71. Of course, these micrographs have shown parts of just two representative fibers. However, numerous other fibers were studied and were all found to demonstrate the same progression patterns observed in these fibers. Also, several other micrographs shown later in this discussion show the entire progression to the S2 layer, including the brief transition discussed thus far. As will be observed, all of these micrographs demonstrate the generalized progression pattern.

Finally, Fig. 76 shows the lumen-surface lamellae (up to and including the rotation reversal) in still another fiber. In the "fanlike" transition (see Fig. 46) of this area, one can count as many as seven or eight lamella edges, depending on one's own interpretation. Furthermore, careful reconsideration of Fig. 71, 72, and 73 suggests the uncertainty of actually counting lamellae within one fiber.

However, in spite of the uncertainty about the exact number of lamellae, the concept of a progression pattern is still judged to be realistic.

Another question which the reader might have raised after studying these pictures is whether the interpretation of overlapping lamellae could be correct. (Certainly, this matter is one of interpretation, since one not only has to explain the pictures he sees; he must also develop a concept of just what original wall structure could have been altered by the random mechanical action to yield the observed exposed surfaces.) One consideration in this question is that the pictures shown were chosen not because they showed broad expanses of single lamellae (though such pictures could have been found), but because they showed many lamellae and thus allowed development of the concept of gradual step transitions involving the several lamellae. In support of the essential lamellar structure, Fig. 77 is included in this discussion. This micrograph shows a large area of overlapping lamellae, but the lamellae are thin enough, and the fibrils separated enough, that one can see through several lamellae at the same time. By careful study, portions of at least five different lamellae can be seen. Thus, the interpretation of overlapping lamellae is considered to be realistic.

The "Transition" Lamellae at the S3-S2 Interface

Just as in the case of the S1-S2 transition, Harada (31, 37) was able to demonstrate the presence of intermediate lamellae between the S3 and S2. Such "transition" lamellae were also found in the longleaf pine tracheids of this work. Two micrographs which display the lamellation of these interface fibrils are given in Fig. 78 and 79. In agreement with the spread-fan concept of Harada (Fig. 46), the fibrillar orientation of each lamella is at a slight angular deviation from that of the lamella above it. (Instead of a comparison to a spread fan, the lamella edges could also be compared to the edges of the treads in a spiral staircase.) Even more

Figure 75. The Succession of Lamella Transition in Another Fiber. Lamellae 1-5 Demonstrate a Counterclockwise Rotation, and 6-11 Demonstrate a Clockwise Rotation. The Rotation Reversal Occurs Between 5 and 6

LS(1): lumen-surface lamella (numbered 1)

Plate Number: 4442 AF

Magnification: 8200X

Specimen Preparation: 0.1N KOH, FD, FWS, lumen surface scraped and peeled, STR


EA
-10-
-8-
-7-
-6-
-5-
-4-
-3-
-2-
-1-
0
1
2
3
4
5
6
7
8
9
10
11
12
13
14
15
16
17
18
19
20
21
22
23
24
25
26
27
28
29
30
31
32
33
34
35
36
37
38
39

Figure 76. A More Detailed View of Lamellae near the Lumen Surface, Including a "Spread Fan" of Lamella Edges. Lamellae 1-8 Represent a Counterclockwise Rotation (Counting from the Lumen Surface Toward the S2), and Lamellae 9 and 10 Begin the Clockwise Rotation. The Rotation Reversal Takes Place Between 8 and 9

LS: lumen surface

Plate Number: 4277 AF

Magnification: 12,600X

Specimen Preparation: 0.1N KOH, FD, FWS, lumen surface scraped and peeled, SFE:10% KOH saturated with barium hydroxide (Fig. 140, Sequence A), FD, STR


WAKE
LAE
SALAMAUA
LAE
SALAMAUA

Figure 77. An Internal Surface of the S3 Showing Five Thin, Overlapping Lamellae. In Several Places, One Can Look Through a Slit in One Lamella and See the Orientation of the Underlying Fibrils. Again, the Line of Orientation Makes a Clockwise Rotation in this Micrograph also

Plate Number: 4450AF

Magnification: 11,700X

Specimen Preparation: 0.1N KOH, FD, FWS, lumen surface scraped and peeled, STR

Figure 78. A View of "Transition" Lamellae at the S3-S2 Interface. Lamellae 1-7 Make a Gradual, Stepwise Transition to the Orientation of the Exposed S2 Layer

H: the hub of the "spread fan"

M: mudlike material retained on the S2

Plate Number: 4446 AF

Magnification: 12,600X

Specimen Preparation: 0.1N KOH, FD, FWS, lumen surface scraped and peeled, STR (other half of fiber shown in Fig. 75)

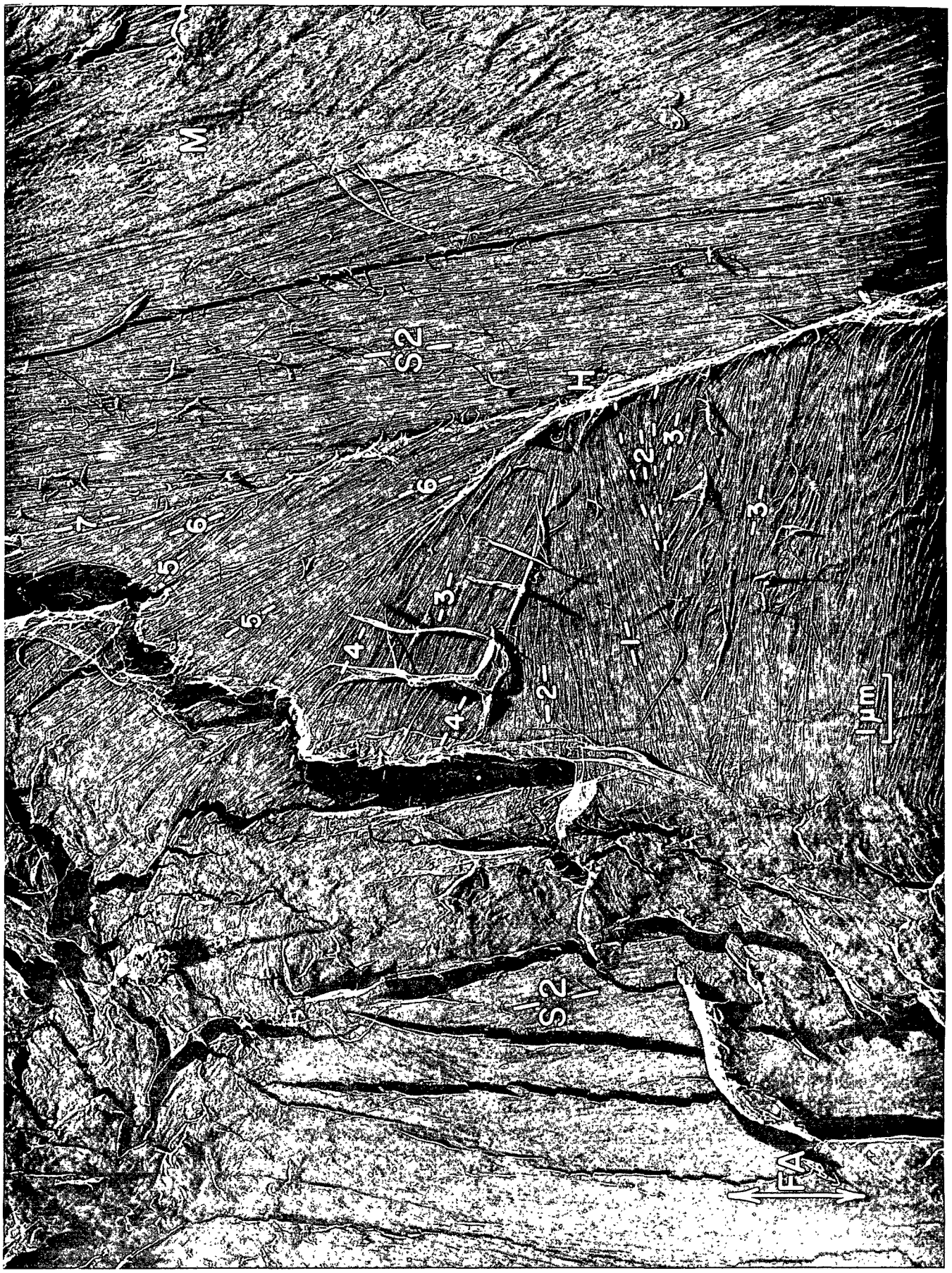
N
S2
F
1
2
3
4
5
6
1m

Figure 79. A View of "Transition" Lamellae at the S3-S2 Interface. This Transition Is Seen to Take Place in Definite Steps

Plate Numbers: 4177, 4178 AF

Magnification: 8300X

Specimen Preparation: 9% KOH, FD, FWS, mounted fiber on rubber cement, scraped lumen surface, extracted surface three minutes with 0.1N KOH, washed with water, air dried


S2
S2
5
2
4
3
S2
PA
5µm

significantly, the incremental rotation of the line of orientation is in a clockwise direction, as if in continuation from the last-mentioned lamellae near the lumen surface.

Figures 78 and 79 showed definite lamella steps. However, other fanlike transitions were found in which the steps could not be easily discerned (Fig. 80 and 81). One could even use these micrographs to support the concept of converging fibrils within a given lamella. Nevertheless, even in Fig. 80, the torn fiber ends at the "hub" of the "spread fan" gave good indication of overlapping lamellar structure.

Overall Views of the S3 Layer

The two previous topics were detailed discussions limited to the S3 lamellae at the lumen surface and at the S3-S2 interface. Therefore, Fig. 82-85 are given to summarize the entire S3 structure. Unfortunately, these micrographs are limited, too, in that the random peeling of the fiber surfaces obscured some of the lamellae shown in the earlier, more detailed regions of transition. Nevertheless, an intercomparison of these five micrographs shows that they do consistently support the emerging concept of the S3 structure. The general picture is one of an S3 layer consisting of at least twelve sublayers or lamellae. As to the orientation of the fibrils in these lamellae, the line of orientation lies nearly perpendicular to the fiber axis on the lumen surface and then rotates in a stepwise fashion as one moves toward the S2 layer. The line rotates first counterclockwise to an angle of at least 30° from the horizontal. Then, the rotation reverses and proceeds clockwise more than 270°, ending with fibrils of the last lamella lying parallel to the fibrils of the S2.

Thus, the generalized S3 structure is discussed as a trend or pattern of fibril orientation. Quite definitely, any citation of specific angles is to be avoided, since the orientation angles do not appear to be constant from one fiber to another.

Furthermore, even the incremental angle between the orientations of successive lamellae does not appear to be constant. For instance, measured increments in the reversal-to-S2 transition have been found to range from 16 to 48°. The average increment would be about 30°. On the other hand, the increments between the lamellae near the surface in the surface-to-reversal sequence are smaller and probably average about 10° or less.

Miscellaneous Features of the Lumen Surface: Wartlike Deposits

The observation and study by others of wartlike deposits on tracheid lumen surfaces were discussed earlier in the Historical Review. The apparent conclusion was that though the warts had been seen in many species and had been found to be generally resistant to chemical action, their composition is still not known.

During the course of this work, the question was raised as to whether the warts are present in longleaf-pine tracheids. Liese (42, 43) had examined 81 other pines and had found some with and some without warts. Jurbergs (97) had examined other pines, including slash and loblolly, but not longleaf pine. One paper was found, though, in which Frey-Wyssling, et al. (98) reported the presence of warts on the pit linings of longleaf-pine tracheids, meaning that warts could probably be found on the lumen surface also.

Thus, in order to verify the presence of warts on the lumen surfaces and to obtain some indication of their size and distribution, a brief effort was made to examine the surfaces of some untreated tracheids. Some untreated wood blocks were softened by boiling in water and then were cut into 40-μm. longitudinal sections. The dried sections were shadowed with palladium, coated with carbon, and then embedded in melted polystyrene. The wood was removed from the replica by alternate treatments with 72% sulfuric acid and 2% sodium chlorite, and then the polystyrene was washed away with benzene.

Figure 80. A Smooth "Spread-Fan" Transition (S3-S2) in Which Lamella Edges Are not Readily Apparent

SF: "spread-fan" transition

H: "hub" of the spread fan

OL: overlapping fibril ends at the hub

Plate Numbers: 4126, 4127 AF

Magnification: 12,600X

Specimen Preparation: 0.1N KOH, FD, FWS, lumen surface scraped and peeled, STR

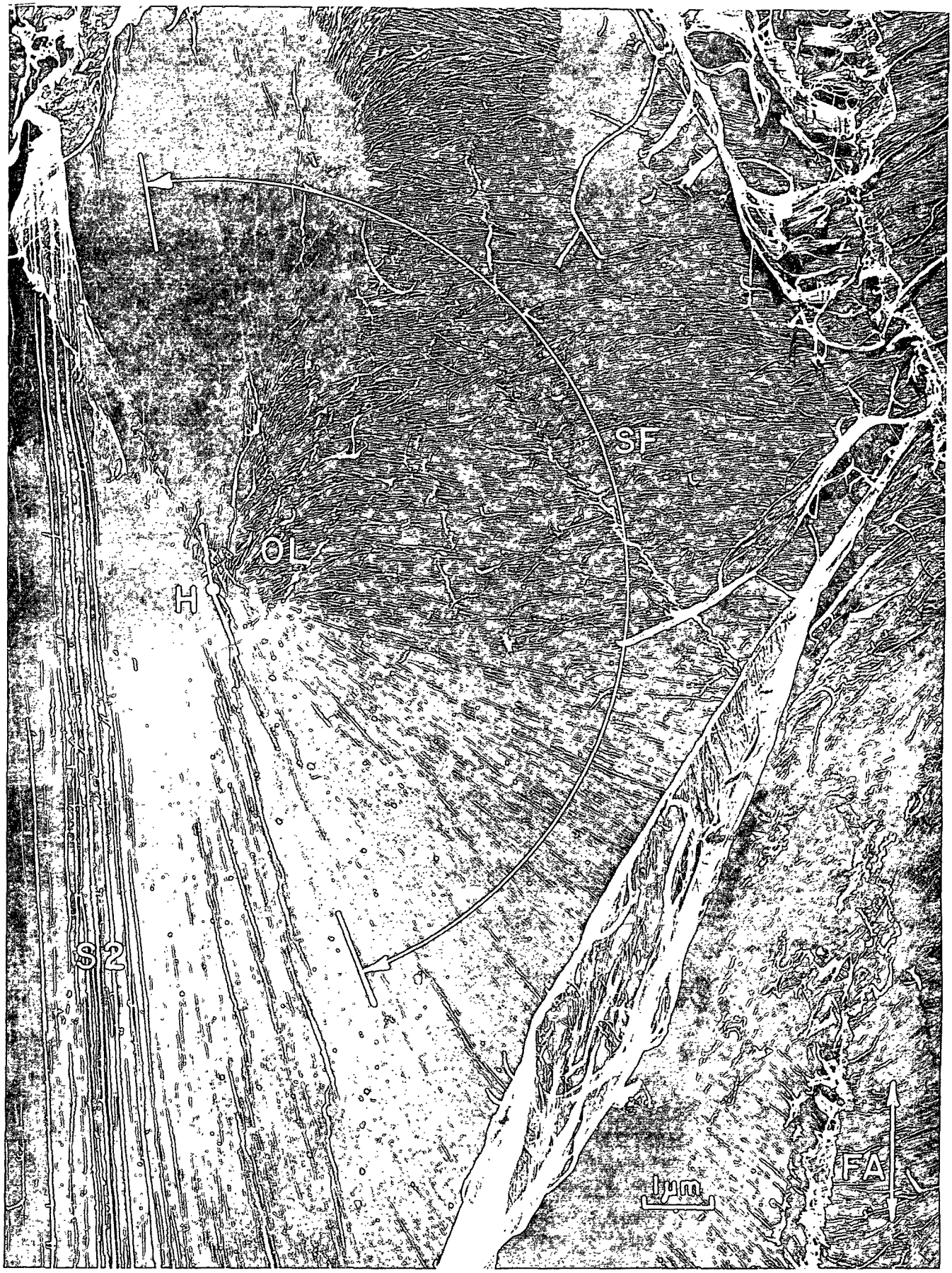
SF
OL
H
S2
1μm
FA

Figure 81. A Smooth, "Spread-Fan" Transition (S3-S2) in Which Overlapping Lamella Edges Are not Apparent

SF: "spread-fan" transition

OL: overlapping lamellae covering part of the spread fan

Plate Number: 4342-4343 AF

Magnification: 10,400X

Specimen Preparation: KOH-BOA, FD, FWS, lumen surface scraped and peeled, STR

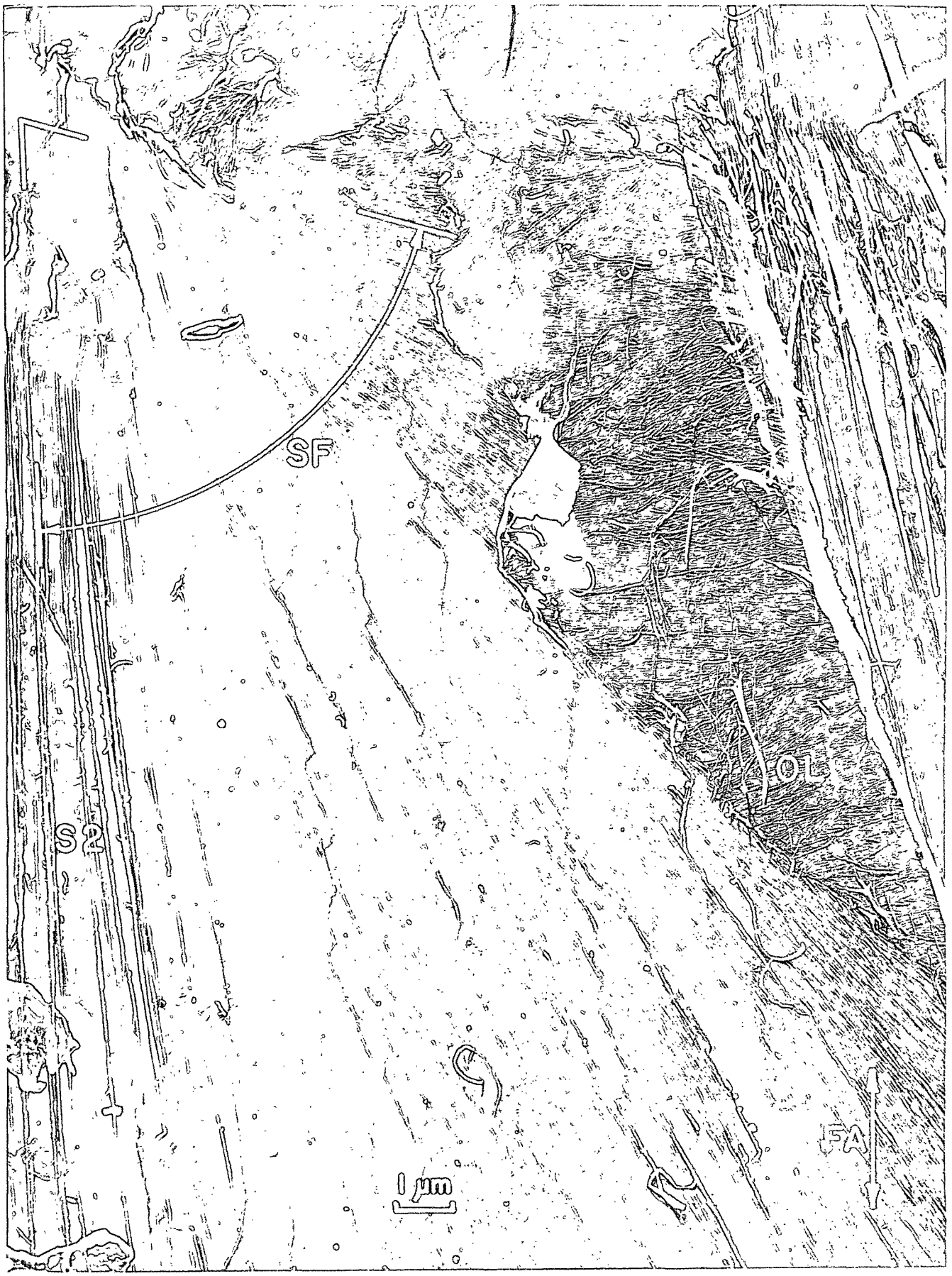
SF
SP
OL
1 mm

Figure 82. An Overall View Summarizing the S3 Structure

LS: lumen-surface lamella (1)

1-5: counterclockwise rotation of orientation

5/6: reversal of rotation

6-12: clockwise rotation

TE: a thick torn edge

M: mudlike material on the surface.

Plate Number: 4457-4458 AF

Magnification: 12,700X

Specimen Preparation: 0.1N KOH, FD, FWS, lumen surface scraped and peeled, STR (other half of fiber in Fig. 77)

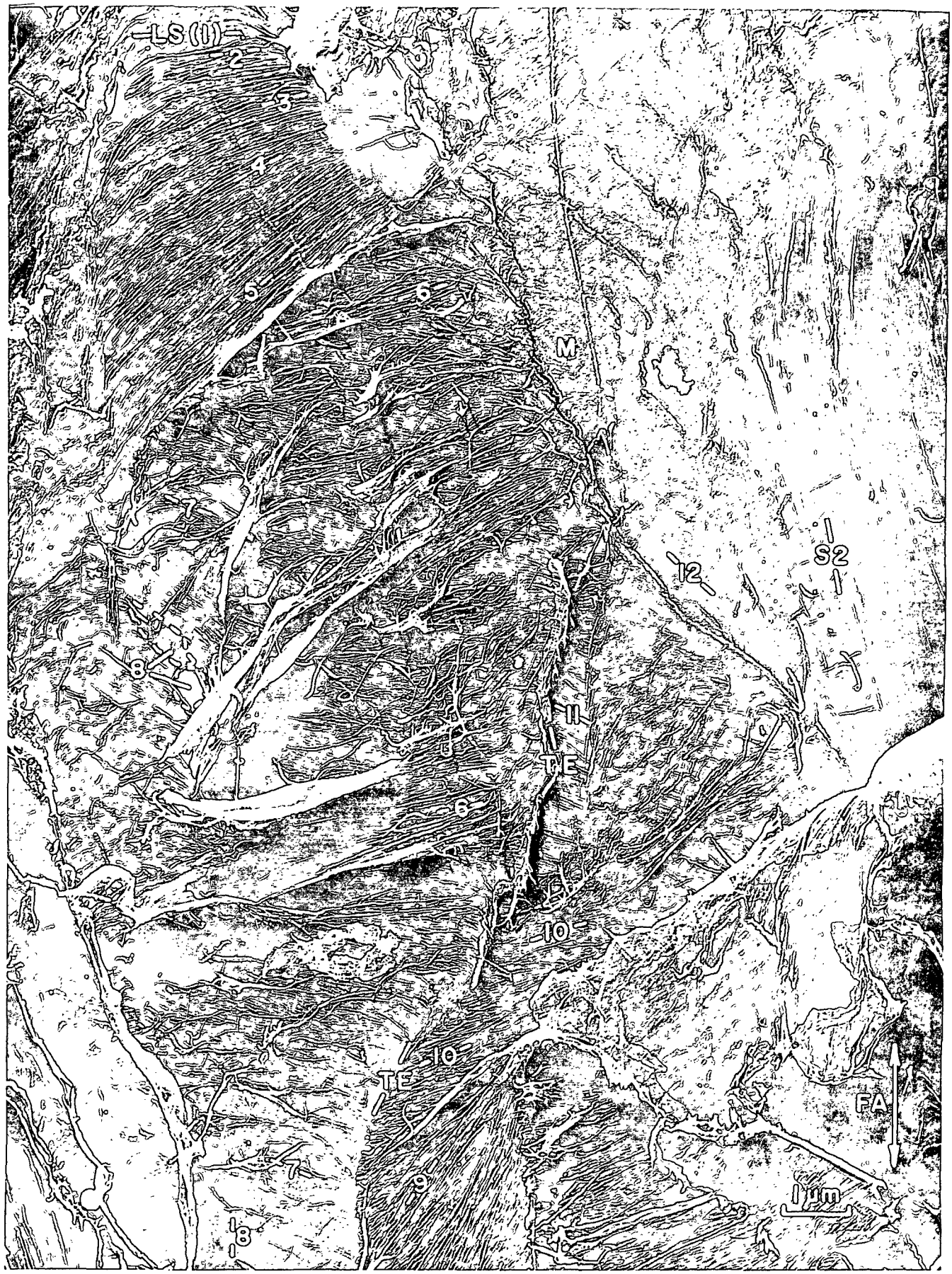
LS (I)
M
S2
PE
TE
FA
1 µm

Figure 83. An Overall View Summarizing the S3 Structure

LS: lumen surface (1)

1-4: counterclockwise rotation of orientation

4/5: reversal of rotation

5-12: clockwise rotation (This micrograph does not show a smooth transition to the S2, though other lamellae making this transition may well have been present in the fiber. Thus, the number of lamellae counted may be a minimal number.)

M: mudlike material retained on the S2

FA: fiber axis (drawn perpendicular to grid bar seen in upper right-hand corner)

Plate Number: 4435-4436 AF

Magnification: 8200X

Specimen Preparation: 0.1N KOH, FD, FWS, lumen surface scraped and peeled, STR


LStr
2
3
4
S2
5
6
M
7
7
S2
9
10
11
FA
12
8
5 µm

Figure 84. An Overall View Summarizing the S3 Structure

LS: lumen surface

1-4: counterclockwise rotation

4/5: rotation reversed

5-12: clockwise rotation (The rotation from 11 to 12 is quite abrupt; so that other lamellae may be present but not visible.)

SC: scraped areas probably touched by dissecting tools

Plate Number: 4496-4497 AF

Magnification: 9700X

Specimen Preparation: 9% KOH, FD, FWS, lumen surface scraped and peeled, STR


S2
S2
10
9
8
SC
LS(I)
7
6
7
3
2
3
4
5
5
7
6
7
SC
SC
LS(I)
FA
1μm

Figure 85. An Overall View Summarizing the S3 Structure

LS: lumen surface (1)

LL: a loose layer torn back to expose the internal S3 structure

1-4: counterclockwise rotation (other lamellae may be hidden in the abrupt tear)

4/5: reversal in rotation

5-12: clockwise rotation (in the case of 5, 9, and 10, only fragments of these lamellae remain)

M: mudlike material retained on the S2 surface

Plate Number: 4281 AF

Magnification: 16,200X

Specimen Preparation: 0.1N KOH, FD, FWS, lumen surface scraped and peeled, STR


LL
LS (I)
LS (II)
M
M
M
S2
S2
S2

Two representative micrographs of these replicas are shown in Fig. 86 and 87. The areas displayed are lumen surfaces of latewood tracheids. As can be seen from these pictures, the cells differed markedly in the number and size of warts on their surfaces. As to variation in size, the warts ranged from less than 0.1 μm. to more than 0.5 μm. in diameter. As to variation in number, some of the tracheids actually had very few warts. Others had many large warts. In any case, these micrographs clearly demonstrate that the wartlike deposits can be found on the lumen surfaces of longleaf-pine tracheids.

The Effect of Alkali Extraction on the S3 Layer

The successive changes in the fibers subjected to progressive stages of alkali extraction were studied for the lumen surfaces as well as the external surfaces already discussed. The objective of this section will be to summarize those stages of change. The changes are considered as relative to the nonextracted surfaces; so the discussion will begin with those surfaces.

The Nonextracted Fibers

Figures 88-90 are three example micrographs of nonextracted lumen surfaces and show much of the surface to be covered over with mud- or plasterlike material. In other areas, though, the microfibrils were plainly visible through the covering layer. These exposed fibrils were, however, slightly covered with fine-grain material.

Over much of the nonextracted surface, small moundlike deposits were visible. Some were small and sharply pointed (Fig. 88), and some were flattened and wider (Fig. 89). These features are assumed to be remnants of the wartlike structures discussed earlier. Dimensionally, this possibility is plausible, since these mounds are generally within the 0.1-0.5-μm. size range found earlier for the untreated warts.

One observation which was quite common through all the stages of extraction was the presence of raised fibrillar arches as in Fig. 90 and 91A. These arches

appeared to be part of the surface layer and, just as the fibrils of that layer, lay nearly perpendicular to the fiber axis. However, no certain explanation for the arches has been found. They were not seen on the untreated lumen surfaces in the wood sections (Fig. 86 and 87), suggesting that they rise after delignification. One can speculate that the fibrils forming the arches could have been under tension before delignification and that they relaxed into the lumen cavity upon being freed. Another possibility is that the tension applied to the inner layer by the spreading out of the cylindrical fiber could have caused some of the surface fibrils to rise from the surface. However, both of these possibilities are questioned when one observes the apparent slackness of the arches in Fig. 90 and 91A. Furthermore, even the suggestion that the structures are not present in untreated wood can be questioned on the basis that the holocellulose fibers and the untreated wood sections (Fig. 86 and 87) were not from the same tree. Thus, the fibrillar arches cannot be conclusively explained, though they were commonly observed.

The Fibers Extracted with 0.1N KOH

The readily apparent effect of the extraction with 0.1N KOH was to remove much of the plasterlike material from the surface fibrils. Also, another effect was to remove all of the wartlike mounds. Figures 92 and 93 are typical micrographs from such extracted surfaces. However, as Fig. 93 shows, portions of the surface still retained patches of the mudlike covering. (The very fine beads on the fibrils in this picture are suspected of being artifacts, because they were also found on newly exposed internal surfaces.) Some of the fibers actually had their lumen surfaces largely covered with the plastering material as in Fig. 94. In this picture, only small areas of exposed fibrils are visible.

One other micrograph of a 0.1N-extracted fiber illustrates a phenomenon which was common in all of the fibers spread open after slitting. Figure 95 shows a jagged crack in a lumen surface. This crack runs along the length of the fiber

Figure 86. A View of an Untreated Lumen Surface Showing Both Large and Small Wartlike Structures

FA: fiber axis (drawn parallel to the wrinkled cut edge)

Plate Number: 4369 AF

Magnification: 12,800X

Specimen Preparation: Explained in adjoining text

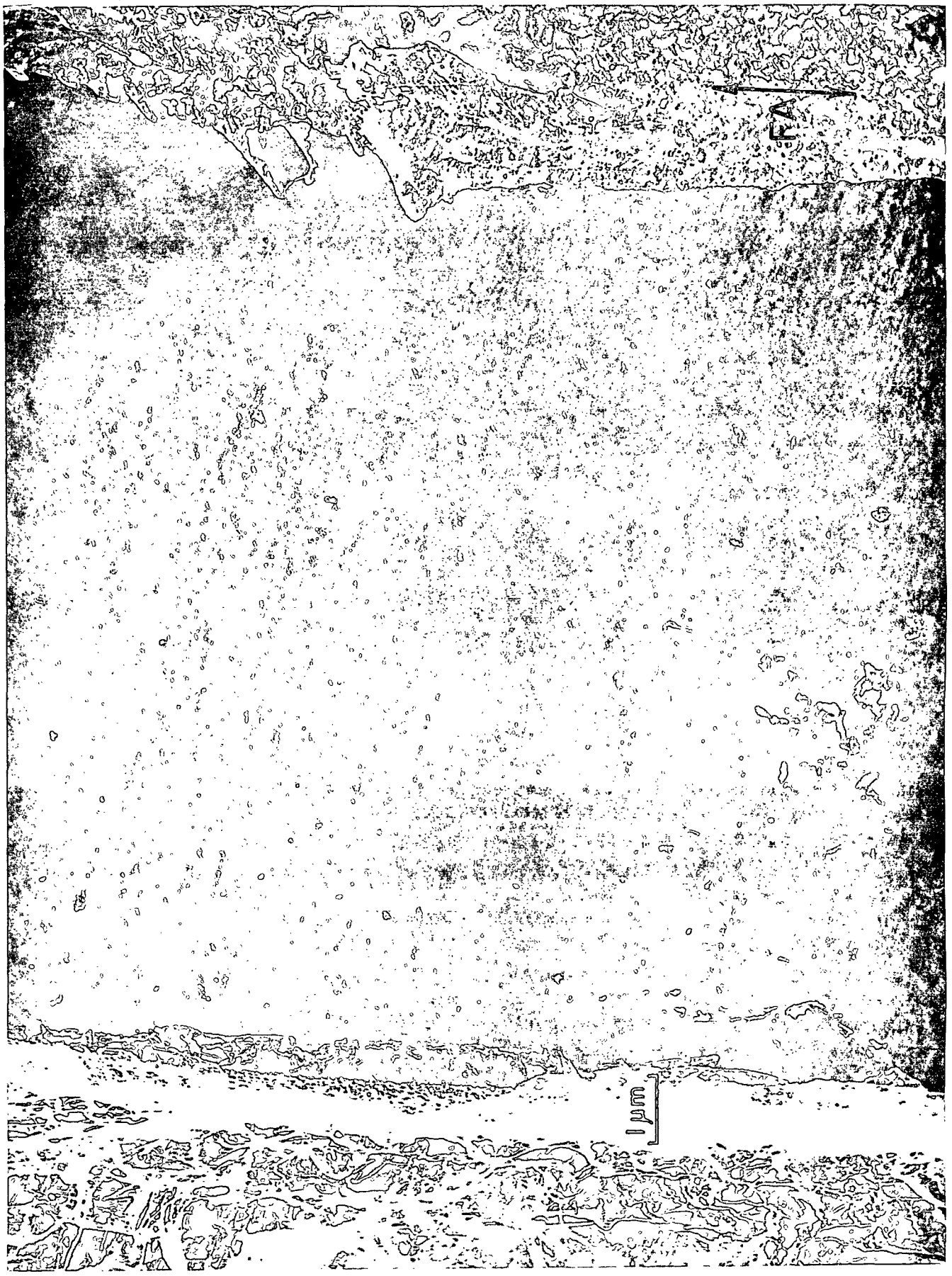
1 µm

Figure 87. A View of an Untreated Lumen Surface Showing Many Large Wartlike Structures

FA: fiber axis (drawn parallel to the cut edge)

Plate Number: 4368 AF

Magnification: 12,800X

Specimen Preparation: Explained in adjoining text. Note: Incidentally, Fig. 86 and 87 are the only electron micrographs in the thesis which show non-delignified wall material. (The light micrograph by Bailey, Fig. 28, shows a nondelignified cross section.)

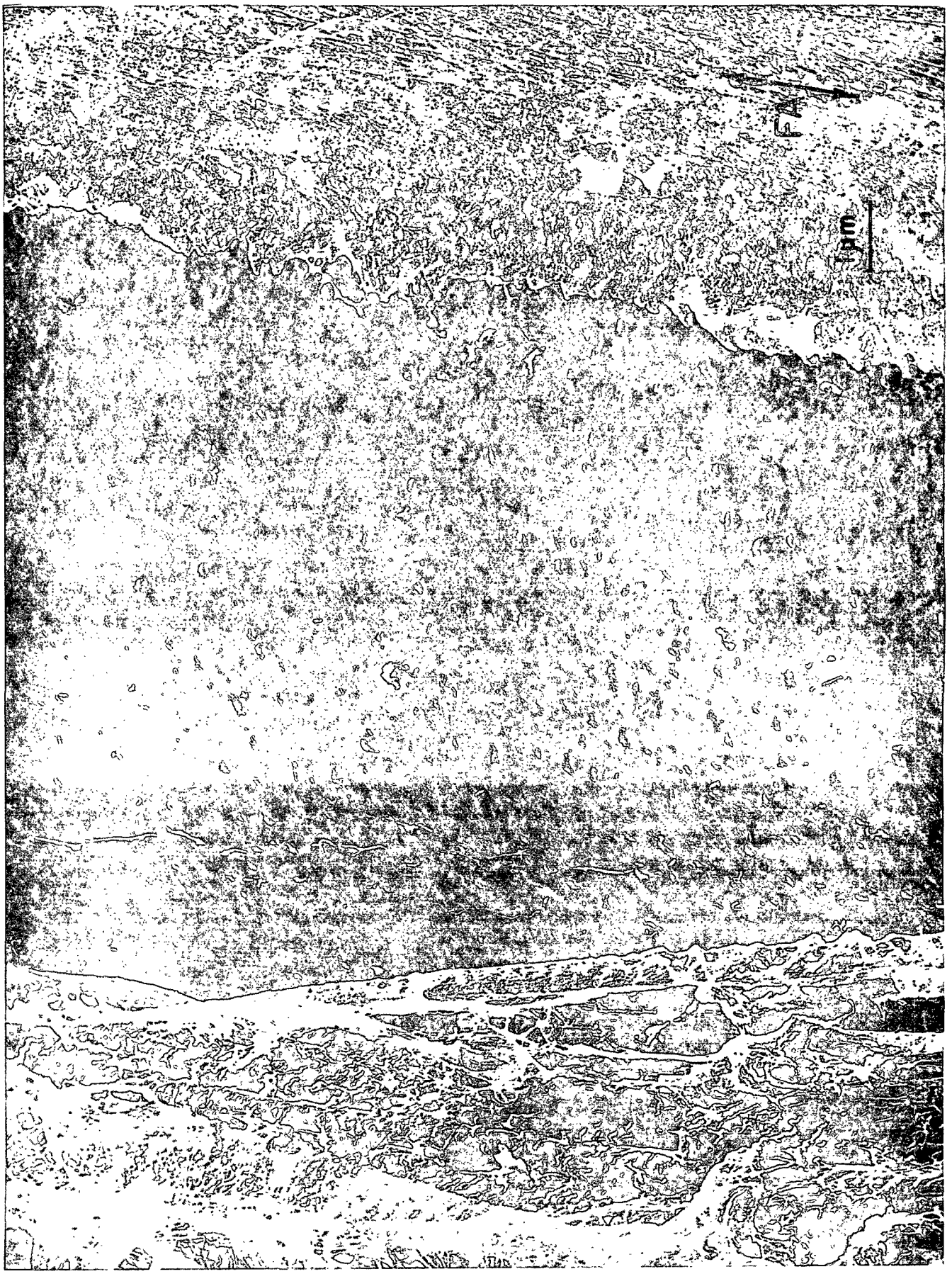
FA
pm

Figure 88. The Lumen Surface of a Nonextracted Fiber, Showing Small, Peaked, Wartlike Structures (Arrows)

M: remaining mudlike material

EF: exposed fibrils (covered with a grainy material)

Plate Number: 3177 AF

Magnification: 23,600X

Specimen Preparation: NONEXTR, FD, FWS, STR


M
FA
1 μm
M

Figure 89. The Lumen Surface of a Nonextracted Fiber, Showing Flattened, Moundlike Structures (Arrows)

EF: exposed fibrils

W: wrinkles in the surface layer

Plate Number: 3175 AF

Magnification: 23,600X

Specimen Preparation: NONEXTR, FD, FWS, STR


FA
1 μm
FF
W
W
W

Figure 90. The Lumen Surface of a Nonextracted Fiber, Showing Raised Fibrillar Arches Nearly Perpendicular to the Fiber Axis

Plate Number: 3170 AF

Magnification: 12,600X

Specimen Preparation: NONEXTR, FD, FWS, STR

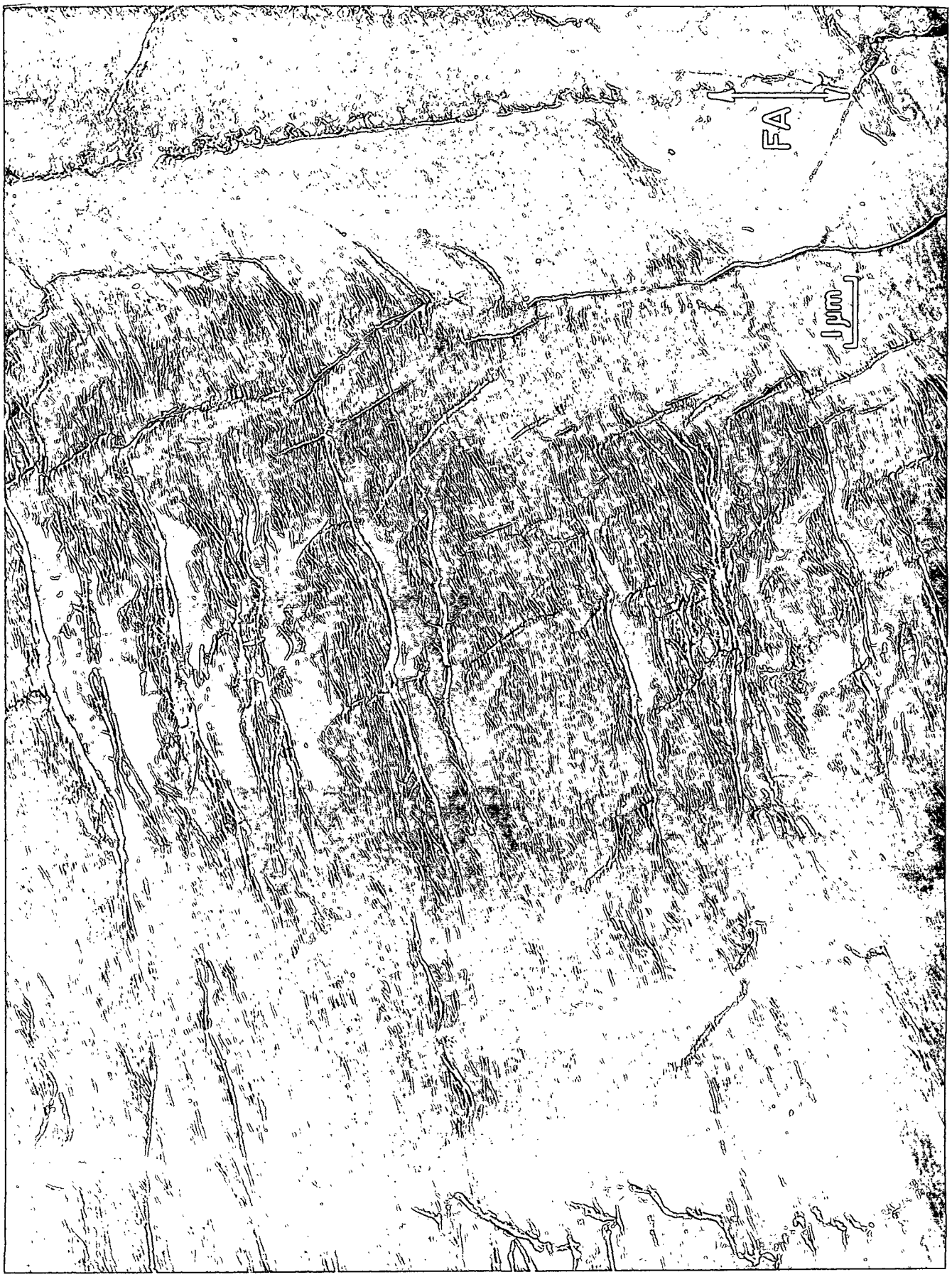
FA
1 μm

Figure 91A. Raised Fibrillar Arches on a Lumen Surface

Plate Number: 5141 AF

Magnification: 4700X

Specimen: Same as in Fig. 90

Figure 91B. A Longitudinal Crack in a Lumen Surface

Plate Number: 5142 AF

Magnification: 3300X

Specimen: 9% KOH, FD, FWS, STR

Figure 91C. Loosened Fibrillar Arches on a Lumen Surface

Plate Number: 5143 AF

Magnification: 10,000X

Specimen: 9% KOH, FD, FWS, STR

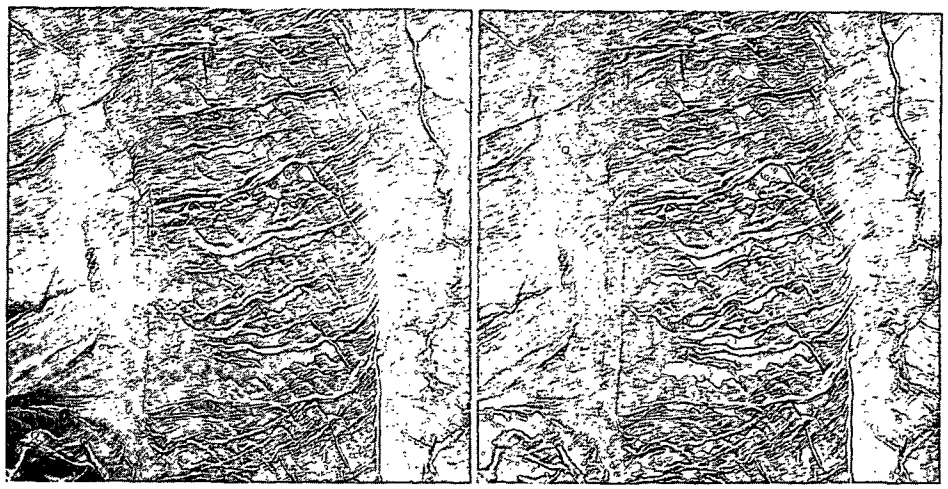

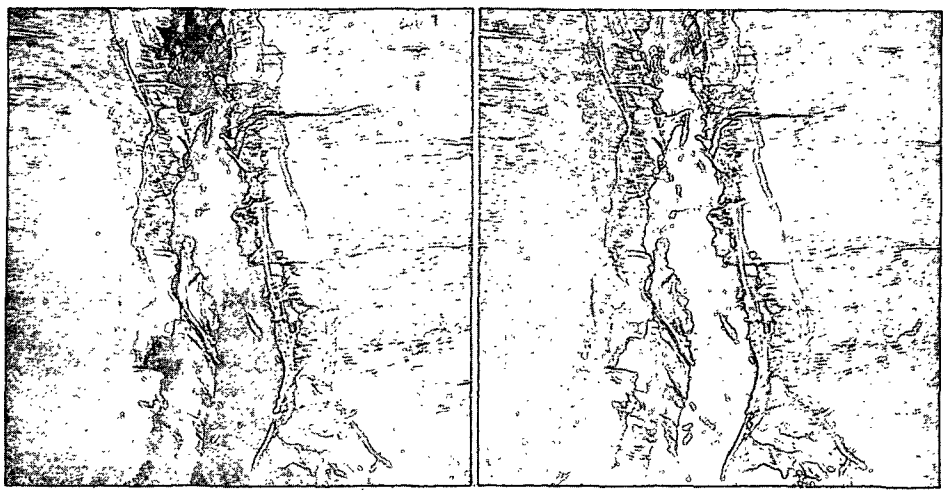

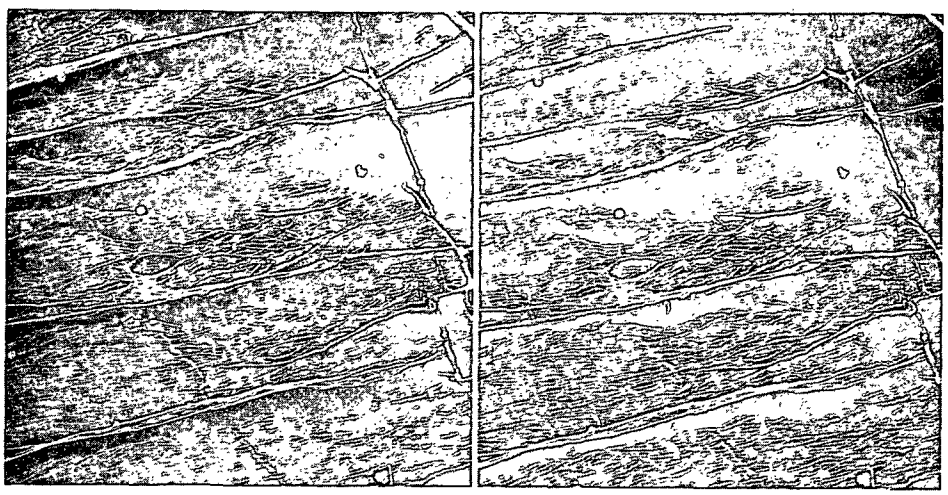

Figure 92. The Lumen Surface of a Fiber Extracted with 0.1N KOH, Showing that the Mudlike Material and Wartlike Structures Have Been Removed

W: wrinkles in the surface layer

Plate Number: 3260 AF

Magnification: 27,500X

Specimen Preparation: 0.1N KOH, FD, FWS, STR


1 μm
FA
W
W

Figure 93. The Lumen Surface of a Fiber Extracted with 0.1N KOH, Showing a Patch of Mudlike Material Retained on the Surface

M: patch of mudlike material

PD: unexplained platelike deposit

B: fine beads (suspected artifacts)

Plate Number: 3233 AF

Magnification: 17,300X

Specimen Preparation: 0.1N KOH, FD, FWS, STR


FA
1 µm
B
PD
M

Figure 94. The Lumen Surface of a Fiber Extracted with 0.1N KOH. Most of the Surface Has Remained Covered with the Mudlike Material, Though the Fibrils Have Been Exposed in some Areas

M: mudlike material

EF: exposed fibrils

RC: replica cracks

H: a hole in the replica (The replica fragments are held together by the secondary carbon coating, which bridges this hole, also.)

Plate Number: 2441 AF

Magnification: 18,400X

Specimen Preparation: 0.1N KOH, FD, FWS, STR

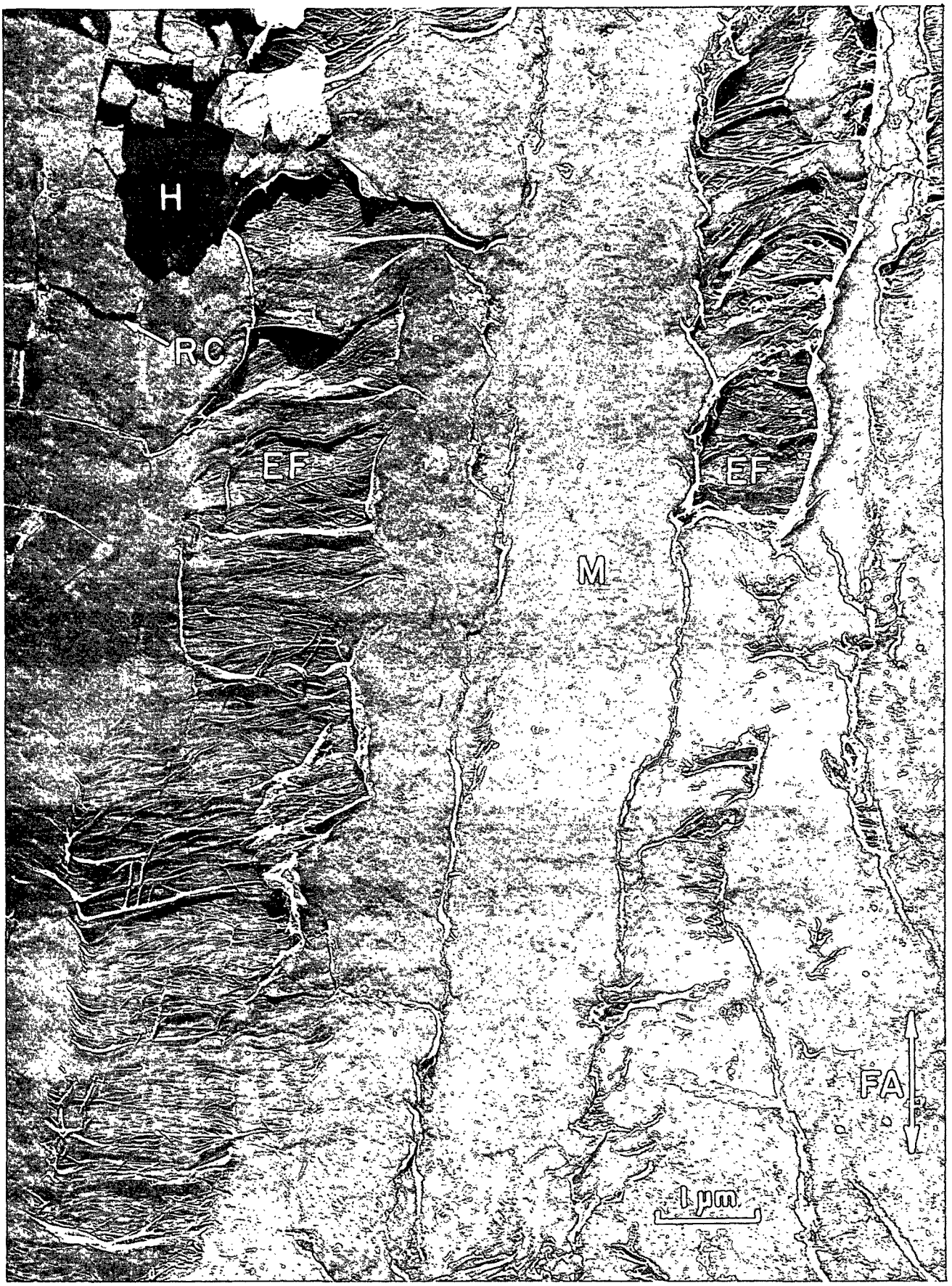
H
RC
EF
EF
M
FA
1μm

Figure 95. The Lumen Surface of a Fiber Extracted with 0.1N KOH, Showing Especially a Crack in the Surface Layer

ES: edges of the surface layer (To show that the surface layer has cracked, one can mentally fit together the edges of the cracked layer. Thus, 1-1 and 2-2 appear to be matching edges of the crack.)

EI: edges of internal lamellae which have also cracked

DF: dense films which are artifacts of replication (Appendix IX)

FA: fiber axis (nearly parallel to the crack)

Plate Number: 2574 AF

Magnification: 27,000X

Specimen Preparation: 0.1N KOH, FD, FWS, STR


DF
FA
DF
DF
ES
DF
1
2
ES
EI
EI
2
EI
ES
DF
1 μm

and exposes inner lamellae of the cell wall. A stereo view of another, similar crack (which happens to be in a fiber extracted with 9% KOH) is given in Fig. 91B. These cracks in the lumen lining are believed to result from the stressing of that layer caused by forcing the slit fiber to spread open (Fig. 96).

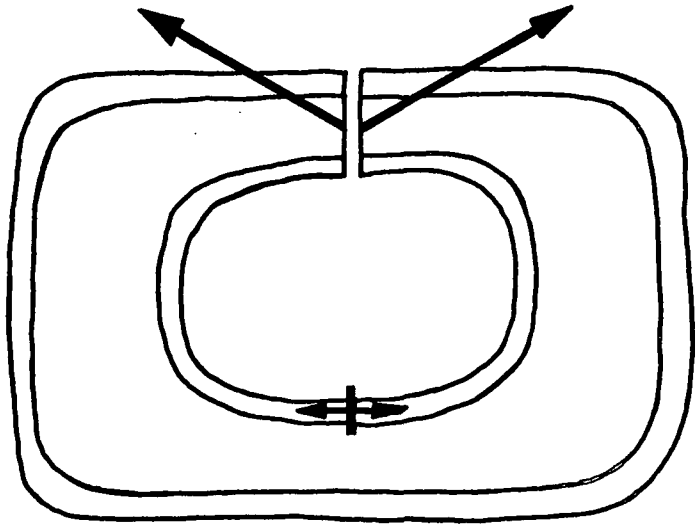

Figure 96. A Cross Section of a Slit-Open Fiber. The Arrows Are Schematic Indicators of the Tension Forces During the Spreading out of the Fibers, Showing How Longitudinal Cracks in the S3 Layer Could Result from This Operation

The Fibers Extracted with 9% KOH

Many of the lumen surfaces extracted with 9% KOH were not greatly different from those extracted with 0.1N KOH. Figure 97 shows one such surface with apparently clean microfibrils and one persistent patch of mudlike material. The surfaces also included the previously mentioned fibril arches (though somewhat loosened) as in Fig. 91C. Also, some of the fibers had large plastered areas with patches of exposed, loosened fibrils (Fig. 98), differing from Fig. 94 only in degree of exposure.

Thus, one general picture of the 9% KOH-extracted lumen surfaces is a picture of microfibrils still in place, though possibly loosened. However, about a third or

fourth of the fibers had areas which showed signs of a detachment of the surface lamellae from the rest of the cell wall. In fact, Fig. 99 and 100 show areas of two fibers in which a general detachment along the entire fiber lengths was apparent. In both of these micrographs the surface lamellae can be seen to be detached and crumpled, lying loosely in the cell cavity. Nevertheless, the surface fibrils appear to be still held in place in the original surface lamellae. Thus, the general condition in many of the 9%-extracted fibers might well be a loosening--or even detachment--of the lumen-surface lamellae from the cell wall, though these lamellae might still lie in place. The greater ease with which the extracted fibers can be scraped and peeled at least supports this possibility.

In agreement with these observations, Bucher (96) had already observed a separation of a thin lamella from the cell wall during maceration with alkali (or acid). He believed that the lamella detached was his "tertiary wall." However, the separation observed in this work took place not between the S3 and S2 layers, but within the S3 layer itself. Even that separation was not a clean delamination between two touching lamellae, but was, rather, a confused disruption involving several lamellae (Fig. 99 and 100).

The Fibers Extracted with 9% KOH plus 3% Borate

About 60% of the fibers extracted with 9% KOH plus 3% borate had their lumen-surface lamellae generally intact, as in Fig. 101 and 102. The remaining 40% of the fibers appeared to have lost some of the surface lamellae. Figures 103 and 104 show the exposed surfaces of two such fibers. The significant observation about these two micrographs is that the lamellae lying just below the uppermost lamellae have orientations slightly clockwise from the lines of those first lamellae. When related to the pattern of S3 structure discussed earlier, this observation means that the detachment of the surface lamellae took place either at the orientation-reversal plane or between that plane and the S2.

Figure 97. The Lumen Surface of a Fiber Extracted with 9% KOH. The Fibrils Are Quite Clean of Mudlike Material, Though One Patch of such Material Does Persist

M: mudlike material

Plate Number: 2910 AF

Magnification: 19,300X

Specimen Preparation: 9% KOH, FD, FWS, STR

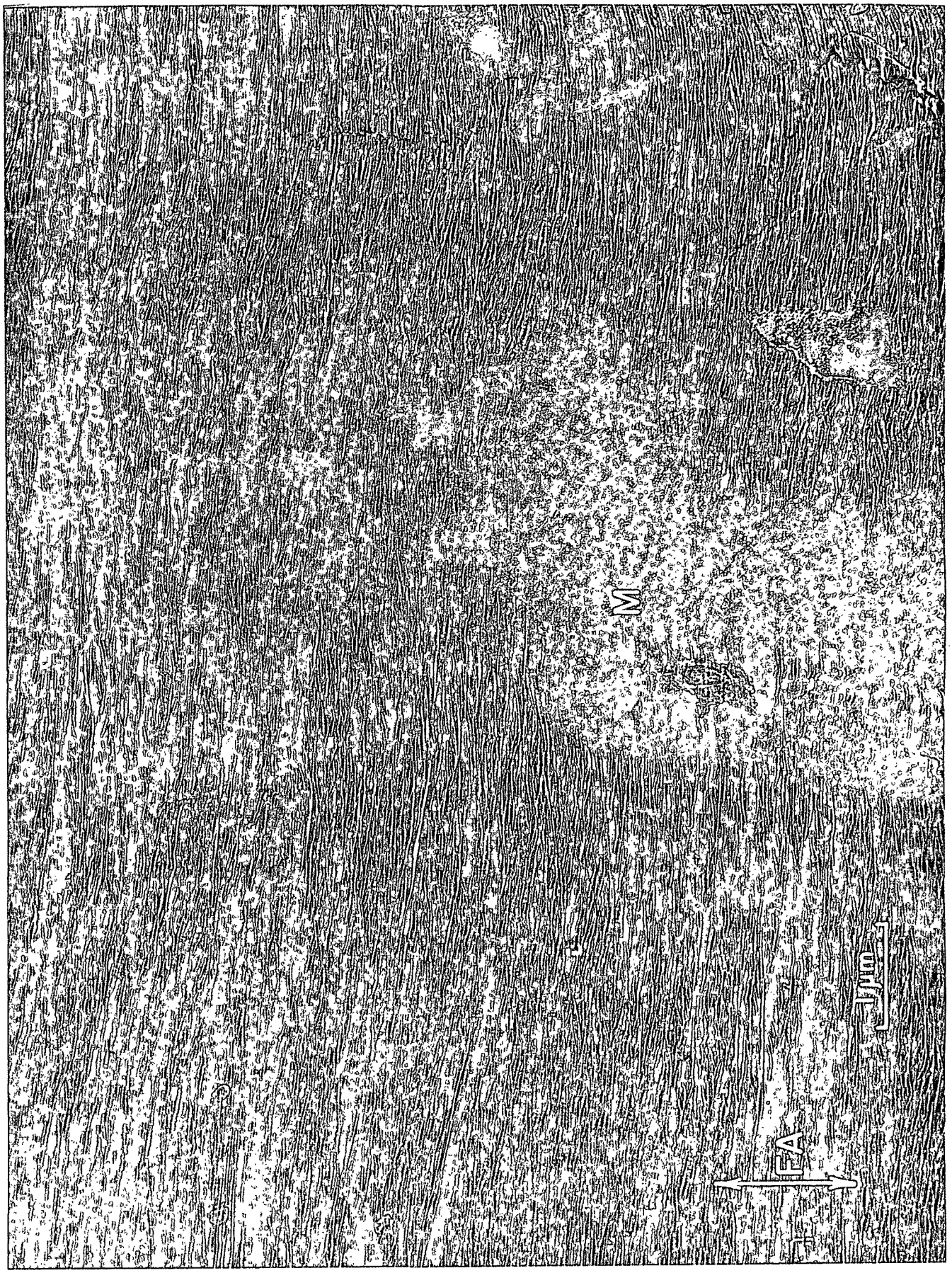
N
FA

Figure 98. The Lumen Surface of a Fiber Extracted with 9% KOH. Though some Mudlike Material Has Been Retained, Most of the Fibrils Have Been Uncovered and Loosened

M: mudlike material

EF: exposed and loosened fibrils

H: a hole in the replica

Plate Number: 2587 AF

Magnification: 12,600X

Specimen Preparation: 9% KOH, FD, FWS, STR

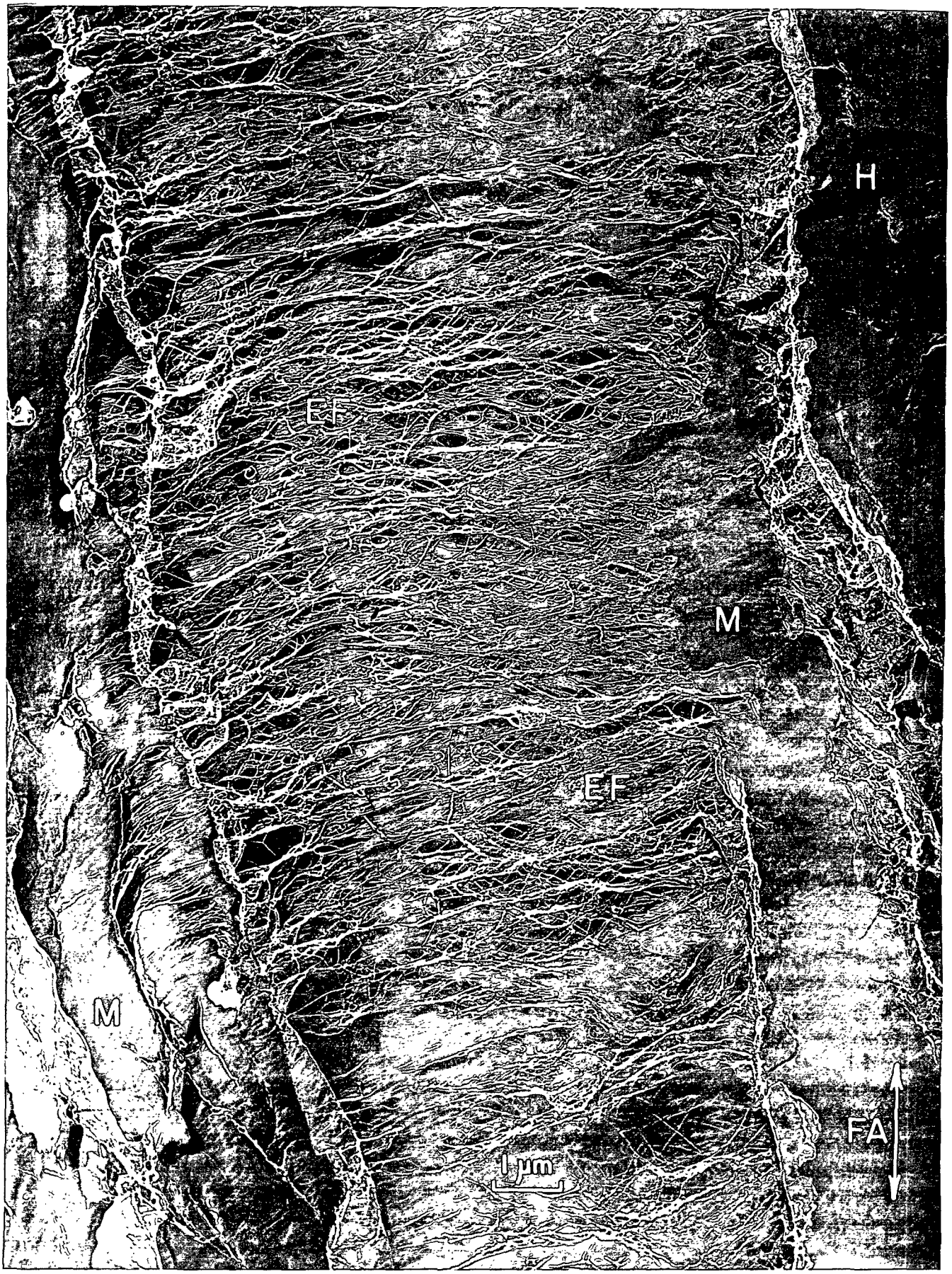
H
EF
M
EF
M
FA
1 μm

Figure 99. The Lumen Surface of a Fiber Extracted with 9% KOH, Showing Especially a Crumpled Flag of Surface Lamellae Folded Back

CF: crumpled flag of loose, surface lamella

I-S3: an internal surface of the S3

LS: lumen-surface fibrils

Plate Number: 3013 AF

Magnification: 7700X

Specimen Preparation: 9% KOH, FD, FWS, STR


FA
S3-1
S3-2
S3-3
S3-4
S3-5
CF
LS
5 mm

Figure 100. The Lumen Surface of a Fiber Extracted with 9% KOH, Showing Crumpled Debris from Loosened Surface Lamellae

CL-LS: crumpled layer of lumen-surface material

I-S3: exposed internal surfaces of the S3

LS: lumen surface

TE: torn edge

S2: S2 fibrils visible through a crack in the surface

LS: lumen surface

RC: replica cracks

Plate Number: 2589 AF

Magnification: 3800X

Specimen Preparation: 9% KOH, FD, FWS, STR


LS
TE
I-S3
CL-LS
I-S3
S2
RC
FA
10 μm

Figure 101. The Lumen Surface of a Fiber Extracted with 9% KOH Plus Borate. The Original Surface Lamella Appears to Be Intact (Though Cracked Along Its Length as Normal)

W: wrinkles in the surface layer

CS: crack in the surface layer

SC: scratches left in the surface by the dissecting tools

Plate Number: 2964 AF

Magnification: 11,300X

Specimen Preparation: KOH-BOA, FD, FWS, STR

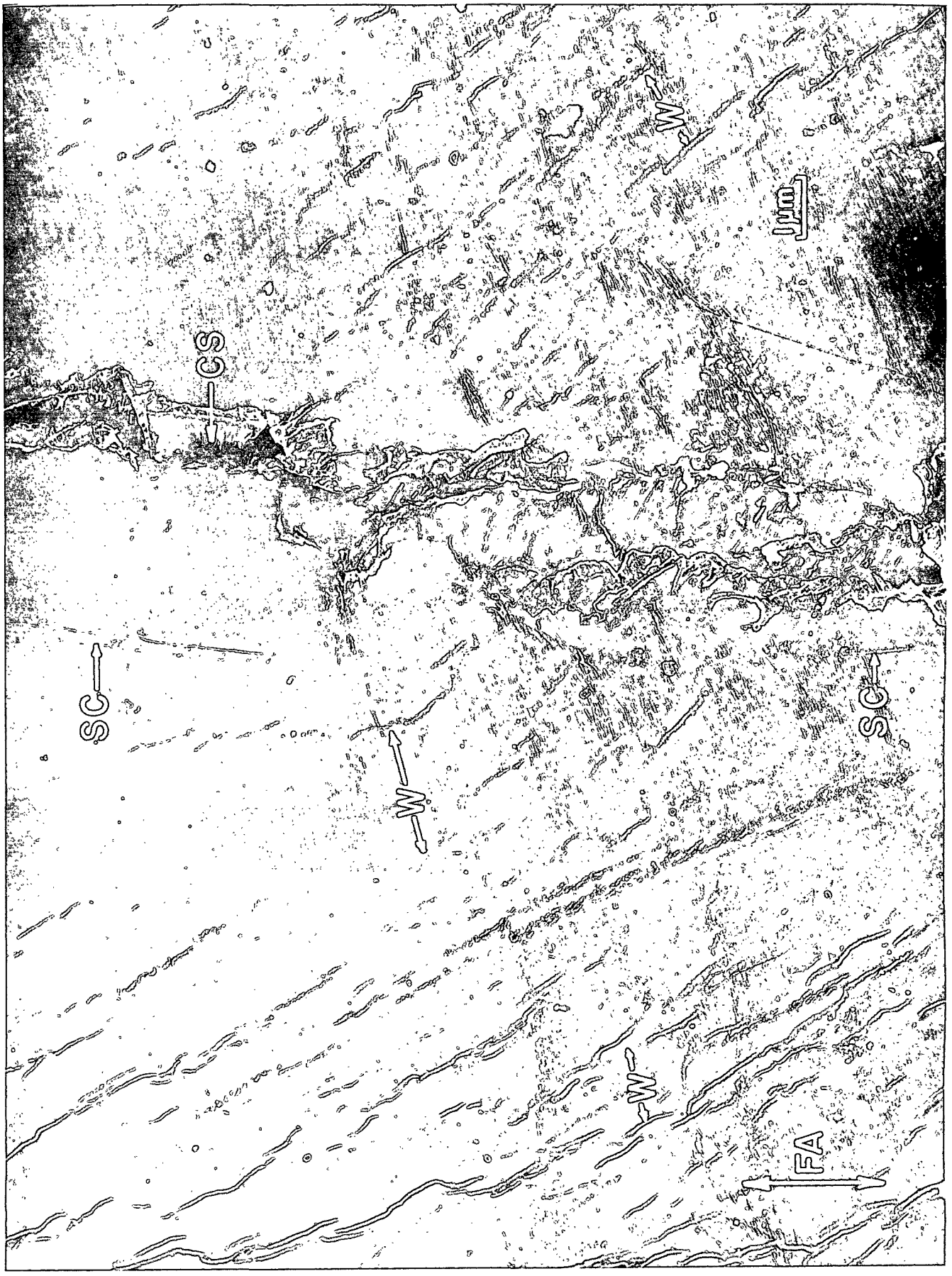
SC
SC
SC
W
W
W
FA

Figure 102. The Lumen Surface of a Fiber Extracted with 9% KOH Plus Borate. The Original Surface Lamella Appears to Be Intact

M: a patch of mudlike material which has persisted through the several extraction stages

RC: replica crack

Plate Number: 2967 AF

Magnification: 30,300X

Specimen Preparation: KOH-BOA, FD, FWS, STR

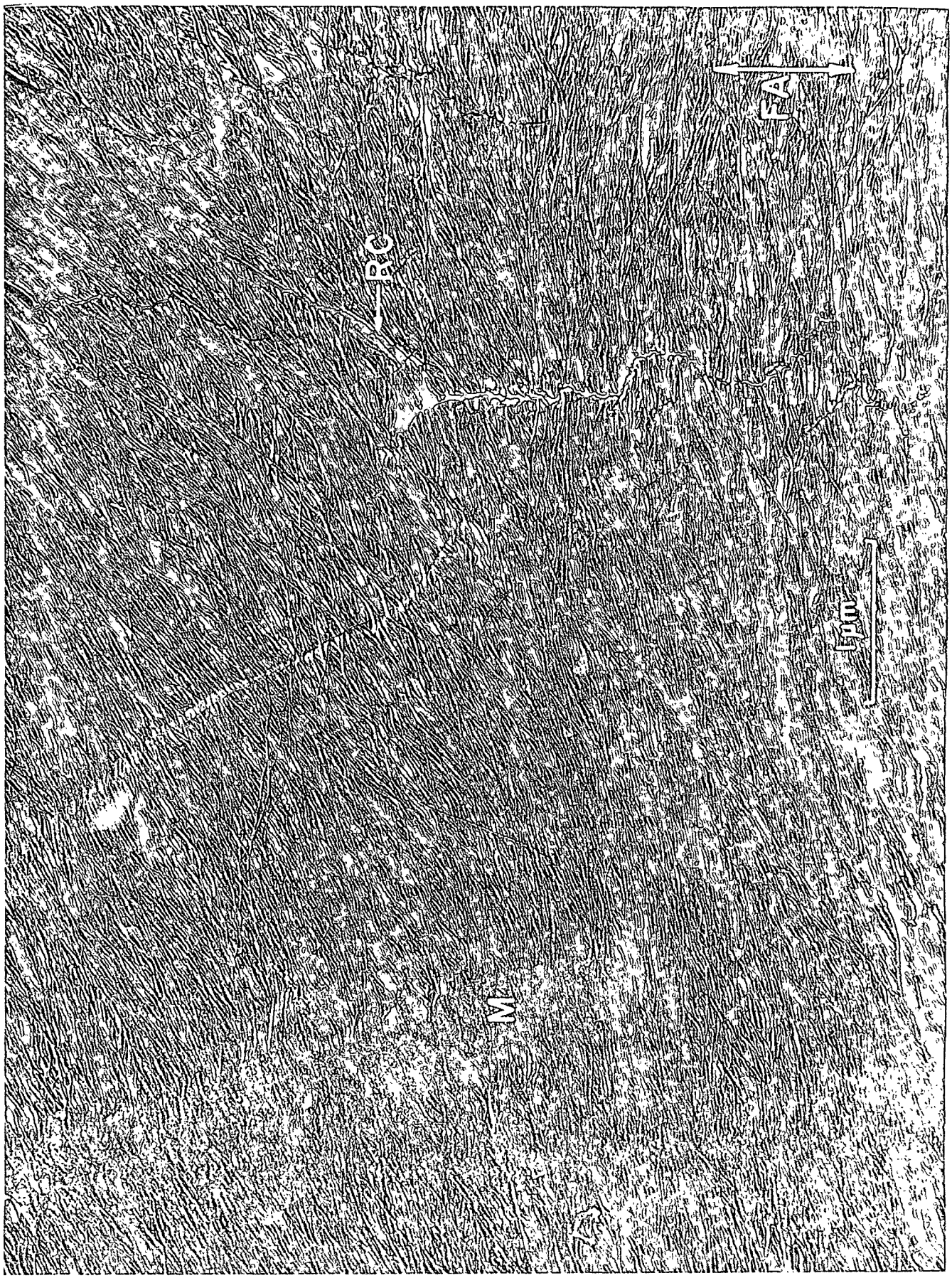
Pbc
Tpm
M

Figure 103. The Lumen Surface of a Fiber Extracted with 9% KOH Plus Borate. Some of the Surface Lamellae Apparently Were Lost During Chemical Treatment of the Fiber

SF: surface fibrils

UL: underlying fibrils

CR: clockwise rotation from the direction of the surface fibrils to the direction of the underlying fibrils (this rotation verifies the removal of the surface lamella believed to have taken place)

M: mudlike material on the internal S3 surface

RC: replica crack

Plate Number: 2966 AF

Magnification: 15,400X

Specimen Preparation: KOH-BOA, FD, FWS, STR


Bridge
Mill
Mill Pond
Mill Pond

Figure 104. The Lumen Surface of a Fiber Extracted with 9% KOH Plus Borate. Some of the Surface Lamellae Apparently Were Lost During Chemical Treatment of the Fiber

SF: surface fibrils

LF: a loose flag of surface fibrils being peeled back

UL: underlying lamella

CR: clockwise rotation from the orientation of the surface fibrils to the orientation of the underlying lamella

P: pit through the cell wall

SC: scratches in the surface caused by the dissecting tools

Plate Number: 2968 AF

Magnification: 10,400X

Specimen Preparation: KOH-BOA, FD, FWS, STR


SC
SF
LF
UL
CR
1μm
P
FA

A brief mention of a related experience might be of interest to the reader at this point. One fiber (Fig. 105) was thought to have had some of its lamellae removed, because the characteristic vertical wrinkles seen in Fig. 101 were not present. On the other hand, the pattern of the surface fibrils looked so much like that of the normal lumen surface that the loss of the surface lamellae was somewhat in doubt. The partial visibility of the underlying lamella and the observed clockwise rotation of this lamella, though, resolved the question. The direction of rotation indicated that these lamellae had lain below the plane of reversal, meaning that the surface lamellae had, in fact, been removed.

Close scrutiny of Fig. 103 and 105 suggests that the separation of the surface lamellae took place either in or very close to the plane of rotation reversal. The reasoning is that within the region between the reversal plane and the S2, two planes of transverse orientation are normally observed--one very near the reversal and one near the S2 layer. Obviously, the surface fibrils in Fig. 103 and 105 lie nearly perpendicular to the fiber axis. Since no hint of the S2 layering is seen in these pictures, the visible transverse fibrils are thought to be equivalent to the transverse fibrils normally observed just below the plane of reversal. Furthermore, a comparison of these figures with those of the earlier section in which the orientation reversal was discussed reveals a close resemblance between these exposed surfaces and those surfaces known to lie just beneath the plane of reversal. Thus, the speculation of the author is that the detachment of the surface lamellae took place close to this plane of rotation reversal, at least for Fig. 103 and 105, which are thought to be representative samples. (The plane of cleavage exposed in Fig. 104 is more uncertain and is thought to be a special case.)

THE S2 LAYER

The boundary surfaces of the S2 layer have already been shown at both the S1-S2 interface (Fig. 43, 44, 47-49) and the S3-S2 interface (Fig. 79-85). However, some discussion of the internal S2 structure is believed to be worthwhile. Figures 106 and 107 are two micrographs showing internal lamellae of the S2 which were exposed by peeling apart the S2 layer. Actually, the two areas would have lain nearly back-to-back in the original cell wall. Figure 106 shows an area on the body of the fiber, and Fig. 107 shows the inner surface of the flag peeled up from the fiber wall. The important observation from these pictures is that the fibrils in the S2 have a distinct uniformity of orientation or alignment. In fact, reexamination of the earlier pictures shows that this distinction is indeed sharp enough to allow one to distinguish between the S2 and the less well-aligned S1 and S3 fibrils without even knowing the angle of orientation. Also, another difference is that many of the S2 microfibrils appear aggregated into larger bundles or fibrils, probably because of their better alignment and, subsequently, their greater ease of aggregation.

Another interesting observation about these two micrographs is the presence of mudlike deposits on the surfaces. Unfortunately, this material cannot be identified from these micrographs. Otherwise, one would be able to draw good conclusions as to the relation of the hemicelluloses to the fibrillar structure. Certainly, some system of staining to be used with surface replicas would be most useful, if such were available. Meanwhile, one approach taken during this work was to wash the surfaces with extracting solutions specific for known compounds of the cell wall. Though the attempt failed, the details of the effort are reported in Appendix VI because of some of the interesting incidental results obtained.

Figure 105. The Lumen Surface of a Fiber Extracted with 9% KOH Plus 3% Borate

SL: surface lamella

UL: underlying lamella (visible through outlined slit)

CR: clockwise rotation from orientation of surface lamella to orientation of underlying lamella

CS: crack in surface lamella

M: mudlike patch

RC: replica crack

Plate Number: 2970 AF

Magnification: 19,200X

Specimen Preparation: KOH-BOA, FD, FWS, STR

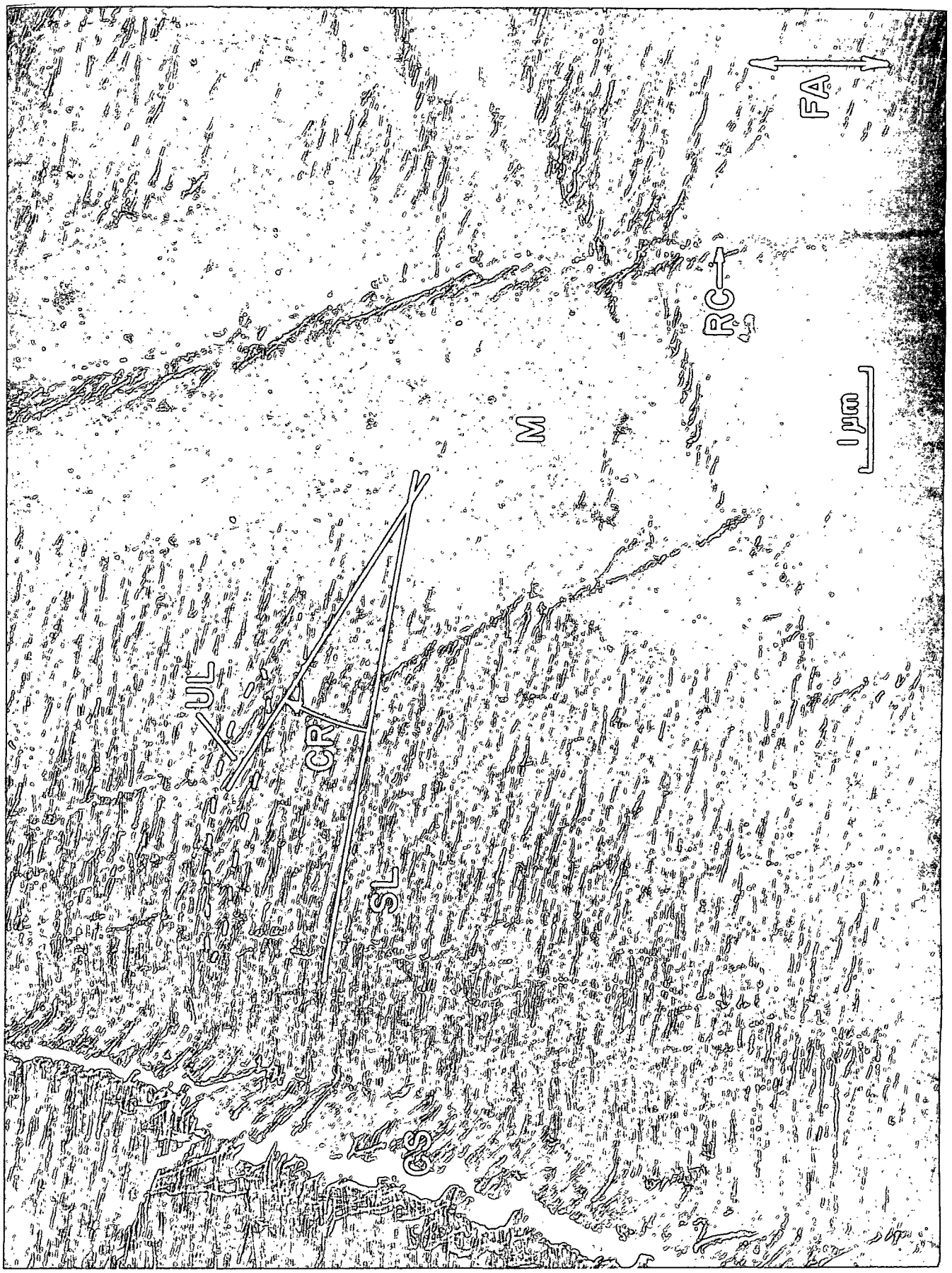
FA
RC
M
1 µm
UL
CR
SL

Figure 106. An Internal Surface of an S2 Layer Exposed by Pulling Back a Partial Layer of the S2

CE: cut edge of the cell wall

GA: grid axis (axis of the grid on which the replica was lying)

Note: This micrograph also illustrates the difficulty one has in designating exact fiber axes for the preceding micrographs. Assuming for a moment that the cut edge is parallel to the original fiber axis, one can see that the fiber replica lies at an angle to the grid axis, even though every effort was made to place the fiber replica parallel to the grid axis. Thus, a simple angular alignment of the grid axis in the microscope is not sufficient to guarantee an accurate record of the fiber-axis direction. On the other hand, the cut fiber edges were not usually visible because of edge wrinkling. Again, even if the edges were visible, they probably are not parallel to the fiber axes.

Plate Number: 4336

Magnification: 7700X

Specimen Preparation: Same specimen as in Fig. 81; KOH-BOA, FD, FWS, lumen surface scraped and peeled (A flag peeled back was not detached but was left lying on the fiber. Figure 107 is a micrograph showing the surface of the flag.) STR


CE
S2
GA
5 µm

Figure 107. The Surface of the Flag Peeled Back from the Surface Shown in Fig. 106. Of Course, This Micrograph also Shows Internal S2 Structure

M: mudlike material

W: wrinkles

SF: a small striplike flag which appears to have been pulled from the surface and then pressed back down

Plate Number: 4337 AF

Magnification: 16,100X

Specimen Preparation: Same specimen as in Fig. 106


1 μm
W
M
SF
W

One other matter which deserves comment is the question of whether the S2 layer is lamellated. Stone and Scallen (35) have embraced the concept that the S2 layer is made up of concentric lamellae that partially separate upon delignification. Actually, the theory that the fibrils are initially deposited in concentric lamellae has been strongly supported by birefringence microscopy (5, 17, 18). However, visual evidence of the suggested separation of the lamellae in the water-swollen condition has been obtained only by study of cell walls embedded in methacrylate, even though the methacrylate medium has been suspected of causing artifacts (36). The ultrathin sections prepared in this work did not show concentric lamellae, though some random checking and sponginess were evident. (These fibers had been embedded in epoxy resin instead of methacrylate. They also differed from the sections of other workers in that the embedding medium had not been washed from the sections before viewing in the microscope.)

On the other hand, many of the exposed and replicated S2 surfaces displayed some separation of fibrillar lamellae (Fig. 108 and 109). Thus, even though the presence of lamellar concentric voids in the cell walls cannot be supported by evidence from the thin sections, the peeling back of surface lamellae at least suggests an easier cleavage along the concentric surfaces.

With regard to fibril orientation in the S2, all of the S2 fibrils observed in this work were seen to lie in right-hand helixes. The helix angles (relative to the fiber axis) varied from about five to twenty degrees. Actually, no effort was made to assemble statistical charts of angle measurements, since the validity of the slit edge as a standard of direction would have to be certified in order for the measurements to be reliable. In other words, the slit edge might not always lie parallel to the fiber axis. Conceivably, a person interested specifically in making fibril-angle measurements could evaluate this possibility and either learn to correct the line of the edge or else devise a different standard of direction.

DISCUSSION OF THE CONCLUSIONS

The Cell-Wall Structure

The cell-wall structure of the longleaf-pine tracheids was interpreted according to the existing concept of a primary wall plus a secondary wall made up of three layers--S1, S2, and S3. The S1 layer was found to include at least three groups of fibrils: one group lying nearly perpendicular to the fiber axis, one group about 25° clockwise from the perpendicular, and one group about 30° counterclockwise from the perpendicular. Any of these groups could consist of one or more lamellae, or aggregates, of fibrils. In fact, the last-mentioned group includes several lamellae which perform a gradual transition to the S2 layer. This transition appears to be a stepwise change from lamella to lamella with the fibrillar orientation of each lamella rotated a slight counterclockwise angle from the one above it.

The S2 layer is made up of fibrils deposited in a right-hand thread and lying at an angle of 5 to 20° with the fiber axis. According to measurements on the thin sections, this layer makes up at least 75-80% of the cell-wall thickness in latewood, though measurements on cell walls embedded in the water-swollen condition can be questioned. The question of whether the S2 fibrils are divided into separated concentric lamellae in the water-swollen condition is still somewhat uncertain.

Adjacent to the S2 layer, the S3 lamellae were found to continue the stepwise transition seen in the S1, but the direction of rotation reverses to a clockwise stepping from one lamella to the next (proceeding from the S2 to the lumen surface and seen from a viewpoint in the S2). This rotation progresses more than 270°, ending with a left-hand helix at about 60° to the axis. Then, another reversal in rotation takes place with a few lamellae making a small counterclockwise rotation to the transverse orientation at the lumen surface.

Figure 108. An Exposed Surface of the S2 Layer

LF: lamellar flags of the S2 layer being peeled back

M: mudlike covering on the S2

Plate Number: 2527 AF

Magnification: 12,600X

Specimen Preparation: 0.1N KOH, FD, FWS, lumen surface scraped and peeled, STR

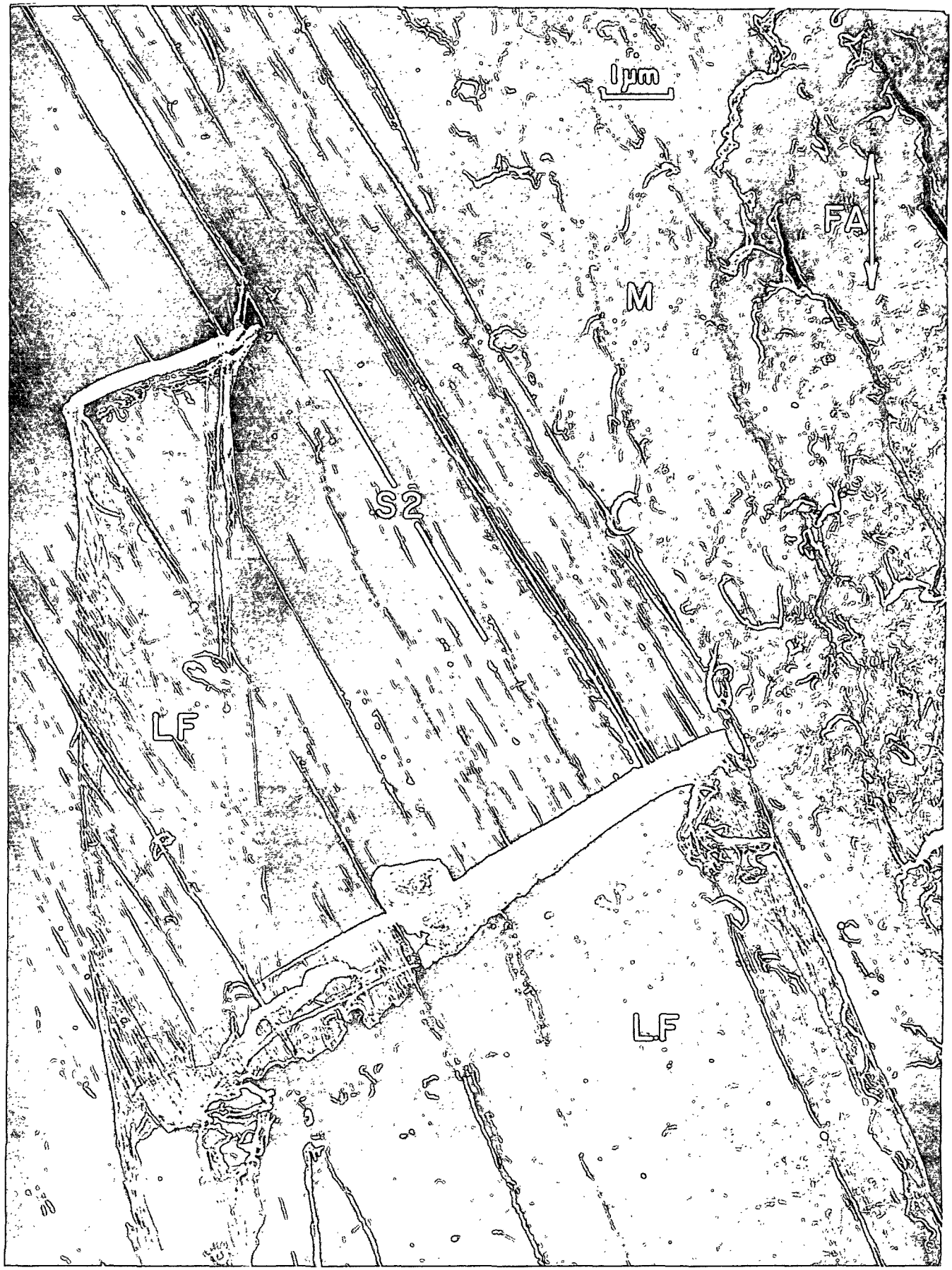
1μm
FA
M
S2
LF
LF

Figure 109. An Internal Surface of the S2 Layer

LL: loose lamellae of S2 fibrils

B: "bubbles" in the surface lamellae

Note: Both the "bubbles" and the loose lamellae indicate a delamination at what would have been concentric surfaces in the whole fiber.

Plate Number: 4540 AF

Magnification: 19,200X

Specimen Preparation: 0.1N KOH, FD, FWS, lumen surface scraped and peeled, STR

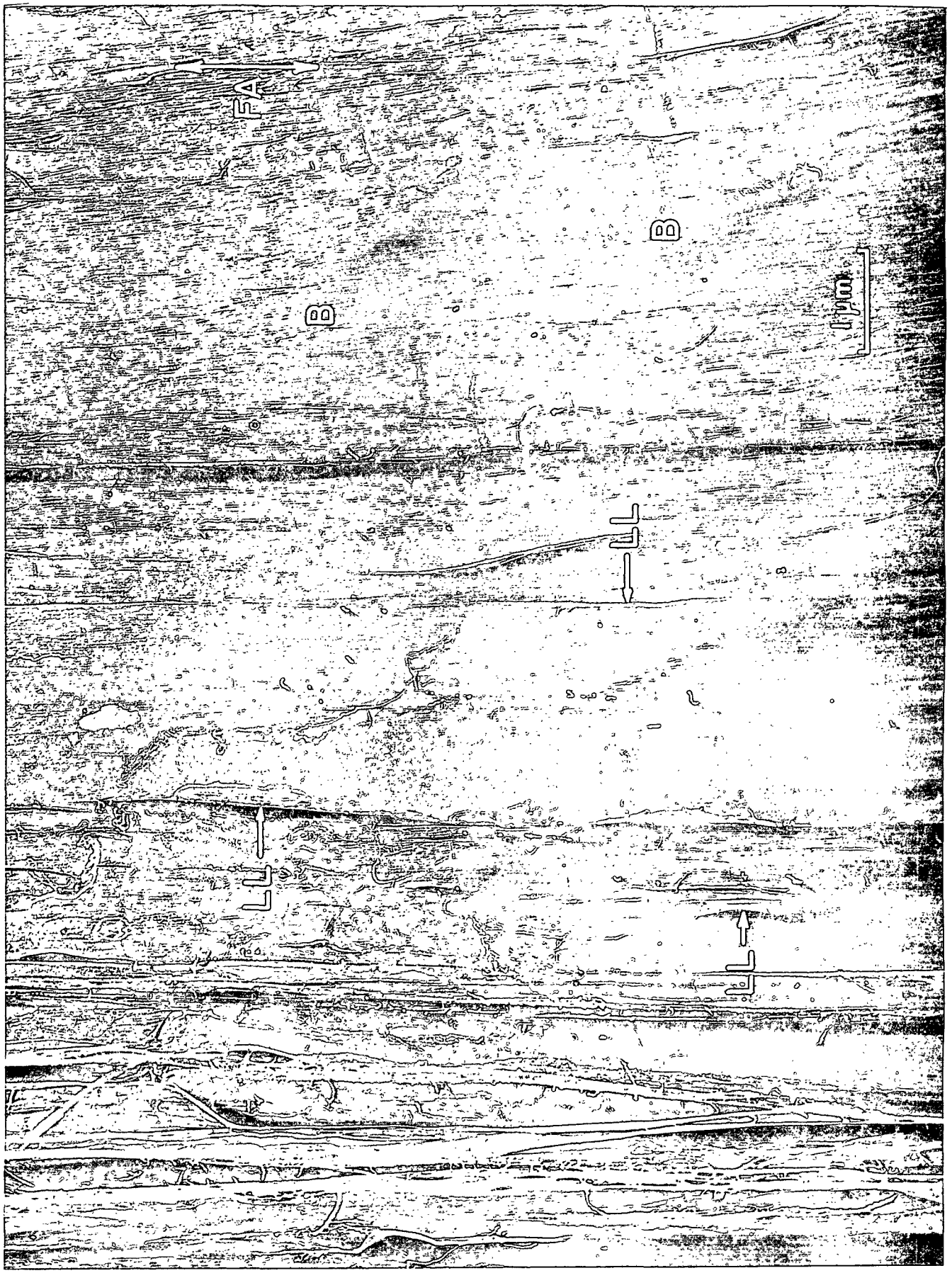

Thus, the results of this work have strongly supported a basic continuity of the secondary wall. In the light of these and similar findings by others, the S1-S2-S3 terminology (based on polarization microscopy) appears somewhat simplified and arbitrary. Nevertheless, the terminology should continue to be used in the sense that the secondary wall consists of a basic, thick central layer bordered by thinner outer and inner layers. The basis of the layer discernment is, of course, the uniform, longitudinal deposition of the central-layer fibrils versus the varying, predominantly transverse deposition of the surface-layer fibrils. In fact, the so-called arbitrary polarization-microscopy differences are reflections of these essential differences. Incidentally, the observation that the S3 layer includes a greater component of longitudinally aligned fibrils than the S1 layer could account for the smaller magnitude of birefringence observed in the S3 by Wardrop (5).

One significant part of this work is the verification of the larger number of S3 lamellae hypothesized by Wardrop and Harada (17) (Fig. 4). They had suggested the presence of zero to six S3 lamellae plus "several" intermediate lamellae between the S3 and S2. Their estimate was based on the division of an assumed lamella thickness of 300 A. into the measured thickness of the S3. Repeating this estimate for the cell walls studied in this work, one finds the S3 layer in Fig. 24 to measure about 6,600 A. This thickness would correspond to 22 300-Angstrom lamellae which, by comparison to the results of the present work, is a good estimate. The minimum number of lamellae from Fig. 82-85 would be about eleven or twelve. This number could be realistically raised to about sixteen by assuming that some of the lamellae seen in more detailed micrographs were present in these fibers but were just not visible in these overall micrographs of the entire S3 transition. On the other hand, the delignified S3 in Fig. 24 could have swollen slightly in water, meaning that the estimate actually is somewhat high. Thus, considering the arbitrary selection of the 300-Angstrom measurement, as well as the other sources of error, the estimate of S3 lamellae appears quite reasonable.

The same calculation for the S1 is not as easily rationalized. This layer, plus the thin primary layer, measures 10,000 A. in thickness, or the equivalent of 33 lamellae. By contrast, Fig. 47-49 show only about five S1 lamellae. This number could be raised to ten by assuming five additional "transition" lamellae. In an attempt to reconcile the difference, several possible sources of error can be pointed out. First, the mudlike material seemed more prevalent in the S1 layer than in the S3. This material could have added to the measured S1 thickness without adding other lamellae, thus accounting for part of the estimate disagreement.

Unfortunately, the mudlike material was effective in another way--in obscuring the S1 lamellae and making the counting of those lamellae much more difficult. Also, the S1 did not peel apart in the same revealing manner of the S3, probably because of the preponderance of transversely oriented lamellae in the S1. In the light of these difficulties, one questions whether other lamellae could have been present in the S1 but yet torn away in such a manner that they were not seen. This speculated condition is not impossible. Nevertheless, the manner in which the different micrographs can be reconciled into a general pattern suggests that any unseen lamellae would not basically alter the pattern.

In spite of the difficulties involved in this method of approach to the problem, these micrographs display more of an overall picture of the lamellar structure than had been seen in micrographs of replicas prepared by other methods. For instance, Wardrop (27) used both immature cell walls and beaten mature walls in studying the S1 structure and could observe large areas of one, or possibly two lamellae. He could not see numerous overlapping lamellae in any given area as one can see in the present micrographs. Nevertheless, he was able to conclude from analysis of his micrographs that the S1 layer of his tracheids (Pinus radiata) consisted of four crisscrossed lamellae with alternating S and Z orientations (left-hand and right-hand spirals). Thus, though the number of and orientations of the lamellae

observed in the present work were slightly different, the newly derived concept of the S1 layer is still basically the same as his concept of the S1 layer. Also, any small differences could be the result of studying different species, instead of differences of interpretation.

As to the organization of the S3 lamellae, Wardrop (5) and Wardrop and Harada (17) concluded that these lamellae alternate between S and Z orientations, or crisscross, in a manner similar to those of the S1. However, the more thorough examination of the S3 in the present work resulted in a different picture--at least for longleaf pine. Certainly, the crisscrossed structure was not observed. Instead, the gradual, incremental, layer-to-layer orientation change found in this work indicates a continuity of the S3 deposition which is not apparent in the model suggested by the earlier workers. Furthermore, this observed continuity of the S3 obviates the designation of the so-called "intermediate" or "transition" lamellae between the S3 and S2 layers. Any labeling of "transition lamellae" would require an arbitrary demarcation between these lamellae and the S3. On the other hand, as long as the S3 layer is defined as a birefrigent inner lining, the "intermediate" lamellae should constitute a portion of that layer. Thus, the author opposes the concept of a transition layer between the S2 and the S3.

The final point in this discussion is to express a tacit assumption involved in the interpretation given to the results of this phase of the work: This assumption is that the cell wall is made up of concentric lamellae which extend the length of the cell. The assumption is generally accepted (1) and, in fact, Wardrop (16, 95) comments, "All layers of the cell wall of a wood fiber exhibit lamellation." Also, he diagrams the lamellae as extending the length of the fiber. Bailey (99) did observe concentric rings in swollen cross sections of cell walls. Presumably, these rings were comparable to the cell-wall lamellae. However, the hypothesis of lamella extensions to the cell ends is yet to be demonstrated. Furthermore, such a

demonstration is not immediately easy. In using dissection techniques such as those developed in this work, one would have to devise a system for cleanly separating two adjacent lamellae. Unfortunately, such a separation would be extremely difficult--if not impossible.

An alternative, indirect approach would be to use the slitting technique to open growing cells in order to observe newly deposited lamellae. If the hypothesis of Wardrop and Harada (17) is correct, each lamella is initiated at the cell center and then grows toward the cell tips. Furthermore, several lamellae would probably be in the process of deposition at the same time. Such simultaneously developing lamellae would probably present the appearance of a system of telescoping tubes. If this multiple growth should be the case, one would still not see the entire length of a given lamella. However, he could at least verify the continuity of each lamella around the circumference of the cell. Furthermore, one could carefully study the growth pattern established in consecutive cells of a given row from the cambium, starting with the youngest cells and proceeding to the mature cells. By thus examining the change from cell to cell, one would achieve a pseudo "time-lapse" effect of lamella growth. This overall picture of cell growth, then, should provide strong indication for or against the concept of center-to-tip lamella extension. This suggested approach of studying maturing cells would have the advantage of being more feasible than the attempt to delaminate adjacent lamellae. Also, the approach should have the double yield of supporting or rejecting the hypothesized growth pattern and also of obtaining an even better picture of the cell-wall structure.

The Effect of Alkaline Extraction

The External Surface

The most noticeable change in surface appearance upon extraction with the first alkali solution (0.1N KOH) was the removal of the obscuring mudlike covering and the revealing of the fibrillar structure of the primary wall. Actually, this sharp

change was not unexpected. Other workers (94, 100-102) had studied holocellulose and delignified high-yield pulps and had shown that the fiber surfaces were plastered over but could be cleared by alkaline extraction. Most of these workers felt that the plastering layer was either hemicellulose or a combination of hemicellulose and lignin residue. On the other hand, Necesany (102) concluded that the mudlike material remaining after delignification was pectin. Unfortunately, his "proof" is questionable. He was able to extract the obscuring grainy material with 0.1N hydrochloric acid (a pectin-dissolving solution) but was not able to extract the grainy layer with 10% NaOH (an extractant for hemicellulose). He therefore concluded that the material was pectin. However, as seen in the present work, even 0.1N KOH can remove the covering layer, meaning that the "failure" of 10% NaOH to dissolve the grainy material should be contended. Fortunately, an incidental facet of the present work (Appendix VI) offers an explanation of Necesany's observation. The pertinent fact was that fiber surfaces extracted with 10% NaOH were found to have lost their fibrillar character--as if some manner of drastic swelling had taken place. Incidentally, a similar appearance had been obtained by Svensson (100) upon treatment of fibers with 18% NaOH at room temperature. Quite interestingly, both of these surfaces closely resembled those shown by Necesany as examples of the retained grainy layer. In other words, the "grainy" material on his unextracted fibers probably was not identical to the "grainy" material on his surfaces extracted with 10% NaOH. In fact, his alkaline extraction probably removed the "grainy" material and then altered the underlying structure, producing another grainy surface.

Thus, Necesany did not prove that the plastering material is pectin. Nevertheless, his speculation could well be correct. The observation in this work that the material can be removed with 0.1N KOH is compatible with the hypothesized pectinaceous character of the material. Furthermore, Sultze (103) had concluded that, at least in the case of aspenwood, the "pectin substances" (polygalacturonic acid,

araban, and galactan) made up two thirds of the compound-middle-lamella carbohydrates. Thus, the material could well be pectin.

One remaining question in the discussion is the significance of the "soluble lignin." Spiegelberg (70) speculated that the unaccounted-for 8% loss of material during the first extraction could have been made up of this little-understood material. Unfortunately, his sugar analysis did not include a determination of galacturonic acid (the backbone unit of pectin). Thus, his undesignated material loss could have been explained, at least partially, as a loss of pectin. In any case, the quantitative significance of pectinaceous material versus soluble lignin in the nonextracted holocellulose is still in question. Consequently, the constitution of the plasterlike surface material is also uncertain. Thus, in light of the foregoing discussion, the surface material removed by the 0.1N KOH is thought to be an unknown mixture of pectin and "soluble lignin."

Though even more mudlike material was removed by the extraction with 9% KOH, the more drastic change brought about during this treatment was a removal of much of the primary wall, leaving the S1 layer exposed. Other workers (12, 16, 94, 100, 101, 104, 105) have discussed the ease of removal of the primary wall, though most of those workers were concerned with commercial pulps. Certainly, the results of the present work emphasize the mildness of treatment sufficient to remove much of the primary wall. Similarly, Preston (104) had already shown that even a shaking of isolated fibers with glass beads was sufficient to remove this material. Presumably, the layer removal that Preston observed could be explained as the result of mechanical action. However, the exact means of layer disruption during the simple extraction used in the present work is uncertain. The mild tumbling induced by the bubbling nitrogen probably would not have been sufficient if acting alone. On the other hand, many areas were observed in which the primary layer appeared to be loosely draped over the fiber surface and not bonded to the remainder of the

cell wall (Fig. 64). This picture of a primary wall loosened by delignification and extraction of carbohydrate material is compatible with the concept of Wardrop (16) that, after pulping, the primary layer exists as a loose, wrinkled sleeve around the fiber. Also of interest to the present discussion is Giertz's (105) observation that the primary layer generally is not removed by fibrillation, even during beating, but is removed as membranelike or skinlike material. Conceivably, then, the extraction leaves the primary wall in a loose condition in which it is vulnerable to even the mildest agitation and, as such, it is removed in sheetlike fragments.

Finally, two other possible factors in the removal of the primary layer should be mentioned. First, one may question whether the microdissection procedure could have resulted in loss of the primary layer. Though such an effect is conceivable, especially in the case of the scraped fiber surfaces, one consideration definitely limits this possibility. Careful examination of the surfaces in question reveals a degree of fibrillation which is not likely to have taken place after the fiber had dried. More probably, the fibrillation was achieved while the fiber was still wet and was then preserved by the freeze drying. Thus, the microdissection was probably not responsible for the fibrillation. Subsequently, since the removal of the primary layer would have preceded the fibrillation of the S1 layer, the microdissection probably was not a factor in the removal of the primary layer, either.

Another possible influence on the primary-layer disruption was the swelling of the cell wall caused by the caustic treatment. However, this possibility is difficult to evaluate at this point. Certainly, the secondary layers would exert a swelling pressure. On the other hand, the transversely and uniformly oriented S1 fibrils could probably contain the swelling pressure without allowing damage to the primary layer. Also, the randomly oriented primary layer should be capable of more stretching without rupturing than the S1 layer. In any case, no examples of

suspected swelling rupture were observed. Contrarily, several cases of multiple rupture not credited to rupture by swelling were observed. Thus, the rupturing of the primary layer is not believed to have been caused by the swelling of the fiber in caustic solution.

Even though the means of layer disruption is not clearly understood, the fact of material removal does offer a comment on one of the questions raised by Spiegelberg (70). Though softwood glucomannan usually has a glucose-mannose (G-M) ratio of 1:2.7, the analysis of his extracted pulp suggested that a 1:1.1 G-M polymer had been removed during the 9%-KOH extraction. Therefore, he speculated that a glucan polymer, in addition to the G-M polymer, might have been removed by the extraction. In the light of the present observations of layer removal, his explanation appears quite reasonable, since the primary layer removed would have consisted largely of cellulose. However, one incidental point is that the fibrillar material probably would have been removed as a colloidal dispersion rather than as a simple solution. Therefore, someone interested in examining this hypothesis might attempt a fractionation of a similar extract by simply filtering the solution through a Millipore filter.

The Lumen Surface

The most noticeable change in the lumen surface upon extraction with 0.1N KOH was the removal of the wartlike structures. Thus, another chemical solubility of the warts can be added to the list prepared by Wardrop, et al. (44) (page 12). In other words, the present observation is that the warts can be dissolved by chlorite treatment followed by extraction with 0.1N KOH. This reaction might be considered similar to the observation of those earlier workers that the warts could be dissolved by a NaOH treatment followed by a chlorine-water treatment.

Though Wardrop, et al. (44) preferred to refrain from speculating about the chemical composition of the warts, one interesting observation is that each of the reactions which has been observed to dissolve the warts involved some form of oxidative treatment. In connection with this observation, the wood constituent which is generally cited as being susceptible to mild oxidative reaction is the lignin. Could the warts, then, be made up at least partially of lignin, or a ligninlike material? Though this question certainly cannot be conclusively answered at this time, interesting support for the speculation is seen in the cross sections of lignin skeletons prepared by Jayme and Fengel (85, 106). Their micrographs indicate a compacted lignin residue occurring at the lumen surface. However, the wart structures themselves are not visible, meaning that the presence of lignin in the warts is still open to question.

One other unknown factor about the warts which must be considered is the significance of the alkali extraction in their removal. Does the delignification leave the lignin in a residue or "soluble-lignin" form which must be removed with alkali, or do the warts consist of a complex of lignin with some other material (carbohydrate, for instance) which is susceptible to a two-step treatment? Thus, the chemical make-up of the wart structures is still not known. This present discussion was simply intended to initiate some considerations which might serve as points of departure for future work.

The other obvious change in the S3 layer was the loosening and detachment of the surface lamellae occurring during the two later stages of extraction. One point from the literature that might be related to the observed detachment is the conclusion of Meier and Wilkie (107) that the "tertiary wall" consists mainly of glucuronoarabinoxylan. Conceivably, this polymer is active in bonding together any cellulosic elements of the S3. Moreover, Spiegelberg (70) observed that the

xylan content of the present pulp decreased sharply upon extraction with the 9% KOH. Thus, the lamellar detachment could have resulted from a decrease in xylan bonding within the S3.

The other question about this detachment is what could have happened to the layers removed. At this point, the author can only speculate as to their fate. One somewhat unlikely possibility is that these lamellae dissolved in the extracting solution. If the lamellae had been removed by solution, one wonders why all of the fibers would not have been attacked at the same time. A more likely speculation is that the layers had been loosened by extraction (as has already been shown) and were simply lost amid the slitting debris. Certainly, this question could bear more detailed study.

Implications in the Hemicellulose-Physical Properties Relationship

Since the extracted fibers examined in this work were taken from the fiber populations tested by Spiegelberg (70), some comment on his results is considered to be relevant. His objective was to examine the effect of the hemicelluloses on the mechanical properties of the single fibers. He approached this objective by extracting the hemicelluloses from the fibers and observing the changes in the fiber properties. However, after seeing in the present work the extent of structural degradation which accompanied the extraction, one at least questions whether the simple removal of the hemicelluloses could be entirely responsible for the change in mechanical properties. For instance, those lamellae which were badly damaged might have been significant in supporting tensile load on the undamaged fibers. However, the lamellae in question constitute probably less than 5% of the cell-wall cross section. Furthermore, the fibrillar orientations of those lamellae are generally perpendicular to the fiber axis--certainly not the optimum orientation for sustaining an axial tensile load. Thus, the author has concluded that the direct load-bearing contribution of the layers in question would have been negligible.

On the other hand, the possibility exists that the damaged layers could have contributed in an indirect manner to the tensile strength of the fibers. For example, the outer and inner layers might be effective in reducing the freedom of the S2 fibrils and in maintaining the uniform steep-helix structure of that layer. Accordingly, damage to these retaining layers might permit the S2 fibrils to be released from their uniform structure. The possible end result of this structure relaxation could be an entanglement of the S2 fibrils and then a piecemeal loading and breaking of single fibrils, rather than a uniform stress distribution and instantaneous breaking of the entire fiber. In other words, the stress-concentration effects in the entangled system could result in a decrease in the breaking stress of the fiber. Unfortunately, the magnitude of this effect cannot be evaluated from present knowledge. Furthermore, even the question about just how much of the S3 is disrupted is still not settled, meaning that one cannot tell how much the S2-retaining capability of the S3 is affected. Thus, the magnitude of change in the mechanical properties brought about by P-S1 and S3 layer damage is not known, but conceivably, the effect may be significant.

One indirect consideration about the observed disruption of the surface layers is the thought that though the surface damage may not affect the mechanical properties, some similar disruption or other form of structural rearrangement could have taken place in the S2 at the same time as the surface damage. Careful examination of the freeze-dried fibers by light microscopy at least supported this speculation. Photomicrographs of fibers from the different extraction stages are given in Appendix VII (p. 382) to illustrate the noticeable changes that took place upon extraction. Actually, one can see little difference between the nonextracted fibers and the fibers extracted with 0.1N KOH (except for the previously discussed fraying of occasional nonextracted fibers). The fibers of both samples are generally straight, except for occasional jointed bends. By contrast, the fibers from the

9%-KOH and KOH-plus-borate extractions are quite twisted and curled, even though the extracting caustic has been washed away. Though the mechanism by which the curling took place is not understood, the fact that the curl is present suggests that the S2 fibrils have, to some unknown degree, departed from their original uniform orientation. This disalignment, or possibly entanglement, could easily explain why Spiegelberg's results indicated that drying under load could be much more significant with the more extensively extracted fibers. In other words, the loads applied to some of the fibers during drying were effective in realigning the fibrils. However, the extensively extracted fibers dried without loading had a certain amount of fibril entanglement set in by drying and thus became subject to stress-concentration effects. Thus, the hypothesis of stress redistribution via drying under load subscribed to by Jentzen and Spiegelberg appears to be meaningful.

Finally, the results of one other incidental experiment during the course of this work suggests an indirect mechanism by which the presence of the hemicelluloses in the cell wall could have affected the mechanical behavior of Spiegelberg's fibers. Other workers (4, 108, 109) had suggested that hemicelluloses and other less crystalline polysaccharides generally have a higher hygroscopicity than cellulose and other high-crystalline materials. Conceivably, then, the fiber samples with higher hemicellulose contents could also have higher equilibrium moisture contents. In order to obtain a simple check on this possibility, small portions of the limited fiber samples were air dried and then oven dried in order to determine the equilibrium moisture content at 50% relative humidity and 73°F. Also, the oven-dried fibers were reconditioned at the same conditions after both absorption and desorption approaches. The results of these measurements are reported in Appendix VIII. The nonextracted and 0.1N-KOH-extracted fibers appeared to retain (or absorb) about three quarters of a percent more moisture than the 9%-KOH- and KOH-plus-borate-extracted fibers (percent of total weight basis). In other words,

the absolute moisture content was about 10% higher in the nonextracted and lightly extracted fibers than in the extensively extracted fibers. (Because of the small quantities tested and the nonduplication of the tests, the differences between the nonextracted and 0.1N KOH-extracted fibers and between the two extensively extracted samples may not be significant.) Thus, the variation of hygroscopicity with hemicellulose content may provide a partial explanation of the hemicellulose "lubricating" effect discussed by Spiegelberg (70). In other words, the hemicellulose may hold water molecules on the surfaces of the microfibrils in such a way as to reduce the bonding between adjacent microfibrils and thus allow the fibrils to creep past one another more easily. In any case, this brief experimentation with and discussion of the moisture relationship is obviously not intended as an exhaustive treatment of the subject, but simply as an indication of a possible role of the hemicelluloses.

THE PIT STRUCTURE

THE STRUCTURE OF THE PIT MEMBRANE

As discussed in the HISTORICAL REVIEW, a question of the exact structure of the cell pits is currently being debated in the literature. Specifically, the debate concerns the structure of the pit membrane and the question of whether the original membrane has a torus structure or a primary-wall-like structure. Though the present work was not planned to answer this question, some incidental observations do permit a meaningful commentary on the question.

The micrographs found most relevant to the discussion of membrane structure were those made from replicas of radial-shive surfaces. Figure 18 was one such micrograph. A similar picture showing a larger area and more pitting is given in Fig. 110. Both of these micrographs (of longitudinal tracheids) show pits grouped in the cross fields or in ray-crossing areas. (The cross fields are areas on the longitudinal tracheids touched by the horizontally aligned ray cells.) In particular,

these figures show one edge of the respective ray crossings. The significant observation is that the pit membranes shown are of two different types. The pit along the edges of the ray crossings have torus-type membranes, as was generally observed for all ray crossings. On the other hand, the pits in the centers of the crossings have primary-wall-type membranes. Figures 111-114 show enlarged representative views of the two different membrane types from Fig. 18 and 110.

One other micrograph of interest to this discussion is given in Fig. 115. This picture shows a ray crossing with some of the ray cells still in place over the longitudinal tracheids. The two upper cells (at the edge of the ray), as well as the lower cell, all appear to have generally retained their shapes, though they are slightly wrinkled. On the other hand, the one cell in the center of the ray appears to be quite thin walled and looks as if it has completely collapsed.

After carefully studying these micrographs, the author's conclusion is that they strongly support the more widely accepted concept of two different membrane types. However, this concept has recently been challenged. The newer, challenging idea is that the torus-type membrane structure is an artifact caused by aspiration of the membrane during drying (55, 58). Nevertheless, several objections to this artifact hypothesis can be derived from the present work. The first objection is simply an intuitive one: The author raises the question as to why two membranes located so close together could still behave so differently upon drying. In other words, if a given pit has its membrane subjected to aspiration because of a retreating air-water interface, one would expect the neighboring pit membranes to be subjected to the same effects. In Fig. 110, for example, one membrane (13) is of the torus type, while two others very close to this one are of the primary-wall type (9 and 10). In any case, this intuitive reasoning is, of course, not conclusive.

Figure 110. A Surface View of a Radial Shive Showing the Tracheid Pitting at a Ray Crossing

G: gap between the two adjacent longitudinal tracheids

ER: edge of the ray crossing

1-12: primary-wall-type membranes over pits

13, 14: torus-type pit membranes

A: suspected replication artifacts--discussed in Appendix IX (In the case of no. 13, the ring under the torus is the suspected artifact.)

FA: fiber axis (parallel to the gap)

Plate Numbers: 3446-3451 AF

Magnification: 2500X

Specimen Preparation: Delignified chip freeze dried, shive manually separated from the dry chip, STR (same specimen as in Fig. 18)

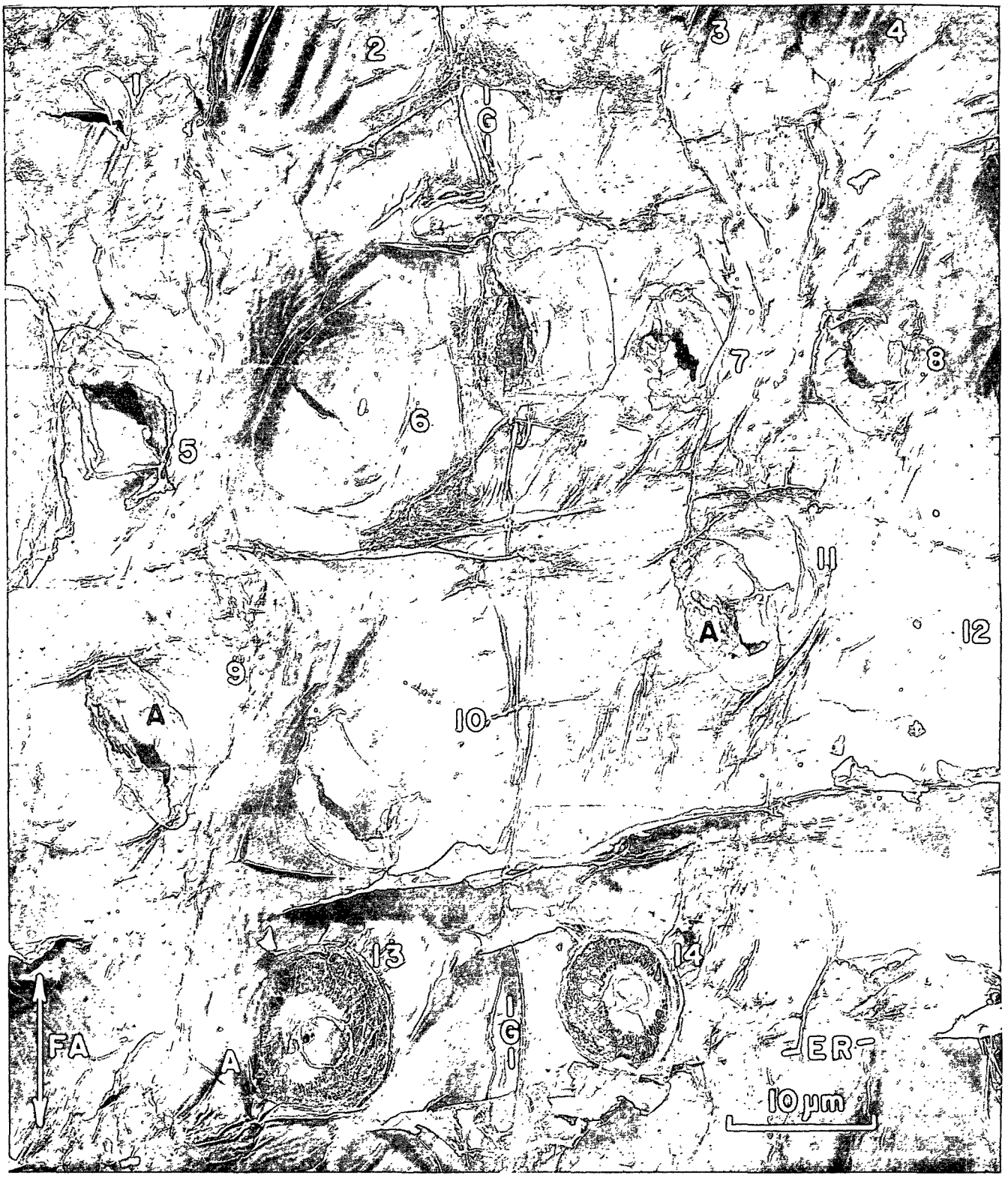
2
3
4
G
7
8
6
5
11
A
12
9
A
10
13
14
FA
A
G
ER
10 µm

Figure 111. A Higher Magnification of a Torus-Type Membrane in Fig. 18 (The Suspended Disk at the Center of the Pit Is the Torus)

SH: "shadows" on the pit lining verify the raised position of the membrane (as opposed to its being aspirated)

A: suspected artifact

FA: fiber axis (determined from Fig. 18)

Plate Number: 3439 AF

Magnification: 15,000X

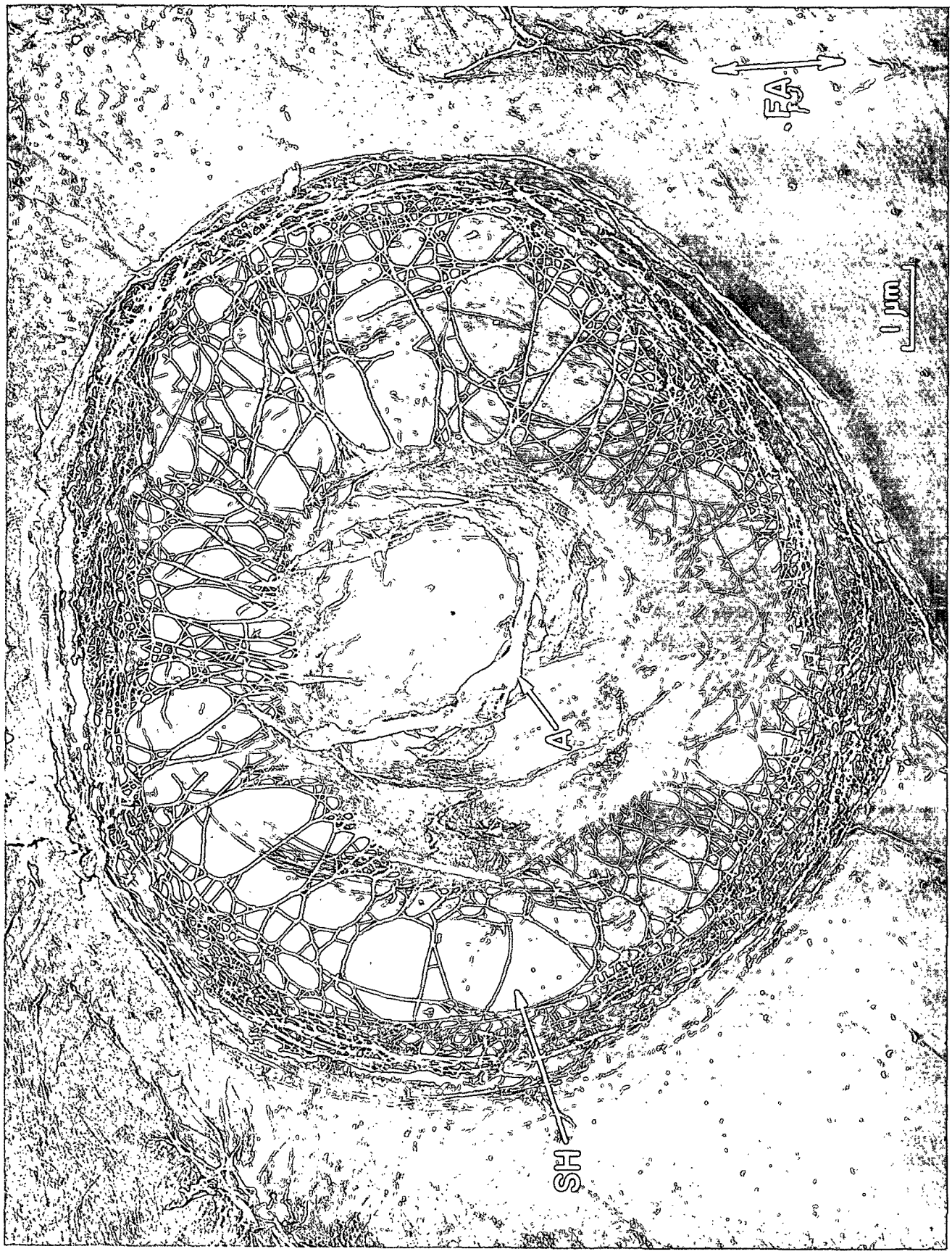
FA
1 mm
A
HS

Figure 112. A Higher Magnification of a Primary-Wall-Type Membrane in Fig. 18

PM: primary-wall-type membrane

AN: pit annulus (outline of membrane area)

CM: crack in the membrane exposing the pit cavity

A: suspected artifact

FA: fiber axis (determined from Fig. 18)

Plate Number: 3438 AF

Magnification: 15,000X


CM
A
PM
AN
FA
1μm

Figure 113. A Higher Magnification of a Torus-Type Membrane in Fig. 110 (The Suspended Disk in the Center of the Membrane Is the Torus)

SH: "shadows" on the pit lining

A: suspected artifact

FA: fiber axis (determined from Fig. 110)

Plate Number: 3453 AF

Magnification: 12,400X


FA
SH

Figure 114. A Higher Magnification of a Primary-Wall-Type Membrane in Fig. 110

FA: fiber axis (determined from Fig. 110)

Plate Number: 3452 AF

Magnification: 12,400X

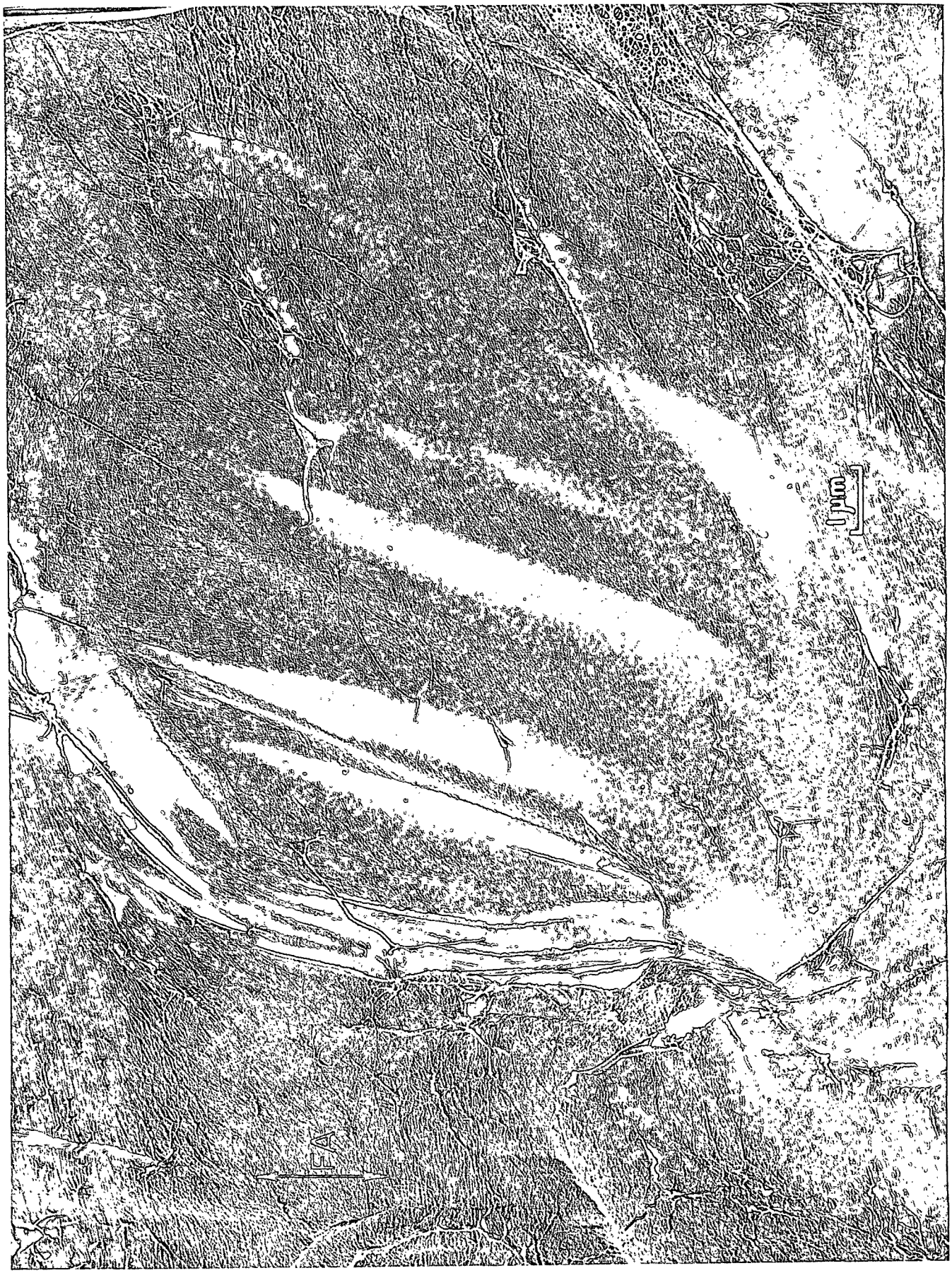
1 μm
1 μm

Figure 115. A Ray Crossing at Which the Ray Cells Are Still in Place

LT: longitudinal tracheids serving as the background in the picture

HW: heavy-walled (thick-walled) ray cells

TW: thin-walled, collapsed ray cell

TM: torus-type membranes in the thick-walled ray cells

PM: primary-wall-type membranes over pits in longitudinal tracheids

Plate Numbers: 3809-3811 AF

Magnification: 2300X

Specimen Preparation: Radial shive extracted 10 sec. with 0.1N KOH, solvent exchanged: absolute alcohol--twice, benzene--twice; air dried; STR


10μm
LT
FA
HW
TM
HW
TM
HW
PM
PM
LT
TW
HW

Actually, a much stronger case against the drying-artifact hypothesis can be developed from consideration of the method of specimen preparation used in the present work. These specimens were freeze dried and, hence, would not have been subject to the capillary-interface effects suspected of causing aspiration and formation of the tori in the pit membranes. Furthermore, one finds upon examining the given micrographs that, indeed, the membranes are not aspirated but are suspended in place above the pit cavities.

Finally, a third argument against the artifact hypothesis of torus formation is the placement of the torus membranes in the ray crossings. These torus membranes are not randomly scattered across the ray crossings but, instead, generally occur along the borders of the crossings. In fact, the author will presently attempt to correlate this preferential placement of the torus membranes with the overall concept of wood structure. Thus, the general conclusion of this discussion is that the results of this work, together with the results of others (54, 60, 61, 63), show definite argument against the artifact hypothesis of torus construction. [The references to Fengel's recent paper (63) is included as he has obtained new evidence from ultrathin sections and concluded that torus formation is not due entirely to aspiration. Instead, he now believes that the radial fibril orientation is largely established during the growth of the cell. However, he still indicates that the aspiration of the membrane is effective in aligning and allowing aggregation of the fibrils. In any case, he is expressing a change in opinion since his coauthorship of the drying artifact hypothesis.]

On the other hand, these results agree quite well with the older concepts of membrane structure (1, 31, 49-52). In softwoods, the wood rays usually include thin-walled parenchyma cells lying along the central bands of the rays. (The thin-walled cell in Fig. 115 is probably one such parenchyma cell.) Also, the pit pairs connecting these parenchyma cells with the longitudinal tracheids are generally

pictured as half-bordered pits (Fig. 6). Furthermore, the membranes of the half-bordered pits are thought to have a continuous-layer structure like the continuous membranes pictured in this work. Thus, the observation of the continuous membranes in the centers of the ray crossings is in agreement with the concept of cell structure accepted by most workers.

Similarly, the torus-type membranes are generally accredited to bordered-pit pairs occurring between adjacent tracheid cells. As for ray tracheids, these cells are believed to lie along the edges, or borders, of the wood rays. (The thicker walled ray cells in Fig. 115 are thought to be ray tracheids.) Thus, the placement of the torus membranes along the borders of the ray crossings is also in complete agreement with the generally accepted concepts of wood structure.

Finally, one other expected location of bordered-pit pairs and torus membranes would be the radial faces between adjacent longitudinal tracheids. Figures 116 and 117 are representative micrographs showing pits of this type. These pits are different from those between longitudinal tracheids and ray tracheids in that their diameters are much larger and their borders much closer together. The observed aspiration of these membranes is a result of the different washing and drying procedures used with these particular samples.

Thus, the present work has not advanced new concepts of pit-membrane structure but has simply developed strong support for the older concepts of structure. This support resulted from the new techniques of preparation that permitted the clean exposure of cell surfaces in a way that had not been done previously. In particular, the exposure of large expanses of ray-crossing area allowed direct comparison of torus-type versus primary-wall-type pit membranes. In conclusion, this work has shown that the torus structure is not a drying artifact, but that it is most probably a real structure produced during cell growth.

Figure 116. Bordered Pits Which Communicated with the Adjacent Longitudinal Tracheid

Plate Number: 3796 AF

Magnification: 5300X

Specimen Preparation: Radial shive extracted 4 hr. with 0.1N KOH at 28°C., solvent exchanged, air dried, STR


FA
10 μm

Figure 117. Bordered Pits Which Communicated with the Adjacent Longitudinal Tracheid

Plate Numbers: 3792, 3793 AF

Magnification: 5300X

Specimen Preparation: Same specimen as in Fig. 116

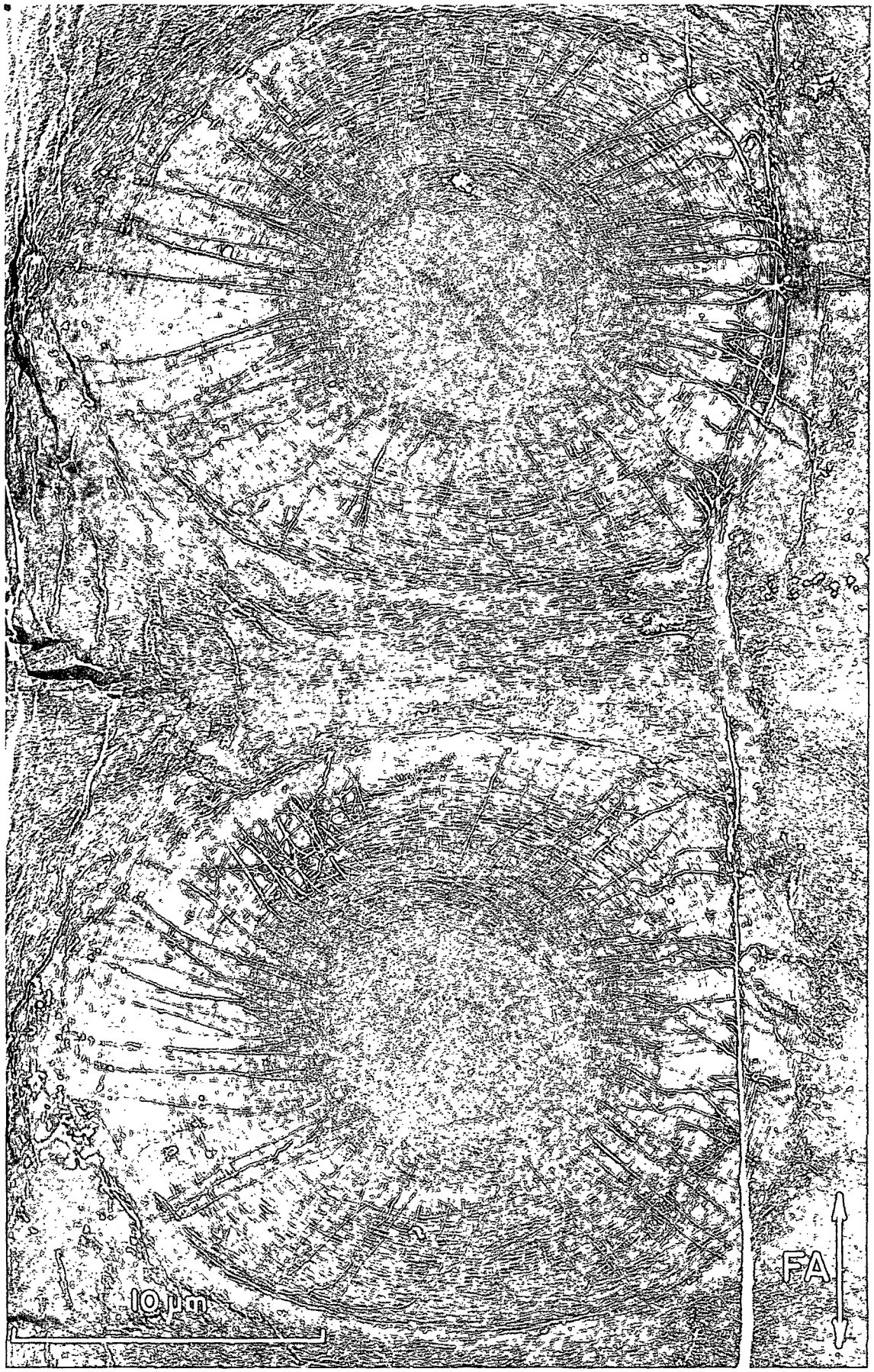
10 µm
FA

Figure 118A. An Electron-Dense Film Lying Underneath a Primary-Wall-Type Membrane

Plate Number: 5144 AF

Magnification: 3300X

Specimen: Radial shive extracted overnight with 0.1N KOH, solvent exchanged, air dried, STR

Figure 118B. A Membrane Torus Suspended in Place. An Electron-Dense Film Can Be Seen Under the Torus

Plate Number: 5145 AF

Magnification: 4700X

Specimen: Same as in Fig. 121

Figure 118C. A Cell Pit from Which a Torus-Type Membrane Has Been Torn Away

Plate Number: 5146 AF

Magnification: 3300X

Specimen: Same as in Fig. 119

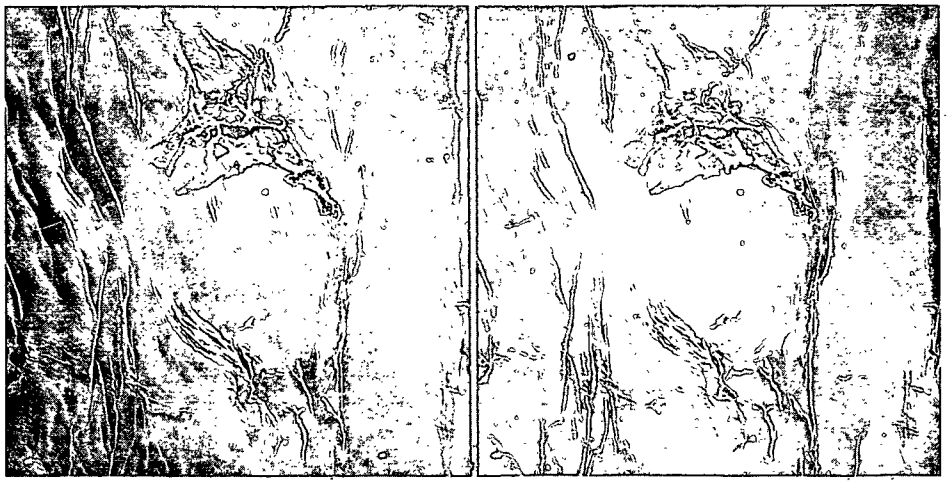

Finally, one other matter which should be mentioned is the designation of some artifacts of replication which can be seen in several of the micrographs. Both the white films underneath some of the torn continuous membranes (Stereo: Fig. 118A) and the white rings underneath some of the torus membranes (Fig. 118B) are believed to be artifacts. A discussion of the origin of these artifacts is given in Appendix IX. Also, this Appendix might be of additional interest to the reader because of its discussion of the submicroscopic behavior of the melted polystyrene.

BEHAVIOR OF THE MEMBRANES DURING TREATMENT OF THE FIBERS

When the surfaces of the extracted fibers were studied, the appearances of the pits were also examined to see how they were affected by the mechanical and chemical treatment. A brief discussion of these observations will be given in this section.

The behavior of the torus-type membranes during the treatments can be quite easily categorized: Practically all of them were torn away. Figure 119 shows the remaining open pit cavity of one typical case (Stereo view in Fig. 118C). Actually, even the designation of the pit as one having had a torus membrane would be quite difficult, except that one can see a few aggregate strands remaining around the border of the pit cavity.

A somewhat unusual case of membrane treatment is seen in Fig. 120. Most of the membrane's moorings have been torn away, permitting it to float to one side. Again, judging from the radially oriented strands on the membrane surface this membrane was also of the torus type. Finally, a very rare case of a torus-type membrane which has survived defibering and extraction treatment is shown in Fig. 121 (Stereo: 118B). In fact, of all the pits observed in the single fibers prepared by Spiegelberg, this pit was the only one having a torus-type membrane preserved so well.

Of the micrographs shown, Fig. 119 and 121 were taken from replicas of fibers extracted with 9% KOH, and Fig. 120 was taken from a fiber extracted with 0.1N KOH. No micrograph of a pit in either a nonextracted fiber or a fiber extracted with borate was shown, but fibers from both of these samples had their torus-type membranes removed in a similar manner. Thus, even though one can pull apart radial shives without disrupting these membranes (Fig. 18 and 110), the membranes appear quite fragile and vulnerable to any tumbling of the fibers in extracting solution.

Many of the continuous, primary-wall-type membranes were also damaged by tumbling in the solutions. Figure 122 shows one such membrane partially torn back. (This micrograph is also interesting in that it shows an uncoiling of the conical pit-cavity lining.) On the other hand, many of the continuous membranes remained intact throughout the extractions. Figure 123 (Stereo: Fig. 124A) is one example of such a membrane. In fact, so many of the continuous membranes were retained in place that one could find examples of several membranes together. Figures 125, 126, and 127 show such groups of several membranes together. These three micrographs also demonstrate the variation between nonextracted, 0.1N-KOH-extracted, and 9% KOH plus borate-extracted membranes, respectively. Incidentally, these three pictures also suggest the difficulty one has in trying to find the covered pits. (One of the first efforts to find hidden pits produced structures exemplified by Fig. 166 in Appendix X. This structure was later thought to be a primary pit instead of a covered pit.) In fact, many of the pits were found only by looking for obvious uncovered pits and then studying the areas around these pits. Also the stereo views of suspected covered pits were quite helpful in verifying the presence of the pits by indicating the protruding outlines of the pit borders (Fig. 124B from Fig. 126).

Thus, in contrast to the torus-type membranes from bordered pit pairs, many of the continuous membranes from half-bordered pit pairs were retained, even on

Figure 119. A Typical Example of a Torus-Type Membrane Torn Away During the Defibering and Extraction

AN: annulus of the pit

MS: membrane strands which once held the torus in place

PL: pit lining made up of conically wound fibrils

PA: pit aperture

Plate Number: 2943 AF

Magnification: 14,000X

Specimen Preparation: 9% KOH, FD, FWS, STR (same specimen as in Fig. 65)


PL
PA
AN
MS
FA
1mm

Figure 120. A Torus-Type Membrane Which Has Been Loosened and Floated to One Side

PM: pit membrane

MS: membrane strands

PL: pit lining

PA: pit aperture

Plate Number: 3227 AF

Magnification: 11,800X

Specimen Preparation: 0.1N KOH, FD, FWS, STR


PL
PA
PM
MS
1μm
F A

Figure 121. A Rare Torus Membrane Which Survived the Defibering and Extraction with 9% KOH

Plate Number: 2905 AF

Magnification: 19,600X

Specimen Preparation: 9% KOH, FD, FWS, STR

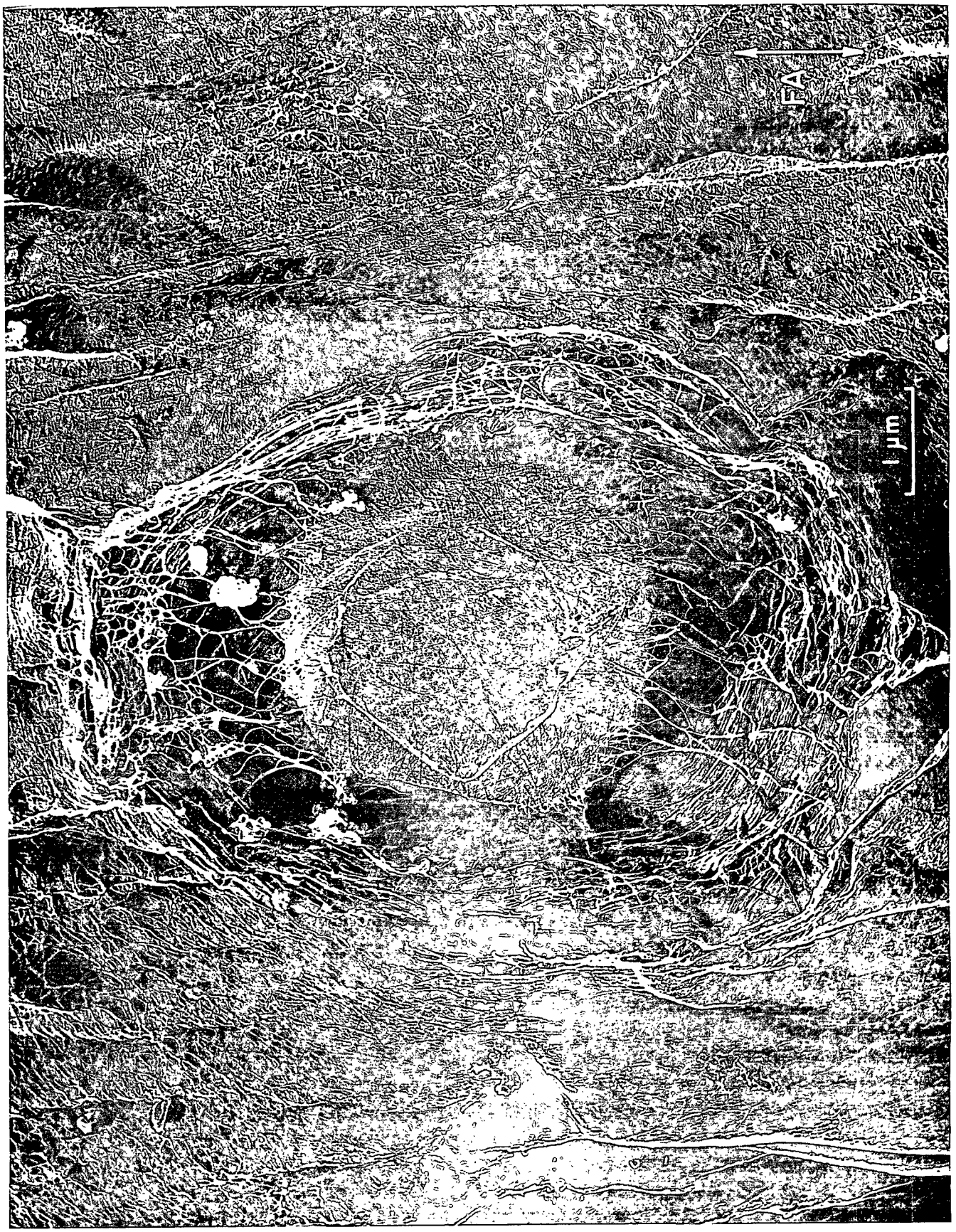
FA
E
E

Figure 122. An Incomplete Tearing Away of a Primary-Wall-Type Membrane:

PM: remaining, overhanging edge of the primary-wall-type membrane

PL: conically wound pit lining

UW: an unwinding strand of the pit lining

PA: pit aperture

Plate Number: 2999 AF

Magnification: 15,100X

Specimen Preparation: 9% KOH, FD, FWS, STR (same specimen as in Fig. 63)


FA
1μm
UW
PL
PL
PA
PM

Figure 123. An Intact Primary-Wall-Type Membrane

PM: primary-wall-type membrane (sunken in pit cavity)

C: fiber corner (fiber axis parallel to this corner)

Plate Number: 3195AF

Magnification: 12,400X

Specimen Preparation: 0.1N KOH, FD, FWS, STR


PM
1 mm

Figure 124A. A Primary-Wall-Type Membrane Which Has Survived Mild Caustic Extraction

Plate Number: 5147 AF

Magnification: 3300X

Specimen: Same as in Fig. 123

Figure 124B. The Protruding Outline of a Covered Pit

Plate Number: 5148 AF

Magnification: 4700X

Specimen: Same as in Fig. 126

Figure 124C. The Lumen Side of a Pit Cavity

Plate Number: 5149 AF

Magnification: 3300X

Specimen: Same as in Fig. 129

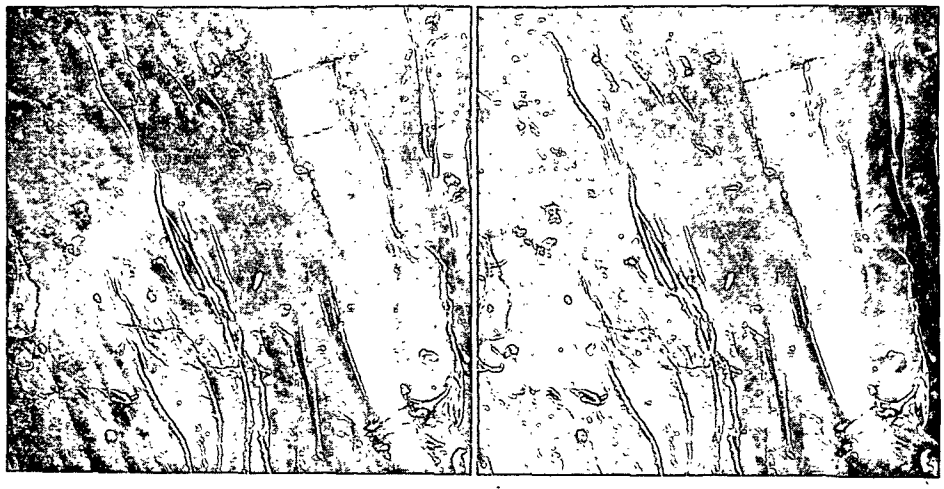

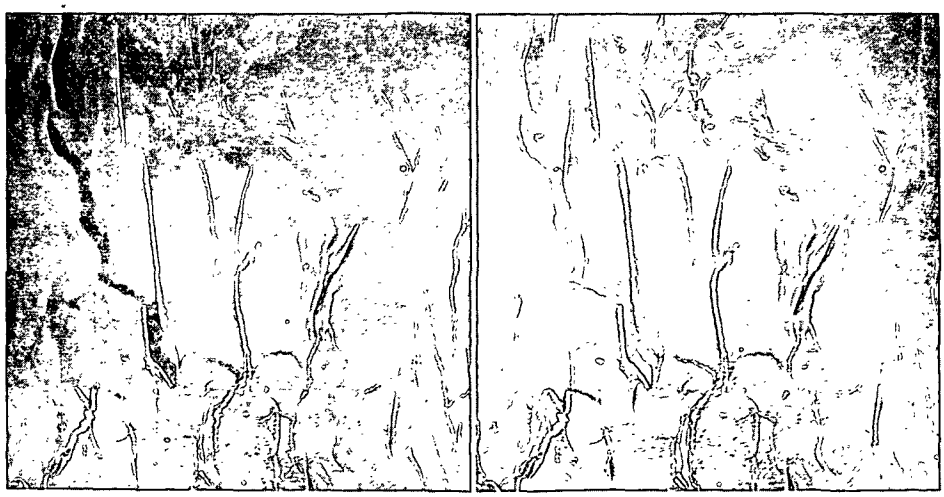

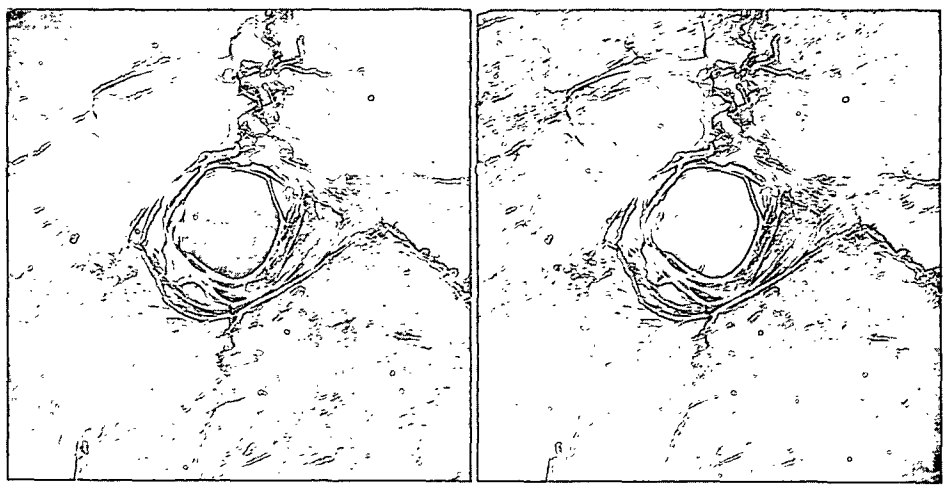

Figure 125. Primary-Wall-Type Pit Membranes on the Surface of a Nonextracted Fiber

PM: primary-wall-type pit membranes

C: corners of the fiber

Plate Numbers: 3151, 3152 AF

Magnification: 5100X

Specimen Preparation: NONEXTR, FD, FWS, STR


C
C
PM
PM
10 µm
PM
PM
C
C

Figure 126. Primary-Wall-Type Pit Membranes on the Surface of a Fiber Extracted with 0.1N KOH

PM: primary-wall-type pit membranes

LL: an unexplained loose lamella that would have at least partially overlapped one of the pits

Plate Numbers: 3210-3212 AF

Magnification: 3160X

Specimen Preparation: 0.1N KOH, FD, FWS, STR (same specimen as in Fig. 60, 61)


PM
LL
PM
PM
PM?
FA
PM
10 μm

Figure 127. Primary-Wall-Type Pit Membranes on the Surface of a Fiber Extracted with 9% KOH Plus 3% Borate

OP: open pits serving to identify the radial face of the fiber and designate the possible location of hidden pits

PM: primary-wall-type membranes

Plate Numbers: 3098-3101 AF

Magnification: 3900X

Specimen Preparation: KOH-BOA, FD, FWS, STR

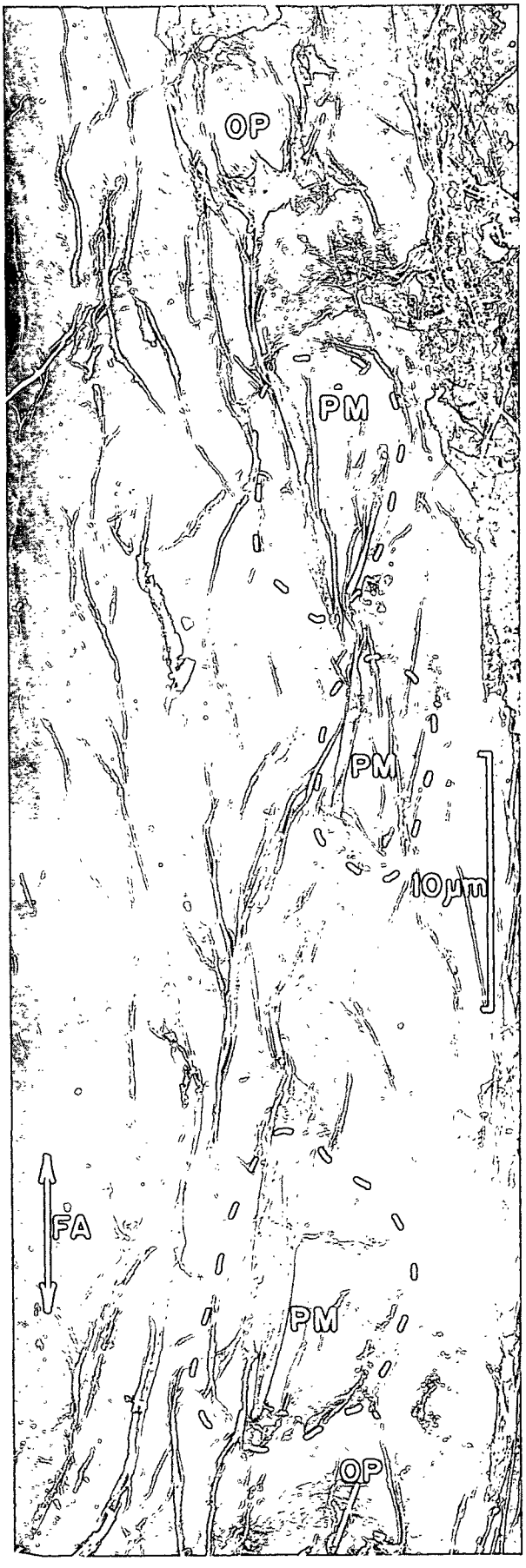
OP
PM
PM
10μm
FA
PM
OP

the extracted fibers. On the other hand, those fibers which had lost their primary walls during the treatment had also lost the continuous membranes, since the membranes are simply a part of the primary wall. At the same time, others of the continuous membranes had been simply torn away from the pits, leaving the remainder of the primary wall intact.

THE LUMEN SIDE OF THE PIT CAVITIES

This final topic is included simply to display some of the typical micrographs showing the lumen side of the pit cavities. Figure 128 shows a lumen surface which includes three such pits together. Around the pits are several typical fibrillar arches. On the other hand, Fig. 129 shows an equally general condition of a pit surrounded by smooth surfaces, including some plasterlike material spread over fibrillar surfaces. (Figure 124C confirms in stereo view the expected depth of the visible open cavity.)

Three other micrographs of lumen-side pit surfaces are given in Fig. 130-132. These pictures are included mainly because of the patterns of fibril deviation around the pit openings shown in the given areas. (Figure 131 also shows the visible lumen side of a continuous membrane, though an even better view of a similar membrane is included in Appendix IX, Fig. 162.) In particular, Fig. 130 and 131 show the patterns of fibrils in interlying areas between adjacent pits. Both of these areas appear to have some exposure of the underlying lamellae because of the deviation of the surface fibrils around the pit openings. On the other hand, Fig. 132 shows one definite pit opening with an area resembling another opening lying beside and apparently linked to the first opening. The resemblance of this area to a pit opening is the result of the swirling of surface fibrils about an open area, exposing the underlying lamella.

Another interesting observation is that these open areas enclosed by swirls of fibrils were not limited to areas beside pits. Three representative micrographs of such independently located "swirls" are given in Fig. 133-135. Again, the surface fibrils appear to be excluded from the given areas and are thus left to swirl around those areas, leaving them totally uncovered. No conclusive explanation of these "swirls" can be offered at this point. However, they do bear a close resemblance to the fibril patterns around the pit openings. Therefore, one possible explanation is that during the growth of these particular cells, the microfibril-generating apparatus behaved as if these areas were to include cell pits and simply deposited the fibrils outside of the designated areas. However, the present information is certainly not sufficient to confirm this explanation.

Another possible guess as to the origin of the "swirls" is that these discontinuities could be artifacts from the alkali extraction (because of their resemblance to the alkali-degraded surfaces in Appendix VI). However, observation of these features in dilute-alkali extracted fibers (Fig. 132 and 134) does not support this speculation. Thus, the explanation of these swirls must be left as an unanswered question.

Figure 128. The Lumen Surfaces of Three Pits Together

P: pit cavities

AR: fibrillar arches

SC: scraped surfaces left by the dissecting tools

Plate Number: 3167 AF

Magnification: 6200X

Specimen Preparation: NONEXTR, FD, FWS, STR

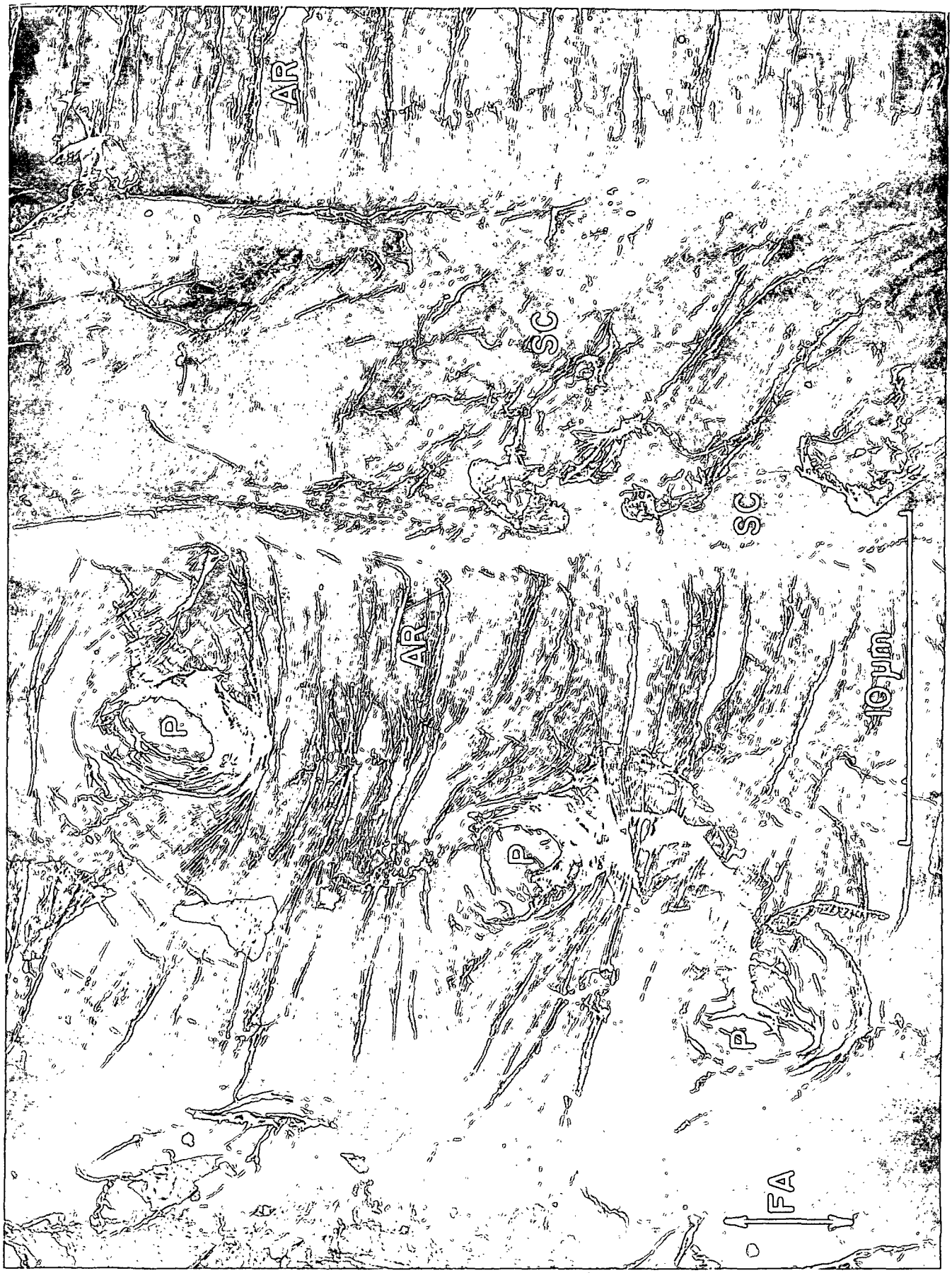
AR
SC
SC
AR
DL
DL
DL
DL
FA

Figure 129. The Lumen Surface of a Single Pit

P: pit aperture

DF: deviation of the fibrils around the pit cavity

CL: crack in the lumen surface

M: mudlike material retained on the surface

AR: a single fibrillar arch

Plate Number: 2908 AF

Magnification: 9400X

Specimen Preparation: 9% KOH, FD, FWS, STR

Figure 130. A Lumen Surface with Two Pits Side by Side

P: pit apertures

DF: deviation of the fibrils around the pits

M: patch of mudlike material retained on the surface

RC: replica cracks

Plate Number: 3232 AF

Magnification: 8600X

Specimen Preparation: 0.1N KOH, FD, FWS, STR (same specimen as in Fig. 93)


RC
L
RC
M
DF
DF
L
5 μm
FA

Figure 131. A Lumen Surface with Two Pits Side by Side

P: pit cavities

PM: a visible primary-wall-type membrane

DF: deviation of the fibrils around the pits

CL: crack in lumen surface

M: mudlike material retained on the surface

Plate Number: 3238 AF

Magnification: 12,400X

Specimen Preparation: 0.1N KOH, FD, FWS, STR


M
P
M
DF
CL
PM
P
1μm
FA

Figure 132. An Open Pit Beside a Structure Resembling the Rim of a Pit Opening

P: pit aperture

SW: swirling of fibrils about an open area (the fibril deviation resembles the deviation around a pit opening)

UL: exposed, underlying lamella

Plate Number: 3258 AF

Magnification: 13,300X

Specimen Preparation: 0.1N KOH, FD, FWS, STR

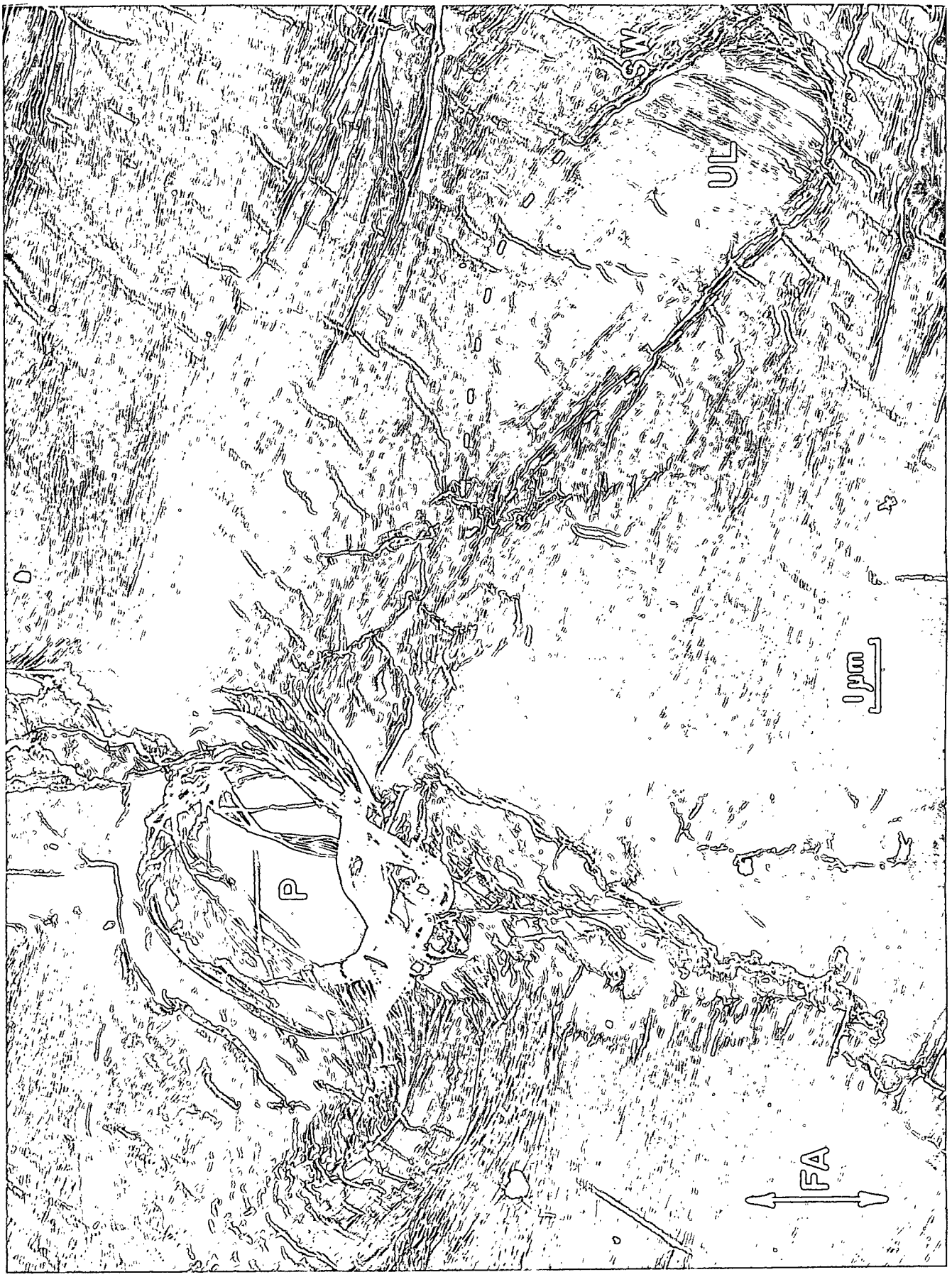
SV
UL
1 µm
P
FA

Figure 133. Swirling of Lumen-Surface Fibrils About an Open Area Exposing an Underlying Lamella

SF: surface fibrils

UL: underlying lamella

Plate Number: 2971 AF

Magnification: 26,200X

Specimen Preparation: KOH-BOA, FD, FWS, STR


SF
UL
SF
1μm
FA

Figure 134. Swirls of Lumen-Surface Fibrils

SW: swirling of the surface fibrils about open areas in the surface lamella, exposing underlying lamellae

SC: scraped surface left by dissecting tools

Plate Number: 3259 AF

Magnification: 12,600X

Specimen Preparation: Same specimen as in Fig. 132


FA
1 km
SW
SW
SC
SW

Figure 135. Swirls of Lumen-Surface Fibrils

SW: swirling of the surface fibrils about open areas in the surface lamellae, exposing underlying lamellae

RC: replica crack

Plate Number: 2963 AF

Magnification: 19,500X

Specimen Preparation: KOH-BOA, FD, FWS, STR (same specimen as in Fig. 101)


SW
SW
SW
RC
FA

SUMMARY OF CONCLUSIONS

The basic conclusions derived from the research can be separated into three main divisions. The first topic concerns the interfiber structure in the delignified chips. The most significant point in this topic was the observation of fibrillar membranes lying in the longitudinal-radial planes and bridging across the interfiber gaps as in Fig. 136. In agreement with the concepts of others, this structure presumably is remnant material of the parent-cell wall. However, the present results are significant in that the membrane structure--seen in surface view for the first time--was found to be quite intact, instead of being severely ruptured as others had concluded. On the other hand, several examples of multiple membrane thicknesses were observed. In these cases, the upper membrane (farthest from the cell wall) could appear stretched and contracted, but the lower membrane (closest to the cell wall) could still be intact. Also of interest is the observation that as many as eleven radially consecutive intercellular gaps could be demonstrated to be at least partially bridged over. Of course, the present observations are limited to latewood cells of longleaf pine. Thus, generalization of this information to include springwood and other species should be done cautiously.

The second topic of conclusions concerns the generalizations of cell-wall structure in the longleaf pine latewood. In agreement with the conclusions of others, the microfibrils were found to be organized in thin lamellae. Presumably, these lamellae are complete envelopes--one within another. In any case, the overlapping lamella edges observed in this work were seen to demonstrate small, stepwise transitions in microfibrillar orientation from one lamella to the next, especially in the S3 layer. Furthermore, the overall picture of these incremental transitions suggests a continuity of deposition during the growth of the cell. Subsequently, this continuity supports the ontogenetic concept of secondary-wall unity.

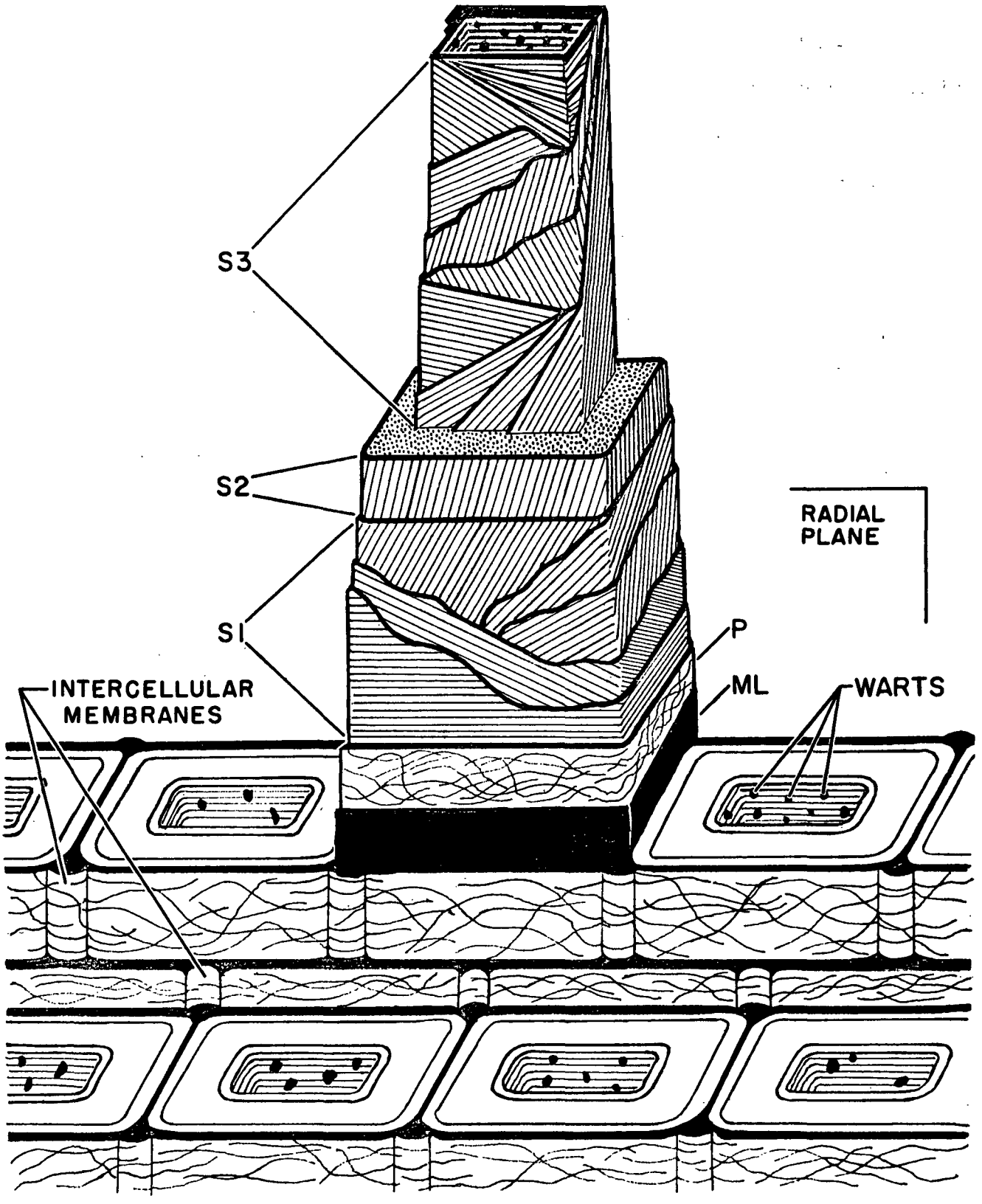

Figure 136. A Schematic Drawing of the Longleaf Pine Cell-Wall Structure

Though the cell walls of different fibers are not identical, a generalized pattern of layer structure was observed and is illustrated in Fig. 136. The model indicates the customary P, S1, S2, and S3 layers, although the arbitrariness of this structure designation according to the results of light microscopy has become more apparent in this study. In general agreement with the findings of others, the S1 layer was found to include at least five or six lamellae. The first lamella has its fibrils oriented nearly transverse to the fiber axis. The fibrils of the second lamella lie in a left-hand thread pitched at about 65° from the fiber axis. The third lamella is a right-hand thread at about 60° from the axis. Then, several "intermediate" lamellae display a gradual stepwise transition to the orientation angle of the S2 layer. This transition is pictured simply as a steepening of each successive thread or helix, with the last helix having nearly the same angle as the S2 fibrils.

In agreement with present concepts, the S2 layer was found to be made up of fibrils deposited in a right-hand thread and lying at an angle of 5 to 20° with the fiber axis. The question of whether the S2 fibrils are divided into separated concentric lamellae in the water-swollen condition is still somewhat uncertain, although an easier mechanical cleavage along concentric surfaces does appear to be possible.

One of the most significant contributions of this work was the elucidation of the S3 structure. This layer was found to consist of at least twelve lamellae. Furthermore, these lamellae display so many different orientations that any concept of average angular orientation becomes meaningless. However, a definite pattern of these orientations was evident in that these lamellae displayed a gradual, stepwise angular transition from the angle of the S2 fibrils to the angle of the fibrils on the lumen surface. If one visualizes a line segment which assumes a direction parallel to the fibrils of any given lamella through which it moves,

this line rotates in an incremental, clockwise manner (as seen from a point in the S2) in stepping from one lamella to the next and moving from the S2 toward the lumen surface. Beginning at the orientation of the S2, the line rotates more than 270°, ending in a left-hand helix at about 60° to the axis. Then, a reversal in the direction of rotation takes place, as the line progresses through a few other lamellae and finally stops in the surface lamella, which has its fibrils nearly perpendicular to the fiber axis.

Regarding the extractable components of the delignified cell wall, the non-extracted fibers were found to have their external surfaces covered with a mudlike coating. This material was seen to be largely removed by the 0.1N KOH and is probably a combination of pectin and "soluble lignin." Likewise, the untreated lumen surface is covered with mudlike material and, also, with wartlike deposits. These warty materials survived the delignification and are visible on the nonextracted surfaces, but they were removed by the extraction with 0.1N KOH. This material too, might be some form of lignin-carbohydrate combination.

The effect of the extractions with 9% KOH and with 9% KOH plus borate, together with any mild mechanical action accompanying the extraction, was a loosening or freeing of surface lamellae. On the external surfaces, much of the primary-layer material was actually removed, permitting the S1 fibrils to loosen and fibrillate. Also, many of the fibers had their lumen-surface lamellae loosened, and even totally removed in some cases. However, the exact explanation of these effects is not definite at this time. Conceivably, some of the hemicellulose acts as an adhesive agent, bonding these lamellae in place on the surfaces. Removal of the hemicellulose, then, would result in a freeing of the bonded lamellae. On the other hand, the alkaline solutions could also be acting through some other mechanism, such as swelling, to provide an additional driving force for lamella removal.

With regard to the effects of alkaline extraction upon the fiber tensile properties found by Spiegelberg (70), the author has concluded that the surface lamellae loosened and removed by the extraction would not have contributed directly to the tensile strength of the fibers. However, these lamellae could have been effective in indirect mechanisms such as restricting the freedom of the S2 fibrils and keeping them in near-optimum configurations. In any case, the extensively extracted fibers were seen to be curled in such a manner as to indicate that the original configurations of the S2 fibrils had most probably been disturbed during the extractions. This curling, then, constitutes evidence in support of the stress-concentration concept of behavior discussed by Spiegelberg. Finally, one other observation was that the equilibrium moisture content of the pulp decreased with the increasing severity of alkali extraction and the concomitantly decreasing hemicellulose content. This circumstantial evidence suggests that the influence of the hemicelluloses on the physical properties of the fibers may be the result of an indirect relationship. In other words, the effect of the hemicelluloses may simply be one of inducing higher moisture contents and greater lubricity within the cell wall.

The third and final topic of conclusions concerns the question of pit-membrane structure. The present work has not advanced new concepts of membrane structure but has simply developed strong support for the older concepts that have recently been challenged. In particular, the exposure of large expanses of ray-crossing areas allowed direct comparison of torus-type *versus* primary-wall-type pit membranes*. Thus, the author concludes that the torus structure is not a drying artifact, as some workers had suggested, but that it is most probably a real structure produced during cell growth.

*Because of the freeze-drying procedure used, these membranes had not been drawn into the pit cavities by retreating water-air interfaces. Instead, the membranes remained suspended in their raised positions.

Finally, in addition to obtaining fundamental knowledge of the cell wall, this work has resulted in the development of potentially important techniques. The techniques of microdissection and replication of single fibers have been found quite successful and have been demonstrated to contribute substantially to the study of wall structure. In fact, if these techniques, or modifications of them, should in time gain widespread use, one may well conclude that the development of the techniques was the most significant contribution of the thesis.

GLOSSARY

FA	fiber axis
FD	freeze dried
FWS	fiber-wall sheet (a fiber which has been slit open and spread out flat)
I	"intercellular substance" (middle lamella)
IPC	The Institute of Paper Chemistry
KOH-BOA	fiber sample which Spiegelberg (70) extracted with 9% KOH plus 3% boric acid
µm.	micrometer
NONEXTR	nonextracted fibers prepared by Spiegelberg (70)
P	primary wall
S1	outer layer of the secondary wall
S2	central layer of the secondary wall
S3	inner layer of the secondary wall
SFE	single-fiber extraction
STR	shadow transfer replica
T	tertiary layer (layer at lumen surface)

ACKNOWLEDGMENTS

In recognition of the many contributions to the thesis by others, the author would like to thank each of these--both students and staff members--for their valuable contributions--both their physical assistance and their broadening discussions. The author would especially like to thank his thesis advisory committee, Dr. J. A. Van den Akker, Chairman, and Dr. Norman S. Thompson and Dr. John W. Green, for their continuing interest and encouragement. Also, Dr. Irving H. Isenberg is warmly recognized for his interest and his helpful discussions with the author. In addition, the author expresses his appreciation to Dr. Gunther Hunger of West Virginia Pulp and Paper Company for the privilege of having worked with him and for the training and experience in electron microscopy gained during that association.

Special recognition is to be given also to those who have given valuable assistance during the experimental work and the preparation of the thesis. The author would like to thank Miss Olga Smith for her cooperation in the electron microscopy and especially for her preparation of the ultrathin sections. Also, the author would like to thank Mr. Fred Sweeney and the Photography and Duplicating Departments for their painstaking work in producing the printed micrographs. In addition, the very careful work of Mrs. Betty Cary in typing the manuscript is gratefully acknowledged.

Finally, the author would like to express appreciation to his wife Beth for her continued devotion and encouragement during student days and also, for her typing of the first draft.

LITERATURE CITED

1. Panshin, A. J., de Zeeuw, Carl, and Brown, H. P. Textbook of wood technology. Vol. I. 2d ed. New York, McGraw-Hill, 1964. 643 p.

2. Kerr, Thomas, and Bailey, I. W., J. Arnold Arboretum 15:327-49(1934).

3. Bailey, Irving W. Contributions to plant anatomy. Waltham, Mass., Chronica Botanica, 1954. 259 p.

4. Roelofsen, Pieter A. The plant cell-wall. p. 209. Berlin, Gebrüder Borntraeger, 1959. 336 p.

5. Wardrop, A. B. The structure and formation of the cell wall in xylem. In Zimmermann's The formation of wood in forest trees. p. 87. New York, Academic Press, 1964.

6. Liese, Walter, and Johann, Ingeborg, Planta 44:269-85(1954).

7. Meier, H., and Yllner, S., Svensk Papperstid. 59, no. 11:395-401(June 15, 1956).

8. Meier, H., Holzforsch. 11, no. 2:41-6(1957).

9. Liese, W., Holz Roh-Werkstoff 18, no. 8:296-303(1960).

10. Liese, W., J. Polymer Sci. (Part C, Polymer Symposia), no. 2:213-29(1963).

11. Bailey, I. W., Phytomorphology 7:136-8(1957).

12. Wardrop, A. B., Holzforsch. 8, no. 1:12-29(1954).

13. Wardrop, A. B., and Dadswell, H. E., Holzforsch. 11, no. 2:33-41(May, 1957).

14. Wardrop, A. B. The structure and organization of thickened cell walls. In Recent advances in botany. Vol. 1. p. 740. Toronto, University of Toronto Press, 1961.

15. Wardrop, A. B., Bot. Rev. 28, no. 2:241-85(April-June, 1962).

16. Wardrop, A. B., Svensk Papperstid. 66, no. 7:231-47(April 15, 1963).

17. Wardrop, A. B., and Harada, H., J. Exp. Botany 16, no. 47:356-71(May, 1965).

18. Wardrop, A. B. Cellular differentiation in xylem. In Côté's Cellular ultrastructure of woody plants. p. 61. Syracuse, N. Y., Syracuse University Press, 1965.

19. Frey-Wyssling, A. Die pflanzliche Zellwand. Berlin, Springer-Verlag, 1959. 367 p.

20. Ruska, V., Kolloid Z. 92, no. 3:276-85(Sept., 1940).

21. Sears, G. R., and Kregel, E. A., Paper Trade J. 114, no. 12:43-9(March 19, 1942).

22. Barnes, R. B., and Burton, C. J., Ind. Eng. Chem. 35, no. 1:120-5(Jan., 1943).

23. Frey-Wyssling, A., Mühlethaler, K., and Wyckoff, R. G. W., Experientia 4, no. 12:475-6(Dec., 1948).

24. Hodge, A. J., and Wardrop, A. B., Austral. J. Sci. Research B 3 no. 3:265-9 (Aug., 1950).

25. Meier, H., Holz Roh-Werkstoff 13, no. 9:323-38(Sept., 1955).

26. Emerton, H. W., and Goldsmith, Valerie, Holzforsch. 10, no. 4:108-15(Sept., 1956).

27. Wardrop, A. B., Holzforsch. 11, no. 4:102-10(Oct., 1957).

28. Emerton, H. W. The outer secondary wall. 1. Its structure. In Bolam's Fundamentals of papermaking fibers. p. 35. Kenley, Surrey, England, Tech. Sect., Brit. Paper & Board Makers' Assocn., 1958.

29. Kallmes, O. The distribution of the constituents across the wall of unbleached spruce sulfite fibers. Doctor's Dissertation. Appleton, Wis., The Institute of Paper Chemistry, 1959. 77 p.

30. Wardrop, A. B., and Dadswell, H. E., J. Inst. Wood Sci. no. 2:8-21(Nov., 1958).

31. Harada, H., Miyazaki, Y., and Wakashima, T. Electronmicroscopic investigation on the cell wall structure of wood. Bull. Govt. Forest Expt. Sta. (Tokyo) no. 104(Jan., 1958).

32. Bailey, I. W., Ind. Eng. Chem. 30, no. 1:40-7(Jan., 1938).

33. Harada, H., J. Japan Wood Res. Soc. 8, no. 6:252-8(Dec., 1962).

34. Jayme, Georg, and Fengel, Dietrich, Holz Roh-Werkstoff 19, no. 2:50-5(Feb., 1961).

35. Stone, J. E., and Scallan, A. M., Pulp Paper Mag. Can. 66, no. 8:T-407-14 (Aug., 1965).

36. Borysko, Emil, J. Biophys. Biochem. Cytol. 2, no. 4, Suppl.:3-14(1956).

37. Harada, H. Ultrastructure and organization of gymnosperm cell walls. In Côté's Cellular ultrastructure of woody plants. p. 215. Syracuse, N. Y., Syracuse University Press, 1965.

38. Kobayashi, K., and Utsumi, N., Sen-i Kenkyusho Koenshu no. 12:159-87(1955).

39. Necesany, V., Drev. Vyskum no. 1:1-26(1966).

40. Berlyn, Graeme P., Forest Prod. J. 14, no. 10:467-76(Oct., 1964).

41. Liese, W., and Hartmann-Fahnenbrock, M., Biochim. Biophys. Acta 11, no. 2: 190-8(June, 1953).

42. Liese, W., Holz Roh-Werkstoff 14, no. 11:417-24(1956).

43. Liese, Walter. The warty layer. In Côté's Cellular ultrastructure of woody plants. p. 251. Syracuse, N. Y., Syracuse University Press, 1965.

44. Wardrop, A. B., Liese, W., and Davies, G. W., Holzforsch. 13, no. 4:115-20 (Oct., 1959).

45. Wardrop, A. B., and Davies, G. W., Nature 194, no. 4827:497-8(May 5, 1962).

46. Liese, Walter. The fine structure of bordered pits in softwoods. In Côté's Cellular ultrastructure of woody plants. p. 278. Syracuse, N. Y., Syracuse University Press, 1965.

47. Wardrop, A. B., and Davies, G. W., Holzforsch. 15, no. 5:129-41(Nov., 1961).

48. Brown, H. D., Panshin, A. J., and Forsaith, C. C. Textbook of wood technology. Vol. I. New York, McGraw-Hill, 1949. 652 p.

49. Harada, Hiroshi, J. Japan Wood Res. Soc. 10, no. 6:221-5(Dec., 1964).

50. Côté, W. A., Forest Prod. J. 8, no. 10:296-301(Oct., 1958).

51. Côté, W. A., Jr., and Krahmer, R. L., Tappi 45, no. 2:119-22(Feb., 1962).

52. Côté, Wilfred A., Jr., J. Polymer Sci. (Part C, Polymer Symposia), no. 2: 231-42(1963).

53. Frey-Wyssling, Albert, and Bosshard, Hans Heinrich, Holz Roh-Werkstoff 11, no. 11:417-20(Nov., 1953).

54. Liese, Walter. Fine structure of bordered pits in conifer wood. In Ross's The proceedings of the third International Conference on electron microscopy, London, 1954. p. 550. London, Royal Microscopical Society 1956.

55. Jayme, Georg, and Fengel, Dietrich, Holz Roh-Werkstoff 17, no. 6:226-30(June, 1959).

56. Jayme, G., and Hunger, Günther, Holz Roh-Werkstoff 13, no. 6:212-15(June, 1955).

57. Jayme, Georg, and Hunger, Günther, Monatsh. Chem. 87, no. 1:8-23(Feb. 15, 1956).

58. Jayme, G., Hunger, G., and Fengel, D., Holzforsch. 14, no. 4:97-105(Oct., 1960).

59. Jutte, S. M., and Spit, B. J., Holzforsch. 17, no. 6:168-75(Dec., 1963).

60. Tsoumis, George. Light and electron microscopic evidence on the structure of the membrane of bordered pits in tracheids of conifers. In Côté's Cellular ultrastructure of woody plants. p. 305. Syracuse, N. Y., Syracuse University Press, 1965.

61. Frey-Wyssling, A., and Mühlethaler, K. Ultrastructural plant cytology. New York, Elsevier, 1965. 377 p.

62. Thomas, R. J., and Nicholas, D. D., Forest Prod. J. 16, no. 3:53-6(March, 1966).

63. Fengel, Dietrich, Svensk Papperstid. 69, no. 7:232-41(April 15, 1966).

64. Ott, Emil, Spurlin, Harold M., and Grafflin, Mildred W., Ed. Cellulose and cellulose derivatives. 2d ed. New York, Interscience, 1954.

65. Hearle, J. W. S., and Peters, R. H. Fibre structure. Manchester, Engl., Textile Institute, 1963. 667 p.

66. Manley, R. St. J. Summary, IPC Pioneering Research Program. p. 88-101. Appleton, Wis., The Institute of Paper Chemistry, 1964.

67. Timell, T. E. Wood hemicelluloses: Part I. In Wolfrom's Advances in carbohydrate chemistry. Vol. 19. p. 247. New York, Academic Press, 1964.

68. Meier, H. General chemistry of cell walls and distribution of the chemical constituents across the walls. In Zimmermann's The formation of wood in forest trees. p. 137. New York, Academic Press, 1964.

68A. Larson, Kenneth C. An investigation of pectic substance in the developing xylem of Populus tremuloides. Doctor's Dissertation, Appleton, Wis., The Institute of Paper Chemistry, 1967.

69. Jentzen, Carl A. The effect of stress applied during drying on the mechanical properties of individual pulp fibers. Doctor's Dissertation. Appleton, Wis., The Institute of Paper Chemistry, 1964. 130 p.

70. Spiegelberg, Harry L. The effect of hemicelluloses on the mechanical properties of individual pulp fibers. Doctor's Dissertation. Appleton, Wis., The Institute of Paper Chemistry, 1966. 115 p.

71. Hill, Richard L. An investigation of the time-dependent structural and mechanical behavior of individual pulp fibers when subjected to an applied stress. Doctor's Dissertation. Appleton, Wis., The Institute of Paper Chemistry, 1967. 119 p.

72. Fischbein, I. W., J. Appl. Phys. 21, no. 12:1199-1204(Dec., 1950).

73. Pye, I. T., Washburn, O. V., and Buchanan, J. G. Structural changes in paper on pressing and drying. In Bolam's Consolidation of the paper web. p. 353. London, Tech. Sect. of the Brit. Paper & Board Makers' Assoc., 1966.

74. Bailey, A. J., Ind. Eng. Chem. Anal. Ed. 8, no. 1:52-5(Jan. 15, 1936); no. 5:389-91(Sept. 15, 1936).

75. Côté, W. A., Jr., Koran, Z., and Day, A. C., Tappi 47, no. 8:477-84(Aug., 1964).

76. Hunger, Günther K. Personal communication, 1964.

77. Jayme, Georg, and Hunger, Günther, Mikroskopie 13, no. 1/2:24-38(1958).

78. Wardrop, A. B. Australia, Council Scientific and Industrial Research. Proceedings of the Seventh Annual Pulp and Paper Co-operative Research Conference 11-45, 1946.

79. Thompson, N. S., Heller, H. H., and Smith, Olga. Unpublished work, 1966.

80. Wardrop, A. B., Nature 170, no. 4321:329(Aug. 23, 1952).

81. Newman, I. V., Phytomorphology 6, no. 1:1-19(March, 1956).

82. Wardrop, A. B., and Dadswell, H. E., Holzforsch. 7, no. 2/3:33-9(1953).

83. Wardrop, A. B., Tappi 40, no. 4:225-43(April, 1957).

84. Meier, Hans, Svensk Papperstid. 61, no. 18B:633-40(Oct. 10, 1958).

85. Jayme, Georg, and Fengel, Dietrich, Papier 16, no. 10a:519-24(Oct., 1962).

86. Fengel, Dietrich, Holz Roh-Werkstoff 24, no. 5:177-85(May, 1966).

87. Klauditz, W., Holzforsch. 6, no. 3:70-82(1952).

88. Harlow, W. M., Paper Trade J. 109, no. 18:38-42(Nov. 2, 1939).

89. Wardrop, A. B., and Dadswell, H. E., Council Sci. Ind. Res. Bull. no. 221: 7-13(1947).

90. Roelofsen, P. A., and Kreger, D. R., J. Exp. Botany 2, no. 6:332-43(Sept., 1951).

91. Harada, H. Personal communication, 1967.

92. Jayme, Georg, and Hunger, Günther, Papier 14, no. 10a:549-53(Oct., 1960).

93. Jayme, G., and Hunger, G. Electron microscope 2- and 3-dimensional classification of fiber bonding. In Bolam's The formation and structure of paper. Vol. 1, p. 135. London, Tech. Sect., Brit. Paper and Board Makers' Assoc., 1962.

94. Jayme, Georg, and Azzola, Friedrich Karl, Ann. Chem. 689:209-20(Nov., 1965).

95. Wardrop, A. B., Appita 16, no. 3:xv-xxx(Nov., 1962).

96. Bucher, Hans. Discontinuities in the microscopic structure of wood fibers. In Bolam's Fundamentals of papermaking fibres. p. 7. Kenley, Engl., Tech. Sect., Brit. Paper & Board Makers' Assoc., 1958.

97. Jurbergs, K. A., J. Polymer Sci. (Part C, Polymer Symposia) no. 11:1-12(1965).

98. Frey-Wyssling, A., Mühlethaler, K., and Bosshard, H. H., Holz Roh-Werkstoff 13, no. 7:245-9(July, 1955).

99. Bailey, I. W., Ind. Eng. Chem. 30, no. 1:40-7(Jan., 1938).

100. Svensson, A. Ake, Arkiv Kemi 10, no. 14:239-50(1956).

101. Jurbergs, K. A., Tappi 43, no. 6:561-8(June, 1960).

102. Necesaný, Vladimír, Drev. Výskum no. 1:27-32(1965).

103. Sultze, Rolland F., Jr. A study of the phenolic and carbohydrate materials in the newly formed tissues of aspenwood. Appleton, Wis., The Institute of Paper Chemistry. Doctor's Dissertation. 1956. 120 p.

104. Preston, R. D., Proc. Royal Soc. Sect. B 134:202(1947).

105. Giertz, Hans W. The effects of beating on individual fibers. In Bolam's Fundamentals of papermaking fibers. p. 389. Kenley, Engl., Tech. Sect., Brit. Paper & Board Makers' Assoc., 1958.

106. Jayme, G., and Fengel, D., Holzforsch. 15, no. 4:97-102(Sept., 1961).

107. Meier, H., and Wilkie, K. C. B., Holzforsch. 13, no. 6:177-82(Dec., 1959).

108. Christensen, G. N., and Kelsey, Kathleen E., Austral. J. Appl. Sci. 9, no. 3:265-82(Sept., 1958).

109. Stamm, Alfred J. Wood and cellulose science. New York, Ronald Press Co., 1964. 549 p.

110. Merchant, Morris V., Tappi 40, no. 9:771-81(Sept., 1957).

111. Haselton, William R., Tappi 38, no. 12:716-23(Dec., 1955).

112. Beélik, Andrew, Conca, Romeo J., Hamilton, J. Kelvin, and Partlow, E. Vernon, Tappi 50, no. 2:78-81(Feb., 1967).

113. Liese, Walter, and Schmid, Roswitha, Holz Roh-Werkstoff 19, no. 9:329-37 (Sept., 1961).

114. Wardrop, A. B., and Dadswell, H. E., Austral. Pulp Paper Ind., Tech. Assoc. Proc. 8:6-26(1954).

APPENDIX I

THE DEFIBERING OF SHIVES FROZEN WITH LIQUID NITROGEN

During the course of the work, freezing of wet specimens with liquid nitrogen was attempted. At the time this medium was tried, an effort was being made to replicate the surfaces of fiber shives. However, the result of the attempt was that shives frozen with the liquid nitrogen were found to be extensively defibered upon sublimation of the ice. Even when shives frozen with liquid nitrogen were subjected to sublimation at the same time as control shives frozen with a dry ice-acetone bath, the test shives defibered, but the control shives did not. Needless to say, this defibering was inimicable to good replication of shives; so the liquid-nitrogen freezing was abandoned in favor of the freezing with dry ice and acetone.

APPENDIX II

CONSIDERATION OF SOLVENT-EXCHANGE DRYING FOR USE IN SPECIMEN PREPARATION

After the method of freeze drying had been tested and adopted for this work, Thomas and Nicholas (62) published the results of a pit-membrane study in which they had used solvent-exchange drying. Since they were mainly interested in membrane structure in untreated wood, they did not examine the surfaces of pulp fibers. Nevertheless, the method of solvent-exchange drying should apply quite well to pulp fibers. In the present work, freeze drying was simply thought to be more convenient. Now that the replica technique has been developed for single fibers and has been shown to preserve the surface fibrillation, someone might be interested in replicating some solvent-dried fibers in an effort to get a more accurate picture of water-swollen fibers. This speculation of a "more accurate picture" is based on Merchant's (110) finding that WAN (water-alcohol-nonpolar solvent) drying preserves much more of the swollen-pulp specific surface area than does freeze drying (up to 196 *versus* 3.17 $m.^2$ per gram). However, one is to be cautioned that special techniques for preparing and replicating the fibers in a dry atmosphere would have to be developed, since Haselton (111) has shown that the specific surface area of WAN-dried pulp decreases drastically upon exposure to atmospheric humidity.

APPENDIX III

PREPARATION OF THE SLITTING KNIVES

The preparation of a slitting knife with a point small enough to enter the fiber lumen is, of course, crucial to the slitting technique. Therefore, the knife preparation will be discussed briefly. The knives used in this work were made from pieces of Gem single-edge razor blades, although any similar blade should be suitable. The first step is to break off a corner of the blade. (This break can be better controlled by clamping that corner between flat metal plates as in Fig. 137A.) Then, the broken edge is ground on a fine emery wheel as in Fig. 137B. Care should be taken not to break or overheat the point or original cutting edge of the blade as both are quite thin. Subsequent grinding of the point is done on an extremely fine hand stone. (The stone used in this work was an "Arkansas" stone polished on one face with number 600 carborundum and on another face with the same powder followed by pink rouge.) The knife is first sharpened to an extremely fine point (Fig. 137C). Then, the last step is to make <u>one</u>, slightly rotating, stroke as lightly as possible with the blade held in a raised position as in Fig. 137D. The purpose of this step is to produce the rounded lower side of the point already mentioned as aiding the "riding" of the point along the fiber lumen surface. Finally, the blade must be inspected microscopically for the presence of "burrs" and then adjusted to suitable form by trial and error.

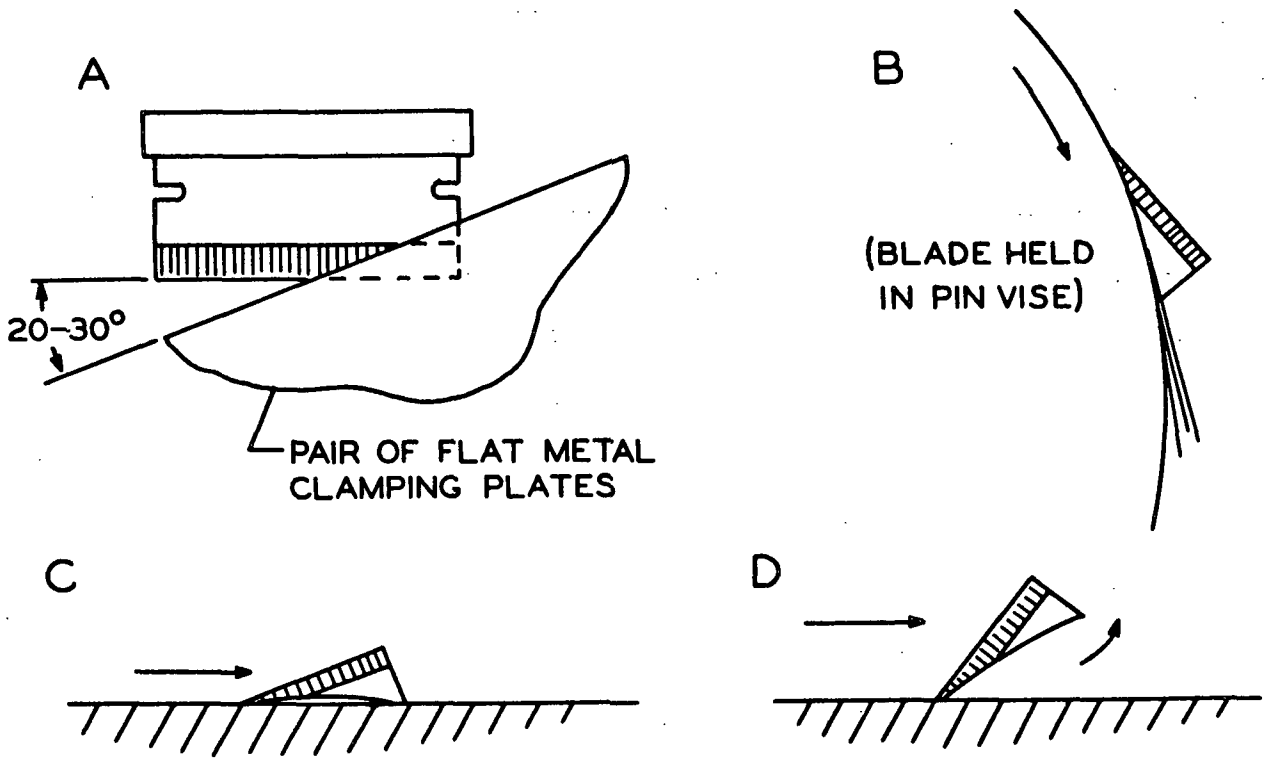

Figure 137. Preparation of the Slitting Knives

APPENDIX IV

THE ATTEMPTS TO SLIT WET FIBERS

Some discussion of the difficulties encountered in developing the slitting technique might be beneficial to the reader. The operation was first attempted with water-swollen fibers. However, several problems were faced. The cell walls were nearly transparent and very difficult to see under water. Even worse, the well-plasticized fibers had very little strength. Even if a very sharp blade was used, fibrils from the outer layers of the fiber tended to "pile up" in front of the moving knife. The resulting cuts were quite ragged, but of even greater consequence is the fact that the very weak fibers tended to pull apart when the knife ground to a halt in accumulated masses of fibrils. Therefore, any fiber wall sheets (FWS) prepared in water were normally quite short and ragged. Also, the operation of spreading the cylindrically shaped split fibers into flat sheets was quite difficult. One could, with patience, spread a portion of the fiber, but once the spreading instrument was removed, the flattened portion quickly re-curled to the original cylindrical shape. Only after repeated stroking of the fiber in the open position did the curling tendency relax.

The fiber slitting was next attempted in ethyl alcohol. Although this modification was made mainly in order to insure that no polysaccharides went into solution upon mechanical disruption of the fibers, an unexpected improvement in the slitting procedure was observed. The fibers became noticeably stiffer and much stronger than they had been in water. These changes greatly improved the reliability of the slitting as well as the quality of the FWS. Furthermore, the spreading of the cylindrical fibers into flat sheets was much easier, because the stiffer fibers tended to remain flat when spread out.

However, the alcohol system was not without difficulties. For instance, the alcohol was suspected of extracting some foreign material, possibly a plasticizer, from the rubber working surface. Also, the absolute alcohol appeared to absorb atmospheric moisture. Subsequently, the alcohol evaporated more quickly than the absorbed water, leaving the water present in an increasing percentage. The water, then, plasticized and weakened the fiber as before the alcohol exchange.

Although these difficulties with the alcohol possibly could have been overcome, the decision to try freeze-dried fibers resulted in such an improvement in the ease of slitting and the quality of the FWS that the use of freeze-dried fibers became standard procedure. These dry fibers were much easier to see and were much stronger than the wet fibers; yet they retained the original cylindrical shape prerequisite for the slitting technique.

APPENDIX V

METHODS OF VIEWING THE STEREO PICTURES

Although several different optical systems are available for viewing stereo pictures, the reader may be interested, for the sake of convenience, in viewing the printed pictures in an unaided manner. Several methods of doing so have been found quite effective. Some workers hold a vertical card between the two stereo pictures as a means of preventing both eyes from focusing on one picture or the other. As an alternative, one can roll up two paper tubes and hold them in binocular fashion to view the pictures.

However, another method used by many workers is even more convenient. One holds the stereo pair at close reading range and then relaxes the eyes as if for viewing an object at a distance. Though the detail of the pictures is not in focus, the lines of vision of the eyes are nearly parallel, permitting the eyes to "fuse" the two images. This fusion is best accomplished by concentrating on a single light or dark feature of the pictures and then allowing the eyes to move until the two images of this feature fuse. Incidentally, the fusion is much easier if the pictures are held so that the two images appear adjusted to the same vertical position (not one above the other). Finally, once the images have been fused, the prints are moved away from the eyes to a more comfortable focusing distance. The eyes are then caused to focus on the detail of the pictures without losing the fused image. In conclusion, this method of viewing might require more practice at first, but it is a more suitable method for continued use.

APPENDIX VI

ALKALI EXTRACTION OF SINGLE FIBERS

After the scraping and peeling of the fibers, many of the fiber surfaces remained covered by mudlike material which prevented any study of lamella structure. This condition was common for both external surfaces (e.g., Fig. 138) and lumen surfaces (e.g., Fig. 139) of the fiber. Considering the possibility that these mudlike materials could be hemicelluloses, a caustic-extraction scheme was set up in an attempt to remove them. Furthermore, the extraction program (Fig. 140) was planned to allow specificity for the xylan and glucomannan polymers. Hamilton, et al. (112) had found that mannose polymers could be insolubilized by the addition of barium to an extracting solution. Therefore, barium hydroxide [$Ba(OH)_2$] was used as a pretreatment solution before the first extraction stage and then as an added compound in the extraction solution itself. Thus, the first stage was intended to remove any xylan present but to leave the mannan in an insoluble form. Following the xylan extraction, the fibers were treated with hydrochloric acid to free the mannan from the barium. Then, the fibers were extracted with sodium hydroxide (NaOH), which was intended to remove the mannan.

In carrying out the extraction, a compromise became necessary. The method of surface replication does not permit one to study a surface, alter it, and then study it again. In order to avoid this problem, three fiber segments were prepared in a similar fashion. Then, one segment was replicated without further extraction; one was subjected to the first extraction stage and then replicated; and one was subjected to both stages and then replicated. Incidentally, in an attempt to overcome the interfiber variation, the three different segments to be compared were all cut from a single fiber, which had already been slit open and spread out. The two segments to be extracted were cemented with epoxy resin (Miller Stephenson 907) to nichrome wires to be suspended in the alkali solutions. After extraction and

Figure 138. The Exterior Surface of a Fiber Which Has Been Scraped, but Which Has Retained Much Mudlike Covering over Its Surfaces

M: mudlike material

P: remnant of the primary layer

S1: probable S1 fibrils (they are too badly plastered over for one to be certain of their identification)

S2: S2 layer (still partially covered over with mudlike material)

SC: possible scraped surface left by the scraping tool

Plate Number: 4320 AF

Magnification: 8100X

Specimen Preparation: KOH-BOA, FD, FWS, exterior surface scraped, STR


W
IS
SC
P
M
S2
M
5mm
FA

Figure 139. The Lumen Surface of a Fiber Which Has Been Scraped, but Which Has Retained Much Mudlike Material on Its Surfaces

M: mudlike material (especially on the surface of the S2 layer)

Plate Number: 4018 AF

Magnification: 8700X

Specimen Preparation: 0.1N KOH, FD, FWS, lumen surface scraped, STR


M
38
M
38
35
E

washing, the two segments were freeze dried and mounted (together with the unextracted segment) for replication.

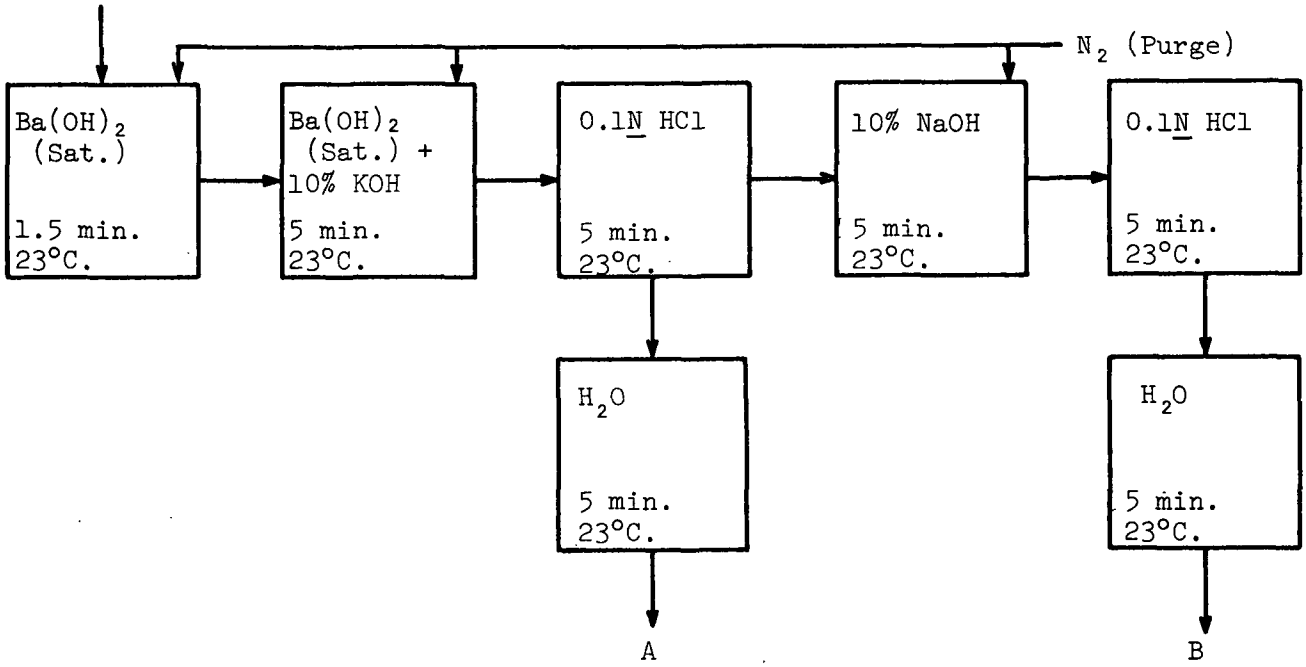

Figure 140. The Extractive Scheme Used in the First Attempt to Extract Single Fibers

Unfortunately, this first extraction scheme was not successful. The first stage did not noticeably remove the plastering material. However, the second stage (10% NaOH) apparently swelled the cell wall so much that even part of the fibrillar structure became smooth, or mudlike. Both the exterior surface (Fig. 141) and the lumen surface (Fig. 142, 143, and 144) lost their characteristic lamellar structures. Incidentally, some form of change was anticipated when the fiber segments were seen to curl severely and display translucent coverings when placed in the NaOH.

The exact explanation of this surface alteration is uncertain. In all likelihood, the distortion resulted from a form of alkali swelling. One might even question whether the appearance of the disoriented fibrils could indicate that

mercerization of the cellulose has taken place. However, according to Ott, et al. (64), mercerization in 10% NaOH, at least of raw cotton, does not set in above 3°C. Therefore, one would be hesitant to conclude on the basis of these micrographs alone that the present material was mercerized. Incidentally, Svensson (100) has treated pulps with mercerizing-strength caustic and has obtained a similar appearance.

Following the failure of the first extraction scheme, a second scheme was set up with a final KOH-plus-borate stage similar to the one used successfully by Spiegelberg (70) (Fig. 145). However, the results of this extraction, too, were somewhat inconclusive. Though some loss of mudlike material was suspected, especially during the KOH-borate extraction, this loss could not be verified without statistical surveys of the areas. Both the outer fiber surfaces (Fig. 146-148) and the fiber-lumen surfaces (Fig. 149-151) retained at least some of their mudlike material throughout the extraction sequence. Thus, any change in appearance would not be an obvious positive-negative difference, but rather a degree-of-exposure difference. For this reason, the results of this work failed to verify in a positive way the removal of hemicellulose materials from the fiber surfaces. Nevertheless, some future worker may be interested to try a similar approach, except to use some means of statistically scanning the surfaces. In any case, many of the fibers prepared during the present attempt became quite useful in the study of cell-wall structure, simply because they displayed good exposure of the lamellar elements. In fact, the reader may have already noticed that many of the micrographs included in the discussion of cell-wall organization showed fiber surfaces which had been reextracted after slitting and scraping.

In trying to explain the mudlike material remaining after alkali extraction, several possibilities would seem reasonable. The material could be lignin residue, though the Klason-lignin content of 0.4% was estimated to be too small to account for all of the plastered areas observed. Another possibility would be that the

Figure 141. The Exterior Surface of a Fiber Which Was Scraped and then Extracted with 10% NaOH. The Fiber Surface Has Lost Its Characteristic Fibrillar Structure

Plate Number: 4293 AF

Magnification: 6100X

Specimen Preparation: 0.1N KOH, FD, FWS, exterior surface scraped, SFE (Fig. 140, Sequence B), FD, STR

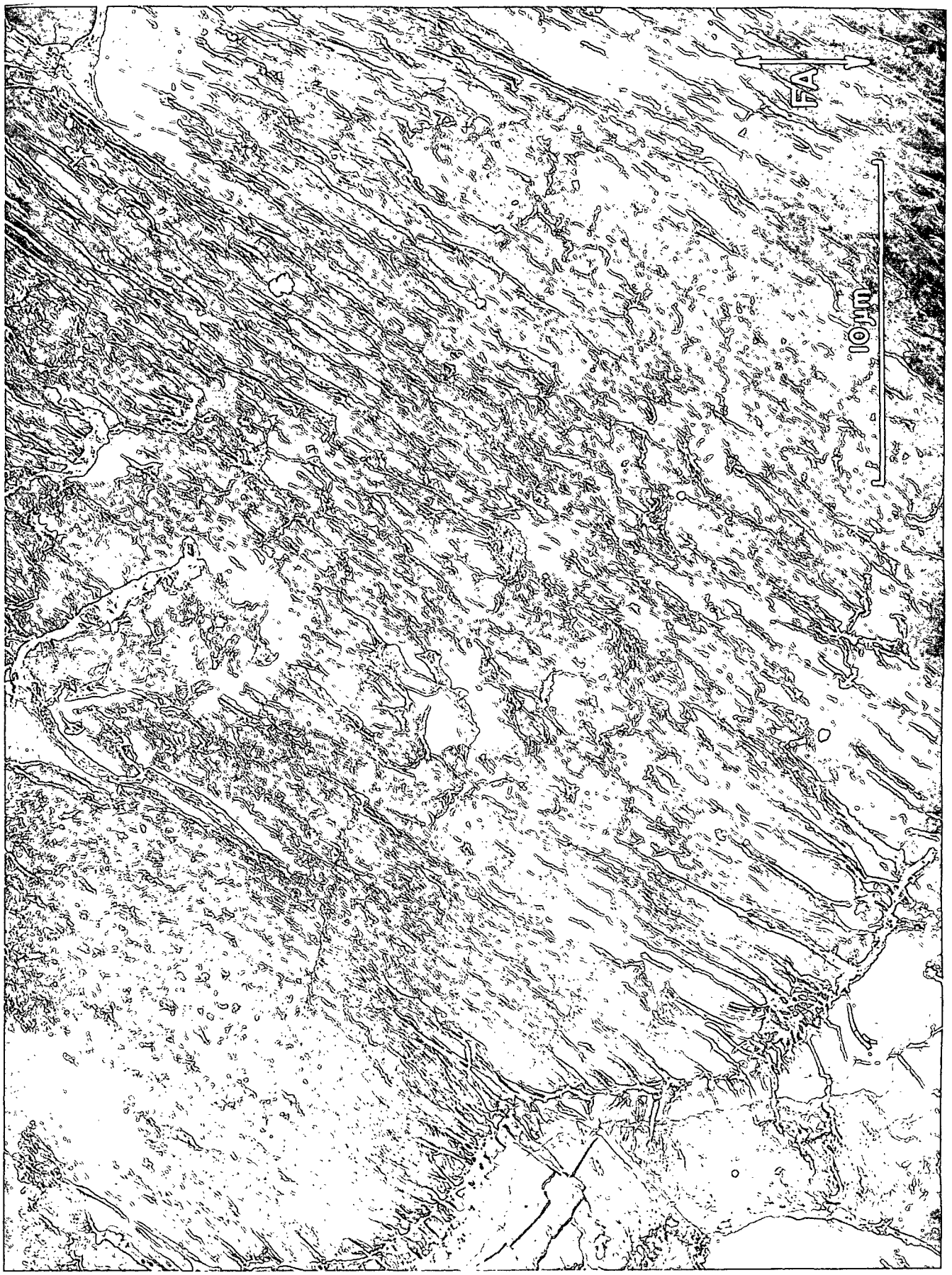
FA
10mm

Figure 142. A Lumen Surface Which Has Been Scraped and Then Extracted with 10% NaOH. Though Some Areas Have Retained a Resemblance of Lamellar Structure, Most of the Area Has None of the Original Structure

Plate Number: 4275 AF

Magnification: 8100X

Specimen Preparation: 0.1N KOH, FD, FWS, lumen surface scraped and peeled, SFE (Fig. 140, Sequence B), FD, STR


FA
5 μm

Figure 143. A Lumen Surface Which Has Been Scraped and then Extracted with 10% NaOH. Very Little of the Original Fibrillar Texture Has Been Retained

Plate Number: 4266 AF

Magnification: 12,500X

Specimen Preparation: 0.1N KOH, FD, FWS, lumen surface scraped and peeled, SFE (Fig. 140, Sequence B), FD, STR


FA
1μm

Figure 144. A Lumen Surface Which Has Been Scraped and then Extracted with 10% NaOH, Showing Still Another Variation of Surface Appearance Observed

Plate Number: 4271 AF

Magnification: 8700X

Specimen Preparation: 0.1N KOH, FD, FWS, lumen surface scraped and peeled, SFE (Fig. 140, Sequence B), FD, STR


5 km

structureless materials are hemicelluloses. Though one would not question the accessibility of hemicelluloses lying on the surface, these materials could be "hornified," having been dried once. One other possibility is that the structureless material is actually fibrillar material which has been mechanically conformed to a smooth or mudlike surface. That such a smoothing over of fibrillar surfaces could take place is demonstrated in Fig. 152 and 153. The first micrograph shows a lumen surface which was mechanically stroked during dissection--probably by the back of the slitting knife. The other picture shows an exposed internal surface of the S3 which was scarred by one of the scraping tools. Thus, both of these pictures demonstrate some degree of conformability of the visible fibrils. Finally, one must recognize the possibility that the mudlike materials may consist of some cell-wall material which has not yet been isolated and identified. Thus, the exact explanation or identity of the mudlike covering material simply remains unknown.

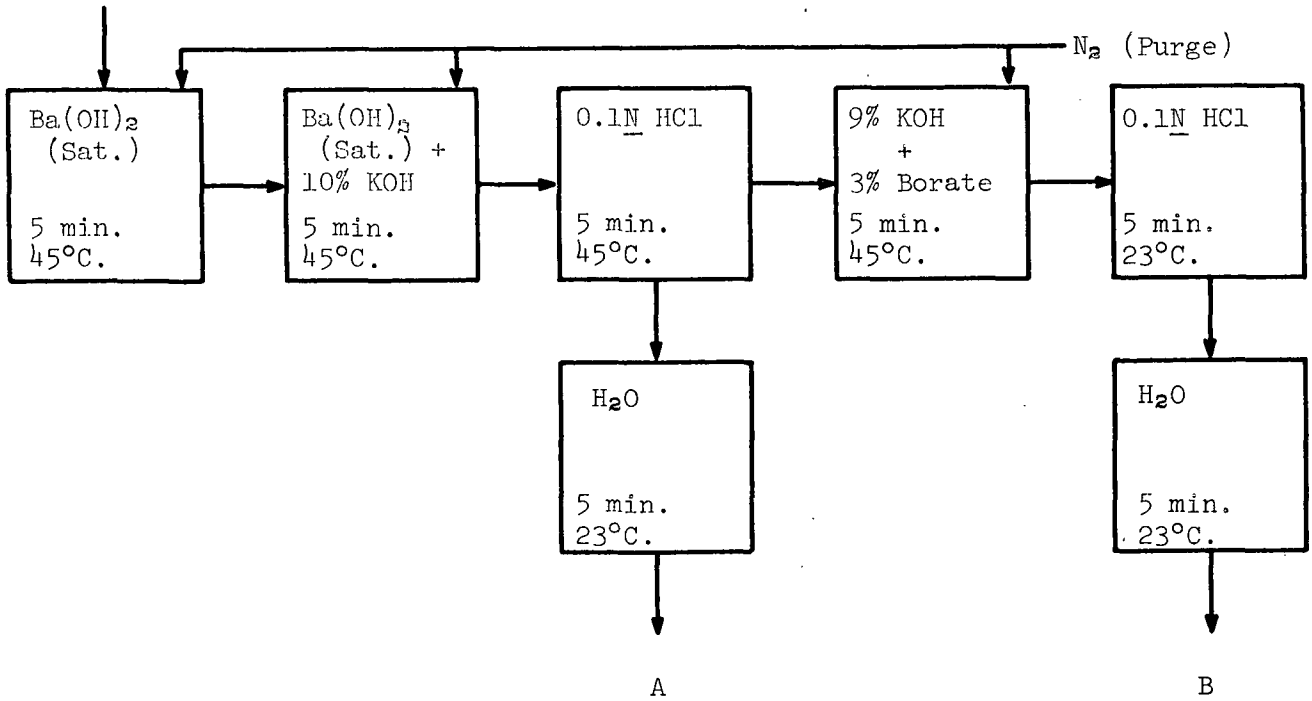

Figure 145. The Extraction Scheme Used in the Second Attempt to Extract Single Fibers

Figure 146. The Scraped Exterior Surface of a Fiber. (After Being Scraped, this Fiber Was Cut into Three Segments. The Segment Shown in this Micrograph Was Replicated After Scraping Without Being Subjected to Further Extraction. The Other Two Segments Were Further Extracted and Are Shown in Fig. 147 and 148)

Plate Number: 4516 AF

Magnification: 13,600X

Specimen Preparation: 0.1N KOH, FD, FWS, exterior surface scraped, STR


FA
1 km
S 22

Figure 147. Another Segment of the Same Fiber Shown in Fig. 146. This Surface Exterior Was Subjected to an Extraction with a 10% KOH Solution Saturated with $Ba(OH)_2$, but Has Retained Much of Its Mudlike Material

P: primary layer

S2: uncovered S2 layer

M: remaining mudlike material

Plate Number: 4518 AF

Magnification: 10,300X

Specimen Preparation: 0.1N KOH, FD, FWS, exterior surface scraped, SFE (Fig. 145, Sequence A), FD, STR


M
S2
P
1mm
FA

Figure 148. Another Segment of the Same Fiber Shown in Fig. 146 and 147. This Surface Exterior Was Further Extracted with 10% KOH Plus 3% Borate, but Still Shows Some Areas of Mudlike Material

Plate Number: 4521 AF

Magnification: 19,000X

Specimen Preparation: 0.1N KOH, FD, FWS, exterior surface scraped, SFE (Fig. 145, Sequence B), FD, STR


FA
S2
1mm
B
D

Figure 149. The Scraped Lumen Surface of a Fiber. (After Being Scraped and Peeled, This Fiber Was Cut Into Three Segments. The Segment Shown in This Micrograph Was Replicated After Scraping Without Being Subjected to Further Extraction. The Other Two Segments Were Further Extracted and Are Shown in Fig. 150 and 151. Incidentally, All Three of These Micrographs Happen to Display Exposed Surfaces of the S2 Layer.)

Plate Number: 4539 AF

Magnification: 30,000X

Specimen Preparation: 0.1N KOH, FD, FWS, lumen surface scraped and peeled, STR

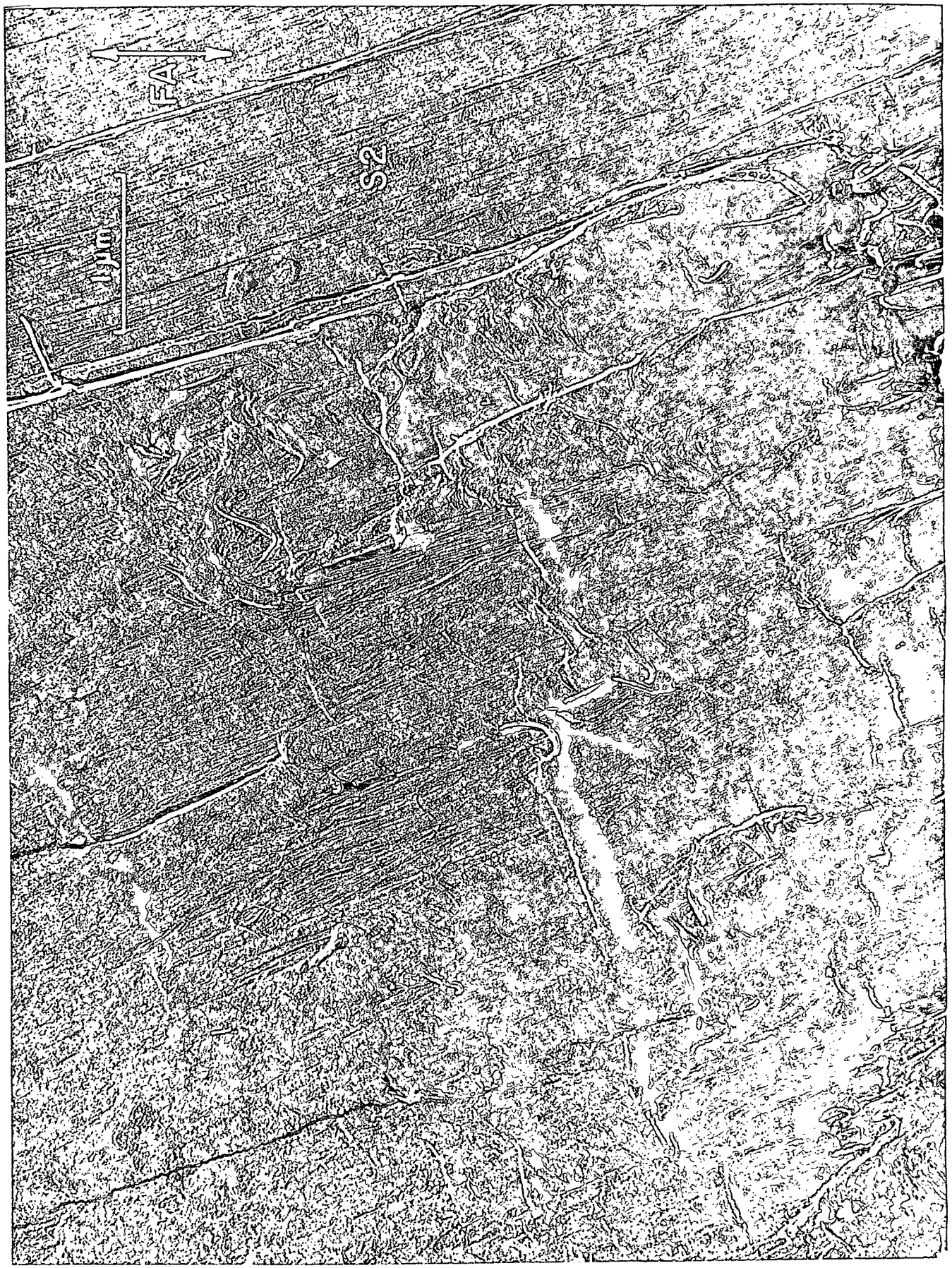
FA1
S2
1 mm

Figure 150. Another Segment of the Same Fiber Shown in Fig. 149. This Surface Lumen Was Further Extracted with a 10% KOH Solution Saturated with $Ba(OH)_2$ but Still Retained Some Mudlike Material

Plate Number: 4545 AF

Magnification: 19,000X

Specimen Preparation: 0.1N KOH, FD, FWS, lumen surface scraped and peeled, SFE (Fig. 145, Sequence A), FD, STR

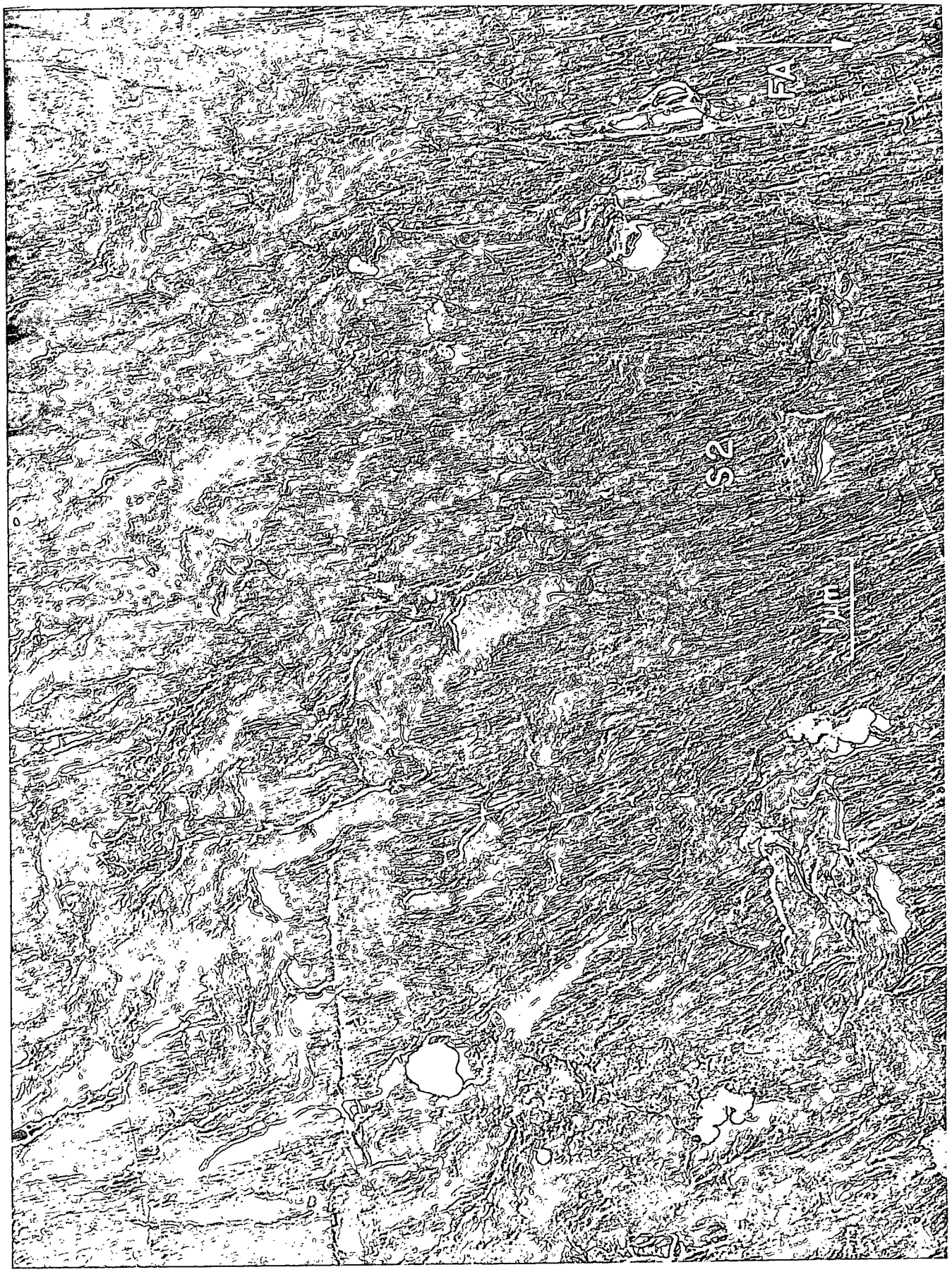
FA
S 97
PIPE

Figure 151. Another Segment of the Same Fiber Shown in Fig. 149 and 150. This Surface Lumen Was Further Extracted with 10% KOH Plus Borate, but Still Shows Some Areas of Mudlike Material

Plate Number: 4549 AF

Magnification: 13,600X

Specimen Preparation: 0.1N KOH, FD, FWS, lumen surface scraped and peeled, SFE (Fig. 145, Sequence B), FD, STR

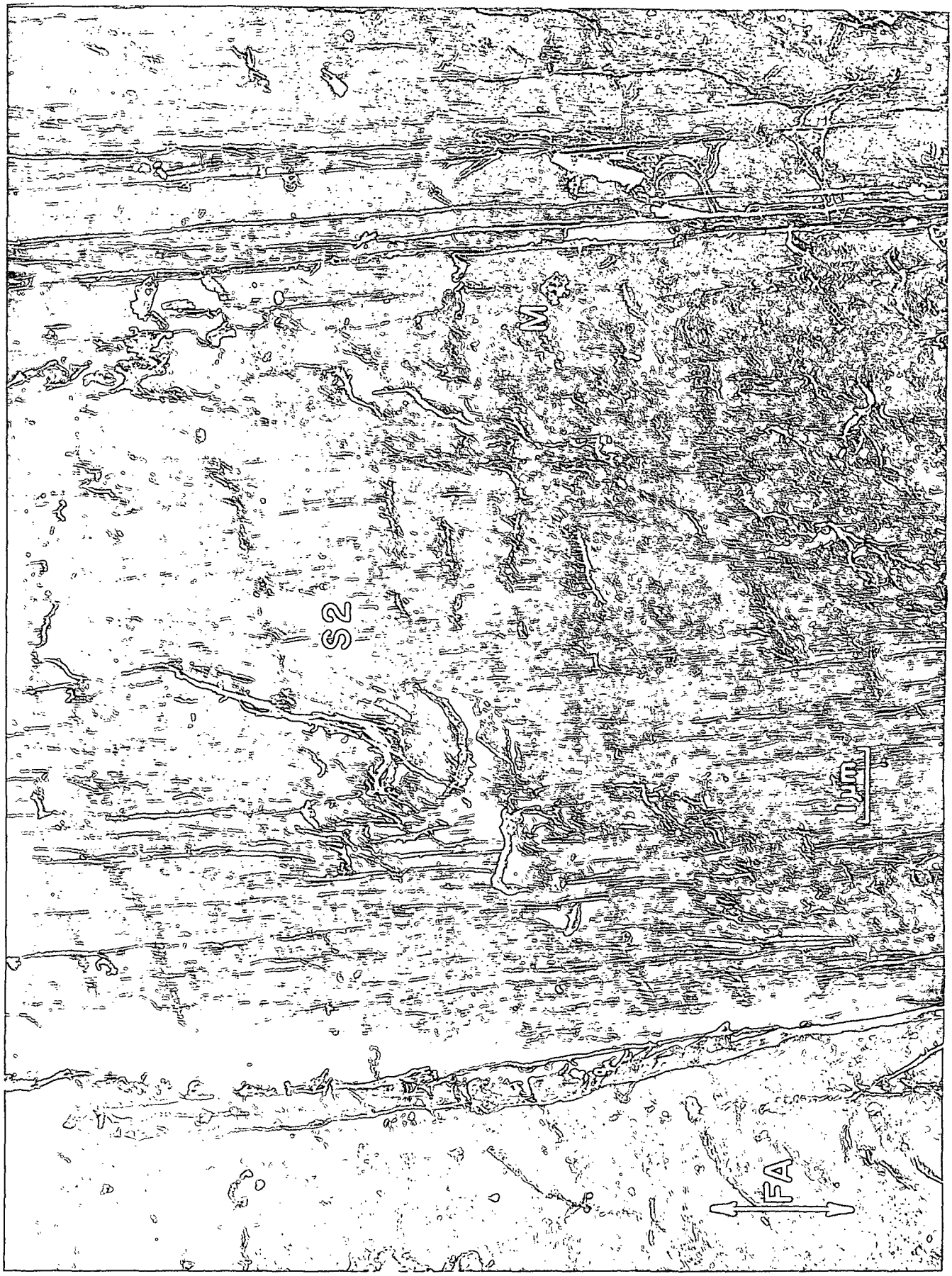
M
S2
FA

Figure 152. A Fiber Lumen Surface Which Demonstrates the Possibility of Mechanically Smoothing over a Fibrillar Surface

LS: lumen surface

GS: grooves in the surface (probably caused by the back edge of the slitting knife)

CS: crack in the surface lamellae

Plate Number: 4335 AF

Magnification: 12,500X

Specimen Preparation: KOH-BOA, FD, FWS, lumen surface scraped and peeled, STR (same specimen as in Fig. 81)

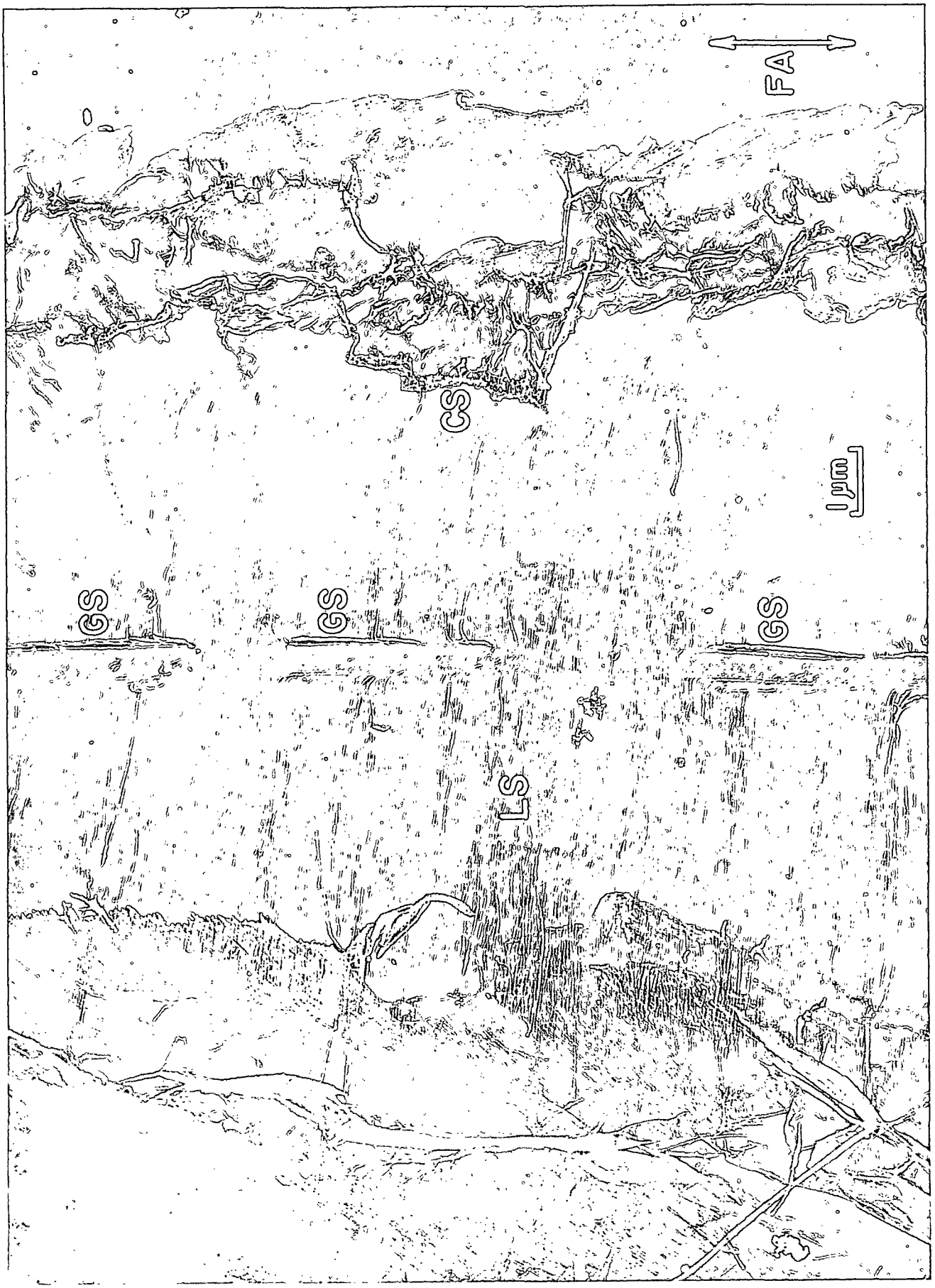
FA
GS
GS
GS
GS
GS
1μm

Figure 153. An Internal S3 Surface Showing a Smooth Scar Left by a Scraping Tool

I-S3: internal S3 surface

SC: scar left by scraping tool

M: mudlike material

Plate Number: 4488 AF

Magnification: 10,300X

Specimen Preparation: 9% KOH, FD, FWS, lumen surface scraped and peeled, STR


M
I-S3
SC
I-S3
I-S3
FA

APPENDIX VII

LIGHT MICROGRAPHS OF FREEZE-DRIED FIBERS

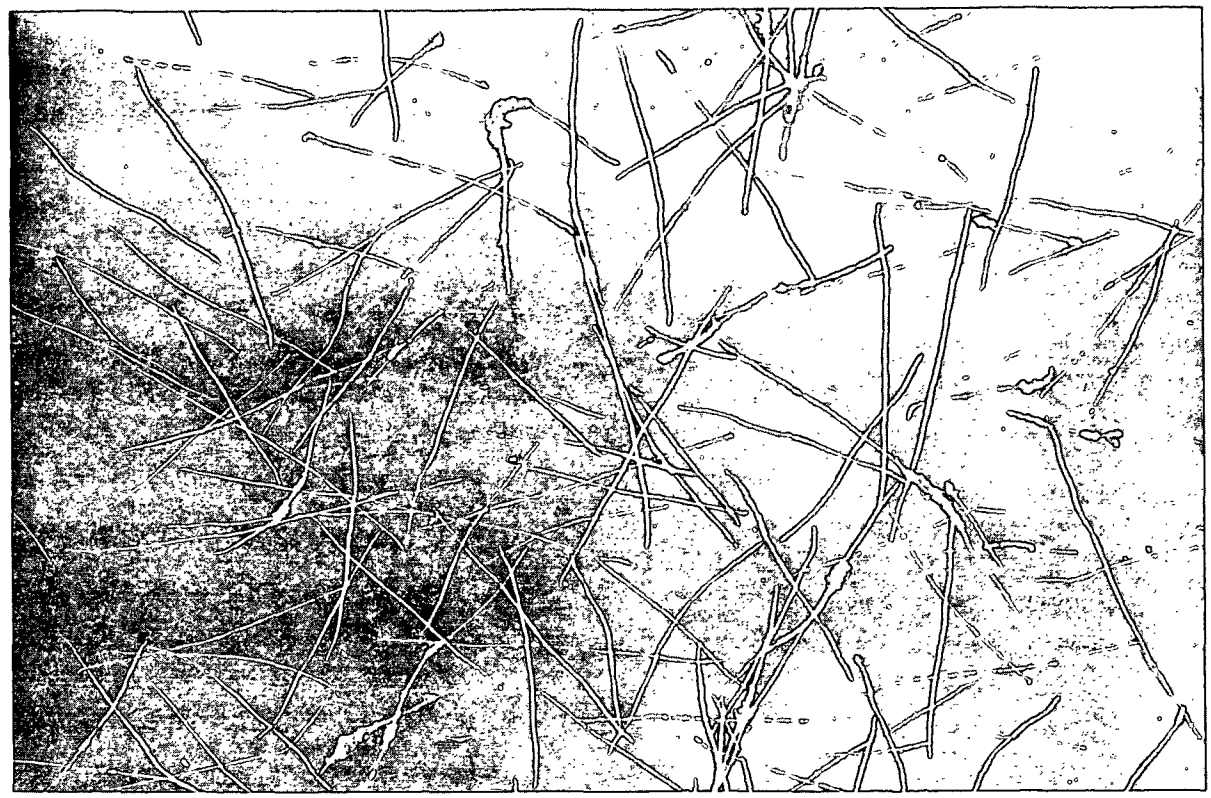

Figure 154. Light Micrograph of Nonextracted, Freeze-Dried Fibers. Negative No. 67M630C, Magnification 8.7X

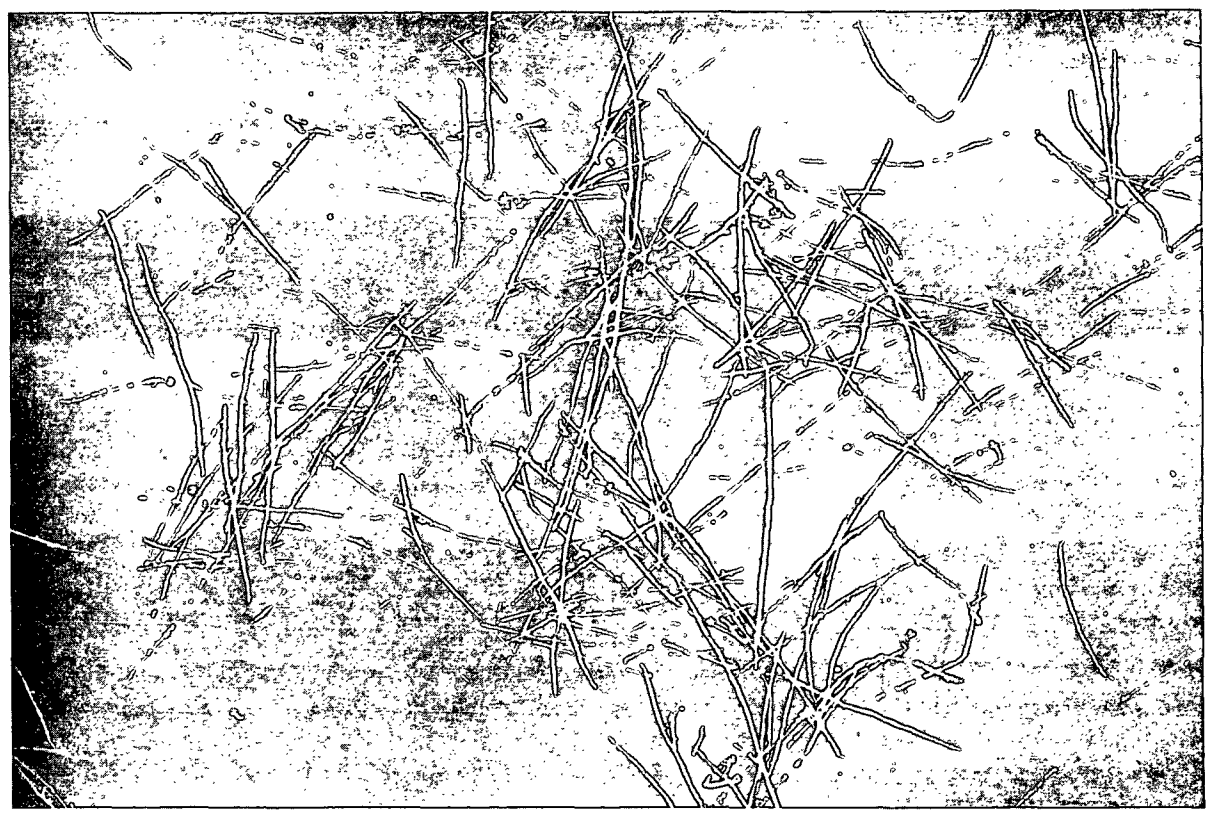

Figure 155. Light Micrograph of Fibers Extracted with 0.1N KOH and Freeze Dried. Negative No. 67M630D, Magnification 8.7X

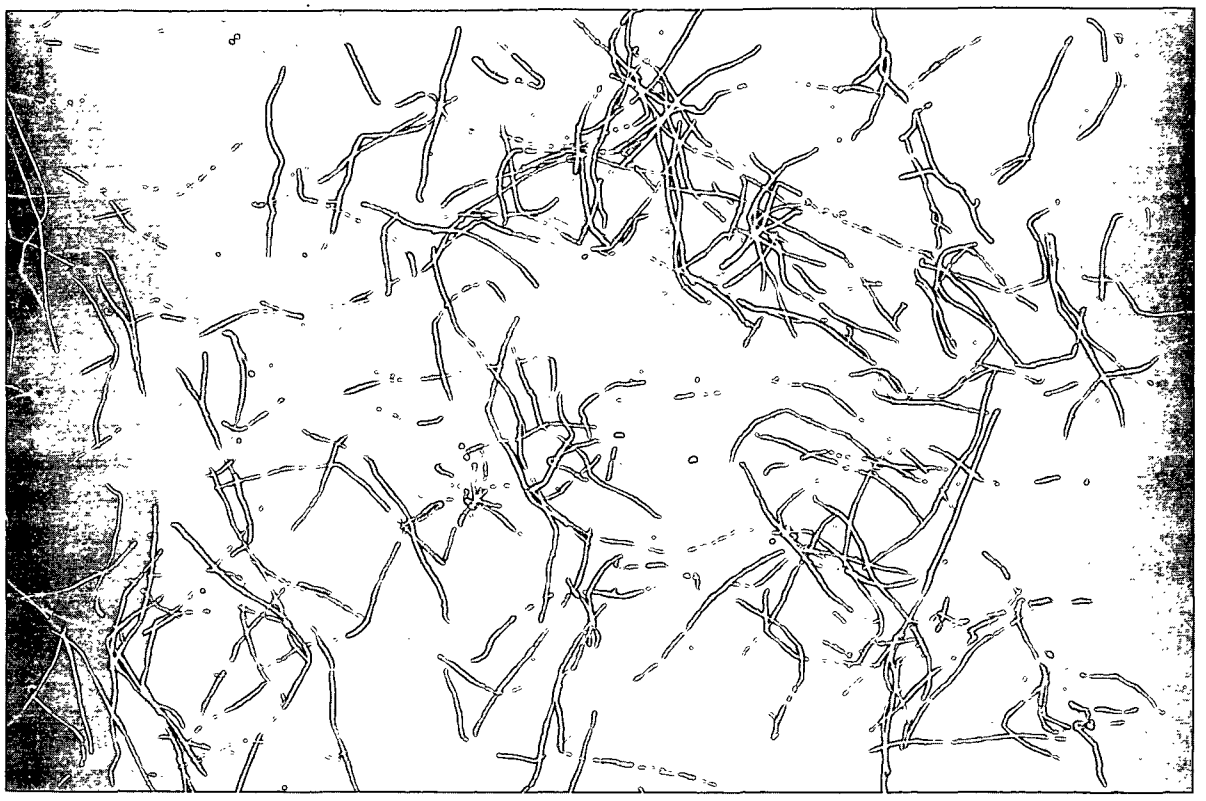

Figure 156. Light Micrograph of Fibers Extracted with 9% KOH and Freeze Dried. Negative No. 67M630E, Magnification 8.7X

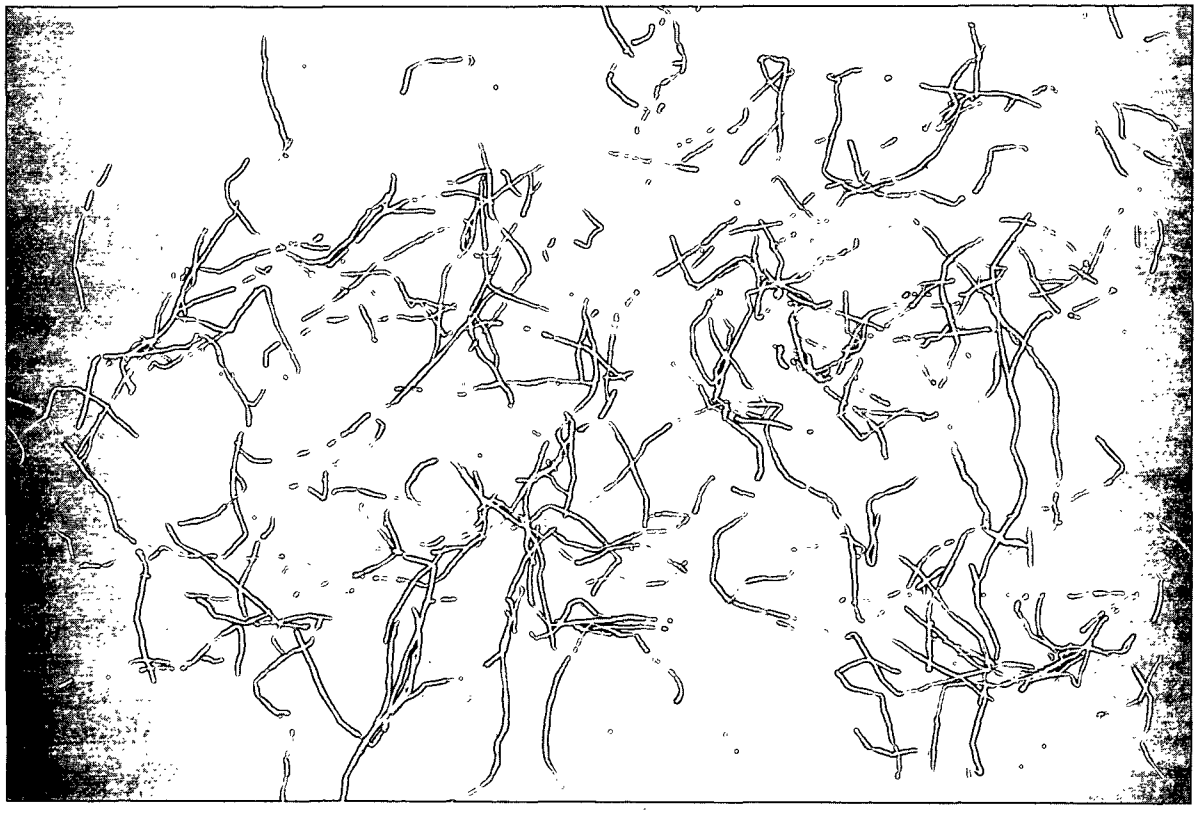

Figure 157. Light Micrograph of Fibers Extracted with 9% KOH Plus 3% Borate and Then Freeze Dried. Negative No. 67M630F, Magnification 8.7X

APPENDIX VIII

EQUILIBRIUM MOISTURE CONTENTS OF THE EXTRACTED PULP SAMPLES

During the course of the present thesis work, the question was raised as to whether the presence of varying contents of hemicelluloses could indirectly influence the mechanical properties of the pulp fibers by effecting different moisture contents in the pulp samples. In order to determine whether, in fact, the moisture contents did vary, meager aliquots (av. 0.27 g.) of the limited pulp samples on hand were air dried at standard temperature and humidity (STH: 73°F., 50% R.H.) for moisture determinations. (The fibers were dried as extremely thin sheets prepared from very dilute suspensions on polyethylene sheets.) After the fibers had reached equilibrium and were weighed, they were oven dried and weighed again. From these measurements, the equilibrium moisture contents at STH were calculated for the first desorption (Table III). The ovendry samples were then again equilibrated at STH to obtain similar measurements for a sorption approach. Finally, the fibers were allowed to sorb at 90% relative humidity and 80°F. and were then subjected to a second desorption to STH. Table III summarizes the results of all these determinations. A more thorough discussion of these results and their implications is given on page 267-8.

TABLE III

EQUILIBRIUM MOISTURE CONTENTS OF THE PULP SAMPLES SUBJECTED TO VARYING DEGREES OF CAUSTIC EXTRACTION

	First Desorption,[a] % moisture[b]	Sorption,[a] % moisture[b]	Second Desorption,[a] % moisture[b]
Nonextracted	9.17	7.76	8.89
Extr. with 0.1N KOH	8.83	7.75	8.58
Extr. with 9% KOH	8.34	7.13	8.07
Extr. with 9% KOH + 3% borate	8.30	7.08	7.98

[a] All at 50% relative humidity, 73°F.

[b] Percent of equilibrium weight.

APPENDIX IX

THE ELUCIDATION OF SUSPECTED ARTIFACTS IN THE REPLICAS

During the early stages of the present work, some unexplained dense films were encountered on the replicas. These films were most readily found either along cracks in the lumen surface (Fig. 158) or else in conjunction with the cell pits (Fig. 159). Actually, the two different structures were not at first recognized as being related. In fact, the dense films along the cracks were questioned as possible lignin residues.

Interestingly enough, an observation with a light microscope was one key which led to an explanation of the dense films. A fiber had been shadowed on its lumen surface, embedded in polystyrene, and then dissolved away from the polystyrene-replica combination. Examination of the embedded replica by means of a light microscope revealed the presence of toadstool- or nail-like studs standing on the surface of the replica. Presumably, these studs were formed by the extrusion of molten polystyrene (PS) up through the cell pits. Starting at the lumen side, the PS would have flowed through the pit aperture and into the enlarged pit cavity (Fig. 160A). The Polypore filter backing the fiber would have stopped the PS at the plane of the exterior fiber surface. Incidentally, the pebbled appearance of the film in Fig. 159 reflects the surface appearance of the Polypore filter.

After the observation of the studs on the surface of the PS-embedded replica, a consideration of the further steps in the replica procedure offered a plausible explanation of the unknown film. The significant point is that the embedded replica would next be coated with an auxiliary deposit of carbon. These studs, then, would intercept some of the carbon, leading to the formation of secondary films separated from the first (Fig. 160B). Finally, a washing away of the PS would allow the secondary carbon film to drape over the first-formed metal-carbon film (Fig. 160C). This collapsed film, then, would be the dense film seen on the replica.

In agreement with the explanation, the dense film in Fig. 159 does lie beneath the replica surface, according to the stereo view (Fig. 161A). In the case of Fig. 159, also, the film lies beneath the replica surface. (Figure 161B shows a similar crack in stereo view.) However, in this case, the molten PS apparently flowed into the open crack and then underneath a slightly raised surface layer. Again, the PS surface thus created and exposed upon hydrolysis would have intercepted the secondary carbon coating.

One might well ask why the separated secondary carbon coating appears so dense; the total carbon deposition in these areas of double films is essentially no greater than in the regions where the secondary carbon film is deposited directly onto the first-formed film. However, Roelofsen (4) indicates that, in general, most of the image contrast is developed by a preferential scattering of electrons, rather than by preferential absorption of the electrons in thicker areas of the specimen. If electron scattering is, in fact, the significant factor of contrast, then one might reason that the double-film structure presents twice as many interfaces--four instead of two--for electron deflection. Thus, these areas might be expected to scatter more of the electrons. Furthermore, whatever the final analysis might indicate about the role of the film surface in electron scattering, one can observe from some of the many micrographs shown that the carbon film alone can display some indication of surface contour. (The speckled or pebbled appearance in Fig. 159 is an example.) Thus, the explanation of the secondary film as an effective electron-scattering agent is at least logically acceptable.

Since the PS penetration into the fiber structure was believed to be important in the formation of the double-film structure, some negative replicas were prepared in order to verify the suspected behavior of the PS. Negative replicas are normally prepared by causing a polymer material to form a negative-contour copy of

Figure 158. A Dense Film Occurring Along a Lumen-Surface Crack

EC: edges of the lumen-surface crack

DF: dense film

Plate Number: 2378 AF

Magnification: 4300X

Specimen Preparation: NONEXTR, FD, FWS, STR

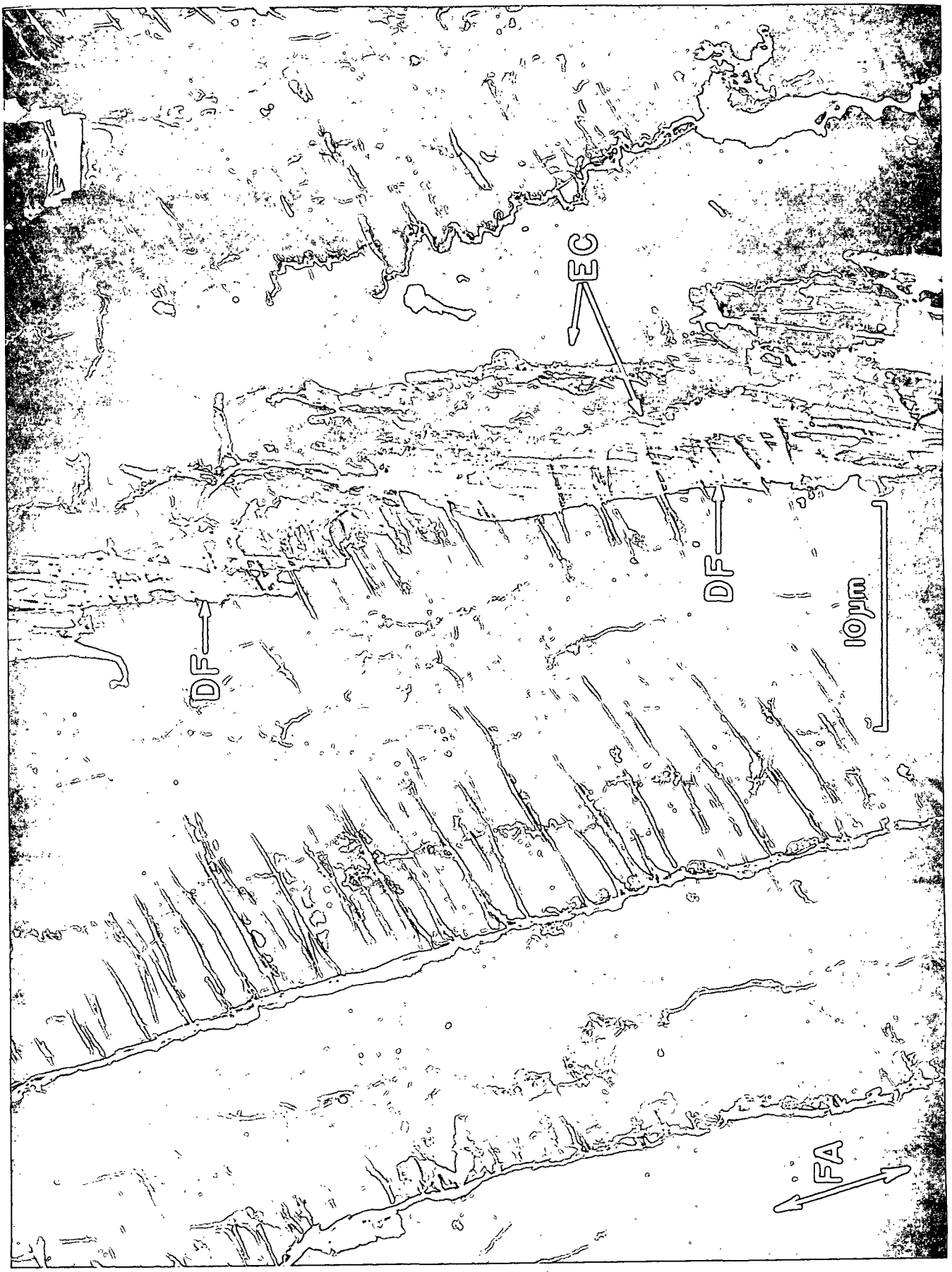
EC
DF
DF
10μm
FA

Figure 159. A Dense Film Occurring with a Cell Pit

LS: lumen surface

PA: pit aperture

DF: dense film

SP: speckled appearance of the film. (This speckled or pebbled appearance reflects the surface appearance of the filter used for a backing material during the polystyrene embedding.)

Plate Number: 2974 AF

Magnification: 10,200X

Specimen Preparation: 9% KOH, FD, FWS, STR


LS
DF
PA
SP
LS
FA
1μm

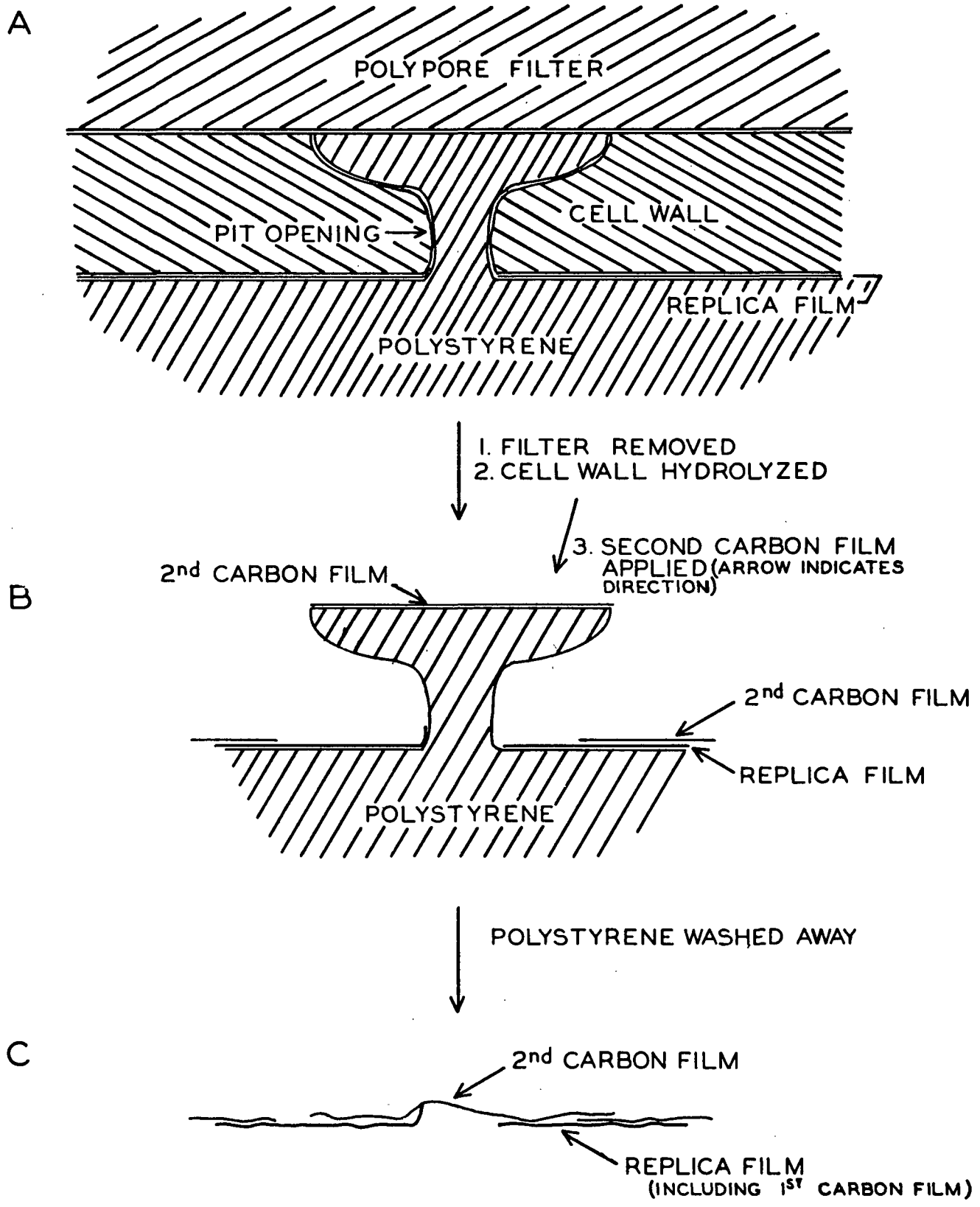

Figure 160. A Schematic Picture of the Replication Process, Indicating the Probable Behavior of the Secondary Carbon Film at a Pit Opening

a surface. Then, after the specimen surface is taken away from the polymer surface, a metal shadowing is applied to the polymer surface. Thus, this type of replica is essentially a record of the polymer's behavior when placed in contact with the given surface. Because of this reasoning, such negative replicas were prepared in order to examine the penetration of the molten PS into the cell structure.

Since the pit areas were especially vulnerable to the formation of the suspected artifacts, these areas were selected for concentrated study. Figures 162 and 163 are example micrographs of primary-wall-type pits. Actually, these two replicas were prepared in slightly different ways. After the application of the PS in Fig. 162, the cell wall was manually pulled away from the PS. Accordingly, most of the pit membrane was left embedded in the polystyrene surface. [Cote (50) had already observed the phenomenon of cell material retained in the PS.] In this particular micrograph, two surfaces of polystyrene penetration through the membrane can be seen. In both cases, the polystyrene surface is recognized because of its conformation to and replication of the pit lining. Incidentally, in addition to demonstrating PS penetration of the membrane, this micrograph also provides a very good view of the cell-wall side of the continuous membrane.

On the other hand, the PS surface shown in Fig. 163 was subjected to acid treatment in order to remove the cell-wall material retained on the polystyrene. This micrograph (Stereo: Fig. 161C) shows the reaction of the PS with two pit structures side by side. The membrane on the left was only partially ruptured and was penetrated only moderately by the PS. However, the membrane of the right-hand pit was severely damaged, and the PS penetrated well into the pit cavity. Furthermore, the surface of the PS looks as if it might have been fractured. Possibly, a core of PS was extruded into the pit aperture and then was broken off when the fiber wall was pulled away from the replica surface. In support of this speculation, Fig. 164 shows an STR (positive replica) of an open pit in a cell wall which had

Figure 161A. A Dense Film Lying Below a Replica Surface

Plate Number: 5150 AF

Magnification: 2500X

Specimen: Same as in Fig. 159

Figure 161B. A Dense Film Lying Below the Crack in a Lumen Surface

Plate Numbers: 2380, 2381 AF

Magnification: 4600X

Specimen: NONEXTR, FD, FWS, STR

Figure 161C. A Negative Replica of Two Primary-Wall-Type Membranes, Showing the Penetration of the Membranes by the Polystyrene

Plate Number: 5151 AF

Magnification: 3300X

Specimen: Same as in Fig. 163

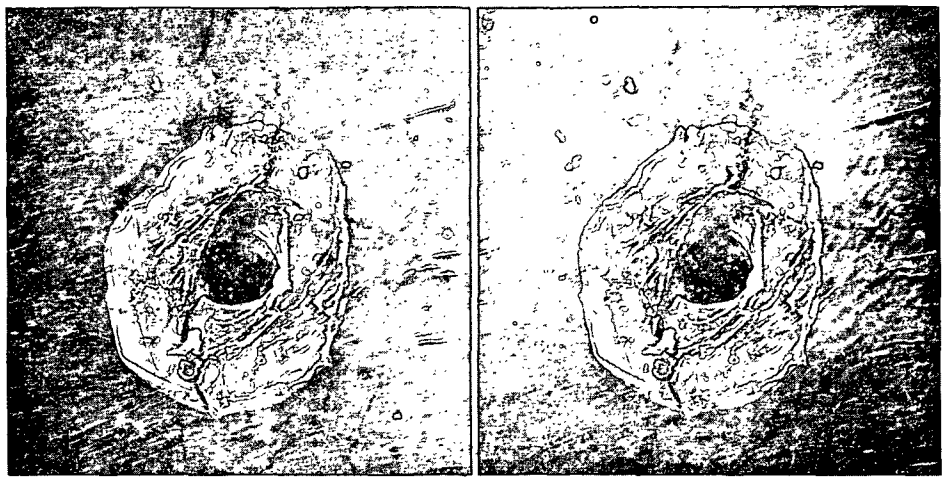

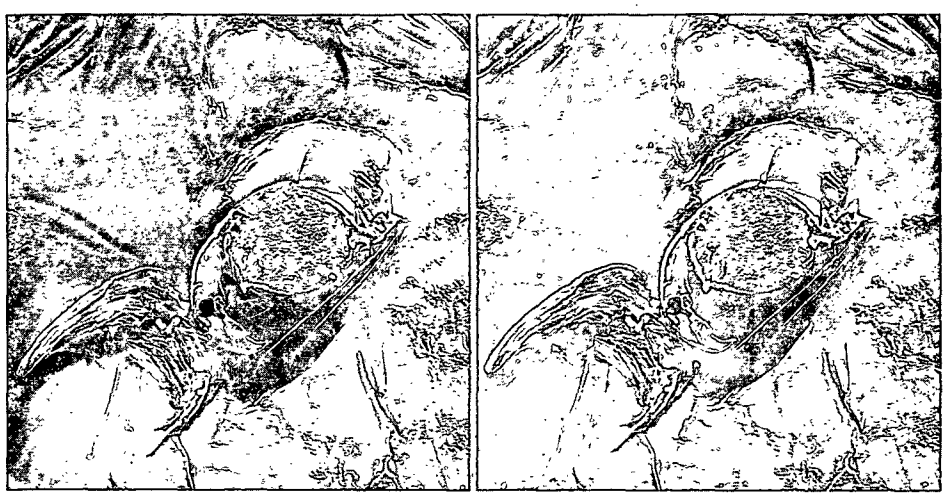

Figure 162. A Negative Replica: the Cell-Wall Side of a Primary-Wall-Type Membrane, Showing Penetration of the Membrane by the Polystyrene (PS)

PM: primary-wall-type pit membrane

PP: polystyrene penetration (the PS surface has taken an impression of the conically wound pit lining)

DS: direction of shadowing (determined by studying the shadows)

F1: a fibril which was present on the surface during shadowing (as evidenced by the build-up of palladium on side of the fibril facing the palladium source)

F2: a negative replica of a fibril. (The fibril was removed from the PS surface before shadowing, leaving a groove in the surface. The palladium atoms have been deposited on the back edge of the groove, leaving a "shadow" behind the front edge)

Note: By studying the surface in the light of the discussion of F1 and F2, one can see that the pit membrane actually remains in place on the replica

Plate Number: 2050 AF

Magnification: 12,300X

Specimen Preparation: 9% KOH, FD, FWS, negative replica: fiber wall embedded in PS, manually pulled away, PS surface shadowed and coated with carbon, PS washed away from replica film


DS
PM
RP
RP
FC
1μm

Figure 163. A Negative Replica of Two Primary-Wall-Type Membranes, Showing Penetration of the Membranes by the Polystyrene

PB: pit borders

PM-1: pit membrane slightly penetrated by PS

PM-2: pit membrane severely penetrated by PS

PP: polystyrene penetration

BS: broken or fractured surface of the PS

PL: replica of the pit lining.

Plate Number: 3730 AF

Magnification: 8600X

Specimen Preparation: Radial shive, FD, negative replica:surface pressed into PS, shive pulled away, PS surface cleaned in 72% sulfuric acid, surface shadowed and coated with carbon, PS washed away


PM-2
PM-1
FA
grm

Figure 164. A Shadow-Transfer Replica Showing an Open Pit in a Fiber Wall. The Fiber Wall Had Been Embedded in Polystyrene and Then Pulled Away

OP: open pit

BS: a broken or fractured surface of a polystyrene core anchored in the pit aperture and then broken off

Plate Number: 3745 AF

Magnification: 16,700X

Specimen Preparation: Radial shive, embedded in polystyrene and then pulled away, STR of the shive surface


1 µm
OP
OP
OP
FA

been pulled away from a PS surface much like the one shown in Fig. 163. In the center of this open pit is a fractured surface similar to the one already shown. Possibly this surface, then, is the broken end of a PS core left anchored in the pit aperture. In any case and whatever the final explanation of the so-called fractured surface, Fig. 162 and 163 definitely demonstrate the penetration of molten PS into membrane ruptures. Thus, the dense films backing the positive replicas of pit membranes can well be explained as carbon films intercepted by the intruded PS surfaces. Incidentally, Jutte and Spit (59) had seen similar films in both their pictures and those by Liese (54, 113). He had explained the films as being remnants of plasma membranes. However, in the opinion of the author, the present explanation as a replication artifact is more reasonable.

One other question raised by the author is how the PS would have behaved around the torus-type membranes. Another curiosity was just how the perceptibly viscous PS could penetrate into the lumen cavity and yet not tear away the fragile fibrils suspending the torus. Figure 165 is included since it at least demonstrates that this penetration is possible. In the case of this replica, too, the fiber wall was simply pulled away from the PS without an acid treatment to clean the surface. Thus, the torus was retained in the PS and, subsequently, was physically present on the replica film studied in the microscope. According to the micrograph, the torus was apparently lying against the pit lining at the time of PS penetration, either as a result of natural aspiration or else as a result of being forced into such a position by the penetrating PS interface. In any case, the torus appears to have limited the extent of PS penetration; only a small raised ridge is visible around a part of the torus. Quite logically, raised rings such as this would be sufficient to intercept secondary carbon rings such as those seen earlier in Fig. 18 and 110.

With regard to the question about the fibrillar strands supporting the torus, Fig. 165 offers further comment. Although part of the strands were apparently pressed against the pit lining and were not engulfed by the PS, some of the other strands appear to have been engulfed or encapsulated by the PS. In fact, careful study of the micrograph reveals very dimly visible strands at just the appropriate location to verify this speculation. These strands, as well as the torus, were retained on the actual replica studied in the microscope and served to scatter part of the electrons not scattered by the metal film above them. Thus, the evidence indicates that the molten polystyrene can actually flow between and around the fibrillar strands without tearing them away. In fact, the encapsulation of the strands in the PS may actually aid in preserving the strands through the acid-treatment step of replica preparation.

Figure 165. A Negative Replica of a Torus-Type Pit Membrane, Showing the Penetration of Polystyrene Around the Torus

PB: pit border

T: torus

MF: membrane fibrils (supporting strands) not engulfed by the polystyrene

RR: raised ring of penetrated polystyrene (small arrows on the polystyrene surface point out supporting strands dimly visible under the replica film)

Plate Number: 4048 AF

Magnification: 13,300X

Specimen Preparation: Radial shive, negative replica:surface embedded in polystyrene, pulled away, polystyrene surface shadowed and coated with carbon, polystyrene washed away


FA
1 µm
MF
PB
RR

APPENDIX X

SUSPECTED PRIMARY PITS

During the search of the radial faces for covered pits, several areas were observed which appeared at first to contain hidden pits. The characteristic appearance of these suspected pit coverings was a concentric deposition of the fibrils in the primary layer. A micrograph of one of these structures is given in Fig. 166. However, as one might guess from this micrograph, stereo views of these areas did not reveal any protruding pit borders which means that the areas probably did not contain covered pits at all. Furthermore, careful study of the center of Fig. 166 reveals a pattern of transversely aligned fibrils lying just beneath the surface. These aligned fibrils closely resemble those of the S1, which again indicates that this area probably does not contain a covered pit.

A probable explanation of these structures is that they are primary pits which did not develop into mature pits at the time of wall thickening. This speculative designation is offered simply on the basis of the resemblance between the presently observed structures and the primary pits pictured by Wardrop and Dadswell (114). They have offered a functional description of these structures:

> On the radial walls there exist thin areas through which the cytoplasm of one cell is connected with the cytoplasm of cells contiguous to it. Aggregates of these points of cytoplasmic penetration of the wall--the plasmodesmata--are called primary pit fields and represent regions which later in the development of the cell may develop into mature pits.

In the example structure shown in Fig. 166, the cytoplasmic strand could have persisted until the primary wall was deposited around it. Then, the strand would have withdrawn, permitting uninterrupted deposition of the S1.

Figure 166. A Suspected Primary Pit

CD: concentrically deposited fibrils

TF: an exposed surface of transversely oriented fibrils encircled by the concentrically deposited fibrils

Plate Number: 2990AF

Magnification: 21,100X

Specimen Preparation: 9% KOH, FD, FWS, STR


GD
GD
GD
1 km